Defining the role of epidermal lipoxygenases and its lipid products in skin homeostasis and disease

A thesis submitted to Cardiff University for the degree of Doctor of Philosophy in the School of Pharmacy and Pharmaceutical Sciences

by

Iestyn Llyr Jones

Cardiff School of Pharmacy and Pharmaceutical Sciences

Cardiff University

January 2022

Summary

Healthy skin forms an effective barrier that prevents infection and rapid water loss from the body. Epidermal barrier disruption is evident in common skin conditions such as psoriasis and eczema, along with significantly affecting adequate wound healing. Essential to a competent barrier are lipids which are metabolised by a group of enzymes known as lipoxygenases (LOX's). The molecular mechanisms by which LOX regulates skin homeostasis and prevent skin disease is unexplored and therefore defining the role of LOX in skin is the primary objective of this study.

RNA-sequencing of 12*R*-LOX deficient and wildtype mouse models was performed and results analysed using various bioinformatics tools, allowing the identification of possible molecular networks and biological processes in which LOX may regulate skin function. Interestingly, Gene Ontology (GO) enrichment analysis identified enriched terms relating to differentiation including "keratinocyte differentiation", "keratinization", "peptide cross-linking" and "cornified envelope". Moreover, the majority of differentially expressed genes (DEGs) following 12*R*-LOX protein deficiency are localised to stratified epidermal layers, suggesting a possible role for 12*R*-LOX derived lipids in differentiated layers. Interestingly, upregulated genes with a 1.5 fold change included genes involved in the epidermal differentiation complex (EDC), such as small proline-rich protein 1b (*Sprr1b*), small proline-rich protein 2d (*Sprr2d*) and repetin (*Rptn*). KO vs. WT dataset also identified the statistically significantly downregulation of peroxisome proliferator-activated receptor gamma coactivator 1 alpha (*Pparγc1α*), hypothesised to be involved in regulating keratinocyte differentiation.

As the RNA-sequencing data pointed towards a possible role for 12*R*-LOX in keratinocyte differentiation, investigation into the effect of 9*R*,10*R*,13*R*-TriHOME terminal product of the 12*R*-LOX / eLOX-3 pathway showed an increasing effect on the protein level of important differentiation markers (*Ivl* and *Krt10*), whilst further *in vitro* experiments ruled out a role in proliferation, migration and apoptosis respectively. It was also identified in this thesis that the 9R,10R,13R-TriHOME activates *Pparγc1α*, which was downregulated in 12*R*-LOX deficient vs wildtype and has previously been demonstrated to be implicated in the process of differentiation.

Bioinformatics and biochemical data indicate a possible role for 12*R*-LOX derived lipids in keratinocyte differentiation which is an important process for the development of an effective skin barrier. These observations raise the possibility of utilising the 9R,10R,13R-TriHOME as treatment for skin disorders with a defective epidermal barrier function.

Acknowledgements

First and foremost, I would like to express my gratitude and offer my special thanks to my supervisor Dr Chris Thomas for his invaluable advice, guidance and continuous support during the last four years of my PhD studies. I am extremely grateful for the opportunity of pursuing such a unique and fascinating PhD under his supervision and would like to thank him for sharing his wealth of knowledge and experience on the subject matter which has helped me enormously throughout this research. The opportunity to present my findings at the Infection and Immunity Annual Conference 2019 was a particular highlight and I am grateful to my supervisors for their belief in me. I would also like to extend my sincere thanks to Professor James Birchall, Professor Valerie O'Donnell, Dr Matthew Ivory and my PGR advisor, Dr Sion Coulman for their insightful knowledge, comments and helpful feedback on experiments and reports throughout my PhD.

The invaluable data obtained from the RNA-sequencing experiment was only made possible from the kind donation of 12*R*-LOX deficient and wildtype mouse pups courtesy of Dr Angela Dick of the University of Erlangen and Nürnberg. A very big thanks and appreciation also go to Dr James Burston for technical support during RNA extraction on 12*R*-LOX deficient mouse models and to Dr Victoria Tyrrell for help with running samples on the LC-MS. Additionally, I would like to acknowledge Dr Robert Andrews for providing bioinformatics support and suggestions on the analysis of the RNA-sequencing dataset. Without their invaluable insight and assistance, these experiments would have been exceedingly difficult and almost impossible.

My thanks also go to other PhD students, undergraduate students and post-doctoral researchers in lab 1.88 for their friendship, advice and constructive coffee breaks! It has been a pleasure sharing the lab with you all. Also, to my friends who have always been a great source of support and encouragement.

Last but not least, I would like to thank mam and dad for their unwavering support and encouragement through the challenging times of the PhD. Also, to my brother Rhys, whose words of wisdom and calming influence has always been a source of comfort and encouragement for me and to that, I am forever grateful.

Hoffwn ddiolch i fy nheulu am eu cefnogaeth dros y bedair blynedd ddiwethaf. Ni fyddwn wedi gallu cwblhau'r ddoethuriaeth heb eu cymorth amhrisadwy a maent wedi bod yn gefn mawr i mi yn ystod fy nghyfnod o ymchwil ac astudio.

Table of contents

Abbreviations

12*R*-LOX	12R-Lipoxygenase
3D	Three-dimensional
AA	Arachidonic acid
AD	Atopic dermatitis
ALA	α-linoleic acid
ARCI	Autosomal recessive congenital ichthyosis
ATCC	American type culture collection
BP	Base pairs
BPE	Bovine pituitary extract
BSA	Bovine serum albumin
Ca^{2+}	Calcium
Casp3	Caspase-3
Ccl	CC chemokine ligands
COX	Cyclooxygenase
CE	Cornified envelope
CER	Ceramide
CHL	Cholesterol
CI	Congenital ichthyosis
CIE	Congenital ichthyosiform erythroderma
CLE	Cornified lipid envelope
DEG	Differentially expressed gene
dH_2O	Distilled water
DMEM	Dulbecco's modified eagle medium

DMSO	Dimethyl sulfoxide
DNA	Deoxyribonucleic acid
DPBS	Dulbecco's phosphate buffered saline
E.coli	*Escherichia coli*
EDC	Epidermal differentiation complex
EDTA	Ethylenediaminetetraacetic acid
EFA	Essential fatty acid
eLOX-3	Epidermal lipoxygenase-3
EOS	Esterified omega-hydroxy sphingosine
EOP	Phytosphingosine
EOH	Hydroxysphingosine
EtOH	Ethanol
FBS	Fetal bovine serum
FC	Fold change
FPKM	Fragments per kilobase of gene model per million mapped reads
GO	Gene ontology
HC	Hierarchical clustering
HCl	Hydrochloric acid
HEPE	Hydroxyeicosapentaenoic acid
HETE	Hydroxyicosatetraenoic acid
HETrE	Hydroxyeicosatrienoic acid
HI	Harlequin ichthyosis
HMG-CoA	3-hydroxy-3-methylglutaryl CoA
HODE	Hydroxyoctadecadienoic acid

HPETEs	Hydroperoxyeicosatetraenoic acid
HPLC	High performance liquid chromatography
HRP	Horseradish peroxidase
hTERT	Human telomerase reverse transcriptase
IPA	Ingenuity pathway analysis
IV	Ichthyosis vulgaris
Ivl	Involucrin
KO	Knockout
Krt	Keratin
LCE	Late cornified envelope
LOX	Lipoxygenase
LTs	Leukotrienes
LXs	Lipoxins
MRM	Multiple reaction-monitoring
mRNA	Messenger ribonucleic acid
MS	Mass spectrometry
MW	Molecular weight
NaCl	Sodium chloride
NCBI	National centre biotechnology information
NCIE	Nonbullous congenital ichthyosiform erythroderma
OS	Omega-hydroxyacyl-sphingosine
PCA	Principal component analysis
PCR	Polymerase chain reaction
PGI	Prostacyclin

PGs	Prostaglandins
PLA2	Phospholipase A2
PPAR	Peroxisome proliferator-activated receptor
PSG	Penicillin streptomycin glutamine
PUFA	Polyunsaturated fatty acids
RIPA	Radioimmunoprecipitation buffer
RNA	Ribonucleic acid
Rptn	Repetin
RT	Room temperature
RXR	Retinoid X receptor
SB	Stratum basale
SC	Stratum corneum
SD	Standard deviation
SG	Stratum granulosum
SPRR	Small proline-rich
SS	Stratum spinosum
TEWL	Transepidermal water loss
TGM	Transglutaminase
TXs	Thromboxanes
TZDs	Thiazolidinediones
UV	Ultra violet
VLFA	Very long-chain fatty acid
WT	Wildtype
XIC	Extracted ion chromatogram

Chapter 1

Introduction

1.1 The human skin

As the largest organ in the human body that comprises around 15% of the total body weight in a human, the human skin has a range of important roles and functions. These include protection against harmful biological and chemical entities, preventing excessive water loss and playing a key role in the body's maintenance of its internal temperature. Other key roles of the skin include the synthesis of vitamin D which is linked to reduced mortality as well as acting as a sensory organ due to the presence of nerve structures (Nair and Maseeh, 2012; Boer et al., 2016; Shipton, 2013). Moreover, the skin consists of a complex system of immune cells required for skin homeostasis, tissue reconstruction and barrier restoration in the event of injury or damage to the skin (Nguyen and Soulika, 2019).

Figure 1.1 shows a detailed observation of the human skin revealing three distinct layers. These include the epidermis, dermis and the subcutaneous tissue (Kanitakis et al., 2002). A clear difference in the thickness of these three layers occurs throughout the human anatomy. The eyelid for example has an epidermal region measuring less than 0.1 mm, whilst a thicker epidermis is observed in the soles of the feet, with a measurement of approximately 1.5 mm (Wong et al., 2015).

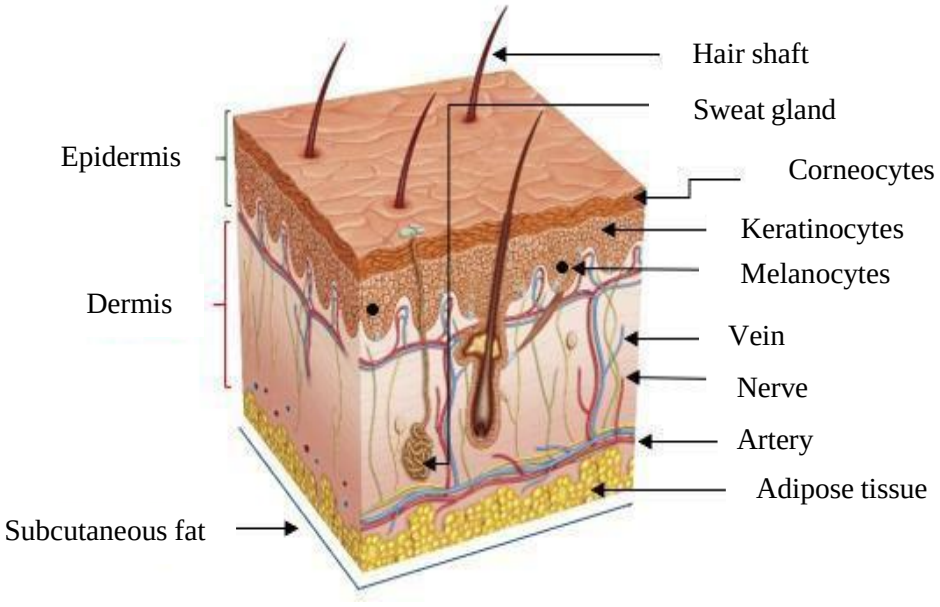

Figure 1.1 A 3-Dimensional depiction showing various layers and structure of the skin. (Image obtained and adapted from http://anatomystructure.net/unlabeled-diagram-of-the-skin).

1.1.1 The epidermis

The epidermis is a continuously renewing epithelial tissue and takes approximately 40-56 days to completely regenerate (Halprin, 1972). It is the outer most layer of the human skin and is mostly composed of a specific cell type known as keratinocytes (Abdo et al., 2020). Other cells found within the epidermis include melanocytes, merkel cells and langerhans cells (James et al., 2006). Melanocytes synthesise an important skin pigment known as melanin which functions as a defence molecule against damaging ultraviolet rays from the sun (Brenner and Hearing, 2007). A merkel cell takes the form of an oval shaped cell and functions as a type 1 mechanoreceptor in human skin (Halata et al., 2010). Langerhans cells are important immune cells that are responsible for regulating an immune response following exposure to harmful substances (Yan et al., 2020). The epidermis is the layer of skin that is exposed to the environment and provides the first line of defence against external stimuli (Chambers and Vukmanovic-Stejic, 2018). **Figure 1.2** shows the epidermis divided into four distinct layers; stratum basale, stratum spinosum, stratum granulosum and the stratum corneum.

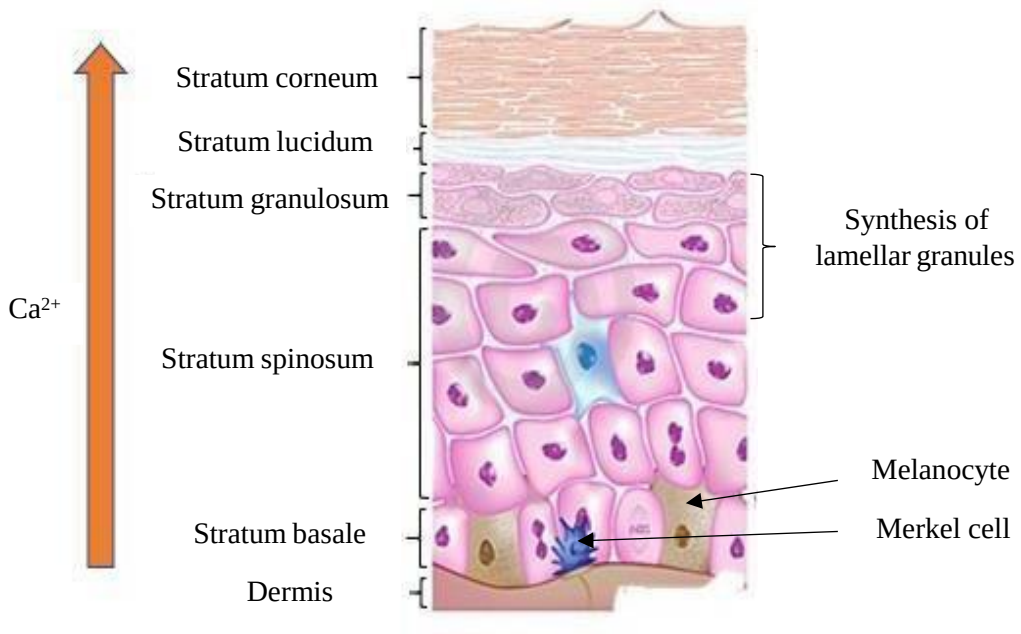

Figure 1.2 A schematic depiction of the outermost layer of the skin known as the epidermis with a demonstration of the increasing calcium gradient and the proliferation and differentiation process. (Image obtained and adapted from http://anatomybody101.com/page/178/).

1.1.2 Keratinocytes

Keratinocytes are the most abundant cell type in the epidermis, accounting for approximately 95% of the entire cell population (Johansen, 2017). Keratinocytes secrete various proteins such as keratins, lipid molecules, cytokines and anti-microbial peptides (Matsui et al., 2015; Chieosilapatham et al., 2021). Keratinocyte proliferation and differentiation are important biological processes essential for the formation of the epidermis (Elias et al., 2005). For effective epidermal barrier formation, epidermal processes such as keratinocyte proliferation and differentiation are highly regulated.

Another important biological process in the epidermis is keratinocyte migration. The initiation of keratinocyte migration is regulated partly by specific combinations of growth factors but might also be controlled by specific individual growth factors (Seeger and Paller, 2015). These molecules which sometimes include proteins and lipids are thought to promote key biological processes of the epidermis such as cell proliferation, migration and differentiation. Cholesterol sulfate is an example of a lipid known to induce keratinocyte differentiation (Feingold and Jiang, 2011). Proteins and lipids that have the ability to act as growth factors might exert their effect as fully functional molecules or may require processing once secreted. Examples of these growth factors include transforming growth factor-α (TGF-α), heparin-binding epidermal growth factor (HB-EGF) and insulin-like growth factor 1 (IGF-1) (Seeger and Paller, 2015). Experimental studies have confirmed the effect of growth factors on cell migration using monolayer cultures of skin cells (Shirakata, 2010).

As keratinocytes migrate from the basal layer of the epidermis, they undergo a unique process known as differentiation. During this process, keratinocytes undergo biochemical and structural changes and express a variety of unique epidermal protein markers during suprabasal migration. Moreover, keratinocytes also synthesise organelles known as lamellar granules during the differentiation process as shown in **Figure 1.2** (Madison et al., 1998). A major biological factor influencing the keratinocyte differentiation process within the epidermis is the existence of a calcium gradient shown in **Figure 1.2**. A high concentration of calcium can be found in the stratum granulosum with the lowest found in the stratum basale layer (Menon et al., 1985). Studies have shown that epidermal proteins such as involucrin, filaggrin and keratins found in the differentiated keratinocytes are regulated by the calcium concentration gradient (Elias et al, 2002). Upon reaching the outer most layer of the epidermis, keratinocytes terminally differentiate resulting in the formation of non-nucleated dead cells

known as corneocytes which are surrounded by a rich layer of lipid molecules known as the corneocyte lipid envelope (Eckhart et al., 2000; Koster, 2009; Akiyama, 2017).

1.1.3 Stratum basale

The inner most layer of the epidermis or the stratum basale (SB), consists mainly of undifferentiated keratinocytes, melanocytes and merkel cells. Keratinocytes found in this layer of the epidermis are described as cuboidal or columnar in shape and orientated on the basement membrane which is the interface between the epidermis and dermis (Yang et al., 2016). This region is often characterised by a single layer of basal cells connected to each other through desmosomal junctions. Melanocytes account for around 5 to 10% of the population of cells found within the basal layer which secrete the melanin pigment involved in UV radiation absorption (Murphy et al., 1997; Yaar and Park, 2012). The basal layer is also a site in which high mitotic activity occurs resulting in cells found in the outer most layer of the epidermis (Matsui and Amagai 2015). Due to the nature of basal stem cells to proliferate rapidly which results in an accumulation of cells, they are known as clonogenic cells with lengthier life spans than any other cell type present within the epidermis (Strachan and Ghadially, 2008). Following infection or damage to the epidermis, surrounding epidermal cells will migrate and proliferate within the affected area resulting in a new, self-renewing epidermal tissue. Key to this process is the presence of stem cells located in the basal layer (Yang et al., 2019).

1.1.4 Stratum spinosum

Above the stratum basale layer lies the stratum spinosum (SS), also known as the squamous layer. Features of the stratum spinosum include a noticeable increase in cell numbers that can be deduced through histological analysis and that range from five to ten cells in thickness. A diverse group of cells with variable structure, shape and cellular properties can be observed with the spinosum layer. However, most cells present here are described as polyhedral in shape and possessing a more rounded nucleus in comparison to the longer nuclei found in basal cells. As we move upwards through the spinosum layer, cells increase in size with a more flattened appearance (Ipponjima et al., 2020).

The abundance of desmosomes between spinous cells aid in strengthening interaction between cells and providing resistance against any physical stress. Surrounding the nucleus in an organised and uniform pattern are keratin filaments whereby they interact with desmosomal plaques, further reinforcing coupling between each cell (Murphy et al., 1997). Desmosomal plaques are also vitally important in regulating calcium concentration that allows the effective

construction and maintenance of desmosomes (Fairley, 1991). The presence of gap junctions is another linkage between cells of the spinous layer, thus allowing interaction through chemical signalling which promotes growth, cell metabolism and the process of differentiation (Caputo and Peluchetti 1977).

1.1.5 Stratum granulosum

The stratum granulosum (SG) is characterised by a profusion of keratohyalin proteins that are found within the cytoplasm of flattened keratinocytes. The keratohyalin granules vary in both shape and size within the cytoplasm of keratinocytes and are key components in the synthesis of interfibrillar matrix which is responsible for connecting keratin proteins together whilst also ensuring that the lining of the stratum corneum is durable. Synthesis of proteins such as a range of keratins occur in the granular layer that are involved in the process of keratinization (Taichman and Prokop, 2010).

Depending on the thickness of the upper most layer, the cornified layer, the stratum granulosum adjusts and is proportional to the thickness of the stratum corneum. Areas consisting of a less thickened cornified layer will be above a granulosum layer comprising of only one to three cells in total thickness. In comparison to a thicker corneum layer as would be evidential on the palms of the hand, the granulosum layer will exceed the thickness of the cornified layer by a factor of ten (Murphy et al., 1997). A process known as parakeratosis occurs when the maturation of epidermal keratinocytes is incomplete, resulting in cells not maturing into a functional corneocyte phenotype (Ruchusatsawat et al., 2011).

Other characteristic features of cells located in the upper spinosum to the granular layer of the epidermis is the presence of lamellar bodies which are specialised secretory organelles consisting of membranous disks surrounding the structure and barrier lipids, proteins and antimicrobial peptides (Madison et al., 1998). The contents of these tubulovesicular organelles include glycoproteins, lipids, free sterols, vast number of hydrolases such as proteases, lipases, acid phosphatases and anti-microbial peptides. An excess of acid hydrolases suggests a function akin to that of lysosomes (Raymond et al., 2008). The role of these lamellar bodies in the upper spinous and granular cells are to produce precursor lipids that can be further metabolised by enzymes in the stratum granulosum, subsequently constructing an effective epidermal barrier. They secrete polar lipids, proteins and enzymatic metabolites into extracellular spaces which helps form the permeability and microbial barrier (Feingold and Denda, 2012; Menon et al., 2018). The secretion of lipid species by lamellar bodies are precursor structures to barrier lipids found in the stratum corneum (Bouwstra et al.,

2000). Typical lipid species found within lamellar bodies include cholesterol, glucosylceramides, phospholipids and sphingomyelin (Feingold and Denda, 2012). The lamellar bodies secrete a large proportion of their contents into the stratum granulosum and stratum corneum interface.

Previous studies using water soluble tracers have detailed how the initial release of lamellar bodies inhibit the entry and diffusion of water from the skin with the precise location being the stratum granulosum-stratum corneum interface (Elias and Friend, 1975). Other studies have aided understanding in the order of events that takes place once lamellar bodies have secreted the vast mix of biological material. Such actions that follow secretion of these granules include fusion of lipid contents of the lamellar bodies and the production of lamellar sheets which occupy the extracellular space between corneocyte (Menon et al., 1992).

Investigations have been performed into the mechanistic processes by which lamellar bodies are formed due to its role in formation and maintenance of the epidermal permeability barrier (Elias and Wakefield, 2014). Interestingly, the incorporation of both lipids and catabolic enzymes occur simultaneously and in an arranged sequence (Rassner et al., 1999). Damage or disruption to the epidermal barrier stimulates the formation of new lamellar bodies with the contents of active lamellar bodies being secreted during barrier distress (Menon et al., 2012). The inhibition of lipid synthesis results in the non-delivery of lipids to lamellar bodies for packaging and has a downstream effect in that enzymes are consequently prevented from being incorporated into lamellar bodies as the process relies on parallel incorporation (Feingold, 2007). However, reintroducing lipids results in their successful delivery into lamellar bodies which subsequently leads to enzymes also being incorporated, emphasising the importance of lipids in enabling enzymes to be transported and perform their biological function once released. Although the relationship between lipid and enzymatic incorporation has been established, it has yet to be confirmed whether lipids are also involved in the transportation of antimicrobial peptides into lamellar bodies. The exact molecular mechanisms and pathways by which lipids are transported into lamellar bodies is yet to be fully understood.

1.1.6 Stratum corneum

The cornified layer, also known as the stratum corneum (SC) is the outer most layer of the epidermis that gives rise to the epidermal permeability barrier that is essential in preventing excessive water and electrolyte loss as shown in **Figure 1.3** (Elias, 2013).

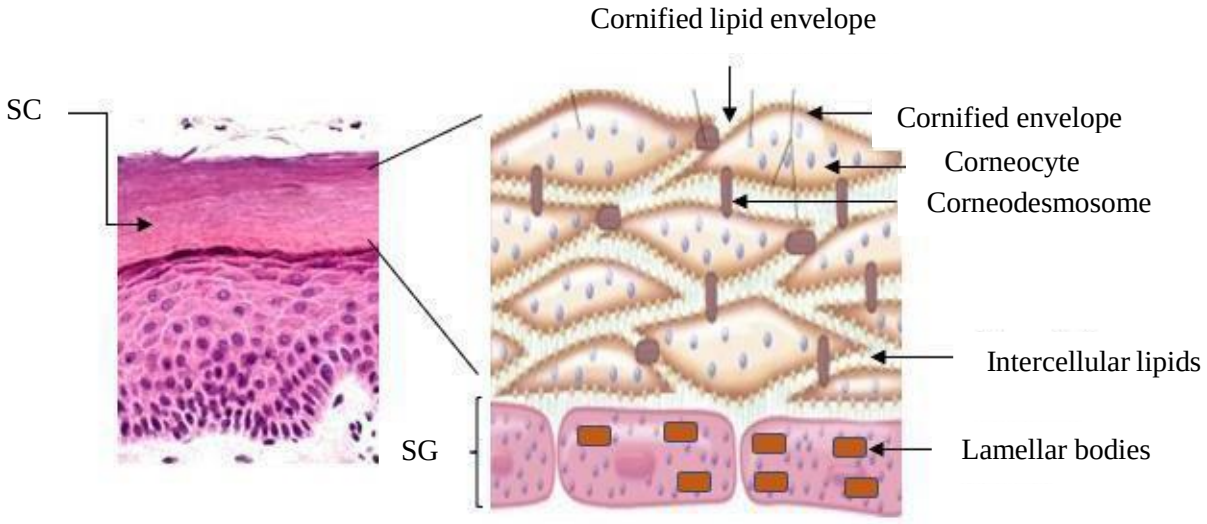

Figure 1.3 A schematic representation of the stratum corneum consisting of corneocytes. Cells are packed with keratin proteins with a rich environment of intercellular lipids. (Image obtained and adapted from Menon et al., 2012).

The structure and organisation of the stratum corneum is often described as "brick and mortar" in which the corneocytes represent the "brick" and the extracellular lipid composition surrounding the corneocytes being described as the "mortar" (Menon et al., 2012). It acts as a defensive barrier to counteract the entry of microorganisms into the human body (Lee et al., 2006). This layer is composed of flat, non-nucleated cells called corneocytes that lack cytoplasmic organelles, normally found in cells of the inner most layers of the epidermis. A close examination of intracellular composition of corneocytes shows a high keratin content that are aligned into cross linked macrofibres through disulphide interaction.

A monolayer of lipids can also be found to be covalently bonded to the cornified envelope which is known as the cornified lipid envelope (Krieg and Fürstenberger 2014). Initiation of the differentiation process in the spinous layer to the terminal differentiation stage takes approximately 14 days (Seo et al., 2005).

An additional layer known as the stratum lucidum is also found in areas such as the palms of hands and soles of the feet and contain keratinocytes (Adabi et al., 2017). Cells forming this unique layer are nucleated and due to the conversion from nucleated cells within

the stratum lucidum to a non-nucleated cell within the cornified layer, they are identified as transitional cells (Gagna et al., 2009).

Stacked between corneocytes is a lipid matrix where they are arranged in an organised layer, thus preventing essential water loss and fluid. Lipids present in the stratum corneum include cholesterol, free fatty acids and ceramides which are found at an equimolar ratio. The exact lipid organisation in the stratum corneum seems to be vitally important in maintaining the integrity of the epidermal permeability barrier. Further investigations performed into the orientation of lipids in the stratum corneum shows lipids parallel to the surface of corneocytes (de Jager et al., 2006). **Figure 1.4** shows the order in which the lipids are packed in the intercellular spaces of the stratum corneum and is described as crystalline lateral packing which has been confirmed using X-ray diffraction and NMR techniques (McIntosh, 2003; Ananthapadmanabhan et al., 2013).

Both human and murine stratum corneum consist of lipids organised in an orthorhombical packing arrangement (White et al., 1988; Bouwstra et al., 1991). Skin barrier disorders such as psoriasis and atopic dermatitis are shown to have an altered ceramide arrangement and composition, suggesting that these specific biomolecules have key roles in maintaining skin health (Pilgram et al., 2001). For example, in atopic dermatitis patients, an increase in hexagonal lattice structure of lipids is observed in comparison with skin of healthy individuals. Furthermore, in lamellar ichthyosis patients, the proportion of hexagonal lattices in comparison with orthorhombic packing was significantly increased reflecting the importance of ceramide organisation and arrangement in the epidermis (Choi and Maibach, 2005).

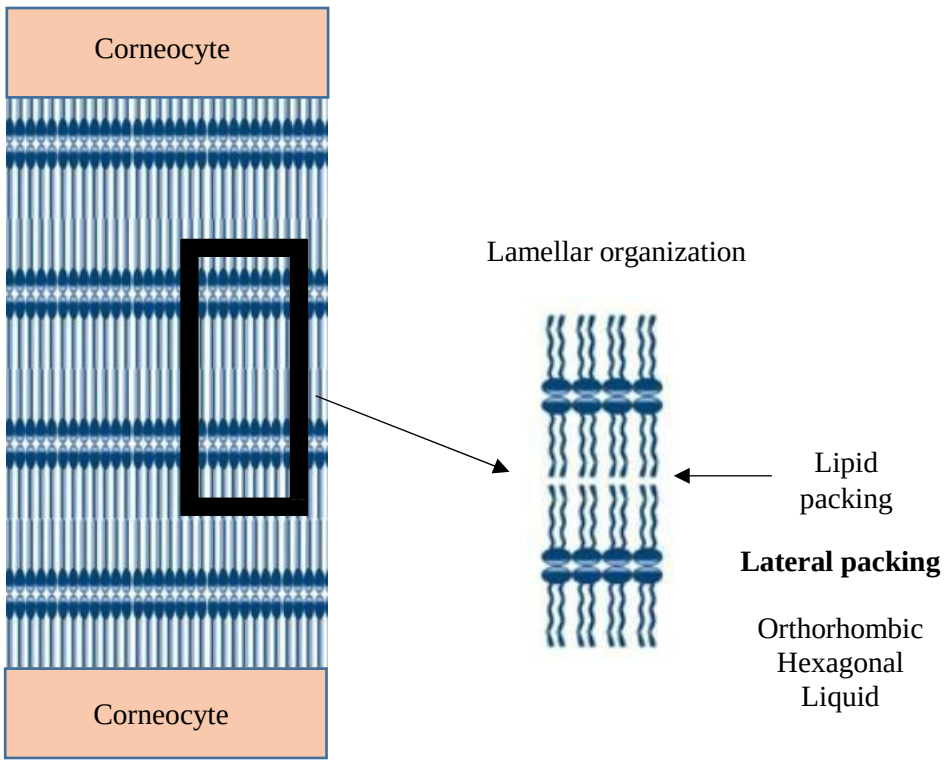

Figure 1.4 A schematic representation of lipid packing in the stratum corneum. (Image obtained and adapted from Ananthapadmanabhan et al., 2013).

Other structural components of the stratum corneum include corneodesmosomes. These modified desmosomes are essential for connecting corneocytes of the stratum corneum together (Haftek, 2014). To allow for the desquamation process to occur in older corneocytes, slow and progressive degradation of desmosome proteins will ensue. A diverse population of lipolytic and proteolytic enzymes are also present in the stratum corneum and have an important role in processing the blend of lipid species and in the degradation of desmosome proteins.

Also scattered in intercellular spaces are secreted biological components of epidermal lamellar bodies. These components include anti-microbial peptides, a range of hydrolytic enzymes that include lipases, proteases, glycosidases and acid phosphatases, along with barrier forming lipids including ceramides, sphingomyelin, free fatty acids, phospholipids and glycosphingolipids which make up the lipid lamellae of the cornified layer (Menon et al., 1992). The combination of all these biological mechanisms and machineries allow for the formation of an effective barrier function and this complex structure and organisation of the stratum corneum can inhibit the penetration or passage of drug molecules.

1.1.7 Proteins involved in terminal differentiation and cornification

A robust structure known as the cornified envelope (CE) is found in the stratum corneum that surrounds corneocytes (Ishida-Yamamoto and Iizuka, 1998). The cornified envelope precursor family encode approximately 32 proteins which constitute the cornified envelope in the outer most layer of the epidermis. Proteins belonging to the cornified envelope precursor family such as involucrin (*Ivl*), filaggrin (*Flg*) and small proline rich proteins form a scaffold-type framework through their cross-linking via the transglutaminase enzyme. This vastly cross-linked assembly of proteins renders the outer most layers of the epidermis extremely insoluble (Kypriotou et al., 2012). The resulting CE surrounds the outer area of differentiated keratinocytes found in the stratum corneum (Schäfer and Werner et al., 2011). Abundantly found in the CE is the loricrin (*Lor*) protein, making up approximately 65-70% of this specific epidermal compartment. In contrast, the involucrin protein forms only a small percentage (2-5%) of the cornified envelope (Hohl et al., 1991). Remaining proteins belonging to the cornified envelope precursor family include the SPRRs. Multiple roles have been attributed to the small proline rich protein gene family such as amino-group donors as well as neutralising reactive oxygen species (Greco et al., 1995). A subset of the small proline rich family known as the late cornified envelope proteins are found to be expressed in the upper layers of the epidermis (Marshall et al., 2001).

The S100 protein family consists of 17 genes that have a range of functions. These include encoding for peptides having antimicrobial properties which are attributed with the S100A7 (psoriasin), S100A15 (koebnerisin) and S100A8/A9 (calprotectin). Specific proteins of the S100 protein family such as S100A15 have shown to be effective against *Escherichia coli* (Abtin et al., 2010). Other functions include the regulation of key biological processes such as cell proliferation, differentiation and apoptosis (Donato et al., 2013). Proteins belonging to the S100 family such as S100A7 and S100A15 are shown to be highly expressed in skin disorders such as psoriasis and chronic eczema (Lei et al., 2017).

The S100 fused type protein family derives from the combination of both the aforementioned cornified envelope precursor protein family and the S100 protein family. Expression of proteins belonging to this EDC family are predominantly detected in stratified layers of the epidermis. Proteins associated with the S100 fused type family such as repetin (*Rptn*), filaggrin (*Flg*), hornerin (*Hrnr*) and cornulin (*Crnn*) constitute the major proteins found in the cytoplasmic matrix of cells. Unlike loricrin (*Lor*), these proteins form a much smaller proportion of the cornified envelope (Marenholz et al., 2001).

Key to epithelial homeostasis is the *Flg* protein, a member of the S100 fused type protein, where its function is to aggregate keratin proteins and intermediate filaments to form a skeletal structure in the granular layer (Sandilands et al., 2009). Mutations in this gene is known to induce a form of ichthyosis known as semi-dominant ichthyosis vulgaris (IV). This skin barrier disease is characterised by retention hyperkeratosis where keratinocytes adhere together which restricts effective desquamation. Additionally, filaggrin (*Flg*) gene mutations are associated with other forms of skin diseases such as atopic dermatitis (AD) (McLean et al., 2006). Filaggrin deficient mouse models display a similar phenotype to 12*R*-LOX deficient mouse models which include a dry and flaky skin appearance. The granular layer of both mouse models appear reduced in size with the loss of nuclei and hyperpigmentation known as acanthosis in filaggrin deficient mouse models (Presland et al., 2000). Processing and expression of another key S100 fused type protein known as filaggrin 2 (*Flg2*) occurs in the granular layer of the epidermis. Furthermore, expression of this protein is abundant in squamous cells of the epidermis. In psoriatic lesions, expression of the *Flg2* protein is greatly reduced, however, a change in expression is unaltered in other forms of skin diseases such as AD (Wu et al., 2009).

Additional members of the S100 fused type protein family include trichohyalin (*Thh*) and trichohyalin-like 1 (*Tchhl1*). *Thh* is predominantly expressed in the upper layers of the epidermis where its role is forming granules in both the root shaft and medulla compartment of human hair (Tarcsa et al., 1997; Lee et al., 1999). Calcium-dependent enzymes found in the epidermis affect the *Thh* protein. For example, an enzyme known as peptidyl-arginine deiminase alters the arginine amino acid into citrulline forming a component of the cornified envelope. The cross-linking of this component is catalysed by a member of the transglutaminase family known as Transglutaminase 3 (*Tgm3*) (Steinert et al., 1996). Along with *Rptn* and the late cornified envelope proteins, the *Thh* protein forms a cross-bridging component that is an essential link between the cornified envelope and keratin filaments (Steinert et al., 2003). The smaller molecular weight protein, *Tchhl1*, is found to expressed in the hair root sheet of the epidermal region. Data demonstrating the localisation and expression of both these proteins indicate an important role in the development of hair (Wu et al., 2011).

Remaining S100 fused type proteins include cornulin (*Crnn*), repetin (*Rptn*) and hornerin (*Hrnr*) in which all three are expressed in the suprabasal layers of the epidermis (Hohl, 2005) (Takaishi et al., 2005). The *Crnn* protein acts a substrate for a Transglutaminase 1 (*Tgm1*) activity in the granular layer of the epidermis and helps protect against ionic

detergents that disrupt protein interactions such as the action of deoxycholate. Furthermore, the EF-hand domain associated with *Crnn* regulates the cellular release of calcium and prevents the process of apoptosis from being induced (Darragh et al., 2006). The expression of *Crnn* is changeable depending on the skin condition. For example, its expression is found to be reduced in eczema, but is found to be unaffected in psoriasis (D'Amato et al., 2009).

The mechanical strength of the cornified envelope is partly due to the cross-bridging *Rptn* protein (Steinert et al., 2003). Interestingly, animal knockout models of loricrin (*Lor*), *krüppel-like* factor 4 (*Klf4*) and kelch-like ECH-associated protein 1 (*Keap1*) show an increase in the expression of *Rptn*. A disrupted barrier is also linked with an upregulation in the *Rptn* protein. In contrast, *Rptn* is shown to be downregulated because of an increase in the expression of a suprabasal protein known as claudin 6. Overexpression of this particular protein is known to cause a severely perturbed barrier function resulting in neonatal death (Turksen and Troy, 2002).

Unlike cornulin's interaction with transglutaminase 1, *Hrnr* is found to be cross-linked *in vitro* via another member of the transglutaminase family known as transglutaminase 3 (*TGM3*). The result of this catalysed reaction are oligomers of high molecular weight that are processed by proteolytic enzymes during the differentiation process in suprabasal layers (Makino et al., 2001; Takaishi et al., 2005). Human and mouse *Hrnr* protein is expressed in the upper layers of the epidermis, with mouse *Hrnr* more strongly induced than is evident in the epidermis of humans (Takaishi et al., 2005). Experimental evidence shows *Hrnr* expression is downregulated in inflammatory skin conditions such as psoriasis and in atopic dermatitis (Schröder et al., 2009; Henry et al., 2011).

1.1.8 The dermis

The dermis is part of the skin that is found between the epidermis and the subcutaneous fat and is mainly composed of elastic tissue and collagen (Prost-Squarcioni et al., 2008) (Wong et al., 2015). It can be further divided into two additional layers known as the papillary and the reticular layers. The main composition of the papillary dermis is the presence of unattached connective tissue, while the reticular dermis is composed of dense connective tissue that forms the majority of the dermal structure. Cells found within the dermis include fibroblasts, macrophages, mast cells, Schwann cells, stem cells and adipocytes (Nguyen and Soulika, 2019). Mast cells are part of the inflammatory network and are responsible for secreting proinflammatory molecules. Adipocytes found in the dermis have a role in energy storage, insulation and hypothesised to be involved in wound healing (Driskell et al., 2014). Collagen is the most abundant component of the dermis, with type I and type III collagen found in copious amounts. The elastic tissue found in the dermis is made of elastin and fibrillin microfibrils with elastin formation and arrangement providing the elastic and stretching properties of the dermis (Green et al., 2014). Other components found within the dermis include, fibroblasts, responsible for synthesising collagen blood vessels, nerve endings and hair follicles.

The dermis plays a key role in thermoregulation and sensation and provides strength and support to underlying layers. The network of blood vessels found in the dermis are essential for providing nutrients to the epidermis, while the presence of neutrophils and lymphocytes in the dermis allows the initiation of an inflammatory response. Specific structures found within the dermis such as glomus bodies produced by glomus cells are integral for thermoregulation (Sethu et al., 2016). Finally, multiple mechanoreceptors, nerve endings and deep pressure receptors allow for touch and feel sensation beyond surface of the skin.

1.1.9 The subcutaneous fat

The inner most layer of the human skin is known as the subcutaneous fat or hypodermis. Components found within this specific layer of skin include blood vessels, sensory neurons, adipose tissue and hair follicles. Cells found in this layer of skin include fibroblasts, macrophages and adipose cells. The main function of the subcutaneous fat is to provide support and protection to underlying muscle tissue through the presence of adipose tissue and protective films secreted by subcutaneous glands (Mittal, 2019). Subcutaneous fat consists of proteoglycan and glycosaminoglycan molecules responsible for drawing fluid into this specific

layer, while leptin secretion is tightly regulated through G protein-coupled receptors (Guimberteau et al., 2010; Amisten et al., 2015).

1.2 Skin lipids

Lipid biomolecules are important for skin homeostasis. Epithelial cells such as keratinocytes and the sebaceous glands are responsible for producing lipid molecules in human skin (Nicolaou and Harwood, 2016). Sebaceous glands in the skin produces and secretes sebum, which is composed of various lipid molecules including triglycerides, squalene, fatty acids and wax esters (Picardo et al., 2009). Lesser quantities of diglycerides, cholesterol and cholesterol esters are also present in sebum (Pappas, 2009). **Figure 1.5** shows examples of lipid species found in the stratum corneum that include cholesterol, linoleic acid and ceramides (Elias and Feingold, 1992). Essential roles of skin lipids include the formation of an effective epidermal barrier, preventing transepidermal water loss, protection from harmful agents and radiation. Lipid biomolecules possess pro and anti-inflammatory features and are implicated in various skin diseases and disorders (Nicolaou and Harwood, 2016). Additional roles of skin lipids include energy storage, cell signalling and forming the semi permeable cell membrane structure (van Meer et al., 2008; Sunshine and Iruela-Arispe, 2017; Welte and Gould, 2017).

Cholesterol

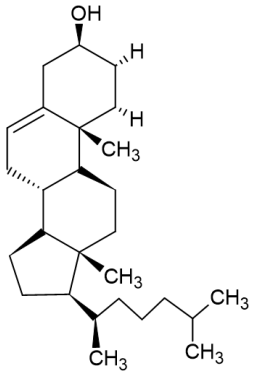

Ceramide [AH]

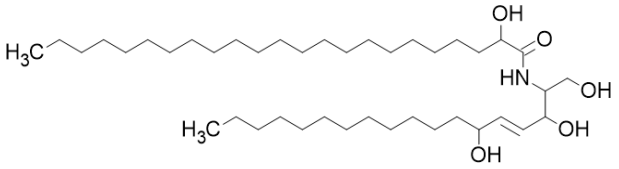

Linoleic acid

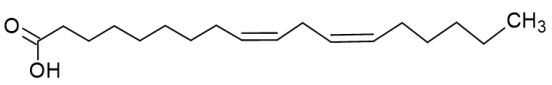

Figure 1.5 Examples of the chemical structure of lipids found in the stratum corneum. These include cholesterol, ceramide [AH] and linoleic acid.

1.2.1 Epidermal lipids

Lipids found in the epidermis play an important role in the formation and function of the epidermal permeability barrier through preventing loss of water, nutrients and electrolytes. Lamellar bodies found in the upper spinosum and granular layer are responsible for the synthesis and secretion of cholesterol, ceramides and free fatty acids that surround the corneocytes found in the stratum corneum (Pappas, 2009).

Epidermal barrier disturbance results in the upregulation of lipid synthesising genes and the increased production of fatty acids, cholesterol and sphingolipids known to be important in re-establishing epidermal barrier function (Feingold, 2009). Previous studies have shown that inhibition of lipid metabolising genes and their associated pathways results in a defective barrier formation, demonstrating the importance of lipids in skin homeostasis. Ceramide molecules unique to the human epidermis have been previously reported and also demonstrated to be important for skin health (Kendall et al., 2017). These ceramides found in the epidermis consists of fatty acid structures of varying carbon atom length. In addition, a proportion of epidermal ceramides consists of ω-hydroxy long chain fatty acids resulting from the enzymatic activity of epidermal lipoxygenase enzymes described in **Section 1.2.9** and **Section 1.2.9.1** (Bouwstra et al., 1998).

1.2.2 Essential fatty acids

Essential fatty acids (EFA) are polyunsaturated fatty acids (PUFA) which the human body is unable to synthesise (Kaur et al., 2012). There are only two important EFAs that exist, namely, linoleic acid (LA) and α-linolenic acid (ALA). These are distinguishable through the position of the first double bond closest to the terminal methyl group. **Table 1.1** shows examples of common PUFA. Fatty acids are important biomolecules that have multiple roles and function in the epidermis (Khnykin et al., 2011). For example, fatty acids can act as signalling molecules and activate transcription factors such as peroxisome proliferator-activated receptors (PPARs) (Schmuth et al., 2008; Sertznig et al., 2008). Furthermore, fatty acids contribute to the acidic pH found in the stratum corneum along with regulating key epidermal processes such as desquamation (Fluhr et al., 2001).

LA is the most abundant fatty acid found in the epidermis and is obtained from dietary sources such as meat and vegetable oils (Whelan and Fritsche, 2013). As aforementioned, LA and ALA are considered EFAs due to the body's inability to synthesise these specific compounds because of the absence of appropriate desaturase enzymes (Sampath and Ntambi, 2011). Previous studies in which rats were supplemented a LA deficient diet has

demonstrated the importance of LA in maintaining epidermal barrier function (Hansen et al., 1985). Historic work performed by George and Mildred Burr in the 1920's identified the importance of LA in epidermal barrier function through feeding rats a fatty acid deficient diet (Burr and Burr, 1930). Rats fed a fatty acid deficient diet exhibited barrier defects accompanied by a redness and scaling of the skin, however, the addition of LA into their diet rescued and recovered epidermal barrier function. As such, this study demonstrated that LA is an essential fatty acid required for skin homeostasis and in preventing the development of skin disease (Spector and Kim, 2015). Further studies conducted in rat models demonstrated the crucial role of LA in barrier formation through substituting the LA for oleic acid. This resulted in epidermal barrier defects and alterations in keratinocyte proliferation (Wertz and Downing., 1983). Changes in fatty acid composition has been observed in psoriasis and atopic dermatitis, suggesting an involvement in the pathophysiology of these skin disorders (Khnykin et al., 2011).

In the epidermis, LA is esterified to the omega-hydroxyl group of ceramides, forming a specific subset of ceramides known as acylceramides. Ceramides also consist of a sphingosine molecule attached to the long chain fatty acid. Forty to fifty percent of lipid species found in the epidermis are ceramide molecules and LA based ceramides are implicated in epidermal permeability barrier function (Hansen and Jensen., 1985; Wertz, 1992). Arachidonic acid (AA) is another example of a n-6 PUFA and is the second most abundant PUFA found in the epidermis (Chapkin et al., 1986). Phospholipids, phosphatidylinositol and phosphatidylserine all contain AA in their structure and the release of AA from the aforementioned molecules occur through an enzymatic reaction with phospholipase A2. Its metabolism results in the formation of epidermal eicosanoids known to mediate inflammatory responses (Nicolaou, 2013).

PUFA family	Name
n-3 PUFA	Stearidonic acid
	Eicosatetraenoic acid
	Eicosapentaenoic acid
	α-linolenic acid
n-6 PUFA	Arachidonic acid
	Linoleic acid
	Adrenic acid
	Tetracosatetraenoic acid

Table 1.1 Examples of common n-3 and n-6 polyunsaturated fatty acids.

1.2.3 Lipid metabolism in skin

The skin is an organ of high metabolic activity as demonstrated by the presence of enzymes that convert endogenous compounds and topically applied pharmaceuticals to a range of metabolites that may be activated or detoxified (Feingold, 2009). Compounds in the skin are able to undergo oxidative, hydrolytic and reductive reactions. For examples, testosterone is metabolised into a mixture of oxidised and reduced metabolites through the CYP450-dependent pathway (Jacques et al., 2014). Molecules such as ceramides, saturated fatty acids, monounsaturated fatty acids and cholesterol can be synthesised in the epidermis. LA is the structural precursor PUFA for molecules belonging to the n-6 FA family, whilst ALA is the precursor for n-3 PUFA as shown in **Figure 1.6**. The deficiency in Δ-5 and Δ-6 desaturase activity in keratinocytes results in the inability to convert LA and ALA to long-chain compounds such as AA, eicosatetraenoic acid (ETA) and docosahexaenoic acid (DHA). As such, these molecules are also considered as essential fatty acids for skin health (Chapkin et al., 1984; Kendall et al., 2017).

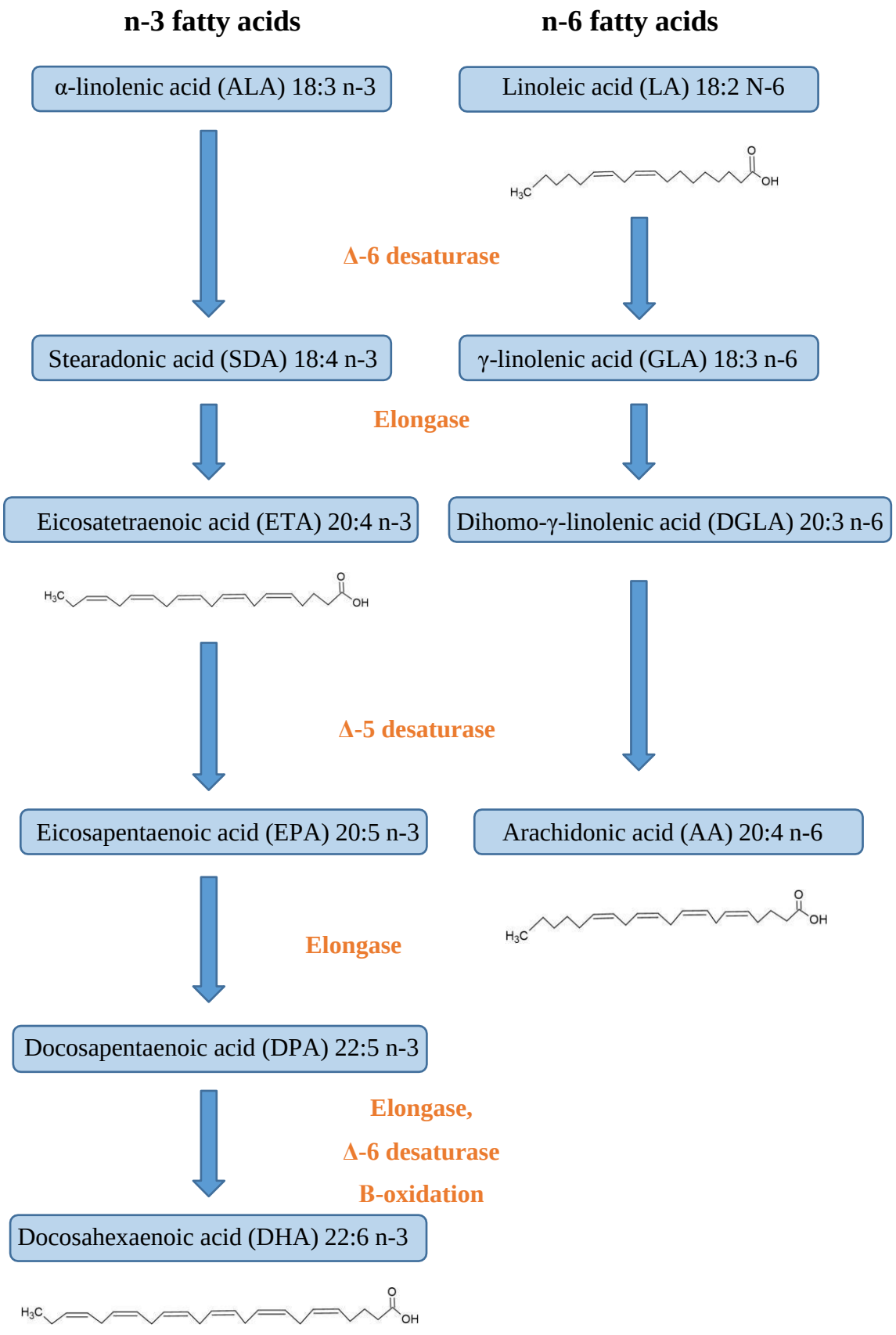

Figure 1.6 The biosynthetic pathway of n-3 and n-6 polyunsaturated fatty acids from linoleic acid and α-linolenic acid. Examples of n-3 and n-6 fatty acid structures are shown.

1.2.4 Fatty acid synthesis

Synthesis of fatty acids occur in the epidermis as demonstrated during barrier disruption studies where epidermal barrier disturbance results in an increased rate of fatty acid synthesis through enzymatic pathways involving acetyl CoA carboxylase and fatty acid synthase (Feingold, 2007). Inhibition of fatty acid synthesis results in acute barrier disruption, highlighting the importance of de novo fatty acid synthesis in epidermal barrier integrity. The process of fatty acid elongation is critical as demonstrated by genetic deletion of a specific elongase known as ELOVL4 in an animal model, resulting in an increased mortality and a significantly compromised epidermal barrier (Vasireddy et al., 2007). Fatty acid desaturase activity is also important in the epidermis as demonstrated by Stearoyl-CoA desaturase 2 knockout animal models where a significantly impaired barrier function, abnormal quantities of lamellar bodies and high mortality rate is observed (Miyazaki et al., 2005).

1.2.5 Epidermal ceramides

Ceramides (CER) represent approximately 50% of lipids found in the stratum corneum. They vary in structure and belong to the sphingolipid family. The structure of a typical ceramide is composed of a sphingoid base that is amide-linked with a variety of fatty acids. The heterogeneity of ceramides is due to variable N-acyl chain length, variety of hydroxylation and saturation. Ceramides can be composed of four different types of sphingoid bases that include sphingosine, phytosphingosine, 6-hydroxysphingosine and dihydrosphingosine (Coderch et al., 2003). Ceramides are thought to play a role in keratinocyte proliferation, differentiation and may serve a function as signalling molecules during apoptosis (Geilen et al., 1997; Burek et al., 2001).

Ceramide species identified in the human stratum corneum are shown in **Figure 1.7**. Acylceramides such as EOS, EOH and EOP contain linoleic acid in their structure that is linked to ω-hydroxy acid molecules. The structural heterogeneity of these ceramides are significant in determining their organization in the epidermis (Coderch et al., 2003).

Ceramide 1 (EOS)

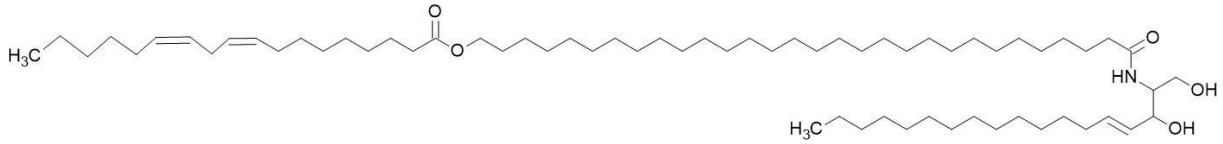

Ceramide 2 (EOP)

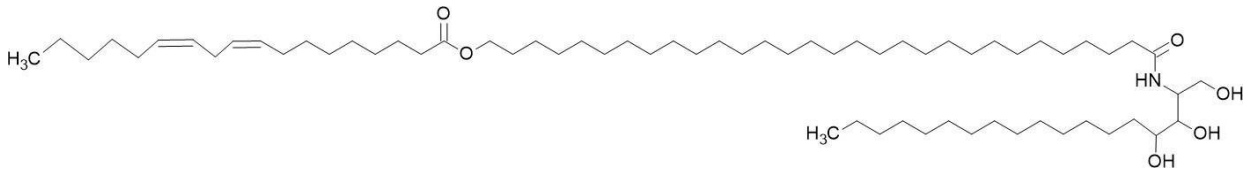

Ceramide 3 (EOH)

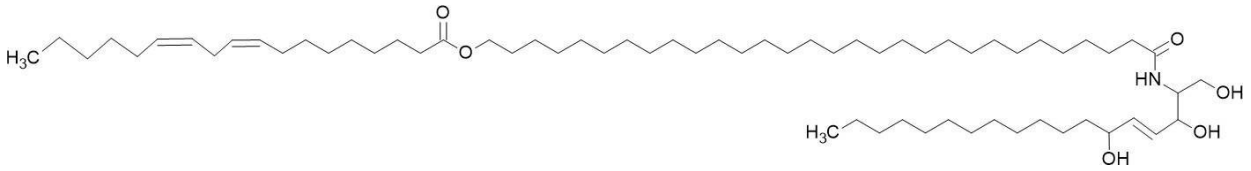

Ceramide 4 (NS)

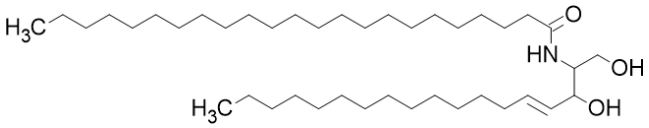

Ceramide 5 (NP)

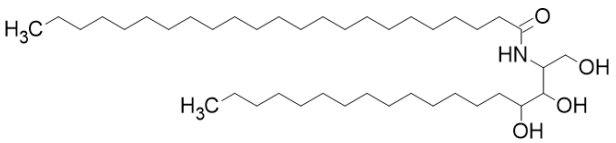

Ceramide 7 (NH)

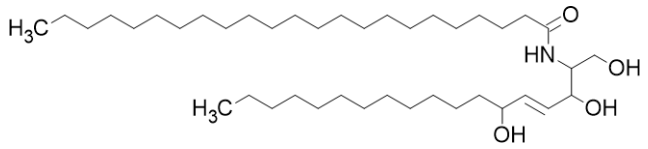

Ceramide 6 (AS)

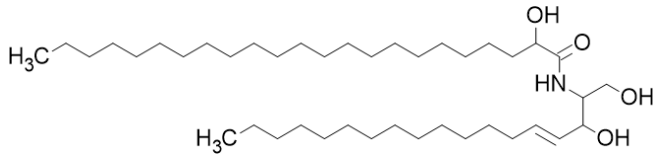

Ceramide 8 (AP)

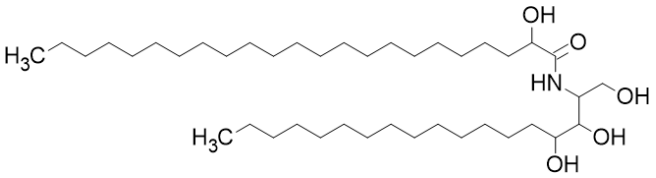

Ceramide 9 (AH)

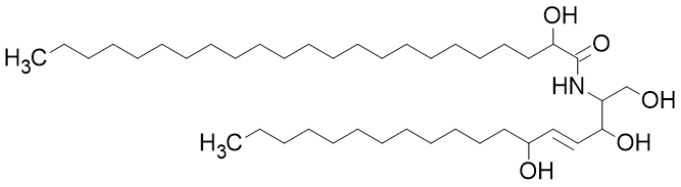

Figure 1.7 Chemical structures of eight major ceramide species found in the epidermis. A = α-hydroxy acid, **E** = Esterified ω-hydroxy acid, **H** = 6-hydroxysphingosine, **N** = nonhydroxy acid, **O** = ω-hydroxy acid, **P** = phytosphingosine, **S** = sphingosine (Image adapted from Coderch et al., 2003).

Two distinct pathways exist to produce epidermal ceramides. The first involves the breakdown of glucosylceramides and sphingomyelin catalysed by β-glucocerebrosidase and sphingomyelinase respectively. The second pathway involves the generation of ceramides from serine and palmitic acid involving the enzymatic action of serine palmitoyltransferase (Holleran et al., 1991). This pathway is illustrated in **Figure 1.8**. Sphingolipid activated protein-C and protein-D are responsible for inducing the activity of β-glucocerebrosidase and

sphingomyelinase (Tayama et al., 1993). Serine palmitoyl transferase is the rate-limiting enzyme involved in the synthesis of sphingolipids, however, inhibition of this key enzyme results in a delayed barrier recovery following its disruption (Holleran et al 1991). Glucosylceramide and sphingomyelin are precursor molecules of ceramides found specifically in the stratum corneum. The glucosylceramide is the main glycosphingolipid found in the epidermis and is synthesised from UDP-glucose and ceramide (Jennemann et al., 2007). Sphingomyelin is an example of a sphingolipid and is a constituent of cell membranes while its structure consists of a phosphocholine and ceramide (Slotte, 2013).

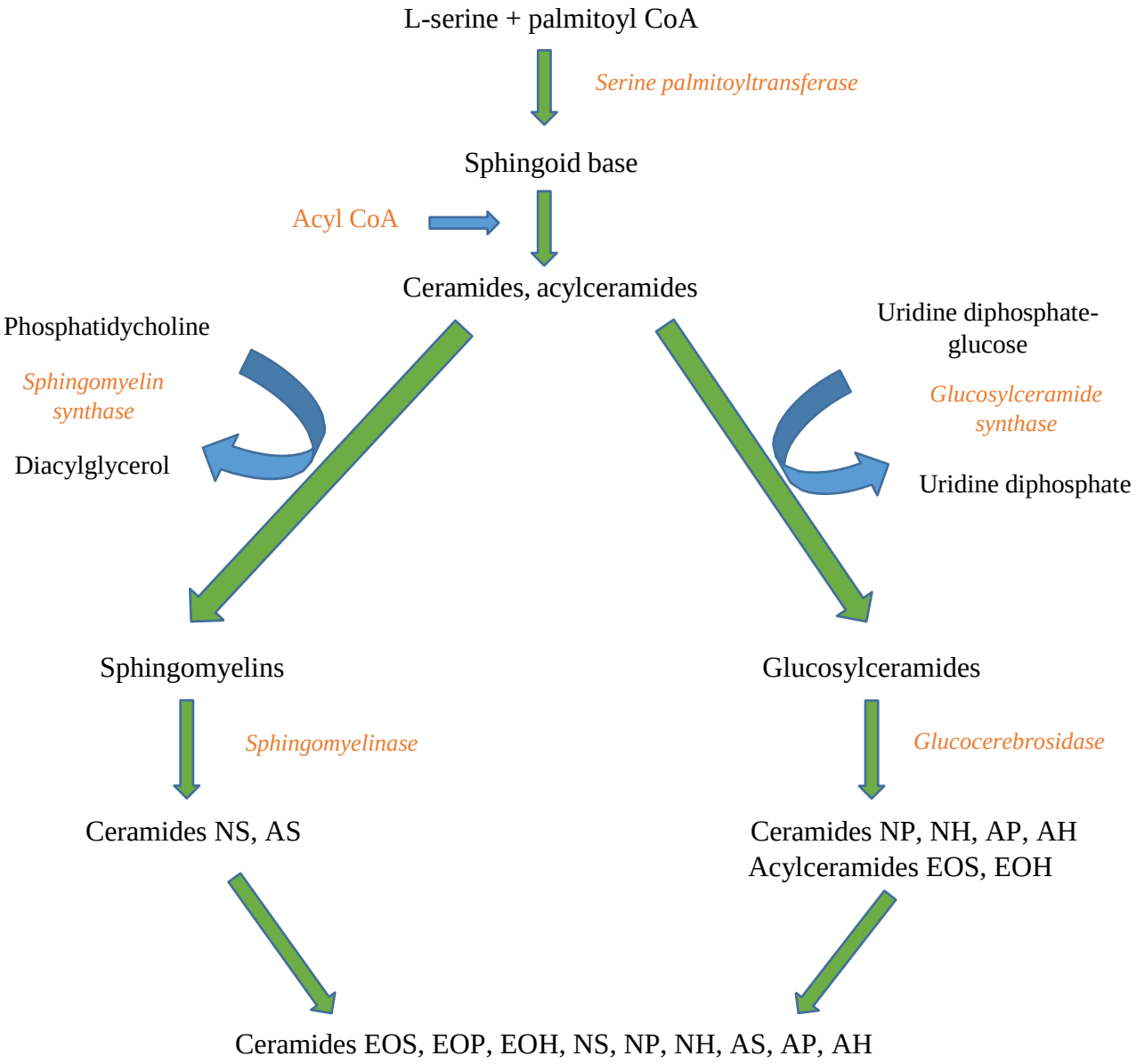

Figure 1.8 Pathway for the production of eight epidermal ceramides. (Image adapted from Coderch et al., 2003).

Decreased quantities and significantly lower weight ceramides have also been observed in atopic dermatitis patients when compared with healthy individuals (Jin et al., 1994; Ishibashi et al., 2003). Additionally, differences in ceramide composition between healthy and atopic dermatitis patients has been demonstrated, where certain free ceramides are found to be significantly reduced in patients with atopic dermatitis, whilst higher levels of cholesterol were observed (Di Nardo et al., 1998; Matsumoto et al., 1999). Similarly, low levels of protein bound ω-hydroxyceramides are detected in the skin, along with a reduction in newly synthesised ceramide species in the skin of atopic dermatitis patients. Studies investigating serine as a substrate for ceramide biosynthesis showed a significant decrease of 46% in lesional skin when compared with healthy skin. These observations indicate that reduced quantities of free and bound ceramide species may play a key role in the abnormal barrier function observed in atopic dermatitis patients (Choi and Maibach, 2005). Furthermore, oxidised ceramide species are reduced in psoriatic lesions along with abnormal metabolism of long chain oxidised ceramides(Tyrrell et al., 2021).

1.2.6 Epidermal cholesterol

Cholesterol (CHL) is another important lipid found in the epidermis and is predominantly synthesised in the liver (Kruit et al., 2006; Pappas, 2009). It is a lipophilic molecule and is thought to play a role in keratinocyte differentiation and contribute to effective epidermal desquamation (Sjövall et al., 2018). Its structure consists of four hydrocarbon rings, a steroid nucleus, a hydroxyl group and a hydrocarbon tail as shown in **Figure 1.5** (Olsen et al., 2009). Other important roles and functions of CHL include forming a structural component of cell membranes, acting as a signalling molecule and serving as a precursor molecule for important biochemical pathways such as the synthesis of vitamin D (Sheng et al., 2012; Cruz et al, 2013; Vona et al, 2021). Cholesterol sulfotransferase (SULT2B1b) converts cholesterol to cholesterol sulfate which has a role in modulating barrier function, keratinocyte differentiation and epidermal desquamation. Cholesterol sulfate is generated in lower layers of the epidermis and its abnormal synthesis results in irregular desquamation along with a perturbed epidermal barrier (Elias et al., 2014).

Cholesterol biosynthesis initially occurs during a condensation reaction between two molecules of acetyl CoA and subsequently forming acyl-CoA. Following this reaction, acetyl CoA and acyl-CoA condense to form 3-hydroxy-3-methylglutaryl CoA (HMG-CoA). A reduction reaction occurs to form mevalonate through activity of the HMG-CoA enzyme. Multiple phosphorylation reactions and a decarboxylation step of the mevalonate occurs to

form isopentenyl pyrophosphate (IPP). Another condensation reaction occurs involving IPP to form farnesyl pyrophosphate (FPP) through geranyl pyrophosphate (GPP) activity. With the aid of squalene synthase, condensation of FPP follows to form squalene. A cyclization reaction of squalene occurs forming lanosterol through the oxidosqualene cyclase enzyme. Lanosterol is then converted into the 27 carbon structure of cholesterol via a demethylation reaction (Berg et al., 2002; Cerqueira et al., 2016).

Following acute barrier disturbance, CHL synthesis is noticeably increased, along with increased expression of enzymes involved in the CHL synthesis pathway such as HMG-CoA synthase and HMG-CoA reductase. An impaired and delayed barrier recovery occurs during the inhibition of key cholesterol synthesis enzymes, emphasizing the importance of cholesterol molecules in skin homeostasis (Feingold, 2007). Additionally, the function and structure of lamellar bodies is significantly affected following inhibition of epidermal cholesterol production (Feingold, 2009). Interestingly, murine models deficient in a key cholesterol converting enzyme known as 3 β-hydroxysterol-delta, result in a significantly perturbed epidermal barrier with a high mortality rate (Mirza et al., 2006).

1.2.7 Biologically active lipid mediators

1.2.7.1 Eicosanoids in the skin

Eicosanoids are important bioactive lipid mediators that play a key role in skin homeostasis. Additional roles of eicosanoids include regulating inflammatory processes through a variety of signalling pathways (Fogh et al., 1989; Nicolaou, 2013; Sivamani, 2014). Moreover, these lipid signalling mediators are involved in processes such as cell migration, proliferation and adhesion (Wymann and Schneiter, 2008). Eicosanoids are produced through the metabolism of n-3 and n-6 PUFA such as AA by lipoxygenases (LOX), cyclooxygenases (COX) and cytochrome P450 as shown in **Figure 1.9** and **Figure 1.10** respectively (Lands, 1992; Nicolaou, 2013). The four families of eicosanoids include prostaglandins (PGs), prostacyclins (PGIs), leukotrienes (LTs) and thromboxanes (TXs) (Wymann and Schneiter, 2008).

The activation of phospholipase A2 (PLA2) is required to initiate eicosanoid biosynthesis with secretory phospholipase A_2 ($sPLA_2$) present in the epidermis and shown to be active in inflammatory skin disorders such as psoriasis (Sjursen et al., 2000; Harizi et al., 2008; Dennis et al., 2011).

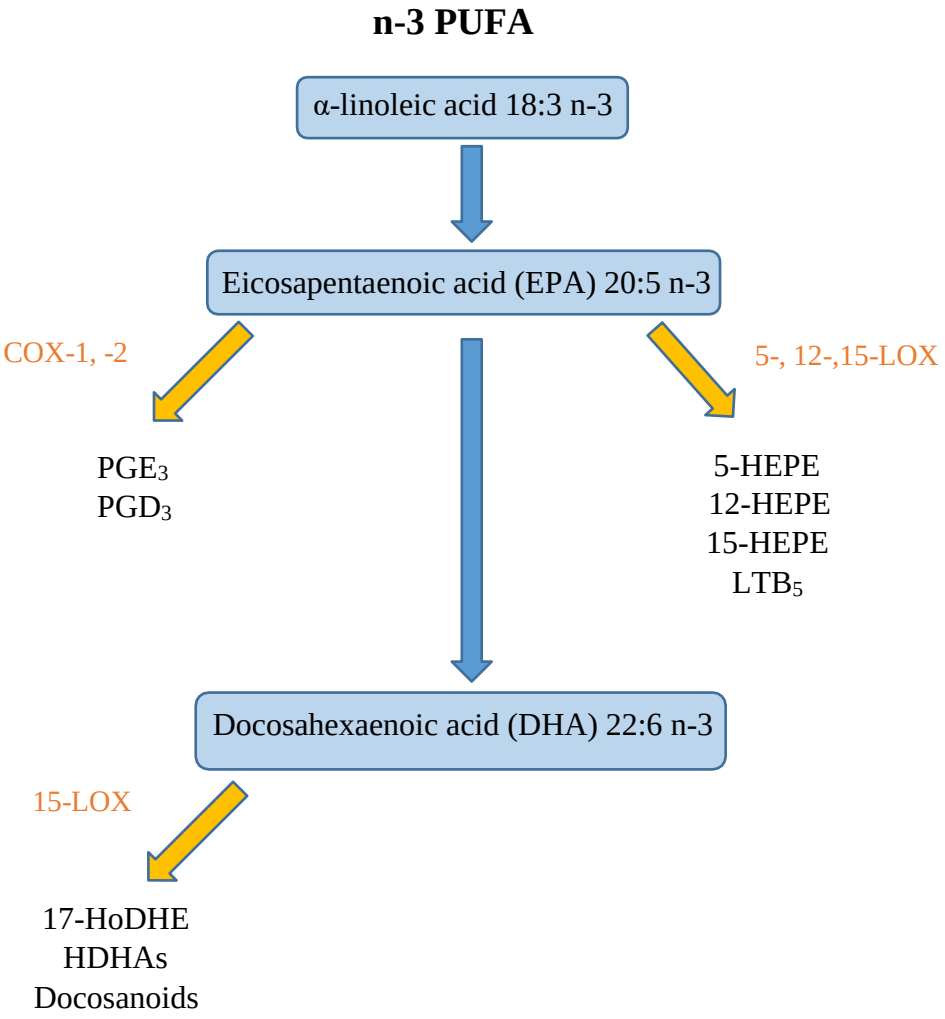

Figure 1.9 Schematic representation of the pathway for eicosanoid biosynthesis from α-linoleic acid.

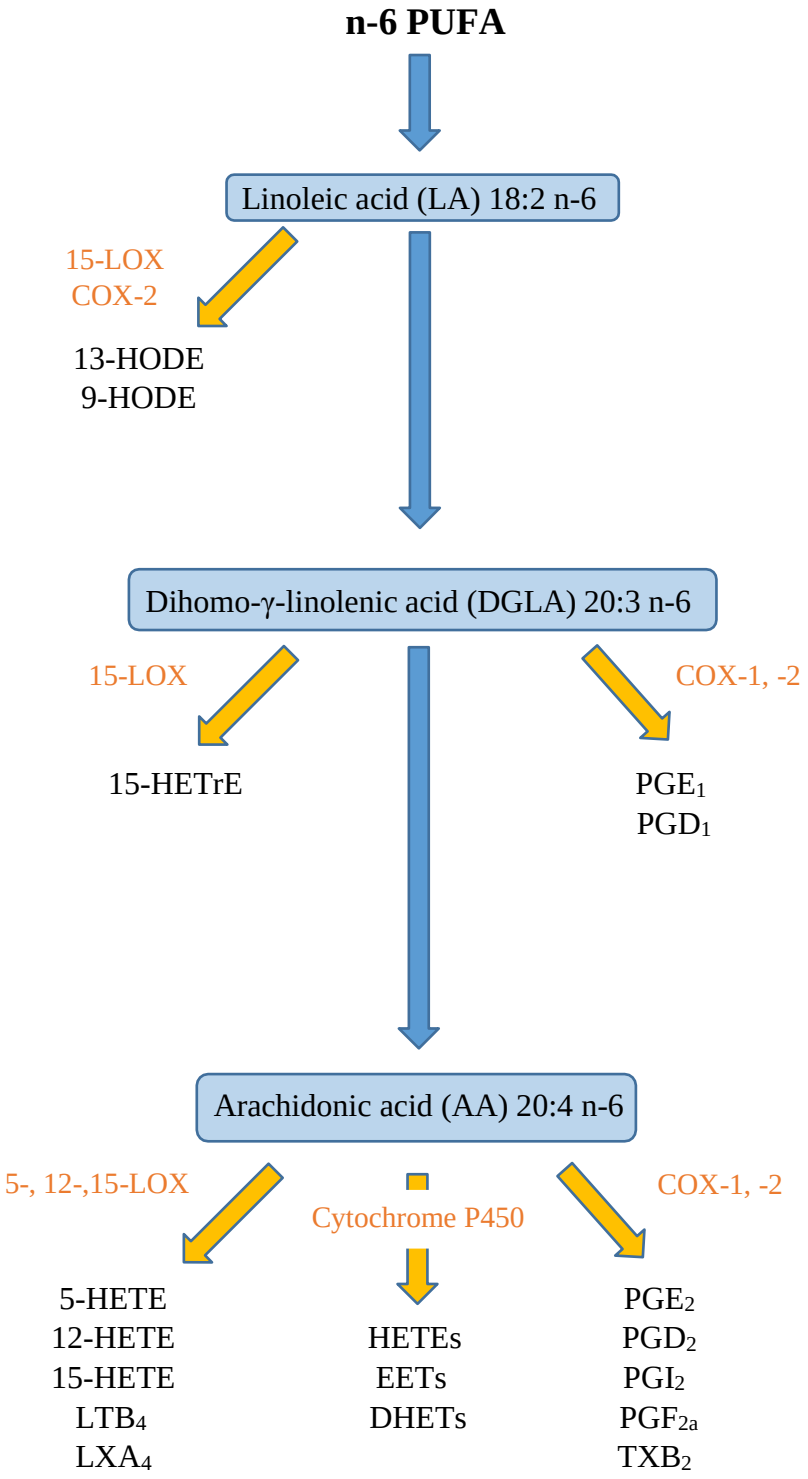

Figure 1.10 Schematic representation of the pathway for eicosanoid biosynthesis from α-linoleic acid.

1.2.8 Cyclooxygenases

Two cyclooxygenase isoforms are found in human keratinocytes which comprise the constitutive COX-1 and the inducible COX-2 isoform (Smith and Langenbach, 2001). Both these COXs catalyse the conversion of a PUFA such as AA to PGH2. Following the production of PGH_2, this metabolite of AA is isomerized to prostaglandins, prostacyclin or thromboxanes (Khanapure et al., 2007; Smith et al., 2011). These family of lipid biomolecules are collectively known as prostanoids. In the skin, prostanoids are produced in response to inflammation and are mediated by prostanoid receptors which include DP, EP, FP, IP and TP (Kabashima and Miyachi, 2004; Smyth et al., 2009). These specific receptors react to the presence of COX metabolites such as PGD_2, PGE_2, PGF_{2a}, PGI_2 and TXA_2 (Kobayashi and Narumiya, 2002).

Both COX-1 and COX-2 produce PGE_2 which is detected in epidermal keratinocytes and has an important role as a pro-inflammatory eicosanoid thought to induce keratinocyte proliferation, differentiation and having a role in immunosuppression (Pentland and Needleman, 1986; Konger et al., 1998; Harris et al., 2002; Honda et al., 2009). These effects are mediated through the G-protein coupled receptor coupled to a Gαi subunit protein known to be expressed in epidermal cells (Pedro et al., 2020).

In addition to PGE_2 eicosanoid production in keratinocytes, the anti-inflammatory PGD_2 prostaglandin is also detected in the skin. The structures of these specific eicosanoids are shown in **Figure 1.11**. PGD_2 is produced from Langerhans cells, dermal mast cells and melanocytes (Harris et al., 2002; Masoodi et al., 2009). Previous studies have demonstrated its anti-proliferative properties (Ikai and Imamura, 1988; Harris et al., 2002). Furthermore, PGD_2 is a precursor to other prostaglandins such as PGJ_2, 15d- PGJ_2 and Δ^{12}-PGJ_2 which also possess anti-inflammatory properties (Straus and Glass, 2001). Other prostanoids found in skin include PGF_{2a} and have been associated with a range of biological processes such as inflammation, skin pigmentation, hair growth and immune responses (Scott et al., 2004; Colombe et al., 2007). Prostanoids such as PGI_2 and TXB_2 have been detected at low concentrations in epidermal cells and are regulators of inflammatory diseases (Sugimoto et al., 2006; Bryniarski et al., 2008; Dorris and Peebles, 2021).

Prostaglandin D_2 – PGD_2

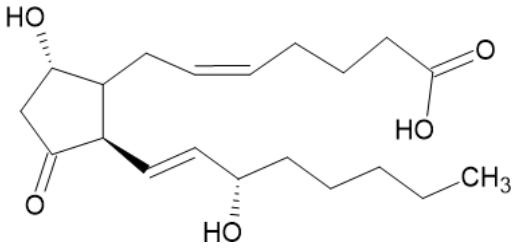

Prostaglandin E_2 – PGE_2

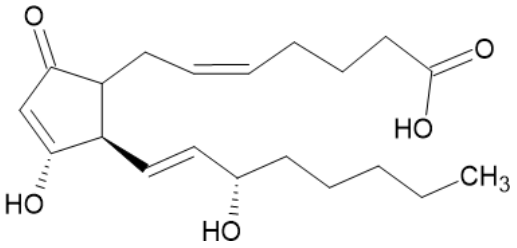

Figure 1.11 PGD_2 and PGE_2 structures produced from COX enzymatic reaction.

1.2.9 Lipoxygenases

To date, the lipoxygenase isoforms in both human and animal skin include 5-, 8- and 15-LOX (Mayer et al., 1984; Ziboh, 1992; Rhodes et al., 2009; Nicolaou et al., 2013). The 12*R*-LOX and eLOX-3 enzymes are of most interest as they are the dominant LOXs found in the epidermis and are involved in the construction of the skin permeability barrier through catalysing the dioxygenation of polyunsaturated fatty acids (PUFA) in a stereo and regio-specific manner resulting in the formation of a range of hydroxyl-fatty acid molecules (Brash, 1999). These PUFA contain a (cis,cis)-1,4-pentadiene bond within their chemical structure. LOXs can catalyse the oxidation of a wide range of PUFA such as AA, LA, EPA, DGLA and DHA resulting in the production of a rich variety of LOX derived metabolites such as those shown in **Figure 1.12**. For example, the hydroxyl-fatty acid molecules produced from AA LOX oxidation include hydroxyeicosatetraenoic acids (HETE) and lipoxins (LXs). LA oxidation by LOX results in the production of hydroxyoctadecadienoic acids (HODE), whilst EPA oxidation generates hydroxyeicosapentaenoic acids (HEPE). Oxidation of DGLA by LOXs form hydroxyeicosatrienoic acids (HETrE) molecules and the oxidation of DHA results in the formation of hydroxydocosahexaenoic acids (HDoHE) (Mayer et al., 1984; Kragballe et al., 1986; Ziboh et al., 1992; Ziboh et al., 2000; Yoo et al., 2008).

13-HODE

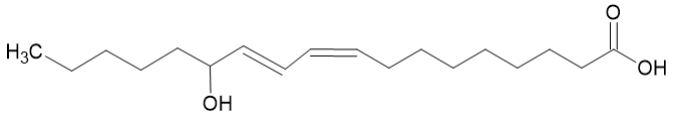

12-HETE

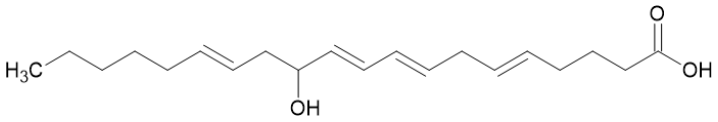

Figure 1.12 Structures of 13-HODE and 12-HETE produced from LOX oxidation of linoleic acid and arachidonic acid respectively.

5-HETE is produced from the activity of 5-LOX, which may also form the LTB_4 leukotriene following a dehydration reaction. Further transcellular metabolic activity occurs to form lipoxins (Serhan and Chiang, 2008; Nicolaou, 2013). In comparison with other LOX actions, the activity of 5-LOX is relatively low in the epidermis. Investigations in the HaCaT cell line showed the expression of 5-LOX is increased during keratinocyte differentiation, whilst a significantly low 5-LOX protein expression was observed in undifferentiated keratinocytes (Janssen-Timmen et al., 1995).

All mammalian LOX genes are found at the human chromosome 17. p13 and located on chromosome 11 in mice. Examination into the chemical structure of LOX reveals a single polypeptide chain which constitutes of around 662-711 amino acids with a molecular mass ranging from 75-81 kDa in the mammalian form of the enzyme. The enzyme also consists of conserved domains and short, recurring patterns in its structure that allow the non-heme iron feature of lipoxygenase to bind. The presence of the non-heme iron is located at the C-terminal of the protein structure with it also being the prime location for substrate binding activity. Distinct isomers are formed in LOX reactions which is dependent on the way in which the substrate is orientated and the volume of the binding cavity of the enzyme. In total, there are six different LOX enzymes in humans that differ in terms of functionality and are categorised on their positional enzymatic activity on lipids. These include 5-LOX, 12-LOX, 12/15-LOX, epidermal LOX (12*R*-LOX, eLOX-3, 15-LOX-2), platelet-type 12-LOX and leukocyte-type 12-LOX (Boeglin et al., 1998; Brash, 1999).

1.2.9.1 12*R*-LOX and eLOX-3 structure and activity

The 12*R*-LOX and eLOX-3 isoforms discovered have been found to play a pivotal role in the construction and maintenance of the epidermal permeability barrier (Krieg and Fürstenberger, 2014). This came about through the identification of 12R-HETE in psoriatic lesions, suggesting that 12*R*-LOX activity occurred in the epidermal compartment of skin, whilst the precise biosynthetic mechanism of 12*R*-LOX production of 12R-HETE in the skin of psoriatic patient was later determined (Hammarström et al., 1975; Boeglin et al., 1998). 12*R*-LOX is the only known LOX protein that can form enantiomeric products with R chirality, as suggested by its name (Siebert et al., 2001). **Figure 1.14** shows the 12*R*-LOX and eLOX-3 isoforms acting sequentially, where the 12*R*-LOX synthesises a fatty acid hydroperoxide and the eLOX-3 converting the fatty acid hydroperoxide into an epoxyalcohol (Zheng et al., 2011). An epoxide hydrolysis reaction follows resulting in production of trioxilins that serve as effective components for epidermal barrier function.

The eLOX-3 isoform also expressed in skin possesses a 54% amino acid similarity to the 12R-LOX protein. Unlike 12*R*-LOX catalytic activity, the eLOX-3 does not oxygenate substrates such as AA and LA. eLOX-3 function was identified as a hydroperoxide isomerase able to transform hydroperoxides produced from 12*R*-LOX activity to epoxyalcohol products as shown in **Figure 1.13**. Whilst structural similarities exist between human and mouse eLOX-3 homologs, slight differences in substrate specificity between the two is observed. For example, human eLOX-3 has a preference towards the oxidised LA, whilst mouse eLOX-3 favours the 12R-HPETE substrate (Gregus et al., 2013; Krieg et al., 2013). 12*R*-LOX and eLOX-3 hepoxilins and trihydroxy linoleate derivatives are shown to be important in the development and function of the epidermal permeability barrier (Krieg and Fürstenberger, 2014). Investigation into the protein structure of 12*R*-LOX and eLOX-3 showed 31 and 41 amino acid subdomains which are found on the catalytic site of both proteins and are essential for substrate binding and catalytic activity (Hallenborg et al., 2010). *ALOX12B* and *ALOXE3* encode the respective 12*R*-LOX and eLOX-3 proteins and consist of an extra intron that is responsible for the catalytic subdomain in each protein (Eckl et al., 2009).

12*R*-LOX and eLOX-3 are expressed in suprabasal layers of the epidermis where keratinocytes are most differentiated. As such, 12*R*-LOX and eLOX-3 are hypothesised to play a key role in the important epidermal process of differentiation (Epp et al., 2007). The tongue, trachea, liver, colon and forestomach are other areas of the human anatomy in which 12*R*-LOX and eLOX-3 are expressed (Heidt et al., 2000). A significantly greater 12*R*-LOX mRNA

expression is observed in psoriatic lesions in comparison with healthy skin, suggesting a role in the pathophysiology of skin disorders. Furthermore, expression of the 12*R*-LOX protein has been observed in prostate cells along with tonsil epithelial cells (Schneider et al., 2001; Krieg and Fürstenberger, 2014). In contrast, eLOX-3 expression has been detected in the brain, ovary, pancreas, placenta and testis (Krieg et al., 2001).

Polyunsaturated fatty acid (Linoleate)

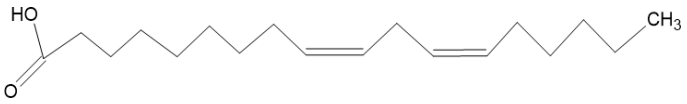

Oxidation — Lipoxygenase (12*R*-LOX)

Fatty acid hydroperoxide (9R-HPODE)

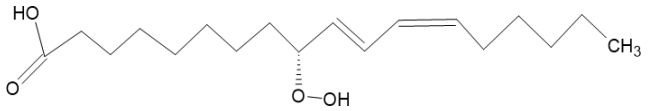

Hydroperoxide isomerase (eLOX-3)

Hepoxilin A-type

And/or

Hepoxilin B-type

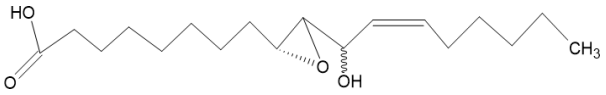

Epoxide hydrolysis

TriHOME

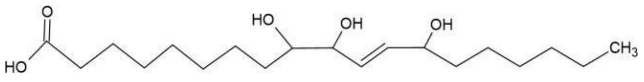

Figure 1.13 Schematic representation of the 12*R*-LOX catalysis of the linoleate substrate to produce trioxilins (trioxilin-type triols). (Image adapted from Muñoz-Garcia et al., 2013).

1.2.9.2 Mutations in 12*R*-LOX and eLOX-3 results skin barrier disease

Previous experimental investigations have shown that mutations in *ALOX12B* and *ALOXE3* genes, responsible for encoding 12*R*-LOX and eLOX-3 give rise to a certain type of ichthyosis known as autosomal recessive congenital ichthyosis (ARCI), highlighting the importance of both 12*R*-LOX and eLOX-3 in skin physiology and maintaining a functional epidermal permeability barrier. ARCI represents conditions such as harlequin ichthyosis, congenital ichthyosiform erythroderma and lamellar ichthyosis (Jobard et al., 2002; Epp et al., 2007; de Juanes et al., 2009).

Certain genes have been identified to be critical in the development of ARCI; *ALOX12B* and *ALOXE3*, *TGM1*, *ABCA12*, *CYP4F22*, *LIPN*, *PNPLA1* and *NIPAL4* (ichthyin) (Fischer, 2009; Grall et al., 2012; Muñoz-Garcia et al., 2013). The TGM1 gene encodes the transglutaminase 1 enzyme that is responsible for cross-linking proteins such as involucrin and small proline-rich proteins of the cornified envelope (Herman et al., 2009). The *ABCA12* gene functions as a lipid transporter in lamellar granules found in the epidermis, whilst *CYP4F22* encodes the *ω*-hydroxylase enzyme essential for the production of epidermal *ω*-hydroxyceramides (Behne et al., 2000; Hotz et al., 2018). *LIPN* is expressed in differentiated keratinocytes and encodes a range of lipases implicated in triglyceride metabolism important for the formation of the epidermal barrier (Israeli et al., 2011). Similarly, PNPLA1 is also involved in lipid metabolism in the epidermis as demonstrated by their lipolytic and acetyltransferase function (Grall et al., 2012). The NIPAL4 gene encodes a granular layer protein known as ichthyin that functions as a receptor to various trioxilin molecules such as A3 and B3 (Li et al., 2012). Studies have been conducted in 520 patients affected by ARCI assessing which gene showed a higher rate of mutation within this cohort. It had concluded that around 32% of patients with ARCI had a mutation in TGM1, 12% in the *ALOX12B* gene, 5% in both *ALOXE3* and *ABCA12* genes (Epp et al., 2007). Mutations in the *ALOXE3* gene gave slightly less severe scaling of the skin in comparison to patients that had mutations in the *ALOX12B* gene as demonstrated by scaling of the skin in patients having a mutation in 12*R*-LOX, whilst a lesser form of scaling and brown patches on the skin of patients with an eLOX-3 mutation is observed. Additional features of patients with a mutation in LOX enzymes include mild to moderate keratoderma and evidence of marked palmoplantar hyperlinearity, where a thickened skin is found on the palms and soles of the feet. Around 15% of patients with ARCI have mutations in the LOX genes with a total of 40 mutations found in both LOX genes that lead to the red, scaly skin phenotype (Jobard et al., 2002; Eckl et al., 2005; Eckl et

al., 2009). Whilst mutations in the 12*R*-LOX protein including nonsense mutations, splice-site mutations, missense mutations and single nucleotide exchanges do not affect the overall binding of the substrate, the overall enzymatic activity of LOX is diminished (Yu et al., 2005; Eckl et al., 2009). This demonstrates the pivotal role in which LOX plays in constructing and maintaining a skin barrier function.

1.2.9.3 12*R*-LOX / eLOX-3 deficient mouse models highlight the importance of 12*R*-LOX in the development and maintenance of the skin permeability barrier

Previous studies involving Alox12b knockout models, which is the gene that encodes for 12R- LOX, have demonstrated the important functional role of 12*R*-LOX and eLOX-3 in the development of an effective epidermal permeability barrier (Epp et al., 2007; Krieg et al., 2013). Various techniques have been used to impair the function of 12*R*-LOX and eLOX-3 proteins that include Cre-loxP systems, ethylnitrosurea induced mouse mutants and tamoxifen induced functional impairment. Whilst these methods differ experimentally, the phenotype of the 12*R*-LOX and eLOX-3 deficient mouse models are consistent with one another. The Cre-loxP technique was used by Krieg et al., 2013 to genetically delete the LOX isoform and resulted in neonatal mortality due to increased transepidermal water loss (TEWL). Interestingly, 12*R*-LOX deficient mice died shortly after birth because of high TEWL, whilst mice deficient in eLOX-3 endured longer survival and appearing to have a less severe phenotype than 12*R*-LOX deficient mice. The phenotype of the 12*R*-LOX deficient mouse models was found to have a reddening, shiny scaling of the skin with histological examination showing a thickened and compressed stratum corneum (Akiyama et al., 2003; Moran et al., 2007). **Figure 1.14** shows a dye permeability assay also performed by Moran et al., 2007 to highlight the defective barrier observed in 12*R*-LOX deficient mice on different embryonic (E) days.

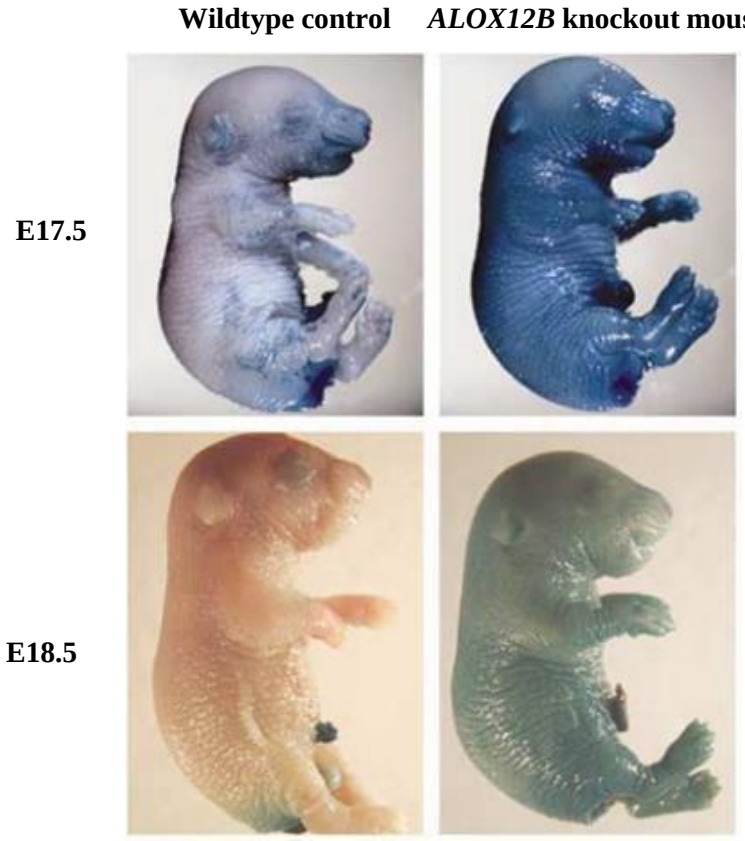

Figure 1.14 *Alox12b* genetic knockout and wildtype mouse models to demonstrate perturbed epidermal barrier. X-gal solution permeation of *ALOX12B* knockout skin significantly greater than X-gal substrate permeation on wildtype mouse skin. (Image obtained and adapted from Moran et al., 2007).

The difficulty with these experiments is that the LOX isoforms knockout results in early mortality in newborns and the ichthyosiform phenotype cannot be further investigated in the maturation stage. However, skin graft studies have overcome this dilemma and allows affected adult mice to be studied. Observable characteristics in 12*R*-LOX deficient mice included a thickened epidermis, hyperproliferation, focal parakeratosis and hyperkeratosis. The result of the adult ichthyosifrom phenotype was subsequently identical to the mice LOX deficient new-borns which was rapid loss of body weight and premature death (de Juanes et al., 2009).

Figure 1.15 shows structural irregularities in both stratum granulosum and stratum corneum of both newborn mice and adult LOX knockout models (de Juanes et al., 2009). This suggests that the lamellar bodies are disturbed in releasing their contents into the stratum corneum for processing by LOX enzymes. Examples of lipids typically found in healthy skin include trihydroxy esterfied omega-hydroxyacyl sphingosine, 12-Hydroxyeicosatetraenoic acid (12-HETE), 13-Hydroxyoctadecadienoic acid (13-HODE), 9-Hydroxyoctadecadienoic acid (9-HODE), 9,10,13-trihydroxyoctadecenoic acid (9,10,13-TriOH) and 9,12,13-

trihydroxyoctadecenoic acid (9,12,13-TriOH). However, in diseased skin, most of these lipids are absent when analysing the epidermis of 12*R*-LOX deficient mice. In addition, the number of bound ceramides to the cornified envelope is greatly reduced in the epidermis of 12*R*-LOX KO mice, demonstrating the effect and impact in which a mutated LOX has on epidermal barrier function. Furthermore, proteins found in the CE such as profilaggrin and filaggrin are either completely absent or have undergone impaired processing. The abnormal CE protein composition of 12*R*-LOX deficient mouse models results in an enhanced fragility in the CE that may be responsible for the increased TEWL and therefore high mortality rate observed in these strains.

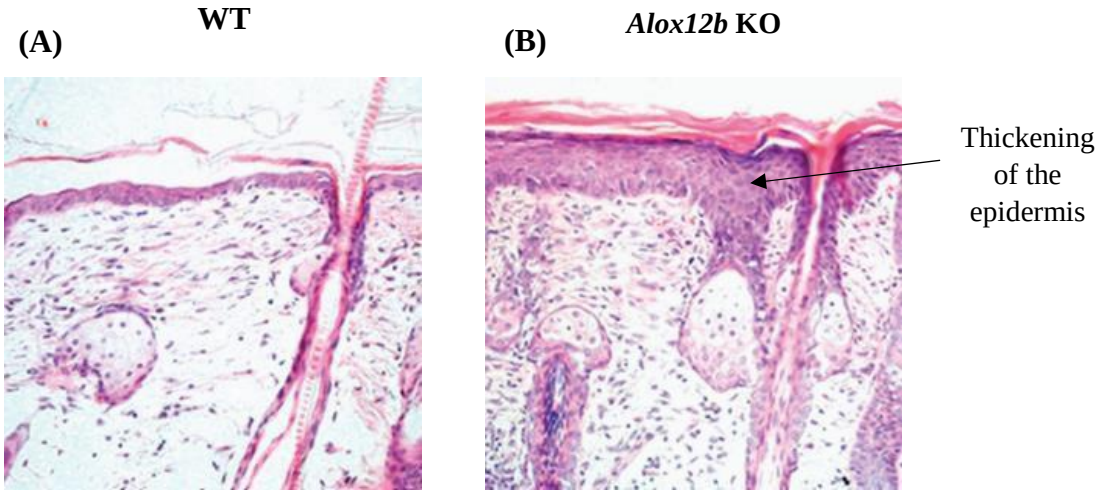

Figure 1.15 Typical ichthyosis phenotype observed in *ALOX12B* knockout mouse model skin sections. *Alox12b* knockout (B) and wildtype skin (A) sections stained with haematoxylin and eosin to demonstrate differences in histology. (Image obtained and adapted from de Juanes et al., 2009).

Lipid analysis by mass spectrometry showed ceramides normally found in healthy skin are found to be unorganised with a reduction in the number of ceramides that are bound to proteins of the CE in the skin of 12*R*-LOX deficient mice. Further analysis conducted on 12*R*-LOX deficient mice by electron microscopy shows an absent cornified lipid envelope (Zheng et al., 2011). To date, Muñoz-Garcia et al., 2013 have confirmed through a series of experiments that both LOX enzymes are involved in metabolising ceramides present within the epidermis and thus forming the CLE as shown in **Figure 1.16**. The LA is specifically esterifed to an omega-hydroxyacyl-sphingosine (EOS, EOH and EOP) and is oxidised by the LOX enzyme resulting in the production of lipids that are vital for skin barrier homeostasis. In healthy skin, it is understood that the linoleate is an important moiety within the ceramide that acts as the substrate for LOX oxidation. The EOS is converted into an omega-hydroxyacyl-

sphingosine (OS) and ω-hydroxy-very long-chain fatty acid (VLFA) via hydrolysis of the oxidised linoleate moiety and a transglutaminase enzyme then catalyses the attachment of the free hydroxy to glutamine proteins present in the CE from involucrin and loricrin to small proline-rich proteins as shown in **Figure 1.16**. This interaction forms the CLE which is integral in preventing transepidermal water loss (Krieg and Fürstenberger, 2014; Muñoz-Garcia et al., 2013).

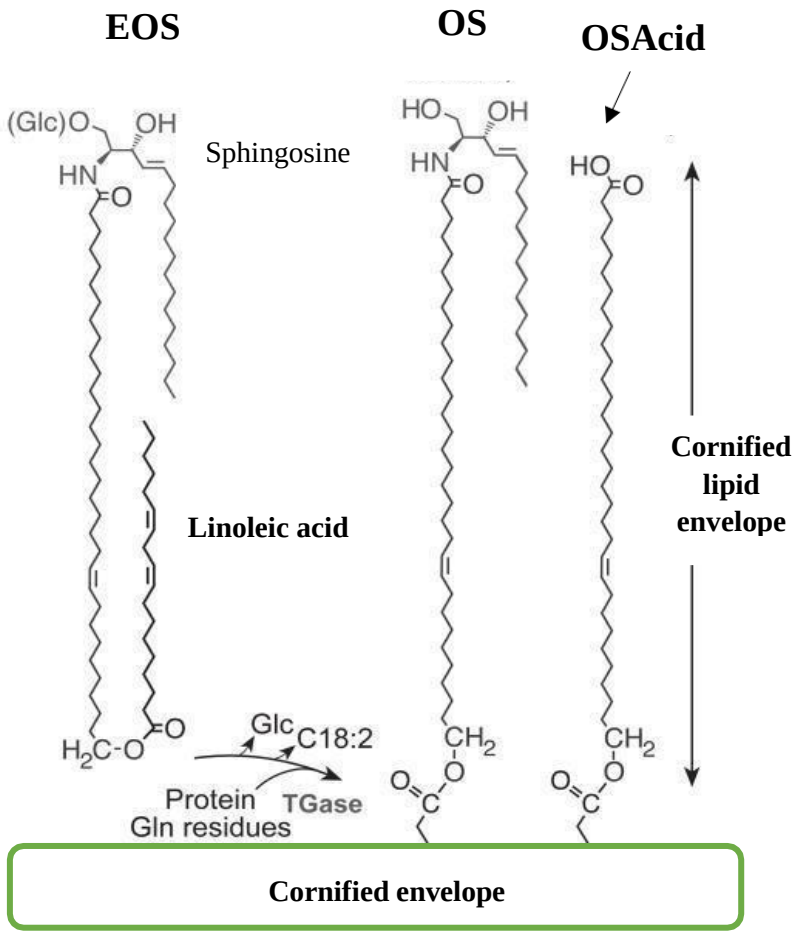

Figure 1.16 Schematic representation of the hypothesised formation of the cornified lipid envelope (CLE). An abundant ceramide known as an esterfied omega-hydroxyacyl-sphingosine (EOS) found in the outer most part of the epidermis is composed of three chemical moieties that include a sphingosine molecule, a linoleic acid and a long fatty acid chain. Hydrolysis of the linoleate occurs which allows transglutaminase (TGM-1) to esterify the resulting omega sphingosine to the cornified envelope (CE). (Image obtained and adapted from Muñoz-Garcia et al., 2013).

Another key observation in 12*R*-LOX knockout models is the lack of metabolites that can be converted into ω-hydroxyceramides along with shorter fatty acid chains that are abundant in wild type strains. TEWL and barrier abnormalities were observed due to the decrease in ceramides bound to the cornified envelope (Krieg et al., 2013). Other evidence in line with 12*R*-LOX and eLOX-3 involvement in barrier formation include the high quantity of

unoxidised linoleic acid present in LOX deficient mice (Uchida and Holleran, 2008; Zheng et al., 2011).

Taken together, a mutation or complete loss of *Alox12b* that encodes for 12*R*-LOX results in a severe phenotype due to the inability to oxygenate linoleic acid. As the cornified lipid envelope is composed of acyl ceramides derived from LOX activity and is known to be critical for the skin permeability barrier, this highlights the importance of 12*R*-LOX in epidermal barrier function. In order to develop novel treatments for patients with ichthyosis, molecular mechanisms and pathways by which LOX contributes to an effective epidermal barrier requires investigation.

1.2.10 Ichthyosis and related skin barrier disorders

ARCI encompasses a range of different ichthyosis conditions such as congenital ichthyosis (CI), harlequin ichthyosis (HI) and congenital ichthyosiform erythroderma (CIE) (Yu et al., 2005; Oji et al., 2010). Approximately 1 in 200,000 individuals in Europe and North America are affected by this genetic skin condition that is characterised by hyperkeratosis and epidermal hyperplasia (Oji and Traupe, 2006). The type of inherited ichthyosis most common in the population is ichthyosis vulgaris that affects around 1 in 250-1000 people according to current NHS figures (Ichthyosis - NHS (www.nhs.uk). Mild scaling, redness and thickening of the skin is observed in the majority of patients with ichthyosis, with neonates exhibiting what can be described as a colloidon membrane (Al-Naamani et al., 2013; Craiglow, 2013). A few weeks after birth, a dry scaling of the skin occurs with mild erythema also observed (DiGiovanna and Robinson-Bostom, 2003). It is possible that enhanced proliferation leading to a thickened epidermis is induced to compensate for the defective barrier that is characteristic of the skin of ichthyosis patients (Krieg and Fürstenberger, 2014).

Rarer forms of ichthyosis include the CIE and HI with extreme scaling of the skin occurring and with neonatal patients requiring intensive care immediately on birth (**Figure 1.17**). CIE can be sub-categorised into a further three types of ichthyosis which include non-bullous, bullous and lamellar. The symptoms observed with the non-bullous form of congenital ichthyosis patients includes severe scaling and redness, whilst symptoms of the bullous form consist of fluid contained blisters that cover large areas of the skin as well as constant shedding. The skin appears less inflamed in lamellar ichthyosis; however, larger and tighter scales can be observed when comparing with the non-bullous and bullous forms of the condition. These types of ichthyosis develop at birth once the collodion membrane has shed which generally occurs one week from birth (Schmuth et al., 2012; Shruthi et al., 2017; Patro et al., 2019).

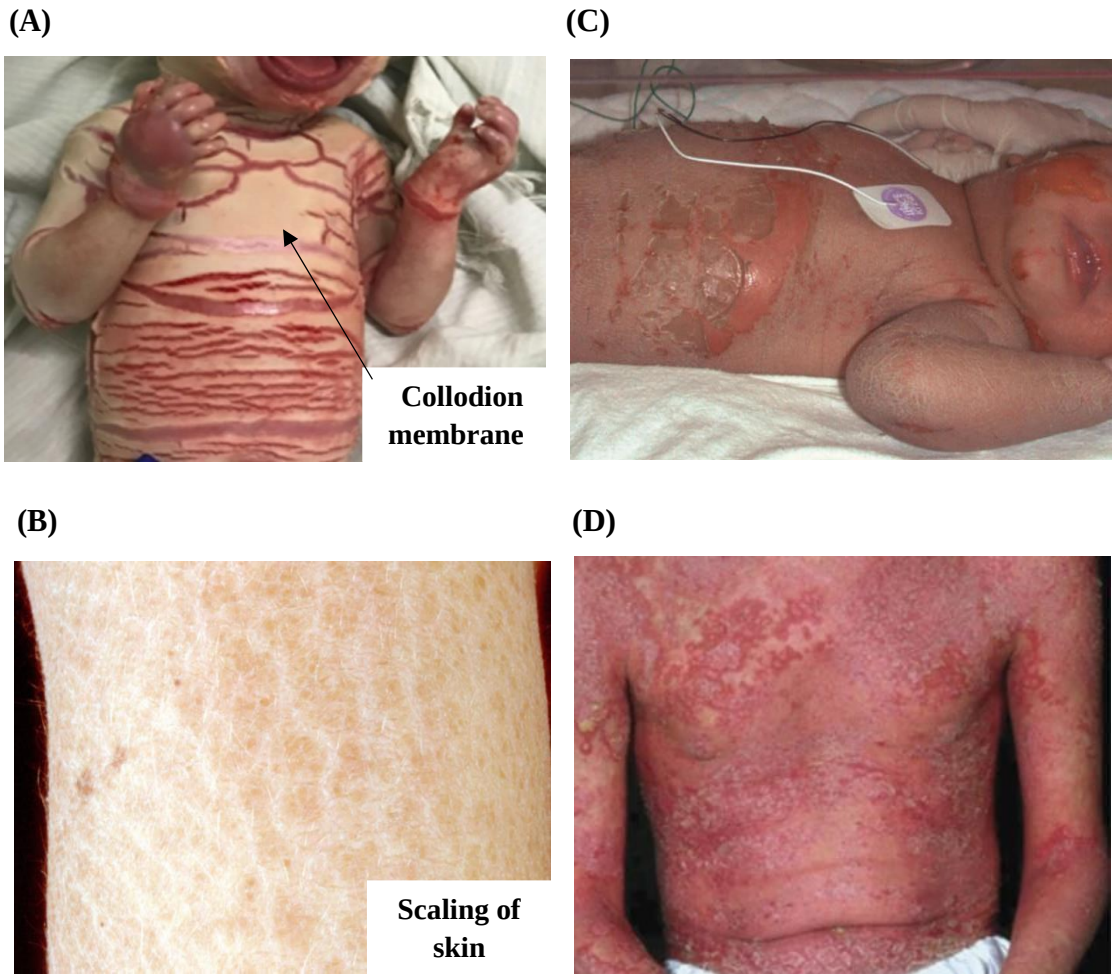

Figure 1.17 Examples of ARCI skin. Classic symptoms of harlequin ichthyosis include hyperkeratosis and thick plate like scales **(A)**. Non-bullous congenital ichthyosiform erythroderma characterised by dry, red soreness and white scaling of skin which are common symptoms **(B)**. Ichthyosis vulgaris is characterised by mild scaling with skin becoming dry and rough (**C**). X-linked ichthyosis again shows scaling found in the torso area (**D)** (Images obtained and adapted from Schmuth et al., 2012 and Shruthi et al., 2017).

Whilst previous types of ichthyosis described are associated with children, adults can also develop a type of ichthyosis known as acquired ichthyosis which has been shown to be linked with other medical conditions such as kidney disease, Hodgkin lymphoma and underactive thyroid (Mishra et al., 2018). Current practise of treating ichthyosis includes the use of emollients that contain lactic acid, urea, various alpha hydroxyl acids or propylene glycol. Additionally, keratolytic agents have been utilised for the treatment of ichthyosis due to its descaling properties (Steensel, 2007; Elias et al., 2010). Acitretin, isotretinoin and alitretinoin are examples of oral retinoids that are used for the treatment of more severe cases of ichthyosis (Vahlquist et al., 2008; Werchau et al., 2011). Patients with ichthyosis often develop infections from the condition and are often prescribed antibiotics and antiseptic

creams. Whilst steroid creams are used for the treatment of other skin disorders such as psoriasis, they are deemed ineffective for the treatment of ichthyosis. No complete cure exists for ichthyosis and current treatments lack adequate efficacy and have the possible risk of side effects. Furthermore, they are treatments that are ultimately used to generate an effective epidermal barrier that would normally be present in healthy skin. A better understanding of the biochemical mechanisms of this skin disorder may pave the way for better and more effective treatment of ichthyosis.

Understanding molecular mechanisms and pathways of these skin disorders may yield a different approach for their treatment instead of novel futuristic and challenging treatments such as gene therapy. Many disorders result due to a deficiency of a specific mechanistic or pathway product. As such, investigations into metabolic products may provide a productive approach for the treatment of disorders such as ichthyosis.

1.2.11 Peroxisome proliferator-activated receptors (PPARs)

Peroxisome proliferator-activated receptors (PPARs) are a superfamily of nuclear hormone receptors implicated in a wide range of diseases due to their involvement in regulating important cellular functions. These ligand-activated transcriptional factors are found in most tissues and are subdivided into three subtypes, PPARα, PPARγ and PPARδ, all of which are expressed in human keratinocytes (Westergaard et al., 2001; Tyagi et al., 2011). PPARs have become a molecular target due to their hypothesised roles in regulating a variety of important biological processes as shown in **Table 1.2**.

Physiological roles of PPARs		
PPARα	**PPARβ/δ**	**PPARγ**
Lipid catabolism	Insulin sensitivity	Adipocyte differentiation
Regulation of inflammatory processes	Glucose homeostasis	Glucose homeostasis
Stimulate fatty acid oxidation	Vascular integrity	Fatty acid oxidation
Fatty acid uptake		Fatty acid uptake and storage

Table 1.2 Physiological roles of each respective PPAR. (Grygiel-Górniak, 2014).

Ligands known to activate PPAR include natural lipid derived substrates and chemically synthesised compounds. PPARs are known to interact with fatty acids such as eicosapentaenoic acid and docosohexaenoic acid which are used in the treatment of metabolic and cardiovascular disease (Bang and Dyberg, 1985). Interaction of ligands with the PPAR receptor results in its translocation to the nucleus, where its structure is altered and consequently regulates the expression of a variety of genes (Rogue et al., 2011). Following their activation, a range of key biological processes is mediated through promoting or repressing genes. For example, the activation of PPARα results in the decrease of triglyceride levels through regulating the transcription of genes implicated in fatty acid metabolism such as lipoprotein lipase, thus, promoting the clearance of unwanted triglyceride (Kersten, 2008). The activation of PPARδ increases fatty acid metabolism via peroxisome proliferator-activated receptor gamma coactivator 1a (PPARγc1α), whilst PPARγ enhances glucose metabolism through upregulating the expression of fatty acid and glucose metabolism genes respectively (Picard and Auwerx, 2002; Kleiner et al., 2009).

In relation to their structure, PPARs are three dimensional proteins consisting of a DNA binding domain and the important ligand binding domain located in the C-terminus (Zoete et al., 2007). Interaction and subsequent binding of ligands to the PPAR nuclear receptor results in a heterodimer formation with another nuclear receptor known as retinoid X receptor (RXR). Specific DNA sequences of genes which bind to PPAR are known as peroxisome proliferator hormone response elements (PPREs) as shown in **Figure 1.18**.

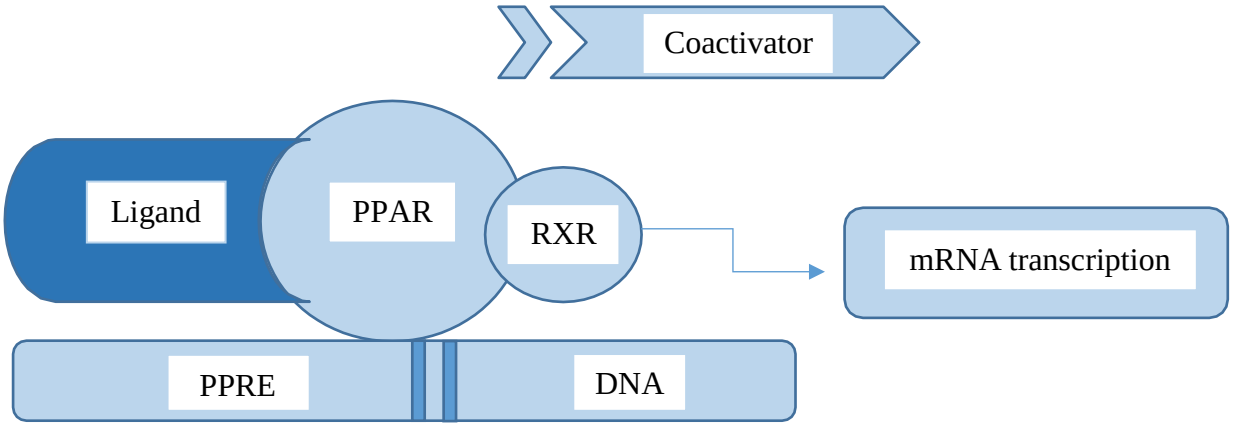

Figure 1.18 Schematic representation of mechanism by which PPARs regulate gene transcription. (Image adapted from Grygiel-Górniak, 2014). **PPAR** = Peroxisome proliferator-activated receptor, **RXR** = Retinoid X receptor, **PPRE** = PPAR response element, **DNA** = Deoxyribonucleic acid.

Moreover, PPAR coactivators also interact with PPAR, permitting the interaction of the PPAR protein with other genes. An example of PPAR coactivators include PPARγc1α and PPARγc1b which interact with the PPARγ nuclear hormone receptor. The PPARγc1α binds to the PPARγ/RXRα heterodimer complex, which in turn can regulate the activity of transcription factors such as the nuclear respiratory factors (NRFs) and estrogen related receptor alpha (Scarpulla, 2002; Taherzadeh-Fard et al., 2011). The function of PPARs is altered in the presence of coactivators via promotion or inhibition of their biological function (Viswakarma et al., 2010). As aforementioned, PPARs encompass three isoforms which differ in relation to biological characteristics such as tissue specificity, physiological roles and ligand specificity (Willson et al., 2000). Once activated by respective ligands, each specific PPAR can stimulate or suppress the expression of various genes that are implicated in lipid homeostasis or energy metabolism for example (Sertznig et al., 2007).

1.2.11.1 Peroxisome proliferator-activated receptor α (PPARα)

Multiple cell types show expression of PPARα which includes hepatocytes, macrophages, endothelial and epithelial cells (Moreno et al., 2004). An essential role of PPARα in human physiology includes providing energy for the normal functioning of peripheral tissues through effective fatty acid oxidation (Lefebvre et al., 2006). Both *in vivo* and *in vitro* studies have shown evidence of PPARα involvement in lipid metabolism (Berger et al., 2005; Jay and Ren, 2007). Natural ligands for PPARα include omega-3 fatty acid derived metabolites that may

include endogenous and synthetic fatty acid compounds (Willson et al., 2000; Bouwens et al., 2007). The nature of the fatty acid structure allows high affinity binding to the PPAR receptor (Sheu et al., 2004). Moreover, omega-3 fatty acids undergo oxidation by various enzymes which in turn produces metabolites which activate PPARs. Interestingly, chemokine expression mechanism studies have shown that oxidised omega-3 fatty acids inhibit NF-κB activation significantly more than unoxidised polyunsaturated fatty acids through the PPARα pathway, suggesting that the enzymatic oxidation of fatty acids can produce a more effective PPARα stimulator (Mishra et al., 2004). Synthetic ligands can also stimulate PPARα and include a class of carboxylic acids known as fibrates. The clinical implication of this binding is a lowering of lipoproteins in the bloodstream as a result of PPARα regulation of the expression of lipoprotein lipase enzymes associated with hypertriglyceridemia (Neschen et al., 2007; Grygiel-Górniak, 2014). In relation to a clinical outcome, the activation of PPARα by clenofibrate, bezafibrate and fenofibrate has shown a decreasing effect on dyslipidaemia through regulating genes which encode hepatic proteins implicated in lipid catabolism. Activation of PPARα by the aforementioned fibrates has been shown to upregulate ABCA1, a known cholesterol transporter, and in turn aiding the facilitation of cholesterol to the liver (Akiyama et al., 2005).

1.2.11.2 Peroxisome proliferator-activated receptors β/δ (PPARβ/δ)

PPARβ/δ is shown to be ubiquitously expressed in majority of tissues such as in the lungs, brain and skin (Girroir et al., 2008). Like PPARα, the PPARδ nuclear receptor is also implicated in lipid metabolism which includes fatty acid oxidation and reducing inflammation through suppressing macrophages (Barish, 2006; Grygiel-Górniak, 2014). PPARδ is involved in changing lipid profiles which is shown to avert obesity development. Mice deficient in PPARδ fed a high fat diet demonstrated an increase in weight and led to obesity. Conversely, activation of PPARδ resulted in effective processing of lipids and thereby preventing obesity (Wang et al., 2003). Its function when activated includes suppressing inflammation and stimulating the processing of fatty acids (Barish et al., 2006). Ligands known to activate and possess high selectivity for the PPARδ nuclear hormone receptor include relatively novel synthetic ligands known as GW610742 and GW501516 (Graham et al., 2005; Nagasawa et al., 2006). Activation of PPARδ has been shown to be associated with a reduced build-up of arterial plaque, demonstrating the potential clinical benefit of its activation. Furthermore, *in vitro* studies have shown that PPARβ/δ activation in adipocytes results in the utilisation and oxidation of fatty acids (Wang et al., 2003). High expression and activation of PPARβ/δ is

linked with the development of colon, prostate and breast cancer and the molecular pathway in the development of these diseases involve the upregulation of COX-2 and excessive production and accumulation of PGE-2 as a result of AA activation of PPARβ/δ (Michalik et al., 2004; Stephen et al., 2004). PPARβ/δ also has a critical role in the initiation of keratinocyte inflammatory responses with its upregulation observed during skin injury through the stress-associated kinase cascade. Cytokines produced during skin inflammation secrete ligands specific to PPARβ/δ, thus allowing its activation and subsequently results in the regulation of apoptotic associated genes (Tan et al., 2001).

1.2.11.3 Peroxisome proliferator-activated receptors γ (PPARγ)

PPARγ expression is detected in a wide range of tissue, from the spleen and large intestine to adipose and skin tissue (Kliewer et al., 1997; Sertznig and Reichrath, 2011). Due to its involvement in macromolecule processing, PPARγ has become a molecular target for treatment of a range of diseases and disorders such as type 2 diabetes (Sarhangi et al., 2020). Its highest expression is found in the adipocytes, where its main role is in the regulation of key processes such as lipid and glucose metabolism. It has a role in regulating the transcriptional activity of genes involved in the release and storage of fatty acids which include fatty acid transporter CD36 and lipoprotein lipase (Lehrke et al., 2005; Medina-Gomez et al., 2007). The development of cancer cells is also regulated by PPARγ as demonstrated by the stimulating or inhibitory action of PPARγ agonists (Feige et al., 2005). Studies have shown the effect of PPARγ activation on tumor development and their role in weakening cancer cell proliferation (Theocharis et al., 2003).

One of the most widely used synthetic PPARγ agonists are a group of compounds known as thiazolidinediones (TZDs), whilst the most abundant natural modulators are fatty acids (Ma et al., 2015). **Figure 1.19** shows examples of drugs belonging to this class of heterocyclic compounds having high affinity for PPARγ that include rosiglitazone and pioglitazone which are used in the treatment of diabetes as they increase sensitivity to insulin (Dumasia et al., 2005). Once ligands such as TZDs and endogenous metabolites interact and bind to the receptor, the PPARs are shown to decrease levels of fatty acids and increased lipid storage capacity in adipose tissue through modulating the expression of genes such as apolipoprotein CII and CII. Both apolipoprotein CII and CII can induce and inhibit the activity of lipoprotein lipase which functions to reduce lipoproteins which are rich in triglyceride content (Deeg and Tan, 2008). The activation and subsequent expression of PPARγ is thought to be implicated in key biological processes such as adipocyte differentiation, energy

metabolism and fatty acid storage via a transcriptional cascade in which PPARγ is part of (Siersbaek et al., 2010). PPARγ has also been shown as a potential biological target for the treatment of diabetes through the high affinity binding of TZDs (Lehmann et al., 1995). Interestingly, ligand activation of PPARγ has been shown to stimulate the expression of proteins associated with lipid metabolism including lipoprotein lipase (LPL), acyl-CoA binding protein (ACBP), fatty acid binding protein 2 (aP2) and phosphoenolpyruvate carboxykinase (PEPCK) (Ferre et al., 2004). Additionally, PPARγ increases the expression of genes implicated in glucose homeostasis such as glucose transporter type 4 (Glut4), phosphoinositide 3 kinase (PI3K) and c-Cbl-associated protein (CAP) (Ahmadian et al., 2013).

Rosiglitazone

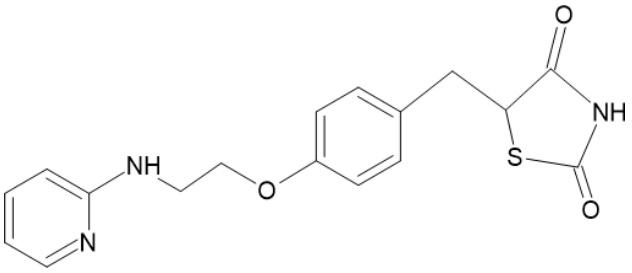

Troglitazone

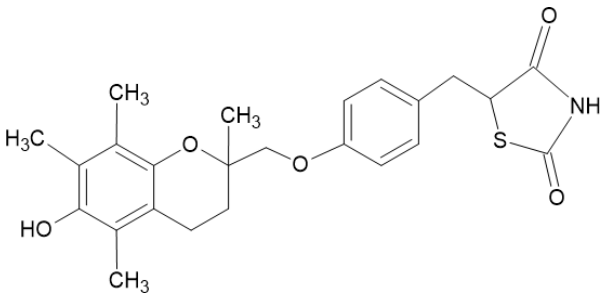

Pioglitazone

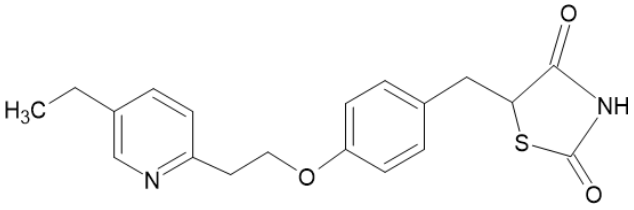

Prostaglandin A1

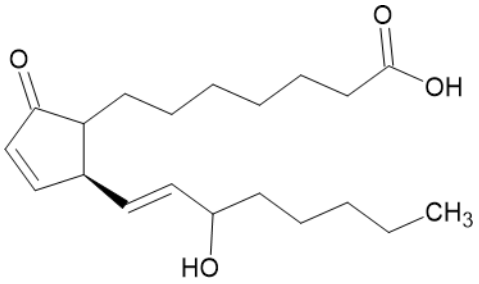

Figure 1.19 Chemical structures of PPAR ligands belonging to the thiazolidinediones (TZDs) family.

1.2.11.4 PPARs in skin homeostasis and disease

Studies using keratinocyte cell lines and ex vivo human skin have demonstrated critical roles for PPARs in maintaining skin homeostasis including, keratinocyte differentiation, proliferation, apoptosis and maturation of the epidermal barrier (Kömüves et al., 2000; Mao-Qiang et al., 2004; Sertznig et al., 2008). These processes are essential for the integrity of the epidermal barrier and PPARs have therefore been identified as molecular targets for the treatment of various skin barrier diseases including psoriasis, atopic dermatitis, skin malignancies and scleroderma (Sertznig and Reichrath, 2011). Experiments performed in rat skin explants revealed accelerated epidermal barrier formation following treatment with PPARα fatty acid ligands (Majewski et al., 2021). Moreover, studies involving a number of PPARα agonists has shown an enhanced barrier maturation as demonstrated by an increase in the expression of epidermal differentiation markers including involucrin, loricrin and profilaggrin-filaggrin, whilst a reduction in transepidermal water loss was also observed (Hanley et al., 1997; Kömüves et al., 2000). Hyperproliferation and impaired differentiation are characteristic phenotypes of skin disorders such as psoriasis and atopic dermatitis, with PPARα ligands having been reported to reduce cell proliferation and promote keratinocyte differentiation (Komuves et al., 1998).

Recent studies have also shown the ability of PPARδ agonists such as GW0742 to suppress keratinocyte proliferation and promote the expression of key mRNA differentiation markers including involucrin, small proline-rich proteins 1a (SPRR1a) and small proline-rich proteins 1h (SPRR1h) (Kim et al., 2005). PPARβ/δ knockout mice exhibited a decrease in the expression of differentiation markers and an increased rate of proliferation. Furthermore, investigations into PPARγ activation by TZDs such as ciglitazone and troglitazone revealed an enhanced expression of epidermal differentiation markers that include involucrin, loricrin and filaggrin (Mao-Qiang et al., 2004). Ligands specific for PPARβ/δ activation also show an increase in the expression of late differentiation markers such as loricrin and filaggrin, further suggesting the essential role of PPARs in promoting epidermal differentiation. Barrier disruption investigations have also been performed to determine whether PPAR agonists are able to restore barrier integrity following treatment with detergents and solvents. The application of the GW1514 PPARβ/δ agonist to mouse skin dramatically improved epidermal barrier function, whilst alleviating the effects of detergent and solvent exposure (Schmuth et al., 2004). Keratinocyte differentiation is also key in inducing changes in genes associated with lipid metabolism known to be essential in maintaining skin homeostasis.

The expression of PPARs is dependent on the stage of epidermal differentiation. For example, the expression of PPARγ and PPARα are associated with late-stage keratinocyte differentiation, whilst PPARβ/δ expression remains consistent through the various layers of the epidermis (Westergaard et al., 2001). To date, both PPARδ and PPARα agonists are shown to increase the expression of keratinocyte differentiation markers, whilst the effects of known PPARγ agonists such as prostaglandin J2 and BRL-49653 on epidermal differentiation is minimal (Rivier et al., 1998; Westergaard et al., 2001). The role of PPARs in maintaining skin homeostasis materialised from studies involving PPAR knockout mouse models (Michalik et al., 2002). Abnormal stratum corneum development and an ultra-thin granular layer is observed in the skin of PPARα deficient mice, suggesting a critical role for PPAR in epidermal homeostasis. Moreover, these defects occur in the outer layer of the epidermis, suggesting a perturbed keratinocyte differentiation process (Komuves et al., 2000). These observations form a strong argument in favour of PPARs participation in the development and homeostasis of the epidermis.

As PPARs are crucial for the development and homeostasis of healthy skin, they have become a target of interest for the treatment of various debilitating skin disorders. More specifically, these include epidermal disorders such as psoriasis which are characterised by hyperproliferation, impaired epidermal differentiation and inflammation. Studies investigating PPARs in skin disease have shown a range of differential expression profiles, from significant increase in PPAR expression to downregulation of the nuclear receptor hormone. For example, psoriatic lesional skin and induced inflammation of mouse skin showed a significant increase in PPARδ expression (Rivier et al., 1998; Tan et al., 2001). The reasoning behind an overexpression of PPARδ is yet to be fully elucidated, however, studies have determined the role of PPARδ in mediating an inflammatory response following a disrupted keratinocyte differentiation process (Tan et al., 2001). In contrast, the expression levels of PPARα and PPARγ are decreased or unaltered in the skin of psoriatic patients (Westergaard et al., 2003).

1.2.12 Possible roles of 12*R*-LOX and eLOX-3 products in the epidermis

There has been much speculation into the role of 12*R*-LOX derived lipids in the epidermis in recent times, from a signalling role to interacting and activating PPARs. The quantities of EOS ceramides is significantly low and is therefore unlikely that these lipids contribute to a structural role in the epidermis. It is possible that 12*R*-LOX oxygenated products may serve as signalling molecules and induce specific biological processes required for the formation and

function of the epidermal permeability barrier (Muñoz-Garcia et al., 2013). Various interactions with a plasma membrane receptor such as ichthyin have been proposed (Lefévre et al., 2004). The ichthyin receptor interacts and binds with a protein known as FATP4 which is responsible for integrating fatty acids into keratinocytes (Li et al., 2013). On the other hand, the production of oxidised products from 12*R*-LOX enzymatic activity may interact and activate PPARs in the epidermis. PPAR activation studies have already shown that oxygenated metabolites and products of AA activates the PPARα subtype (Yu et al., 1995).

1.3 Study background

In healthy skin, an effective permeability barrier prevents the rapid loss of water and pathogen ingress from and into our bodies respectively. Disrupted epidermal barrier occurs in skin disorders such as ichthyosis which increases the risk of infection. Key in maintaining the integrity of the epidermal barrier and regulating homeostasis is the presence of lipid molecules including ceramides and cholesterol. Synthesis of oxidised lipids in the epidermis is in part a result of the enzymes 12*R*-LOX and eLOX-3. As discussed, mutations in these enzymes results in the development of a scaly skin disorder known as ichthyosis (Yu et al., 2005; Moran et al., 2007). Furthermore, 12*R*-LOX deficient mice die shortly after birth and display an altered lipid composition, highlighting the importance of the 12*R*-LOX pathway in skin physiology (Epp et al., 2007). The exact biochemical pathway and molecular mechanisms by which 12*R*-LOX lipids regulates skin physiology and their role in disease is currently unknown.

Whilst it has been established that LOX enzymes are required for the maintenance of the epidermal permeability barrier and its full functioning in preventing water loss and infection, the role of LOX-derived lipids in regulating skin physiology and in diseases such as ichthyosis is unknown. It is yet to be determined whether these lipids metabolised by LOX provide structural support, signalling to other cells via activation of transcriptional factors such as PPARs within the epidermis or restoring barrier integrity after damage. Interestingly, PPARs are implicated in proliferation, differentiation, wound healing and lipid metabolism (Hanley et al., 1998; Komuves et al., 2000; Mao-Qiang et al., 2004). Furthermore, inhibition of LOX by MK886 has been shown to downregulate all PPAR isoforms and studies have confirmed the activation of PPARα by the 8R-hydroxy-11R,12R-epoxyeicosa-5Z,9E,14Z-trienoic acid product of the epidermal lipoxygenase pathway (Kehrer et al., 2001).

Novel molecular profiling techniques such as RNA-sequencing of the 12*R*-LOX deficient mice transcriptome will be utilised to identify key transcriptional regulators and a series of genes that may be involved in regulating important epidermal processes. The

identification of key epidermal processes and transcriptional regulators would permit further investigation into the role of 12*R*-LOX lipids through utilising human skin cell culture models. The addition of 12*R*-LOX lipids following *in vitro* silencing of the *ALOX12B* gene would further aid in establishing the transcriptional networks by which 12*R*-LOX regulate skin homeostasis.

1.4 Hypothesis

It is hypothesised that 12*R*-LOX / eLOX-3 derived lipids play a role in maintaining skin health and preventing disease through modulating important biological processes in the epidermis. These specific LOX products may be involved in regulating key epidermal processes such as keratinocyte differentiation, proliferation or interacting with transcriptional regulators.

1.5 Aim

The aim of this study is to define the role of 12*R*-LOX / eLOX-3 derived lipids such as the 9R,10R,13R-TriHOME in epidermal homeostasis and disease.

1.6 Objectives

- Explore the molecular mechanisms and pathways by which 12*R*-LOX regulates skin physiology through utilising bioinformatics platforms.
- Identify biological processes and transcriptional factor involvement.
- Characterise and identify gene clusters of interest impacted following 12*R*-LOX silencing.
- Evaluate the epidermal localisation of differentially expressed genes following 12*R*-LOX silencing.
- Evaluate whether 12*R*-LOX derived lipids promote key epidermal processes including keratinocyte proliferation, differentiation, migration and apoptosis through utilising molecular biology techniques such as western blotting.
- Characterise the effect of 12*R*-LOX derived lipids on PPARs using gene reporter assays.

Chapter 2

General materials and methods

2.1 Cell culture

2.1.1 Materials for HaCaT cell culture

All reagents were purchased from Thermo Fisher Scientific, UK unless otherwise stated. The immortalized HaCaT keratinocyte cell line was obtained from the School of Pharmacy and Pharmaceutical Sciences, Cardiff University and was characterised by Ahmad Moukachar as described in Moukachar, 2021. Free calcium Dulbecco's Modified Eagles Medium (DMEM), fetal bovine serum (FBS) (Biowest #S1810-500), penicillin-streptomycin-glutamine 100x (PSG) (#10378016), trypsin-EDTA (0.25%) (#25200056), chelex 100 molecular biology grade resin (Biorad, UK #1421253), calcium and magnesium free Dulbecco's Phosphate Buffered Saline (DPBS) (#14190144) and T75 cm^2 flasks (VWR, UK #734-2313) were all the reagents used in the culture of the HaCaTcell line.

2.1.2 Culture of the HaCaT keratinocyte cell line

HaCaT cells were cultured in a calcium free DMEM that included 10% FBS, 1% PSG 100x. The calcium contained within the FBS was removed with a chelator complex for 1 hour at 4ºC. HaCaT cells were treated independently with calcium chloride ($CaCl_2$) to achieve final calcium (Ca^{2+}) concentrations of 0.03 mM, 1.8 mM and 2.8 mM to induce the proliferative and differentiated phenotypes of the epidermis. The cells were incubated in a humidified atmosphere at 37ºC and at 5% CO_2. The culture medium was renewed every 2-3 days to provide a fresh source of nutrients to cells. Cells were passaged by removing the old medium, washing twice with calcium and magnesium free DPBS and then incubating with 1x trypsin-EDTA (0.25%) at 37 ºC for 5 minutes to detach cells. Inactivation of the trypsin was performed using growth medium before seeding cells into T75 cm^2 flasks at the desired cell density.

2.1.3 Materials for hTERT immortalized human keratinocyte cell culture

All reagents were purchased from Thermo Fisher Scientific, UK unless otherwise stated. The hTERT immortalized human keratinocyte cell line Ker-CT (ATCC CRL-4048TM), KGM™ Gold Keratinocyte Growth Medium BulletKit™ (1 vial with 0.50 mL hydrocortisone, 1 vial with 0.50 mL transferrin, 1 vial with 0.25 mL epinephrine, 1 vial with 0.50 mL GA-1000, 1 vial with 2.00 mL BPE, 1 vial with 0.50 mL hEGF, 1 vial with 0.50 mL insulin and 0.1 mM $CaCl_2$) (Lonza, UK #00192060), trypsin-EDTA (0.05%), calcium and magnesium free DPBS and T75 cm^2 flasks (VWR, UK #734-2313) were all the reagents used in the culture of the hTERT immortalized human keratinocyte cell line.

2.1.4 Culture of the hTERT immortalized human keratinocyte cell line

The hTERT immortalized human keratinocyte cell line were cultured in KGM™ Gold Keratinocyte Growth Medium BulletKit™. hTERT cells were incubated in a humidified atmosphere at 37ºC and at 5% CO_2 to achieve the desired confluence. The culture medium was renewed every two days to provide a fresh source of nutrients to cells. Cells were passaged by removing the old medium, washing twice with calcium and magnesium free DPBS and then incubating with 1x trypsin-EDTA (0.05%) at 37 ºC for 5 minutes to detach cells. Inactivation of the trypsin was performed using 1% FBS before seeding cells into T75 cm^2 flasks at the desired cell density.

2.1.5 Assessment of shape and morphology of cells

The shape and morphology of the HaCaT keratinocyte cell line and hTERT immortalized human keratinocyte cell line was analysed daily by inverted phase contrast microscopy (Olympus BX50 fluorescence microscope). Images were captured at 10x magnification using the inverted phase contrast microscopy equipped with a Nikon digital camera at the desired timepoints and intervals.

2.1.6 Materials for A549 cell culture

All reagents were purchased from Thermo Fisher Scientific, UK unless otherwise stated. The A549 cancer cell line and Ham's F-12K medium supplemented with 2 mM L-glutamine was generously gifted by Professor Arwyn Jones and Jared Whitehead, PhD student (School of Pharmacy and Pharmaceutical Sciences, Cardiff University). Fetal bovine serum (FBS) (Biowest #S1810-500), penicillin-streptomycin-glutamine 100x (Pen-Strep) (#10378016), trypsin-EDTA (0.25%) (#25200056), calcium and magnesium free DPBS (#14190144) and T75 cm^2 flasks (VWR, UK #734-2313) were all the reagents used in the culture of the A549 cancer cell line.

2.1.7 A549 cancer cell culture

The A549 cancer cell line were cultured in Ham's F-12K medium supplemented with 2 mM L-glutamine, 10% FBS and 1% penicillin-streptomycin-glutamine 100x. A549 cells were incubated in a humidified atmosphere at 37ºC and at 5% CO_2 to achieve the desired confluence. The culture medium was renewed every 2 days to provide a fresh source of nutrients to cells. Cells were passaged by removing the old medium, washing twice with calcium and magnesium free DPBS and then incubating with 1x trypsin-EDTA (0.25%) at 37ºC for 5 minutes to detach

cells. Inactivation of the trypsin was performed using growth medium before seeding cells into T75 cm^2 flasks at the desired cell density.

2.2 Skin sample for western blot

Human skin samples used for the positive control in western blot experiments were obtained from female patients that had undergone mastectomy or breast reduction surgery at the Royal Gwent Hospital, Newport, UK. Informed patient consent and local ethical committee approved its use for experiments at the School of Pharmacy and Pharmaceutical Sciences, Cardiff University (Cardiff University – Code of practice for human tissue research) (CU/13/HTA14/5.0). Following surgery, the skin samples were transferred in DMEM and 1% penicillin/streptomycin at 4ºC. Once arrived at the laboratory, the underlying subcutaneous fat was removed using a scalpel. The remaining skin sample was placed into a beaker containing PBS and placed on a heating mantle at 90ºC for 10 minutes until the epidermis could be peeled from the dermis using tweezers. The peeled epidermis layer was then homogenised in 10 ml of radioimmunoprecipitation (RIPA) lysis buffer containing Mini protease and phosphatase inhibitor cocktails. Protein extraction procedure in **Section 2.3** was then performed.

2.3 Protein extraction and quantification

Cells were washed with ice-cold PBS and a RIPA lysis buffer (50 mM Tris-HCl (pH 8.0), 5 mM EDTA, 0.1% SDS, 150 mM NaCl, 1.0% Triton-X, 0.5% sodium deoxycholate) was used to lyse cells at 4ºC for 30 minutes. The RIPA lysis buffer also consisted of Mini protease and phosphatase inhibitor cocktails (Sigma Aldrich, UK #11836153001). Samples were left on ice for 30 minutes and then sonicated (5x for 5 seconds), followed by centrifugation at 13.000 rpm for 10 minutes at 4ºC and the supernatant collected. Samples that were not used immediately were frozen at -80ºC. The soluble protein extracts were then quantified through using the Pierce™ Coomassie (Bradford) Protein Assay Kit as per manufacturer's instructions (Thermo Fisher Scientific, UK #23200).

2.4 Western blot analysis

All reagents were purchased from Thermo Fisher Scientific, UK unless otherwise stated. Protein lysates were denatured for 10 minutes at 100 ºC and variable protein quantities (20-50 μg) was separated on a Novex™ WedgeWell™ 10% Tris-Glycine, 1.0 mm, mini protein gel (#XP04120BOX) and transferred to either a nitrocellulose transfer membrane, 0.45 µm *(*#77010*)* or a polyvinylidenedifluoride transfer membrane, 0.45 µm (PVDF) (#88585) for 1 h at 25V, using transfer buffer (25 mM TrisHCl, 190 mM glycine, 20% methanol, and 0.05%

SDS). To confirm successful transfer, the membrane was soaked in Ponceau S (#BP103-10) for a few seconds and then washed with deionised water. The membrane was blocked in blocking buffer (PBS that contained 0.05% Tween and 5% powdered non-fat milk, pH 7.4) at room temperature (RT) for 1 hour. After blocking, membranes were blotted at RT for 2 hours with various primary antibody dilutions (specific antibodies and dilutions shown in respective chapters). The membranes were then washed 3 times with PBS-0.25% Tween and incubated for 2 hours at RT with horseradish peroxidase-linked secondary antibodies. The blots were developed using Pierce^{TM} ECL Western Blotting Substrate (#32209) through following the manufacturer's protocol. Protein bands were detected using chemiluminescence using the G:BOX Chemi XX6/XX9 detection system. β-actin was used to normalize the levels of protein detected. Western blot densitometry band quantification was performed using ImageJ analysis software.

2.5 RNA-Sequencing study

2.5.1 Generation of 12*R*-LOX deficient mouse models

Generation of the 12*R*-LOX deficient (n=6) and wild-type (n=3) mouse models were performed by Angela Dick from the Department of Paediatrics, University of Erlangen-Nürnberg, Germany and were kindly donated for the RNA-sequencing experiment. As the *Alox12b* gene encodes for the 12*R*-LOX protein, this specific gene was targeted using the Cre-*loxP* system. The mechanism by which deletion of the *Alox12b* gene was performed is as follows; Intron 7 and exon 8 of the *Alox12b* gene is targeted using a vector possessing *loxP* sites. Electroporation of the vector consisting of the *loxP* sites into embryonic stem cells was performed. Two embryonic stem cells possessed the alleles required to produce chimeric mouse strains. Cre engineered mice were mated with mice possessing the *Alox12b* gene flanked by *loxP* sites. The generated heterozygous *Alox12b*$^{+/-}$ mice were bred with each other to produce homozygous *Alox12b* knockout mice (Epp et al., 2007). The mice used in the RNA-sequencing study were culled immediately after birth.

2.5.2 Validating the 12*R*-LOX deficient mouse models

Validation of 12*R*-LOX protein deficiency was also performed at the Department of Paediatrics, University of Erlangen-Nürnberg, Germany. This was confirmed by RT-PCR and western blotting and the 12*R*-LOX deficient mouse models were shipped over in dry ice to the School of Pharmacy and Pharmaceutical Sciences, Cardiff University, UK.

2.5.3 Isolation of skin and total RNA extraction

An incision was made dorsally using a scalpel and the entire skin peeled from all mice. The skin tissue of all samples were then weighed (range - 43-45 mg) and transferred into a new RNAase free tube. Ice cold TRIzol reagent (Thermo Fisher Scientific, UK #15596026) was added (1 ml) and each mouse skin tissue was subsequently homogenized using the bead ruptor elite (Cole-Parmer-UK). Each tube was then placed in ice to cool, followed by agitation at RT for 5 minutes. Tissue homogenate was then treated with 1-bromo-3-chloropropane (0.2 ml), vortexed and centrifuged at 10,000g for 15 minutes at 40ºC giving a three phase solution (bottom trizol phase containing proteins, interphase containing DNA and top aqueous phase containing RNA). The aqueous phase was treated with solution B (0.7 ml isopropanol + 0.25 ml sodium acetate, pH 3-4) and then vortexed. The samples were then centrifuged at 5000g at 40ºC for 10 minutes to pellet the RNA. After removal of solution B, the pellet was washed with 70% ethanol and re-centrifuged. The ethanol was removed and the pellet left to air-dry at RT for 5 minutes. The RNA pellet was then diluted in RNAase free water (50µl) and column clean-up was performed using the RNeasy Mini kit (Qiagen) per manufacturer's instructions.

2.5.4 Experimental design of the RNA-sequencing study

RNA sequencing analysis was performed at Wales Gene Park on the Next Generation Sequencing (NGS) Illumina HiSeq 2500 platform. A cDNA library was also constructed using PCR amplification at Wales Gene Park. The exact length of RNA fragments from each sample was detected by the Agilent 2100 Bioanalyzer Instrument (Agilent, USA). Low quality reads or Adapters were filtered in the process using the Perl Script programming. The design of this experiment follows the ENCODE "Guidelines and best practice for RNAseq quantification". This includes at least three biological replicates per condition, sequencing to a depth of 20-25 million mapped reads per replicate of each condition, generating 50bp paired-end reads. The pipeline employed in this study for gene discovery and expression analysis involves the TopHat and Cufflinks bioinformatics software platforms undertaken by Dr Robert Andrews (Institute of Infection & Immunity, Cardiff University). The TopHat analysis platform allows the reads from the RNA sequencing to be aligned with a reference genome which is the wildtype control in this study. Cufflinks analysis on the other hand will collect all reads generated and convert into possible transcripts, yielding a final transcriptome reading. Through both TopHat and cufflinks analysis, gene expression levels can be generated, that is, fragments per kilobase of gene model per million mapped reads (FPKM). As a result, differential gene expression analysis can be performed.

2.5.5 Differentially expressed gene analysis (DEG)

To identify DEG's, the R package DESeq2 was performed using the raw gene counts and the data normalized. DESeq2, a statistical tool package, generates the differential gene expression through a negative binomial distribution (Love et al., 2014). To determine differentially expressed genes that are of significance, a t-test was conducted which in turn produces *p* values for each respective gene in the dataset. Statistically significant DEGs was defined as a *p* value of < 0.05 included genes with a ≤ -1.5 and ≥ 1.5-fold change (FC).

2.5.6 Sequence annotation

Investigations on DEG's of interest (FC, ≤ -1.5 and ≥ 1.5) were compared against protein / bioinformatics databases such as (https://www.genecards.org/), (https://jax.org/), National Centre for Biotechnology Information (NCBI), the Swiss-Prot database, the non-redundant protein (Nr) database and the scientific and medical literature available.

Chapter 3

Investigation of 12*R*-LOX expression in the HaCaT and hTERT cell lines

3.1 Introduction

Primary human keratinocytes are frequently utilised for investigating keratinocyte function, however, a constant supplementation of growth factors are required for their survival and they are also observed to have a reduced *in vitro* life span, preventing long term investigative studies (Schurer et al., 1993). Furthermore, primary human keratinocytes undergo cell death once differentiation has been induced and are therefore unsuitable for long term investigative studies. Variable growth rates have been observed in human primary keratinocytes when comparing donor to donor, resulting in complex interpretation of experimental data and expression of proliferative and differentiation markers are altered following several passages of primary human keratinocytes (Colombo et al., 2017). Additionally, purchase of human primary keratinocytes from commercial suppliers is costly and a large quantity of primary epidermal cells are required to create a 3D skin model for study of skin physiology and disease (Smits et al., 2017).

Due to various drawbacks associated with primary human keratinocytes, the HaCaT cell line is often preferred and chosen as the *in vitro* model for the study of human skin keratinocytes function in skin physiology and disease (Seo et al., 2012). The HaCaT cell line is a spontaneously immortalized, monoclonal cell line, modified for long term growth in culture, without the constant supplementation of growth factors and nutrients (Schurer et al., 1993). Moreover, HaCaT cells display identical shape and morphology to human keratinocytes, along with expressing specific protein markers known to be associated with human keratinocytes including both proliferative and differentiation markers such as keratin 10 and involucrin respectively (Micallef et al., 2009). An advantage of utilising HaCaT cells is their ability to revert back and forth between a proliferative and differentiated state following alterations in calcium concentration and cell contact inhibition, while studies have shown that HaCaT cells are able to reconstruct an epidermal structure following *in vivo* transplantation (Garach-Jehoshua et al., 1998; Deyrieux and Wilson 2007; Smits et al., 2017).

Whilst certain proteins known to be expressed in human keratinocytes are also found to be expressed in HaCaT cells, expression profiles of proteins such as filaggrin and loricrin are dissimilar in comparison with primary human keratinocytes (Boukamp et al., 1988). Furthermore, irregular stratification of the epidermis is observed in the HaCaT cell line models in comparison with human keratinocytes, along with abnormal expression of epidermal differentiation markers. It has also been reported that growth of HaCaT cells in culture does not form a stratum corneum as would be observed in primary keratinocytes (Smits et al., 2017).

A recently developed immortalized cell line known as human telomerase reverse transcriptase (hTERT) primary keratinocyte cell line combines the native features and characteristics of primary keratinocytes with the immortalized cell line quality of surviving multiple passages in culture. This specific cell line has provided a breakthrough in the study of epidermal biology and has been created through transducing the human telomerase reverse transcriptase gene into human primary keratinocytes and through deletion of the pRB/$p16^{INK4a}$ pathway (Dickson et al., 2000). The hTERT cell line shows extended proliferative and differentiation features associated with human keratinocytes and has been extensively used in epidermal biology investigations. For example, mRNA and protein expression of epidermal differentiation markers such as loricrin, keratins 1 and 14 and filaggrin have been investigated using the hTERT cell line and compared with human primary keratinocytes (Smits et al., 2017). Moreover, hTERT cells exhibit normal epidermal barrier permeability, form a stratified epidermal layer observed in human primary keratinocytes and display a comparable epidermal morphology to primary keratinocytes (Smits et al., 2017). The lipid composition and ultrastructural characteristics of hTERT cells is highly comparable to that of primary human keratinocytes, suggesting that the hTERT cell line is a biologically relevant model for epidermal biology studies.

3.2 Aims

- Generation and characterisation of phenotypically different hTERT keratinocyte cell line to determine expression of 12*R*-LOX in proliferative or differentiated state.
- Investigate whether the 12*R*-LOX protein is expressed in both HaCaT and hTERT cell lines.

3.3 Objectives

- Evaluate the expression of proliferative (keratin 5) and differentiation (involucrin) markers following collection of cells at 30% and 100% confluence.
- Explore whether cell confluence and calcium (Ca^{2+}) concentration has an influence on the detection of the 12*R*-LOX protein.
- Investigate whether 12*R*-LOX lipid products are present in hTERT cells.

3.4 Materials and methods

Materials, equipment and routine cell culture of the HaCaT keratinocyte cell line and hTERT immortalized human keratinocyte cell line are described in **Section 2.1.1, 2.1.2**, **2.1.3** and **2.1.4** respectively.

3.4.1 Cell culture

3.4.1.1 Culturing of the HaCaT keratinocyte cell line to induce proliferative and differentiated epidermal phenotypes

HaCaT keratinocyte cells were seeded at a density of 500,000 cells into a T75 cm^2 flask containing DMEM culture media. HaCaT keratinocyte cells were cultured for a total of 8 hours in DMEM media consisting of 0.03 mM Ca^{2+} concentration to induce a proliferative phenotype found in the epidermis, a total of 24 hours in DMEM media consisting of 1.8 mM Ca^{2+} concentration to induce a middle differentiated layer phenotype found in the epidermis and a total of 48 hours in DMEM media consisting of 2.8 mM Ca^{2+} concentration to induce the most differentiated layer phenotype found in the epidermis.

3.4.1.2 Culturing of the hTERT keratinocyte cell line to induce proliferative and differentiated epidermal phenotypes

hTERT immortalized keratinocyte cells were seeded at a density of 500,000 cells into a T75 cm^2 flask containing KGM™ Gold Keratinocyte Growth Medium BulletKit™. The KGM™ Gold Keratinocyte Growth Medium BulletKit™ used to culture hTERT immortalized keratinocyte cells already contains a 0.1 mM Ca^{2+} concentration which is the approximate Ca^{2+} concentration in proliferative to early differentiated layers of the epidermis. A higher Ca^{2+} concentration of 1.8 mM and 2.8 mM was used in HaCaT cells to induce a differentiated state, however, it is unknown as to whether a 0.1 mM Ca^{2+} concentration can induce significantly differentiated layers of the epidermis. To overcome this, allowing cells to reach a higher confluence is known to induce keratinocyte differentiation (Borowiec et al., 2013).

To induce the proliferative layer of the epidermis, hTERT immortalized keratinocyte cells were cultured in KGM™ Gold Keratinocyte Growth Medium BulletKit™ for a total of 6 hours to achieve 30% cell confluence. To induce differentiated layer of the epidermis, hTERT immortalized keratinocyte cells were cultured in KGM™ Gold Keratinocyte Growth Medium BulletKit™ for a total of 48 hours to achieve a 100% cell confluence.

3.4.1.3 Analysis of shape and morphology of the HaCaT and hTERT keratinocyte cell lines

Shape and morphological analysis of the HaCaT keratinocyte cell line and hTERT immortalized human keratinocyte cell line are described in **Section 2.1.5**.

3.4.2 Protein extraction and quantification of HaCaT and hTERT keratinocyte cells

HaCaT keratinocyte cells cultured in 0.03 mM, 1.8 mM and 2.8 mM Ca^{2+} concentrations were harvested once cells reached a proliferative or differentiated phenotype. hTERT immortalized keratinocyte cells were harvested after reaching a 30% and 100% confluence respectively. Protein extraction and quantification of HaCaT keratinocyte cells and hTERT immortalized keratinocyte cells is described in **Section 2.2**.

3.4.3 Antibodies used for investigating 12*R*-LOX, keratin 5 and involucrin expression

Two different primary antibodies raised against 12*R*-LOX were used in investigating 12*R*-LOX presence in HaCaT keratinocyte cells and hTERT immortalized keratinocyte cells. These include a primary mouse polyclonal IgG anti-12*R*-LOX (1:500) (Fisher Scientific, UK #89-004-014) and a primary mouse monoclonal IgG anti-12*R*-LOX (1:100 and 1:500) kindly received from Dr Peter Krieg at the German Cancer Research Center, Heidelberg, Germany. Other primary antibodies used in this chapter include rabbit monoclonal IgG recombinant anti-cytokeratin 5 (1:1000) (Abcam, UK #ab52635), rabbit polyclonal IgG anti-involucrin (1:500) (Abcam, UK #53112) and rabbit polyclonal IgG anti-β-actin (1:1000) (Abcam, UK #ab8227). Secondary antibodies used were goat anti-mouse IgG (HRP) (1:3000) (Abcam, UK #ab97023) and goat anti-rabbit IgG (HRP) (1:2000) (Abcam, UK #ab6721).

3.4.4 Western blot analysis for the detection of 12*R*-LOX

The western blot protocol for investigating 12*R*-LOX protein expression in HaCaT keratinocyte cells and hTERT immortalized keratinocyte cells is described in **Section 2.3**.

3.4.5 Lipid extraction of HaCaT and hTERT keratinocyte cells

Both HaCaT keratinocyte cells and hTERT immortalized keratinocyte cells were harvested at the desired confluence (4 million cells) and centrifuged at 1000 g for 5 minutes at 4ºC. Cells were washed with ice-cold PBS, homogenized with chloroform/methanol (1:1 v/v) and transferred to glass vials. Extraction of lipids from HaCaT keratinocyte cells and hTERT immortalized keratinocyte cells was done following the Bligh and Dyer method (Bligh and

Dyer, 1959). The aqueous phase was discarded whilst the organic phase was then transferred into a new tube. This was then dried under a stream of nitrogen gas for about 30 minutes. The lipids extracts were then suspended in 500 µl of 1:1 (v/v) chloroform/methanol solution.

3.4.6 LC-MS analysis for the detection of oxidized ceramides products of 12*R*-LOX and eLOX-3

Lipid extracts from the hTERT immortalized keratinocyte cells were separated and analysed by reverse-phase HPLC using the Spherisorb ODS2 3 µm C18 150 x 2 mm column (Waters, Hertfordshire, UK) using a 20% - 0% A gradient for over 5 minutes. This was the followed by a 100% gradient B for 50 minutes using a flow rate of 200 µl min^{-1} (A: water, 5 mM ammonium acetate; B methanol:THF, 80:20, 5 mm ammonium acetate). The 12*R*-LOX and eLOX-3 oxidized lipid products were quantified on the ABSciex 6500 Q-Trap instrument equipped with a Shimadzu UPLC and electrospray ionization (ESI) using multiple reaction monitoring (MRM) mode to monitor precursor to product transition. Settings included declustering potential -20 V, collision energy -42 V, collision cell exit potential 13 V, curtain gas 35, ionSpray voltage -4,500, source temperature 350°C, nebuliser gas 40 and heating gas 30. (Tyrrell et al., 2021). **Appendix 1** shows all MRM transitions with the individual parameters.

3.4.7 Statistical analysis

Experiments were carried out in three independent biological replicates (n=3) and data are expressed as the mean ± SD. Statistical significance between treatments was determined using Student's t-test with $p < 0.05$ considered of statistical significance and is represented with an asterisk. Statistical analysis was done using GraphPad Prism 9.0 software (GraphPad Software Inc., San Diego, CA, USA) and Microsoft Excel software.

3.5 Results

3.5.1 Investigation of 12*R*-LOX expression in the HaCaT cell line

3.5.1.1 HaCaT keratinocyte cell line cultured under different calcium (Ca^{2+}) concentrations results in proliferative and differentiated epidermal phenotypes

As 12*R*-LOX is thought to be expressed in differentiated layers of the epidermis, HaCaT cells were cultured in increasing Ca^{2+} concentrations known to induce differentiation and therefore mimic the differentiated layers of the epidermis. Previous characterisation of HaCaT cells had been performed by Moukachar, 2021 where keratin 5 and involucrin expression were shown in proliferative and differentiated cells respectively. Investigation of HaCaT cells cultured at a calcium concentration of 0.03 mM under a light microscope revealed a shape and morphology that is, long, thin and spindle like in shape that resembles the biological characteristics of cells found in the basal layer of the epidermis. **Figure 3.5.1** shows HaCaT cells cultured at a Ca^{2+} concentration of 1.8 mM and 2.8 mM display a difference in shape with cells being cuboidal rather than a spindle like shape, whilst also appearing more closely packed. HaCaT cells grown at a Ca^{2+} concentration of 1.8 mM are representative of cells that would be found between the basal layer and cornified layer, that is the stratum granulosum and stratum spinosum. Examination of HaCaT cells cultured at the higher Ca^{2+} concentration of 2.8 mM shows cells in larger colonies with very tight packing.

(A) 8 hours – 0.03 mM Ca^{2+} **(B)** 24 hours – 1.8 mM Ca^{2+}

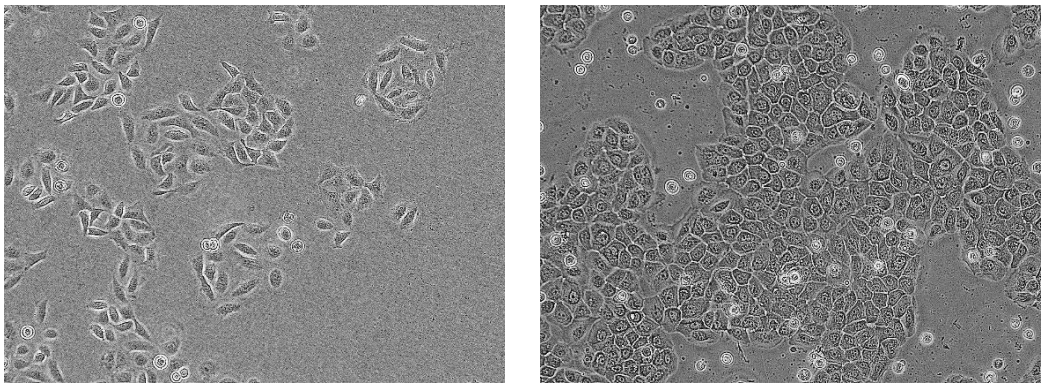

(C) 48 hours – 2.8 mM Ca^{2+}

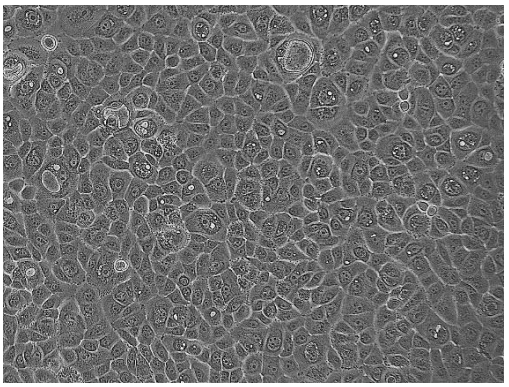

Figure 3.5.1 Culturing HaCaT cells at different calcium concentrations induces changes in shape and morphology to mimic the biological characteristics of cells found in different epidermal compartments. (A) Phase contrast image of HaCaT cells cultured in 0.03 mM calcium concentration for 8 hours to induce a proliferative phenotype found in the epidermis. (B) Phase contrast image of HaCaT cells cultured in 1.8 mM calcium concentration for 24 hours to induce a middle differentiated phenotype found in the epidermis. (C) Phase contrast image of HaCaT cells cultured in 2.8 mM calcium concentration for 48 hours to induce the most stratified differentiated phenotype found in the epidermis. Phase contrast images were taken at the indicated times at 10x magnification.

3.5.1.2 12*R*-LOX protein expression could not be detected in the HaCaT cell line using western blot analysis

Figure 3.5.2 shows a western blot with 20 µg of extracted protein loaded to the gel, however, both 12*R*-LOX and GAPDH expression could not be observed at the respective molecular weights of 80 kDa and 36 kDa in HaCaT cells cultured in different Ca^{2+} concentrations of 0.03 mM, 1.8 mM and 2.8 mM. An intense band appears in the human skin extract sample at approximately 55 - 60 kDa, however, this is not at the molecular weight in which 12*R*-LOX is detected. 12*R*-LOX has a molecular weight of 80 kDa, whilst GAPDH has a molecular weight of 35 kDa but no clear bands could be observed at these molecular weights.

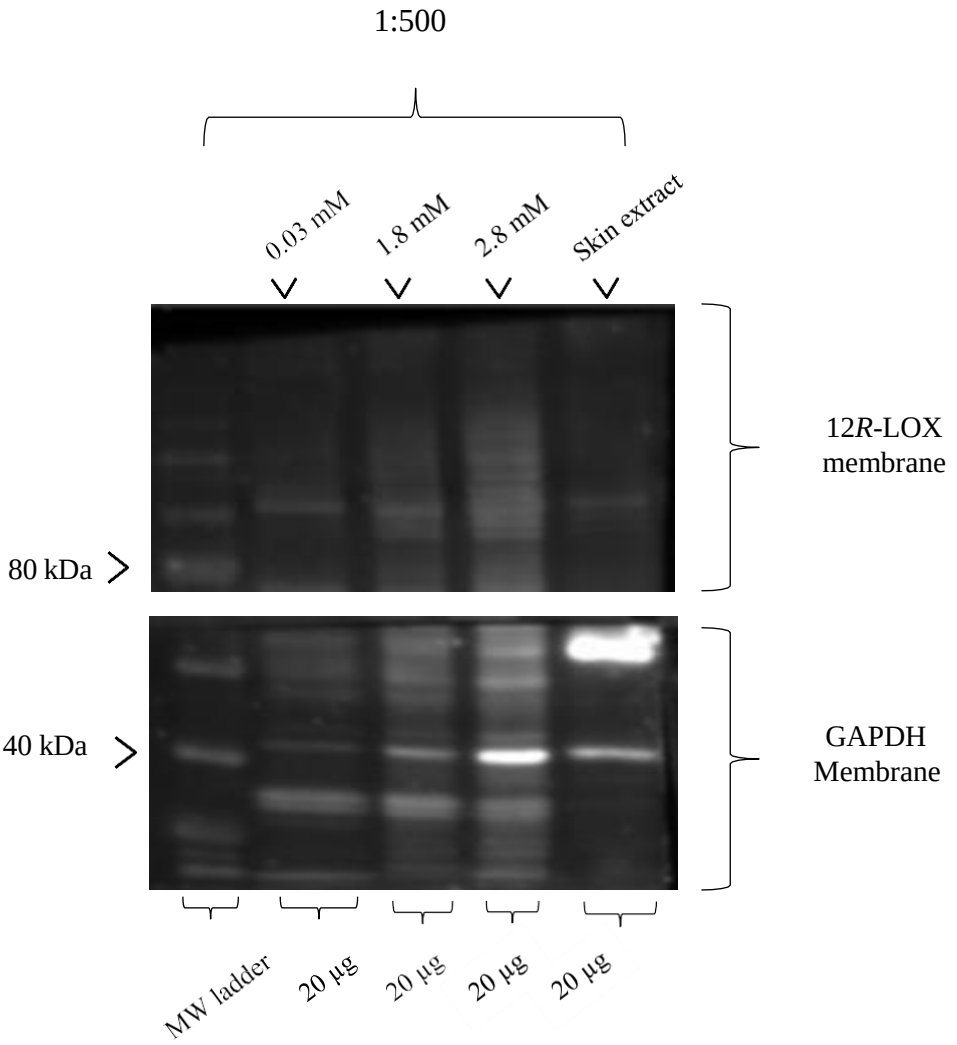

Figure 3.5.2 Investigating whether 12*R*-LOX (80 kDa) is expressed in the HaCaT cell line cultured in different Ca^{2+} concentration using western blot analysis. A total of 20 µg of protein was extracted from 10^6 cells and then loaded to an SDS-PAGE gel which was then electrotransferred onto a nitrocellulose membrane. Rabbit polyclonal antibodies was used in an attempt to detect proteins of interest. A 12*R*-LOX primary antibody dilution of 1:500 was used. No band can be observed for the 12*R*-LOX protein and GAPDH control.

Another immunoblot experiment was conducted with a greater protein amount of 40 µg, whilst keeping all other conditions unchanged. The 12*R*-LOX protein expression at the predicted molecular weight of 80 kDa could not be detected in HaCaT cells cultured in different Ca^{2+} concentrations of 0.03 mM, 1.8 mM and 2.8 mM as shown in **Figure 3.5.3**. Moreover, no clear band could be observed for the GAPDH control at the predicted molecular weight of 36 kDa in any of these samples. Additionally, the 12*R*-LOX protein expression and GAPDH control could not be detected in the human skin sample when adding 40 µg and 50 µg of protein.

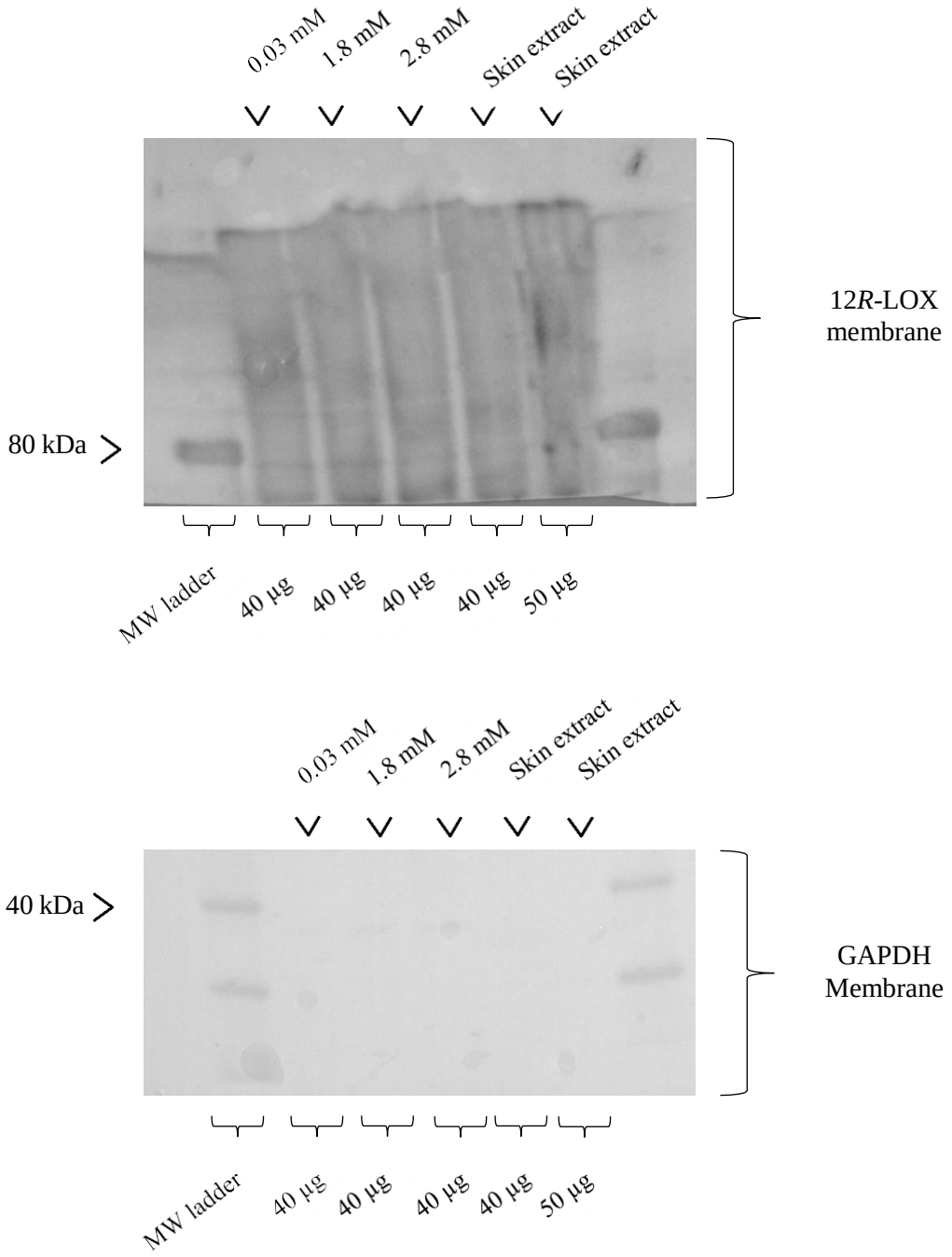

Figure 3.5.3 Evaluating whether increasing protein amount aids in 12*R*-LOX (80 kDa) detection in the HaCaT cell line cultured in different Ca^{2+} concentrations using western blot analysis. A total of 40 µg of protein was extracted from 10^6 cells and then loaded to an SDS-PAGE gel which was then electrotransferred onto a nitrocellulose membrane. Rabbit polyclonal antibodies were used in an attempt to detect the proteins of interest. A 12*R*-LOX primary antibody dilution of 1:500 was used and a GAPDH primary antibody dilution of 1:500 was used. No band can be observed for the 12*R*-LOX protein and GAPDH control.

As the GAPDH housekeeping protein could not be detected in previous western blots, an alternative housekeeping protein was used known as β-actin. **Figure 3.5.4** shows a band at a molecular weight of 42 kDa for β-actin in HaCaT cells cultured in different Ca^{2+} concentrations of 0.03 mM, 1.8 mM and 2.8 mM. **Figure 3.5.4** also shows a band for β-actin is also observed in human skin sample.

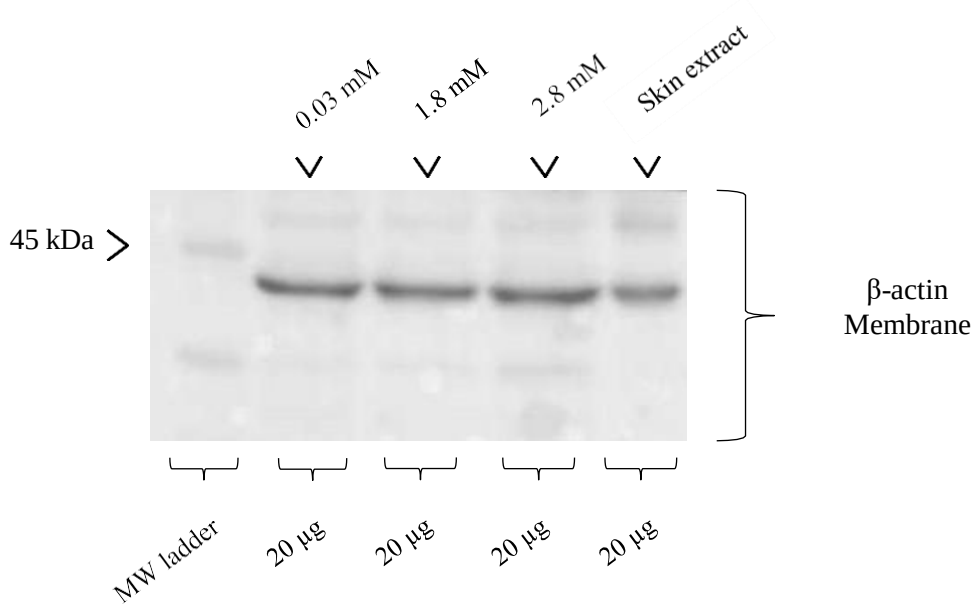

Figure 3.5.4 Evaluating whether expression of an alternative housekeeping protein, β-actin, is observed in HaCaT cells cultured in different Ca^{2+} concentrations. A total of 20 µg of protein was extracted from 10^6 cells and then loaded to an SDS-PAGE gel which was then electrotransferred onto a nitrocellulose membrane. 1º antibody (Anti- β-actin) 1:5000 dilution, white background developing.

A higher sensitivity PVDF membrane was used to investigate whether 12*R*-LOX protein expression could be observed. **Figure 3.5.5** shows that 12*R*-LOX protein expression at the predicted molecular weight of 80 kDa could not be detected in HaCaT cells cultured in different Ca^{2+} concentrations of 0.03 mM, 1.8 mM and 2.8 mM using the higher sensitivity PVDF membrane. The 12*R*-LOX protein expression was also not observable in the human skin sample control using the PVDF membrane. However, a band at 42 kDa for the β-actin control can be observed in **Figure 3.5.5**.

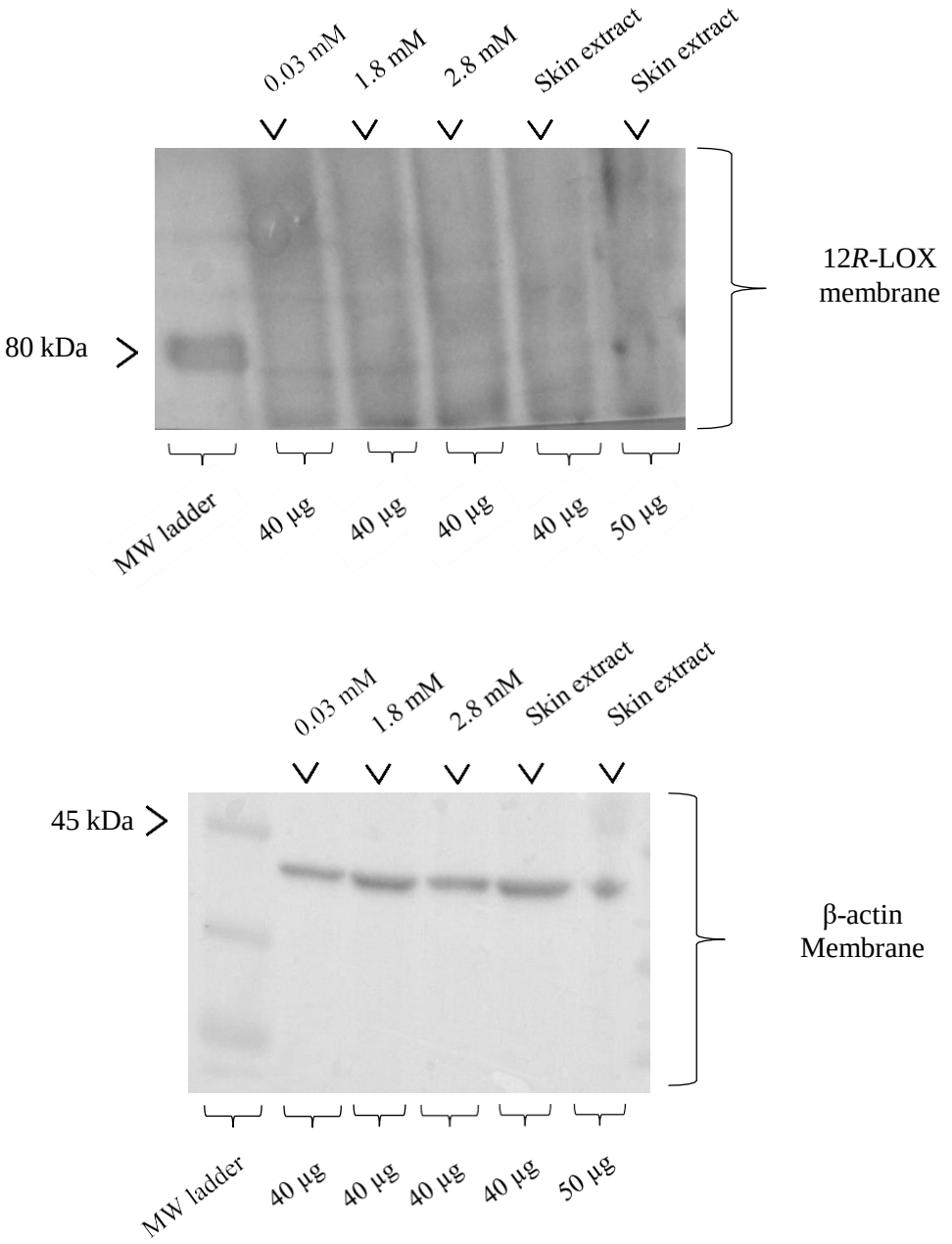

Figure 3.5.5 Evaluating whether a higher sensitivity membrane aids in 12*R*-LOX (80 kDa) detection in the HaCaT cell line cultured in different Ca^{2+} concentrations using western blot analysis. A total of 40 µg of protein was extracted from 10^6 cells and then loaded to an SDS-PAGE gel which was then electrotransferred onto a PVDF membrane. The proteins of interest were attempted to be revealed by rabbit polyclonal antibodies. A 12*R*-LOX primary antibody dilution of 1:500 was used and a β-actin primary antibody dilution of 1:500 was used.

Figure 3.5.6 fails to show a band for 12*R*-LOX protein expression at the anticipated molecular weight of 80 kDa in HaCaT cells cultured in different Ca^{2+} concentrations of 0.03 mM, 1.8 mM and 2.8 mM when incubating for a longer period overnight with the primary 12*R*-LOX antibody. 12*R*-LOX protein expression could not be observed in human skin sample controls with the longer incubation times of the primary antibody. A band at 42 kDa for the β-actin control is shown in **Figure 3.5.6**.

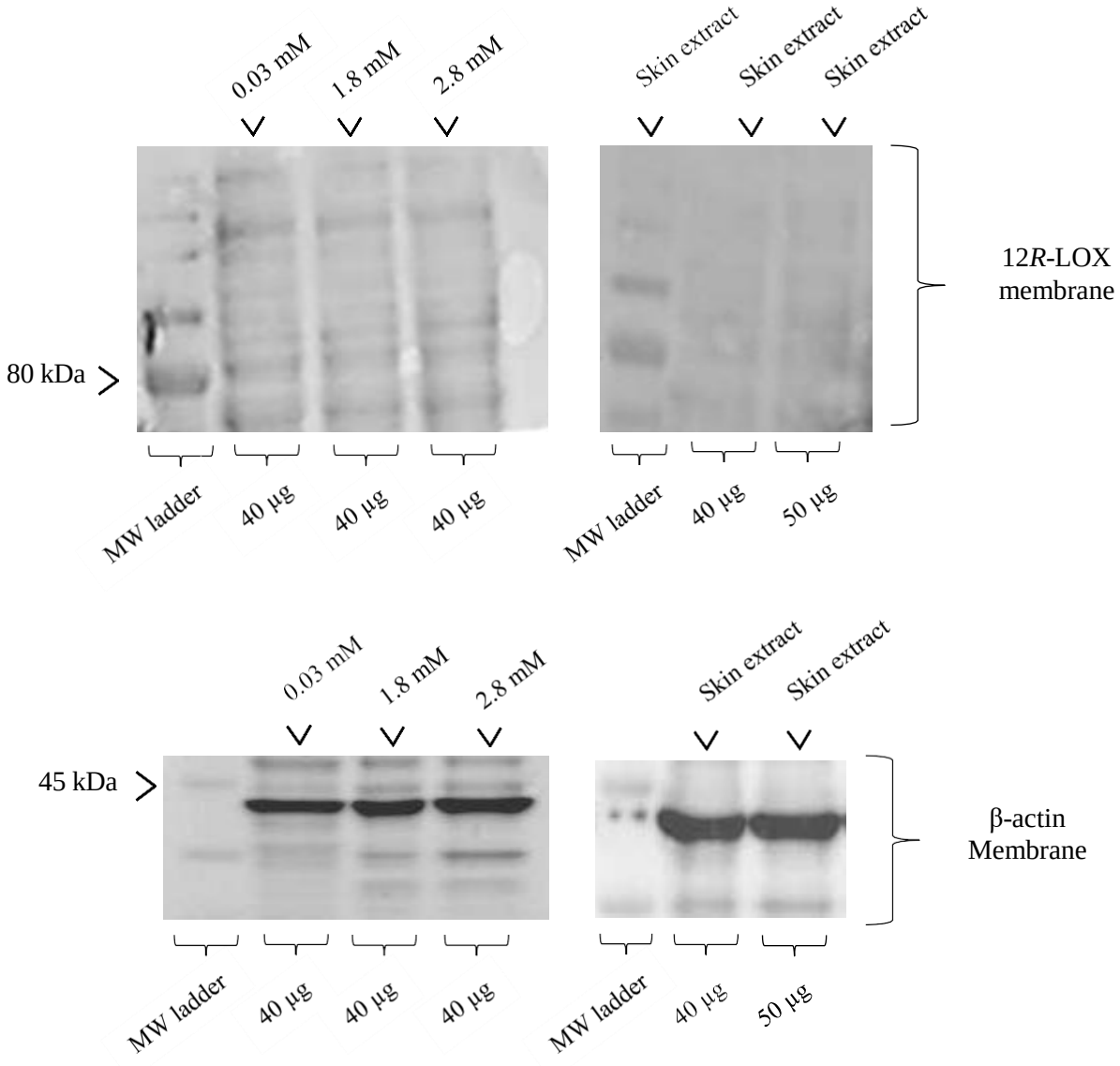

Figure 3.5.6 Evaluating whether a longer overnight 12*R*-LOX primary antibody incubation aids in 12*R*-LOX (80 kDa) detection in the HaCaT cell line cultured in different Ca^{2+} concentrations using western blot analysis. A total of 40 µg of protein was extracted from 10^6 cells and loaded to an SDS-PAGE gel which was then electrotransferred onto a PVDF membrane. 12*R*-LOX primary antibody dilution of 1:500 was used and a β-actin primary antibody dilution of 1:500 was used.

An alternative 12*R*-LOX primary rabbit polyclonal antibody kindly received from the University of Erlangen, Germany was used instead of the 12*R*-LOX primary antibody from the commercial supplier to investigate whether a change in primary antibody made a difference in detecting 12*R*-LOX. **Figure 3.5.7** shows no band at the anticipated molecular weight of 80 kDa for the 12*R*-LOX protein in HaCaT cells cultured in different Ca^{2+} concentrations of 0.03 mM, 1.8 mM and 2.8 mM. Disappointingly, the 12*R*-LOX protein could not be detected in the human skin control as shown in **Figure 3.4.7**. A protein band at 42 kDa for the β-actin control is shown in **Figure 3.5.7** in all samples along with the human skin extract.

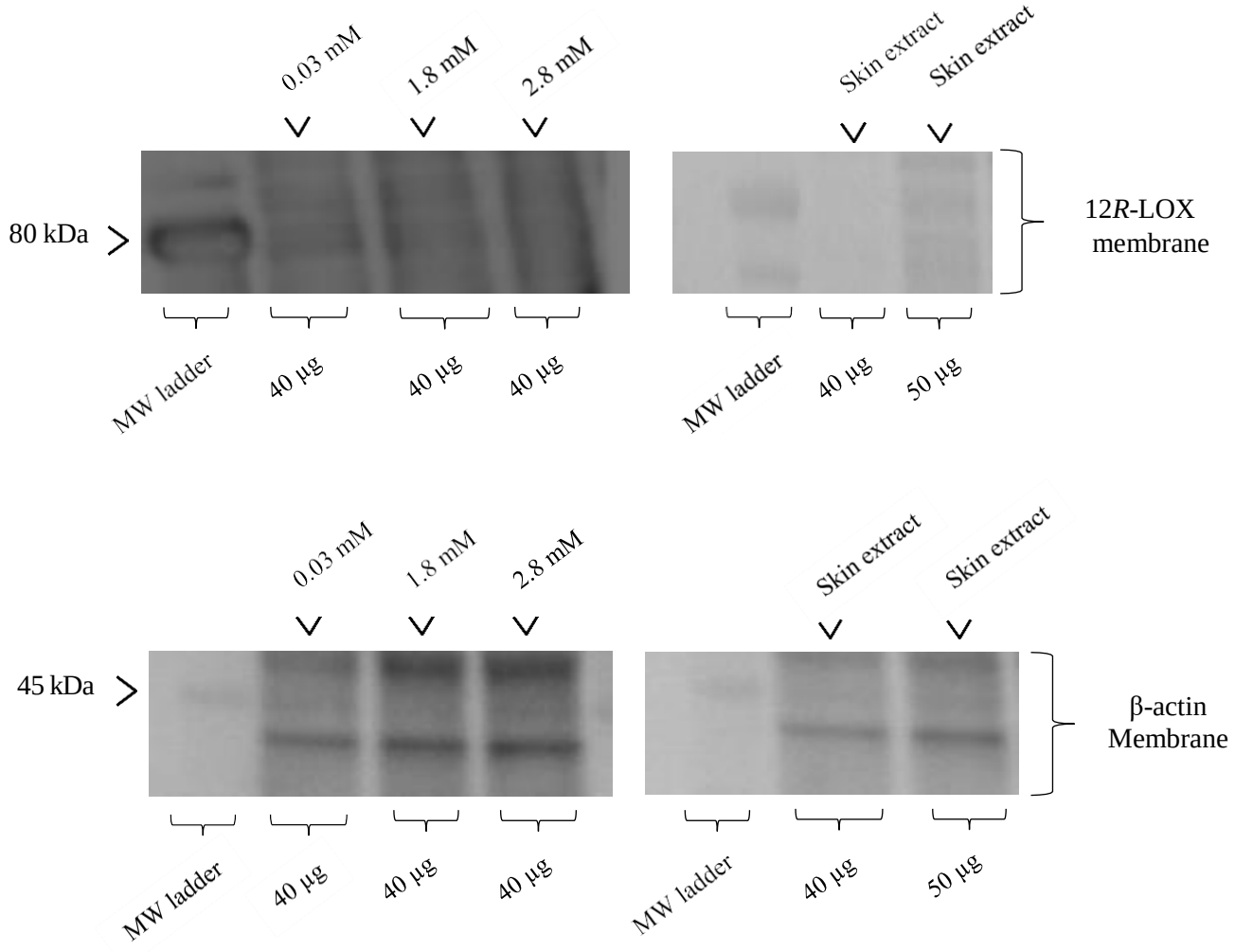

Figure 3.5.7 Evaluating whether an alternative 12*R*-LOX primary antibody (80 kDa) has an effect in western blotting for the 12*R*-LOX protein in the HaCaT cell line cultured in different Ca^{2+} concentrations using western blot analysis. A total of 40 µg of protein was extracted from 10^6 cells and loaded to an SDS-PAGE gel which was then electrotransferred onto a PVDF membrane. 12*R*-LOX primary antibody dilution of 1:500 was used and a β-actin primary antibody dilution of 1:500 was used.

3.5.2 Characterisation of the hTERT keratinocyte cell line

3.5.2.1 hTERT keratinocyte cells collected at 30% and 100% confluence display a morphological difference

As 12*R*-LOX protein expression was unable to be detected in the HaCaT cell line, focus shifted to an alternative keratinocyte cell line known as the hTERT epidermal cell line which is more biologically similar to primary keratinocytes than the HaCaT cell line. Calcium was already present in hTERT cell culture media and the addition of further calcium to the media was not recommended by the manufacturer as it is unknown what effect this would have on the other supplements provided by the manufacturer. In this case, to replicate the proliferative or differentiated phenotype of cells, they were grown to different confluencies as previously described (Poumay and Pittelkow, 1995; Borowiec et al., 2013). **Figure 3.5.8** shows the hTERT cell line grown to a 30% and 100% cell confluence. Examination of hTERT cells at these respective cell confluence reveals a difference in shape and morphology. hTERT cells at 30% confluence display a spindle-like shape, are less compact and exhibit no tight cellular junction observed between cells (**Figure 3.5.8 A**). A total time of 48 hours was required to achieve a 100% cell confluence of hTERT cells. Examination of hTERT cells grown for 48 hours from seeding to a confluence of 100% shows cells having a cuboidal shape, tight cell to cell junctions and are significantly more compact then hTERT cells grown to 30% confluence as would be expected (**Figure 3.5.8 B**).

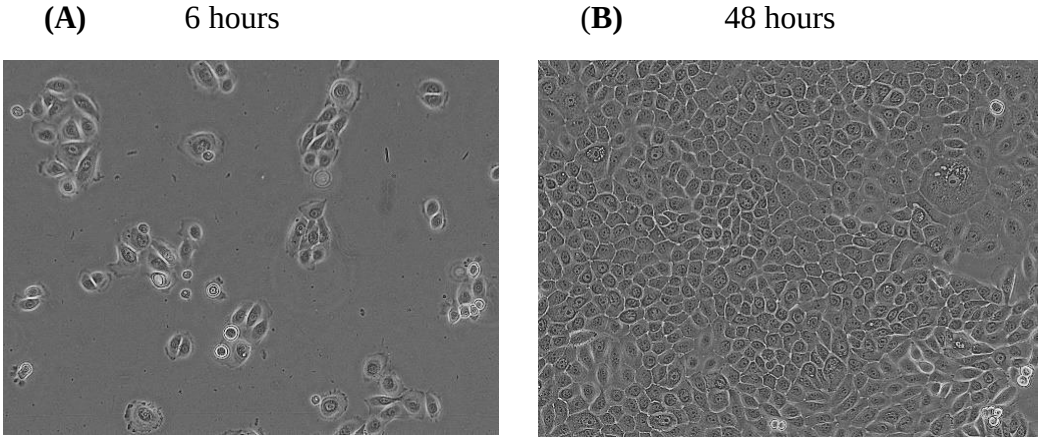

Figure 3.5.8 Evaluating changes in in shape and morphology of hTERT cells at two different cell confluence. (A) Phase contrast image of hTERT cells to 30% confluence to mimic proliferative layer of epidermis. (B) Phase contrast image of hTERT cells grown to 100% confluence to mimic differentiated layer of epidermis. Phase contrast images were taken at the indicated times at X10 magnification.

3.5.2.2 Increased keratin 5 and involucrin expression dependent on hTERT keratinocyte cell confluence

Figure 3.5.9 shows a denser band is observed in hTERT cells collected at 30% confluence in comparison with hTERT cells at 100% confluence. **Figure 3.5.10** shows that the relative protein level of keratin 5 (*Krt5*) (proliferative marker) is statistically significantly greater in hTERT cells collected at 30% confluence in comparison with hTERT cells collected at 100% confluence.

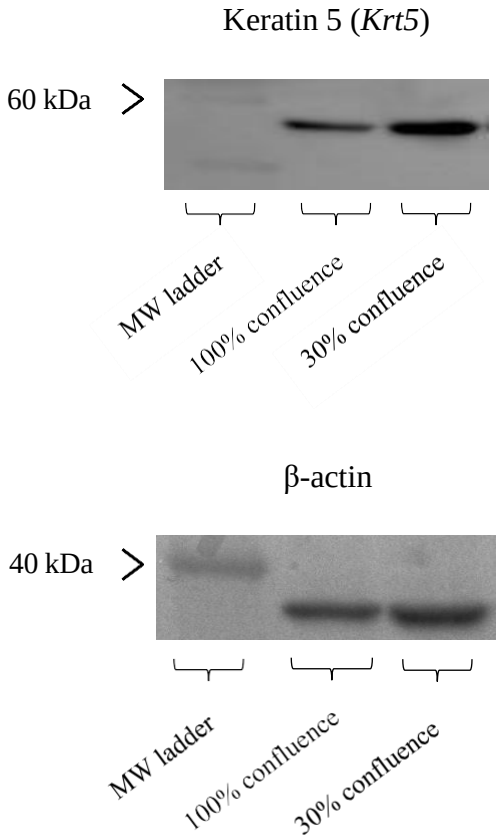

Figure 3.5.9 Representative images of western blots in the detection of the proliferative *Krt5* marker. A band corresponding to *Krt5* and β-actin was detected at the predicted molecular weight of 58 kDa and 42 kDa respectively.

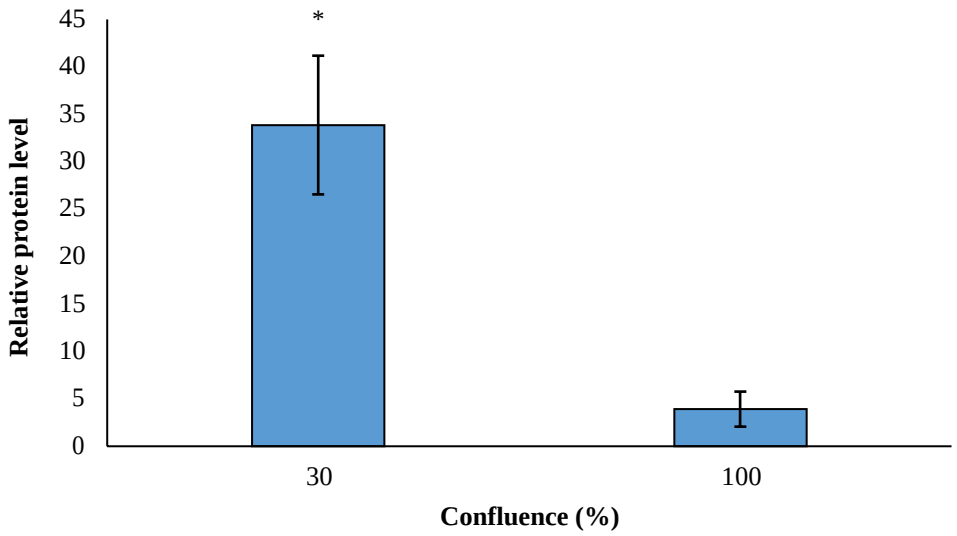

Figure 3.5.10 Western blot quantification of *Krt5* expression in 30% and 100% confluent hTERT cells. hTERT cells were collected at 30% and 100% confluence respectively. Relative protein levels are represented as mean protein values normalized to β-actin using ImageJ, ± SD (n = 3). * $P < 0.05$ when compared with hTERT cells collected at 100% confluence.

Figure 3.5.11 shows a denser band in hTERT cells collected at 100% confluence in comparison with hTERT cells collected at 30% confluence. Whilst the relative protein level of *Ivl* is shown in hTERT cells collected at 60% confluence, it was not used for quantification comparison purposes as shown in **Figure 3.5.12**. **Figure 3.5.12** shows that the relative protein level of involucrin (*Ivl*) (differentiated marker) is statistically significantly greater in hTERT cells collected at 100% confluence when compared with the relative protein level of *Ivl* in hTERT cells collected at 30% confluence.

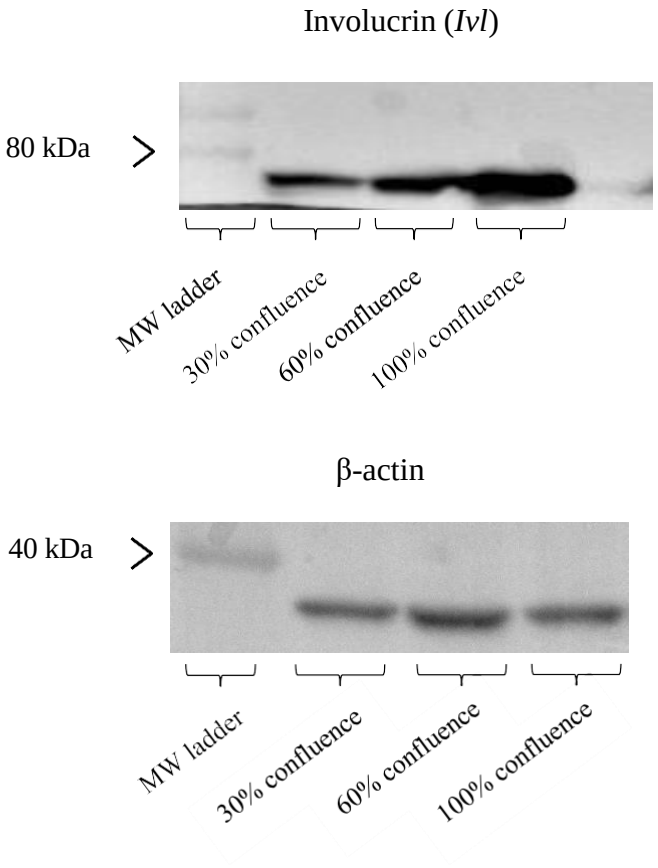

Figure 3.5.11 Representative images of western blots in the detection of the *Ivl* differentiation marker. A band corresponding to *Ivl* and β-actin was detected at the predicted molecular weight of 69 kDa and 42 kDa respectively.

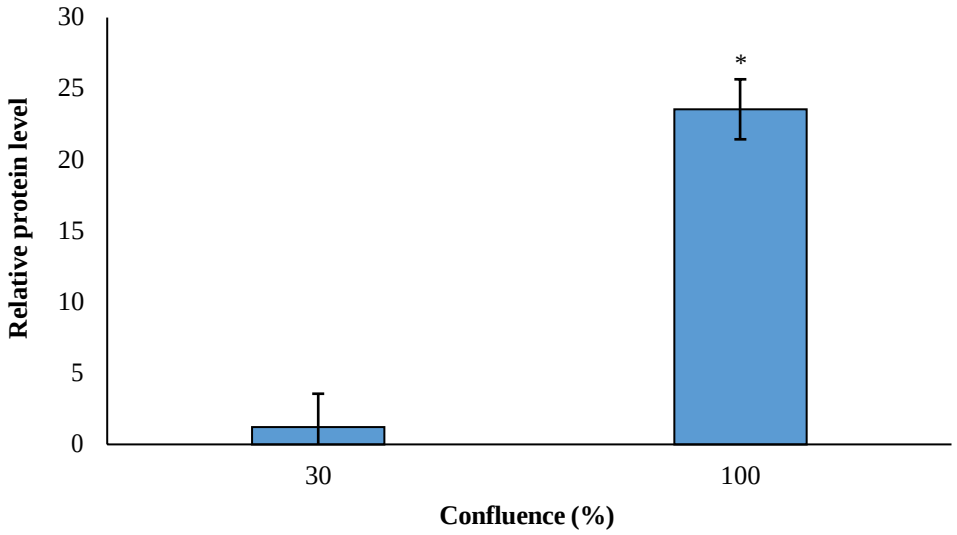

Figure 3.5.12 Western blot quantification of *Ivl* expression in 30% and 100% confluent hTERT cells. hTERT cells were collected at 30% and 100% confluence respectively. Relative protein levels are represented as mean protein values normalized to β-actin using ImageJ, ± SD (n = 3). * $P < 0.05$ when compared with hTERT cells collected at 30% confluence.

3.5.3 Investigation of 12*R*-LOX expression in the hTERT cell line

3.5.3.1 12*R*-LOX protein expression could not be detected in the hTERT keratinocyte cell line using western blot analysis

Figure 3.5.13 shows a western blot with 40 µg of extracted protein loaded to the gel with a 12*R*-LOX primary mouse monoclonal antibody dilution of 1:500 and 1:1000. A band for 12*R*-LOX protein expression could not be observed at the anticipated molecular weight of 80 kDa in primary immortalized hTERT cells cultured to a confluence of 100%. This is surprising as keratinocyte cells at this confluence would be differentiated which is where the 12*R*-LOX protein is thought to be expressed. A band for 12*R*-LOX protein expression could not be observed at the anticipated molecular weight of 80 kDa in primary immortalized hTERT cells cultured to a confluence of 30% as keratinocyte cells at this confluence resemble highly proliferative cells of the epidermis. The western blotting results for 12*R*-LOX expression should resemble a similar pattern to the the *Ivl* western blotting results, where the *Ivl* protein expression is observed in differentiated keratinocytes rather than in proliferative keratinocytes. 12*R*-LOX protein expression was also not detected in the human skin extract sample. A protein band at 42 kDa for the β-actin control is shown in **Figure 3.5.13** in hTERT cells collected at 30% and 100% confluence along with the human skin extract.

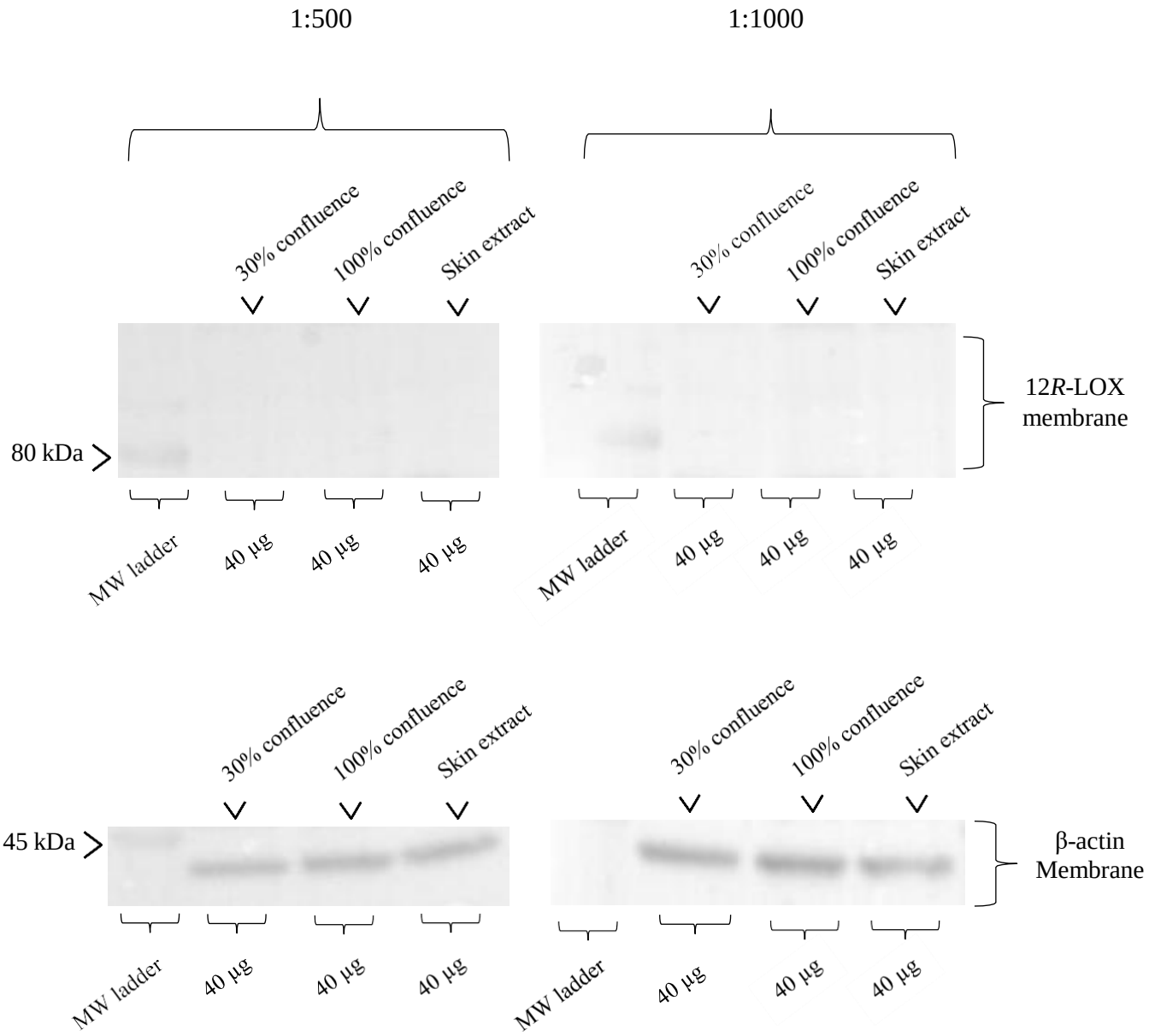

Figure 3.5.13 Evaluating whether the 12*R*-LOX protein (80 kDa) is expressed in the hTERT cell line cultured and collected at different cell confluence. A total of 40 µg of protein was extracted from 10^6 cells and loaded to an SDS-PAGE gel which was then electrotransferred onto a PVDF membrane. 12*R*-LOX primary antibody dilutions of 1:500 and 1:1000 was used.

Figure 3.5.14 does not show a band for 12*R*-LOX protein expression at the anticipated molecular weight of 80 kDa in the hTERT cell line cultured to 30% and 100% confluence when incubating for a longer period overnight with the primary 12*R*-LOX antibody. 12*R*-LOX protein expression could not be observed in human skin sample controls with the longer incubation times of the 12*R*-LOX primary mouse monoclonal antibody. A band at 42 kDa for the β-actin control is shown in **Figure 3.5.14**.

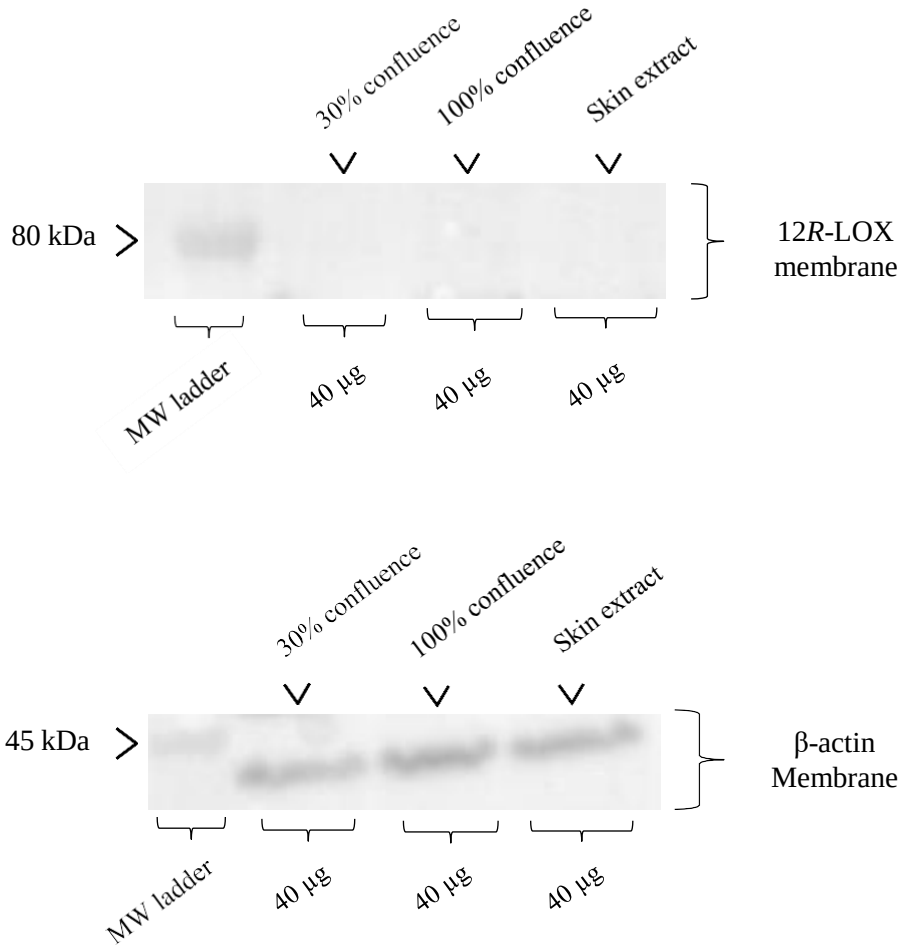

Figure 3.5.14 Evaluating whether a longer overnight 12*R*-LOX primary antibody incubation aids in 12*R*-LOX (80 kDa) detection in the hTERT cell line cultured and collected at 30% and 100% confluence using western blotting. A total of 40 µg of protein was extracted from 10^6 cells and loaded to an SDS-PAGE gel which was then electrotransferred onto a PVDF membrane. 12*R*-LOX primary antibody dilution of 1:500 was used and a β-actin primary antibody dilution of 1:500 was used.

Figure 3.5.15 shows a western blot with 40 µg of extracted protein initially loaded to the gel with a 12*R*-LOX primary antibody dilution of 1:100 and a reduced wash time of 5 x 30 seconds. A band could not be detected for 12*R*-LOX protein expression at the anticipated molecular weight of 80 kDa under these optimised conditions in primary immortalized hTERT cells at confluences of 30% and 100%. The 12*R*-LOX protein expression was also not detected in the human skin extract sample. A protein band at 42 kDa for the β-actin control is shown in **Figure 3.5.15** in hTERT cells collected at 30% and 100% confluence along with a protein band for the β-actin control in human skin extract.

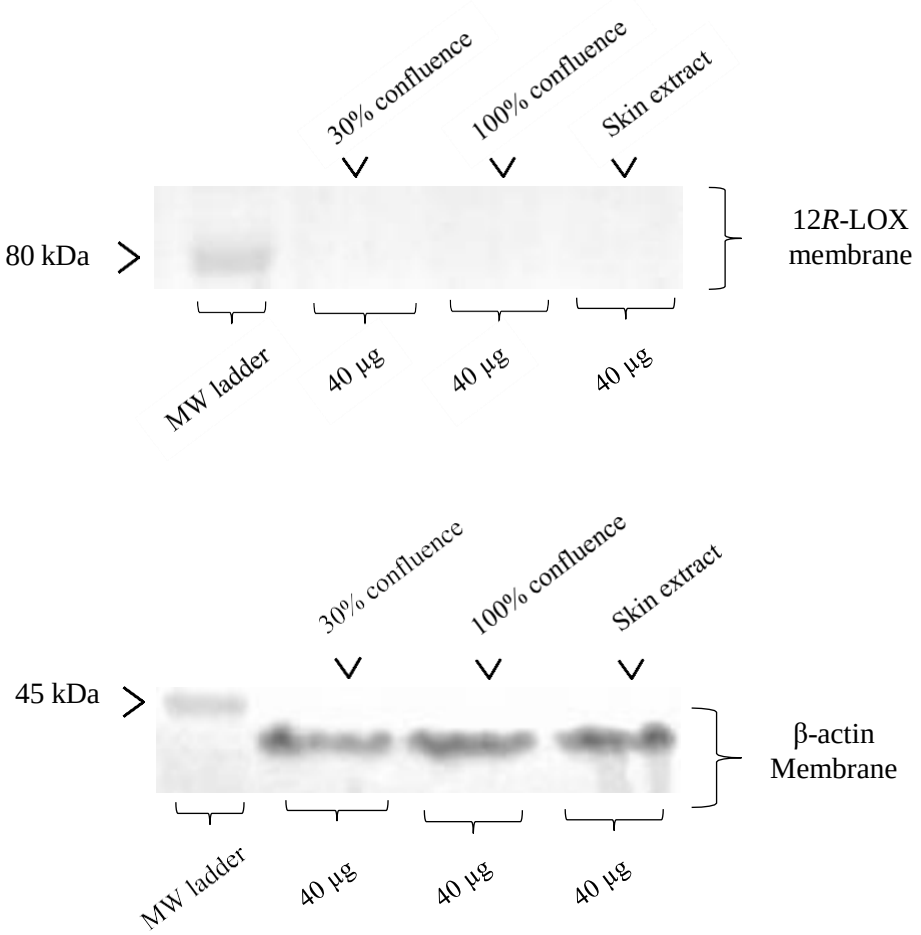

Figure 3.5.15 Evaluating whether a concentrated 12*R*-LOX primary antibody incubation aids in 12*R*-LOX (80 kDa) detection in the hTERT cell line cultured and collected at 30% and 100% confluence using western blotting. A total of 40 µg of protein was extracted from 10^6 cells and loaded to an SDS-PAGE gel which was then electrotransferred onto a PVDF membrane. 12*R*-LOX primary antibody dilution of 1:100 was used with an overnight incubation and a reduced tween wash time of 5 x 30 seconds. β-actin primary antibody dilution of 1:500 was used.

3.5.3.2 Low quantities of oxidized ceramides detected in the hTERT cell line using LC-MS analysis

Due to the inability of western blotting to detect the 12*R*-LOX protein in any samples above in the hTERT keratinocyte cell line and the skin extract control, the focus of detection was shifted to analyse for 12*R*-LOX / eLOX-3 products using mass spectrometry (MS). The MS methodology has been described extensively in Tyrrell et al., 2021 to quantify ng amounts of these products in human epidermal tape strip samples. **Appendix 2** shows MRM chromatograms for C32 EOS, EOH and EOP ceramides in hTERT media, hTERT cells collected at 30% and 100% confluence.

Figure 3.5.16 shows no detectable peak above base line noise for C32 EOS, EOH and EOP 9-HODE in hTERT media. **Figure 3.5.17** and **Figure 3.5.18** shows indication of some signals at 11 – 15 minutes for C32 EOS, EOH and EOP 9-HODE in hTERT cells collected at 30% and 100% confluence, however, Tyrrell et al., 2021 indicates EOS/EOH/EOP- HODE ceramide should elute between 16 – 19 minutes.

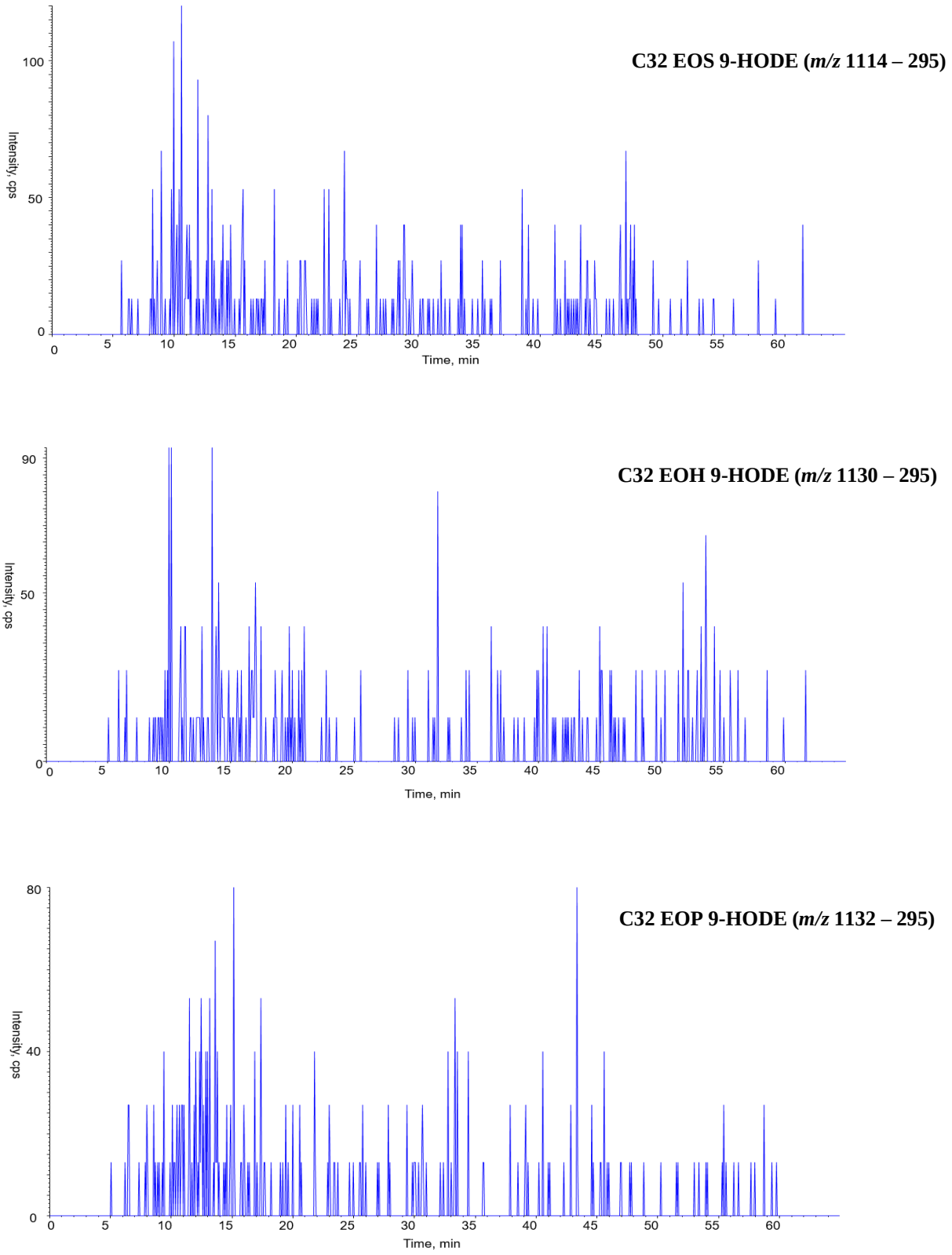

Figure 3.5.16 Extracted ion chromatogram (XIC) of C32 EOS, EOH, EOP 9-HODE ceramides detected as precursor ([M-H+CH3CO2H]-) → 295 in hTERT media.

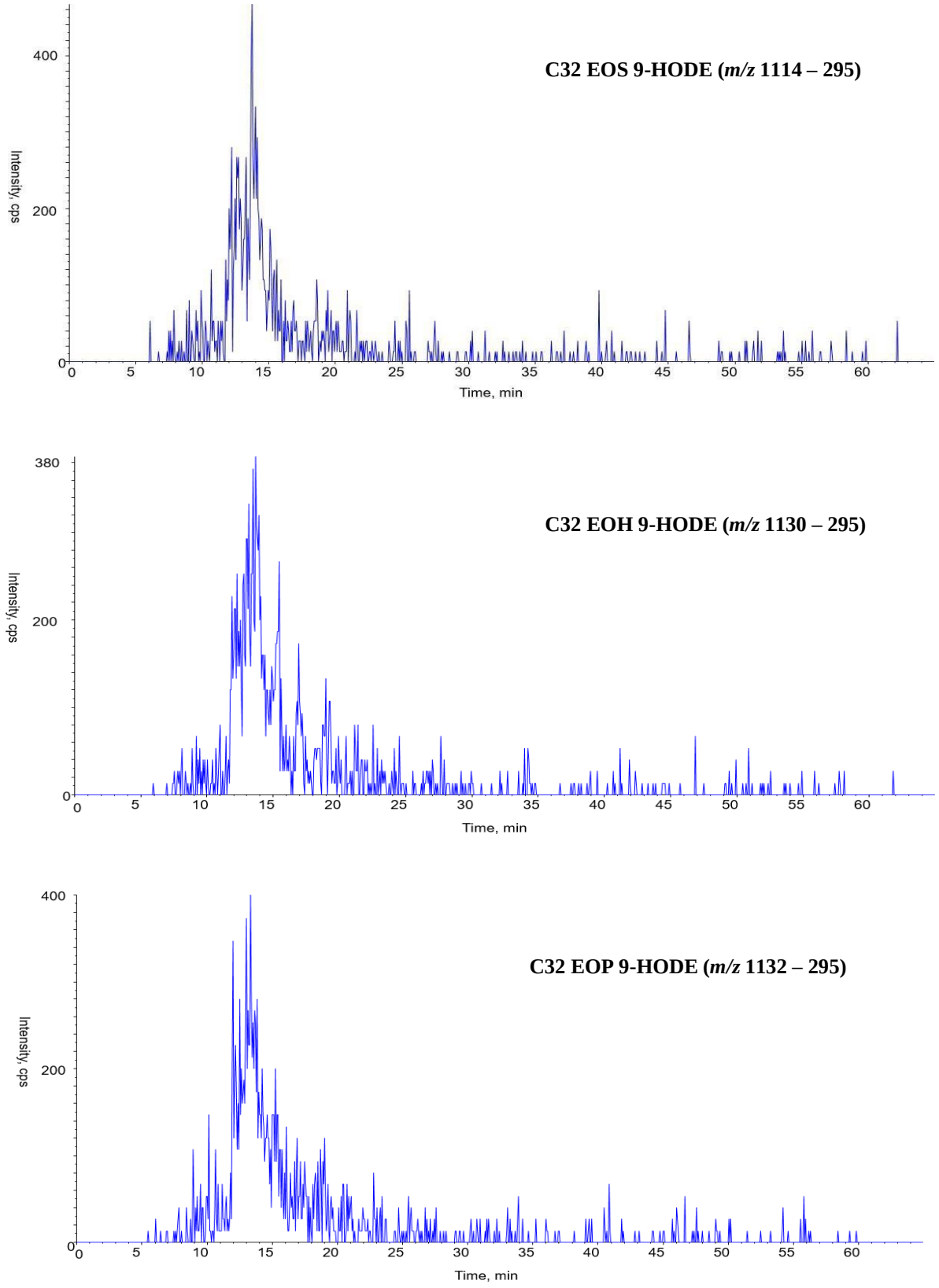

Figure 3.5.17 Extracted ion chromatogram (XIC) of C32 EOS, EOH, EOP 9-HODE ceramides detected as precursor ([M-H+CH3CO2H]-) → 295 at 30% confluence.

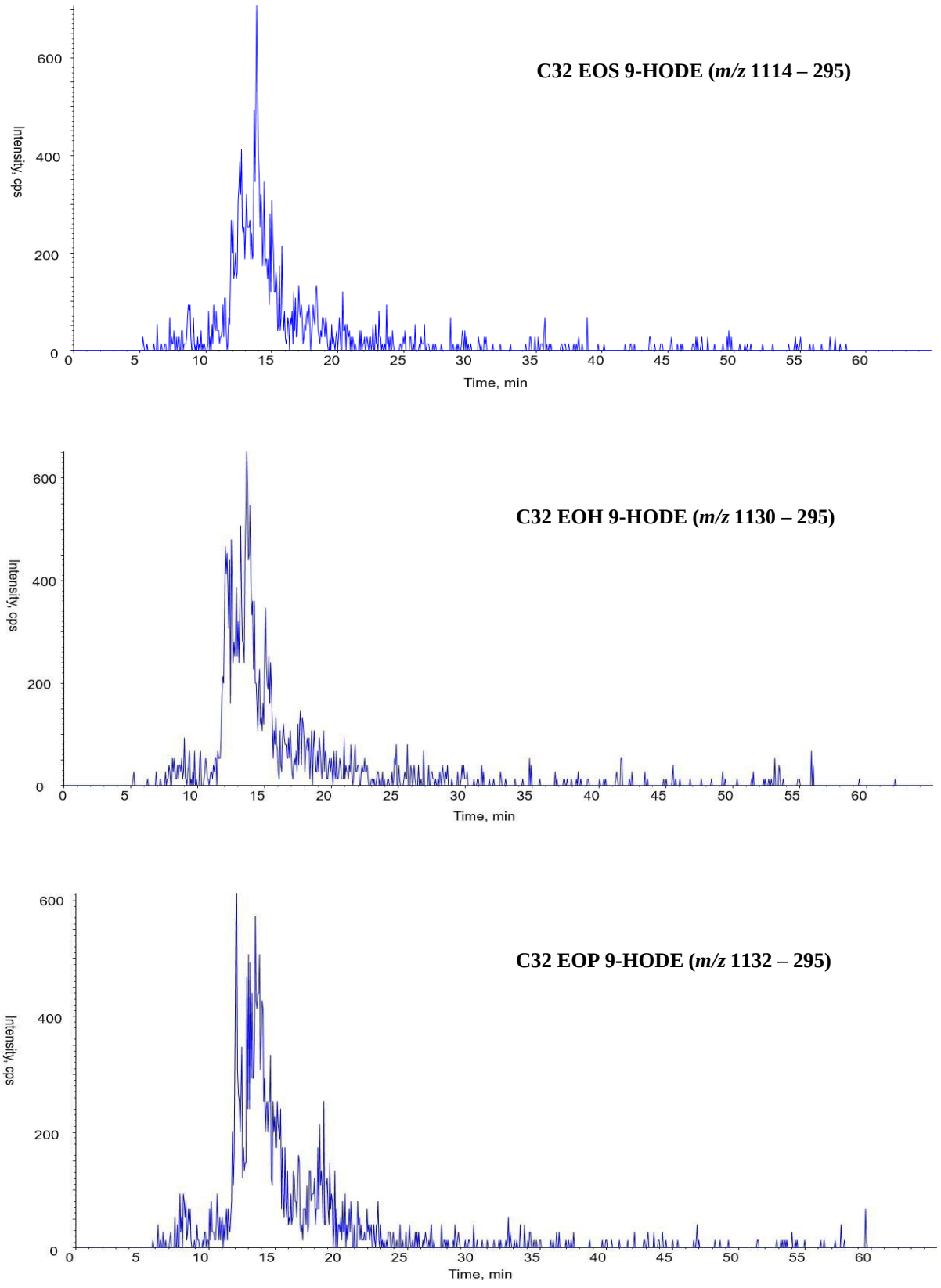

Figure 3.5.18 Extracted ion chromatogram (XIC) of C32 EOS, EOH, EOP 9-HODE ceramides detected as precursor ([M-H+CH3CO2H]-) → 295 at 100% confluence.

Figure 3.5.19 shows no detectable peak above base line noise for C32 EOS, EOH and EOP 9R,10R,13R-TriHome in hTERT media. Whilst a signal appears for C32 EOS, EOH and EOP 9R,10R,13R-TriHome in hTERT cells collected at 30% and 100% confluence as shown in **Figure 3.5.20** and **Figure 3.5.21**, at an expected elution time these signals would not pass the limit of detection (LOD) for these specific compounds and the peak shape does not infer a single compound representing the MRM transition.

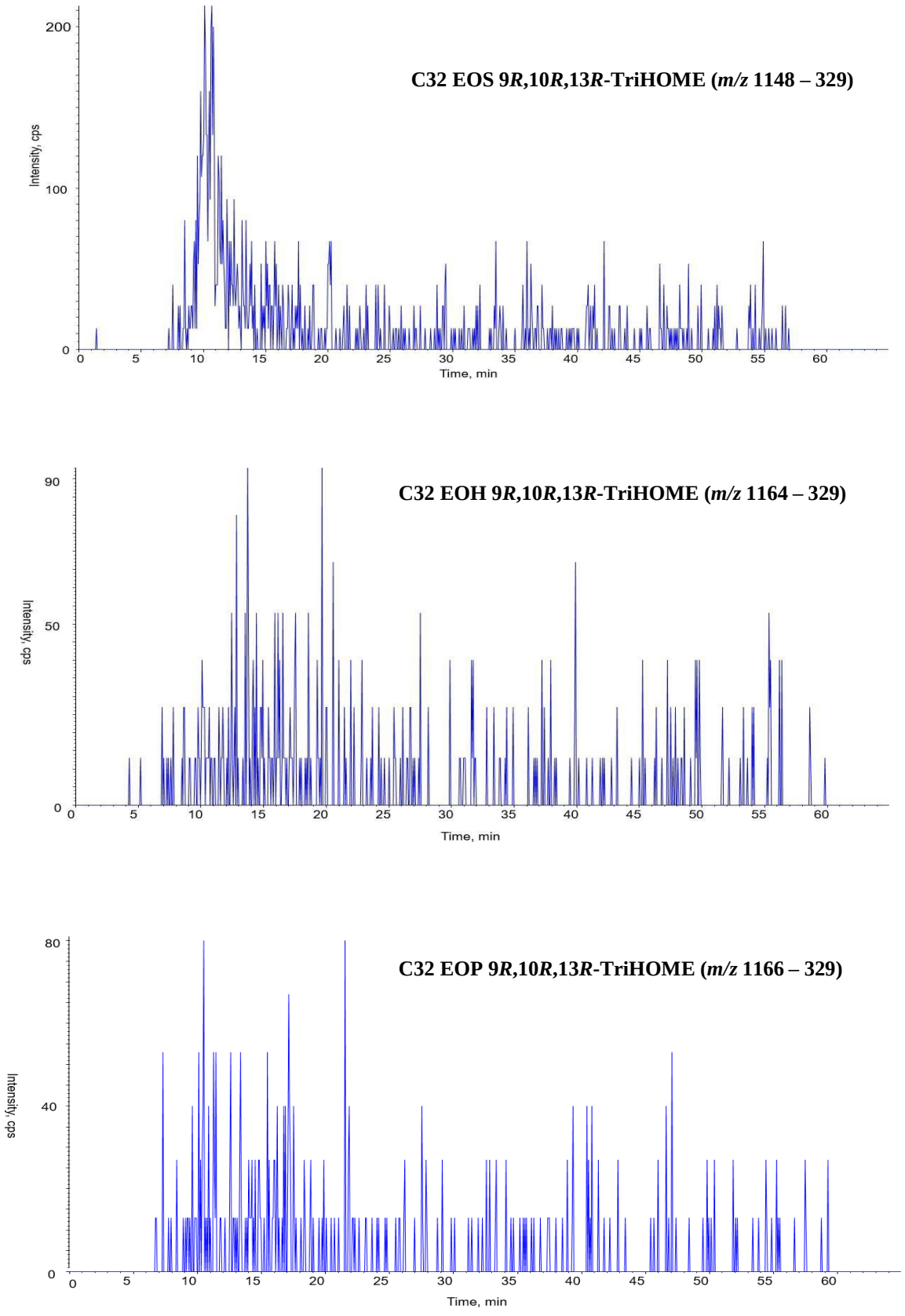

Figure 3.5.19 Extracted ion chromatogram (XIC) of C32 EOS, EOH, EOP 9R,10R,13R-TriHome ceramides detected as precursor ([M-H+CH3CO2H]-) → 329 in hTERT media.

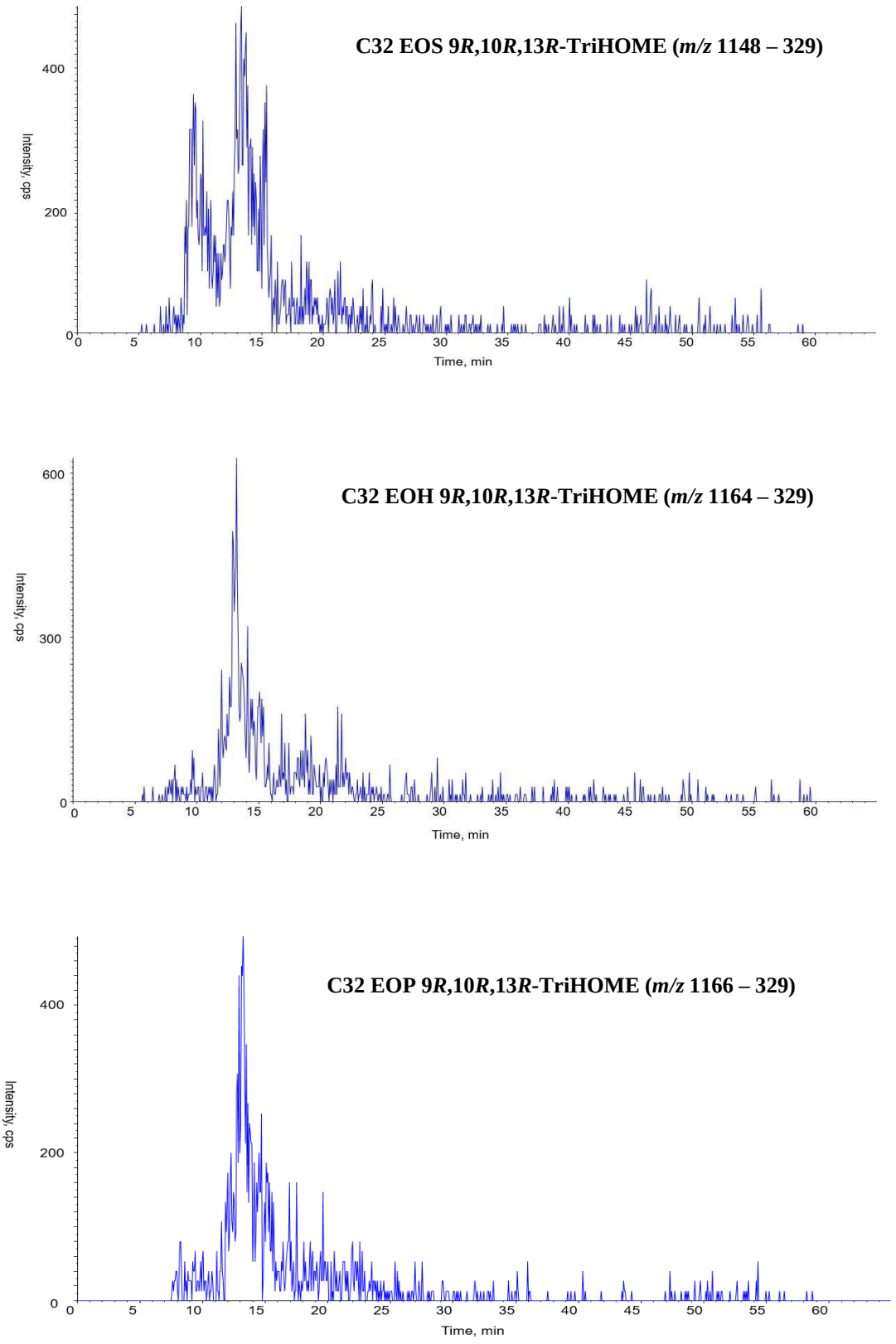

Figure 3.5.20 Extracted ion chromatogram (XIC) of C32 EOS, EOH, EOP 9R,10R,13R-TriHome ceramides detected as precursor ([M-H+CH3CO2H]-) → 329 in hTERT cells collected at 30% confluence.

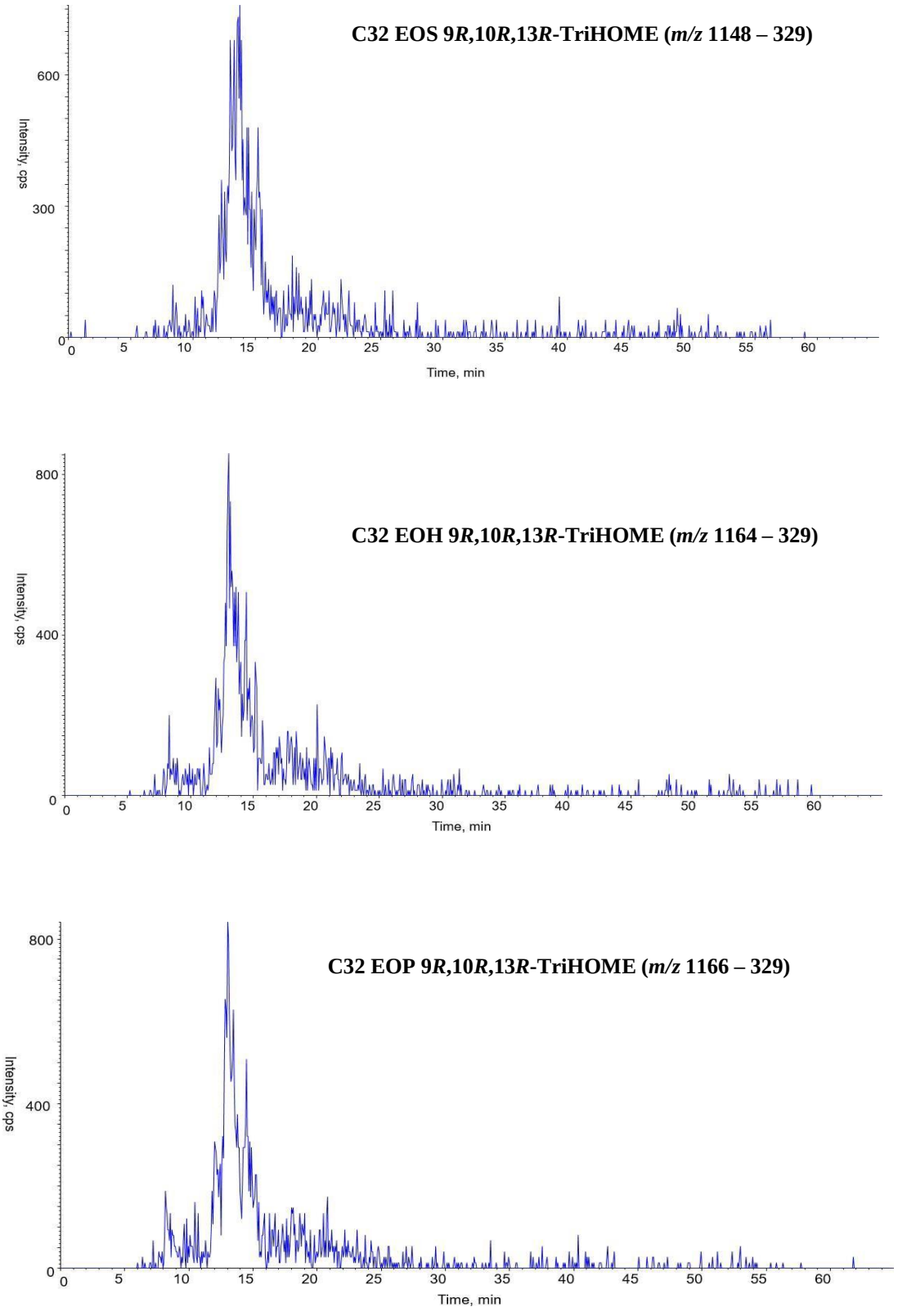

Figure 3.5.21 Extracted ion chromatogram (XIC) of C32 EOS, EOH, EOP 9R,10R,13R-TriHome ceramides detected as precursor ([M-H+CH3CO2H]-) → 329 in hTERT cells collected at 100% confluence.

3.6 Discussion

The initial hypothesis for this investigation was the discovery of a keratinocyte cell line that expressed 12*R*-LOX / eLOX-3 to be used in silencing experiments to further monitor genetic, phenotypic and morphological changes in the absence of the LOX enzyme. As it has been shown that LOX is expressed *in vivo* in keratinocytes forming stratified layers of the human epidermis and thus cells undergoing differentiation, to mimic the human epidermis and the possible expression of LOX, HaCaT cells were cultured in three different Ca^{2+} concentrations representing basale, spinosum and granulosum levels, 0.03 mM, 1.8 mM and 2.8 mM respectively. To ensure HaCaT cells retained their unique proliferative and differentiated keratinocyte characteristics, cells were collected at specific time points. To mimic the middle layer of the epidermis, HaCaT cells cultured for a prolonged period of time risk losing their distinctive granular phenotype and may become too differentiated and therefore resemble terminally differentiated keratinocytes. Moreover, to retain basal keratinocyte characteristics, cells cultured in 0.03 mM Ca^{2+} concentration were collected after 8 hours as prolonged culturing of cells grown in low Ca^{2+} medium can initiate the process of differentiation and therefore lose basal keratinocyte features (Deyrieux and Wilson 2007). Microscopy analysis was performed to determine whether the HaCaT cells grown in the different Ca^{2+} concentrations maintained either their basal cell phenotype, that is, spindle like shaped cells with tight junctions, or the suprabasal cell characteristics in which cells are cuboidal in shape and closely packed (Hennings et al., 1980). Once a reliable and consistent growth of three *in vitro* growth conditions of HaCaT cells had been established that mimicked different layers of the epidermis, a protein extraction could be performed ready for investigating 12*R*-LOX protein expression using western blotting. Whilst the HaCaT cell line is routinely used as a keratinocyte *in vitro* model, continuous passaging of cells can result in protein expression alterations which may no longer mimic the cell line being investigated (Toouli et al., 2002). This may negatively influence and alter the expression of the 12*R*-LOX protein and could explain the difficulty in its detection.

3.6.1 Optimisation of the western blot protocol did not result in the detection of the 12*R*-LOX protein in the HaCaT cell line

Optimisation of the protein extraction procedure was required to obtain sufficient protein to perform western blotting. A commonly used Tris-HCl, EDTA and SDS buffer was used initially, however, protein concentration values were insufficient to proceed to western blotting and therefore a RIPA assay buffer was prepared for the extraction. This buffer aims to release

maximal protein content from cells, from nuclear proteins to mitochondrial proteins, however, insoluble protein fractions may still remain (Janes, 2015). As the exact cellular location of 12*R*-LOX within keratinocytes is unknown, a buffer that can solubilize proteins in different cellular compartments is the more practical approach in identifying the presence of 12*R*-LOX in the immunoblot. Protease and phosphatase inhibitor cocktails were added to various buffers used to prevent the degradation of the 12*R*-LOX protein. The addition of chemical components such as sodium deoxycholate, an ionic detergent, aids in dissociating and disrupting interactions between proteins in the hope of obtaining as much protein quantity as possible. Triton-X is also a component of RIPA buffer which is a non-ionic detergent allowing effective solubilization of both membrane and cytoplasmic proteins. This specific component prevents degradation of proteins, thus allowing the native state of proteins to be retained (Pchelintsev et al., 2016).

Several optimisation experiments were performed in attempting to detect the 12*R*-LOX protein in the HaCaT cell line. For example, increasing protein quantity to be added for western blotting, longer incubation with the 12*R*-LOX primary antibody, alternative 12*R*-LOX primary antibody and more concentrated 12*R*-LOX primary antibody dilutions did not result in the detection of the 12*R*-LOX protein in the HaCaT cell line. Moreover, a higher sensitivity PVDF membrane in comparison to nitrocellulose membrane did not result in the detection of the 12*R*-LOX protein. It's possible that the 12*R*-LOX protein is present in significantly low quantities within these specific cell lines and is therefore difficult to detect using western blotting. Furthermore, the 12*R*-LOX protein was also not detectable in the human skin control sample, suggesting that the 12*R*-LOX primary antibodies used may not be specific enough to detect this epidermal protein. If the 12*R*-LOX protein is of low abundance in these *in vitro* models, reducing the wash time with PBS/tween and using a more sensitive membrane may aid in the detection of the 12*R*-LOX protein. However, altering to these specific conditions did not result in the detection of a band for 12*R*-LOX. Alternative methods such as immunoprecipitation may aid in the detection of low abundant proteins through isolating and enriching the 12*R*-LOX protein from the cell extract samples (Kaboord et al., 2015). Determining whether 12*R*-LOX is expressed on an mRNA level using PCR would give indication of whether these cell lines produce the 12*R*-LOX protein or not. However, silencing of the 12*R*-LOX protein requires its detection on a protein level as it's the 12*R*-LOX protein that is responsible for generating oxidized lipid molecules in which their role will be investigated. Whilst 12*R*-LOX protein expression has been detected in mouse skin studies using western blotting, it has yet to be detected in human skin (Epp et al., 2007; Krieg et al., 2013). It's possible that these specific primary antibodies used in the western blots do not recognise the unique 12*R*-LOX peptide

sequence in the human skin sample control. Highlighted in **Figure 3.6.1** are the differences in amino acids in the peptide sequences of human and mouse 12*R*-LOX orthologues.

Human 12*R*-LOX peptide sequence

```
MATYKVRVATGTDLLSGTRDSISLTIVGTQGESHKQLLNHFGRDFATGAVGQYTVQCPQD
LGELIIIRLHKERYAFFPKDPWYCNYVQICAPNGRIYHFPAYQWMDGYETLALREATGKT
TADDSLPVLLEHRKEEIRAKQDFYHWRVFLPGLPSYVHIPSYRPPVRRHRNPNRPEWNGY
IPGFPILINFKATKFLNLNLRYSFLKTASFFVRLGPMALAFKVRGLLDCKHSWKRLKDIR
KIFPGKKSVVSEYVAEHWAEDTFFGYQYLNGVNPGLIRRCTRIPDKFPVTDDMVAPFLGE
GTCLQAELEKGNIYLADYRIMEGIPTVELSGRKQHHCAPLCLLHFGPEGKMMPIAIQLSQ
TPGPDCPIFLPSDSEWDWLLAKTWVRYAEFYSHEAIAHLLETHLIAEAFCLALLRNLPMC
HPLYKLLIPHTRYTVQINSIGRAVLLNEGGLSAKGMSLGVEGFAGVMVRALSELTYDSLY
LPNDFVERGVQDLPGYYYRDDSLAVWNALEKYVTEIITYYYPSDAAVEGDPELQSWVQEI
FKECLLGRESSGFPRCLRTVPELIRYVTIVIYTCSAKHAAVNTGQMEFTAWMPNFPASMR
NPPIQTKGLTTLETFMDTLPDVKTTCITLLVLWTLSREPDDRRPLGHFPDIHFVEEAPRR
SIEAFRQRLNQISHDIRQRNKCLPIPYYYLDPVLIENSISI
```

Mouse 12*R*-LOX peptide sequence

```
MATYKVKVATGTDFFSGTLDSISLTIVGTQGESHKQRLNHFGRDFATGAVDDYTVQCQQD
LGELIIIRLHKEPHSFLAKDPWYCNYVQICAPDCRVYHFPAYQWMDGYETLALREATGKI
TADDTLPILLEHRQEEIRAKKDFYHWRVFVPGLPNYVDIPSYHPPPRRCRNPNRPEWDGY
IPGFPILINIKATRFLNSNLRFSFVKTASFFYRLGPMALAFKLRGLVDRKRSWKRLKDIK
NIFPATKSVVSEYVAEHWTEDSFFGYQYLNGINPGLIRRCTQIPDKFPVTDEMVAPFLGE
GTCLQAELERGNIYLADYRILDGIPTVELNGQQQHHCAPMCLLHFGPDGNMMPIAIQLSQ
TPGPDCPIFLPNDSEWDWLLAKTWVRYAEFYSHEAVAHLLESHLIGEAFCLALLRNLPMC
HPLYKLLIPHTRYNVQINSIGRALLLNKGGLSARAMSLGLEGFAQVMVRGLSELTYKSLC
IPNDFVERGVQDLPGYYFRDDSLAVWYAMERYVTEIITYYYPNDAAVEGDPELQCWVQEI
FKECLLGRESSGFPTCLRTIPELIEYVTMVMYTCSARHAAVNSGQLEYTSWMPNFPSSMR
NPPMQTKGLTTLQTYMDTLPDVKTTCIVLLVLWTLCREPDDRRPLGHFPDIHFVEEGPRR
SIEAFRQNLNQISHNIRQRNKCLTLPYYYLDPVLIENSISI
```

Figure 3.6.1 12*R*-LOX peptide sequence of human and mouse orthologues. (Sequence obtained from ALOX12B - Arachidonate 12-lipoxygenase, 12R-type - Homo sapiens (Human) - ALOX12B gene & protein (uniprot.org)and Alox12b - Arachidonate 12-lipoxygenase, 12R-type - Mus musculus (Mouse) - Alox12b gene & protein (uniprot.org) respectively).

3.6.2 Prolonged culturing of HaCaT cells may induce the expression of the 12*R*-LOX protein

The 12*R*-LOX protein expression could not be identified in any of the HaCaT cells cultured in different Ca^{2+} concentrations of 0.03 mM, 1.8 mM and 2.8 mM, suggesting that the 12*R*-LOX protein is likely not be expressed at these specific concentrations. Prolonged culturing and exposure of HaCaT cells in the higher Ca^{2+} concentrations of 1.8 mM and 2.8 mM may have allowed cells to reach a stage of greater differentiation, thus allowing the detection of the 12*R*-LOX protein. These specific Ca^{2+} concentrations are selected to induce specific changes to mimic the stratified layers of the epidermis and this is the hypothesised localisation of the 12*R*-LOX protein. HaCaT cells may not have been significantly differentiated to allow for 12*R*-

LOX protein detection following their culturing in different Ca^{2+} concentrations of 0.03 mM, 1.8 mM and 2.8 mM. Moreover, the prolonged culturing of HaCaT cells would result in a greater cell count and protein quantity which may facilitate the detection of the 12*R*-LOX protein. However, cell cycle arrest and apoptosis is likely to occur when allowing cells to exceed confluence due to limited nutrient and supplement availability (Wright Muelas et al., 2018). Moreover, alterations in gene expression is known to occur in keratinocytes in *in vitro* models when cells reach a higher confluence (Lai and Pittelkow, 2004). For silencing experiments, this may influence the resulting protein expression changes and show differences not solely caused by the downregulation of LOX, however, collecting cells at a greater confluence could mimic the tight and compact cell-cell junction's characteristic of the stratified layers of the epidermis where 12*R*-LOX is hypothesised to be localised.

3.6.3 The use of the alternative hTERT immortalized primary keratinocyte cell line did not result in the detection of the 12*R*-LOX protein

As the presence of 12*R*-LOX could not be determined in the HaCaT cell line, the hTERT primary keratinocyte cell line was chosen as an alternative route of investigation as it is more biologically comparable to primary keratinocytes, genetically stable and retain the same protein expression profiles over prolonged periods of subculturing (Smits et al., 2017). Due to such advantages, it was deemed as an appropriate and suitable *in vitro* model for investigating 12*R*-LOX presence. Moreover, the hTERT keratinocyte cell line is shown to undergo differentiation as demonstrated in **Figure 3.5.11** and **Figure 3.5.12** by the expression of key epidermal markers such as involucrin during the characterisation of the hTERT cell line. This is important as 12*R*-LOX is hypothesised to be expressed in differentiated keratinocytes.

Here, it was shown that the 100% confluence growth of hTERT cells induced moderate differentiation as demonstrated by the significant expression of *Ivl*. 12*R*-LOX protein was not detected in hTERT cells grown to a confluence of 30% as expected or at the hypothesised differentiated 100% confluence, suggesting that the 12*R*-LOX epidermal protein is not detectable at this induced differentiated state. Similar to the experiments performed in HaCaT cells, optimisation of the western blot protocol in the detection of 12*R*-LOX protein expression was performed. These included increasing the protein quantity, prolonged incubation with the 12*R*-LOX primary antibody and a more concentrated 12*R*-LOX primary antibody dilutions. These alterations did not result in the detection of the 12*R*-LOX protein in the hTERT cell line.

The literature suggests that 12*R*-LOX expression is predominantly found in stratified layers of the epidermis, but the exact localisation of 12*R*-LOX is yet to be determined (Tyrrell

et al., 2021). That is, the 12*R*-LOX protein could be expressed anywhere from the lower granular layer to the upper cornified layer of the epidermis. hTERT cells collected at 30% and 100% confluence may only represent a defined area of the epidermis that does not express 12*R*-LOX. hTERT cells collected at different confluence could be further investigated for the presence of 12*R*-LOX. It's possible that 12*R*-LOX expression may only be expressed in significantly differentiated layers of the epidermis and hTERT cells collected at 100% confluence are not differentiated enough for 12*R*-LOX to be expressed. As such, once hTERT cells reach a 100% confluence, these could be cultured an additional 2-3 days and then collected and investigated for 12*R*-LOX protein expression. Allowing the keratinocyte cell line to differentiate further may facilitate and induce 12*R*-LOX expression. Previous studies involving keratinocytes have reported an increase in the expression of specific proteins such as prosaposin following prolonged culture after reaching 100% confluence (Yamamoto-Tanaka et al., 2014). Other studies have also shown that mRNA expression levels of an epidermal transcription factor known as MAF BZIP transcription factor B is also greater in keratinocytes at 120% confluence than in keratinocytes collected at a 100% confluence (Miyai et al., 2016). Again, the lack of 3D environment allowing specific cell-cell interaction could also be a limiting factor in 12*R*-LOX expression.

3.6.4 LC-MS analysis shows low levels of 9-HODE and 9R,10R,13R-TriHOME products of 12*R*-LOX and eLOX-3 pathway in hTERT cells

Further analysis by LC-MS was performed to determine whether 12*R*-LOX and eLOX-3 products, C32 9-HODE and 9R,10R,13R-TriHOME acyl ceramides were present in the hTERT cell line. If 12*R*-LOX was present and enzymatically active within hTERT cells, it should be clear from chromatographic data of the presence of both C32 9-HODE and 9R,10R,13R- TriHOME acylceramide compounds. It is the 9R,10R,13R-TriHOME terminal product of 12*R*- LOX / eLOX-3 in which their role in skin homeostasis and in skin disorders is yet to be fully understood. The LC-MS data shows very low levels of 9-HODE and 9R,10R,13R-TriHOME in hTERT cells at 30% and 100% confluence and would not pass the LOD. As aforementioned, hTERT cells may not be in a differentiated state where the 12*R*-LOX protein may possibly be expressed. As such, this may explain the low levels of 9-HODE and 9R,10R,13R-TriHOME observed as the hTERT cells collected for the LC-MS analysis are not sufficiently differentiated and subsequently lacks 12*R*-LOX activity needed to generate C32 9-HODE and 9R,10R,13R-TriHOME acylceramides.

3.7 Conclusion

Following multiple attempts of optimisation, western blotting did not detect the presence of the 12*R*-LOX protein in two separate keratinocyte cell lines, namely the HaCaT and hTERT primary keratinocyte cell lines. The HaCaT and hTERT keratinocyte cell lines were cultured in different Ca^{2+} concentrations and confluence to induce the proliferative and differentiated states that is present within the epidermis. Furthermore, LC-MS analysis of C32 9-HODE and 9R,10R,13R-TriHOME acylceramides in hTERT cell line revealed low levels in the investigated samples. As such, progressing to silencing of the 12*R*-LOX protein without confirming its presence in both these keratinocyte cell models would not be feasible as it would not be possible to confirm whether downregulation of the 12*R*-LOX protein was successful. Instead, 12*R*-LOX deficient mouse models can be utilised to determine and characterise the regulation of gene expression in the epidermis by 12*R*-LOX lipids such as C32 9R,10R,13R-TriHOME acylceramide terminal product of 12*R*-LOX / eLOX-3 pathway. A global screening approach known as RNA-sequencing can then be performed to determine changes in gene expression and possible biological processes in which these genes are thought to regulate. These mouse model results could be further extrapolated and specific genes of interest further studied in human skin.

Chapter 4

Global transcriptome analysis of the 12*R*-LOX deficient mouse model

4.1 Introduction

Engineering of the 12*R*-LOX deficient mice models was performed at the University of Erlangen by utilising the Cre-*loxP* system. This specific technology is widely used in the research community for deletion of genes due to its simple manipulation technique. The technique utilises a Cre recombinase enzyme that specifically recognises and subsequently excises two *loxP* sites that flank the gene of interest. This method requires a mouse strain expressing the Cre recombinase enzyme and a second mouse strain with the gene of interest flanked by *loxP* sites. Knockout models are then produced through subsequent breeding of both these strains (Kim et al., 2018).

The 12*R*-LOX deficient model developed by Krieg et al., 1999 has been used previously to demonstrate the importance of the 12*R*-LOX protein in the formation of an effective epidermal barrier. Previous studies performed utilising 12*R*-LOX deficient mice included barrier-dependent dye exclusion assay that revealed defective barrier formation resulting in neonatal death because of rapid transepidermal water loss. Further investigation of 12*R*-LOX deficient mouse skin revealed structural differences in the upper layers of the epidermis when compared with the control. An irregular lipid content was also observed in 12*R*-LOX deficient mouse models, with significant changes in lipid species bound to the cornified envelope. In conjunction with these findings, 12*R*-LOX deficient mice exhibited enhanced fragility of cornified envelopes located in the upper most layers of the epidermis (Epp et al., 2007).

RNA-sequencing is a revolutionizing method in the field of medical research that is used to provide an invaluable understanding into the transcriptome of a cell or tissue (Hrdlickova et al., 2016). A transcriptome is described as the total sum of messenger RNA (mRNA) transcripts that are expressed in a cell or tissue for a physiological disorder or at a specific stage of organism development (Wang et al., 2010; Wang et al., 2019). Initial steps of an RNA-sequencing study include RNA extraction, enrichment of mRNA, synthesis of cDNA and finally the construction of a sequencing library. The prepared library is then sequenced on a high-throughput instrument to the desired read depths, usually 10-30 million reads per condition. Read depth is defined as the average number of times a specific nucletide in a genome has been read or represented in a defined experiment (Sims et al., 2014). Following platform sequencing of the samples, computational work is performed to align the reads to a transcriptome, quantifying the number of reads and conducting normalization between samples being investigated (Stark et al., 2019). Advantages of RNA-sequencing over traditional sequencing techniques such as Sanger-sequencing and microarray include a greater detail,

higher coverage and resolution of the transcriptome under investigation. Furthermore, low background signals and highly accurate gene expression results are observed in RNA-sequencing studies in comparison with DNA microarray technologies. This is due to the DNA being specifically mapped to the transcriptome, thus reducing possible high background (Nagalakshmi et al., 2008). Moreover, high reproducibility and substantially less RNA sample required are additional benefits of RNA-sequencing (Wang et al., 2019).

Gene expression studies are primarily performed to determine differential gene expression through utilising complex statistical approaches. A gene is identified as a differentially expressed gene (DEG) during the analysis of RNA-sequencing data if changes in the level of expression for a given gene, between two conditions are statistically significant. Selection of fold change is arbitrary, however, the majority of RNA-sequencing studies employ fold change ratio values of between >1.5 and >2.0 (McCarthy et al., 2009; Dalman et al., 2012). Common statistical tools specifically used in the identification of differentially expressed genes include Cufflinks, Tophat and Bowtie (Trapnell et al., 2012). Supporting these statistical packages for differentially expressed genes include DESeq, DEGseq and edgeR (Robinson et al., 2009; Anders and Huber, 2010).

RNA-sequencing also allows identification of transcriptional factors, spliced genes and the detection of previously undiscovered transcripts (Kukurba and Montgomery, 2015). Prior to advances in sequencing techniques, low throughput technologies such as quantitative polymerase chain reaction (qPCR) were utilised to determine changes in gene expression. Limitations of these technologies included the ability to only measure single transcripts and inaccurate quantification of highly and lowly expressed genes, whilst recent developments in the field of genome sequencing allowed global quantification of the entire genome. Improvements in sample preparation, sequencing instruments and bioinformatics platforms has resulted in a more in-depth analysis of the transcriptome along with identifying genes underlying pathological disorders (Kukurba and Montgomery, 2015).

Whilst knockout models have been used extensively to study the transcriptome of other skin disorders such as atopic dermatitis and psoriasis over the past decade, investigation into the transcriptome of 12*R*-LOX inactivation has yet to be investigated. Other knockout mice models exhibiting skin barrier defects include the krüpel-like factor 4, claudin and E-cadherin knockout mice models (Segre et al., 1999; Furuse et al., 2002; Tunggal et al., 2005). In comparison with these knockout mice models possessing a defective epidermal barrier, the 12*R*-LOX phenotype displays the most severe phenotype with excessive water loss leading to premature death. Examination of changes in the transcriptome in response to 12*R*-LOX protein

deficiency have not been fully investigated and this study would elucidate possible molecular mechanisms, pathways and functions underlying skin barrier diseases such as ichthyosis, along with an understanding on how 12*R*-LOX derived lipids regulates skin physiology.

4.2 Aim

- Identify molecular mechanisms and epidermal processes affected following *Alox12b* gene knockout that encodes 12*R*-LOX, and the likely lipid effect on the regulation of skin physiology and pathways underlying skin barrier disorders.

4.3 Objectives

- Evaluate and compare the expression profiles of each respective condition used in this experiment, including 12*R*-LOX deficient mice and wildtype mice.
- Explore the localisation of differentially expressed genes (DEGs) in the epidermis.
- Explore which biological processes, molecular processes and cellular compartments the DEGs of 12*R*-LOX deficient mice are associated with.
- Explore whether DEGs belong to a specific epidermal family of proteins and characterise their function in the epidermis.

4.4 Materials and methods

Generation of *Alox12b* knockout mouse models encoding 12*R*-LOX and validating the 12*R*-LOX deficient mouse models is described in **Section 2.5.1** and **2.5.2**. Isolation of 12*R*-LOX and wildtype mouse skin and the total RNA extraction protocol is described in **Section 2.5.3**. Experimental design of the 12*R*-LOX deficient vs wildtype RNA-sequencing study is described in **Section 2.5.4**. Identification of differentially expressed genes (DEGs) in the 12*R*-LOX deficient vs wildtype dataset is described in **Section 2.5.5**.

4.4.1 RNA quality and quantity determination

The RNA concentration and purity were measured using the Nanodrop spectrophotometer (Thermo Scientific, USA) along with the total amount of RNA (ng/µl). The purity was evaluated based on the A260/A230 and A260/A280 ratio. A sample of RNA deemed as "pure" should have an A260/280 ratio value of 1.8-2.1 and an A260/A230 ratio value of 2.0-2.3 (Desjardins and Conklin, 2010).

4.4.2 Principal component analysis (PCA)

To determine variables within the RNA-sequencing dataset and allow ease of data visualisation, a statistical software known as principal component analysis (PCA) was employed. This was performed with the aid of our in-house bioinformatician, Dr Robert Andrews. Similar transcriptome profiles should be observed in each respective condition (12*R*-LOX deficient and wildtype) as skin was the only form of tissue extracted for this study and not any other form of tissue. If the latter was the case, we would possibly expect different expression profiles. Additionally, it is preferable that all samples are subject to RNA-sequencing analysis at the exact same time. If this is not done in a timely manner and samples are run on different days for example, we would expect greater variability in these transcriptomes.

4.4.3 Identification of differentially expressed genes found in human skin

A literature search was performed using protein sequence and function databases such as UniProt, National Centre for Biotechnology Information (NCBI), Ingenuity Pathway Analysis (IPA) and human protein atlas in an attempt to determine the localisation and/or the linking of both upregulated and downregulated genes in the 12*R*-LOX deficient vs WT dataset to specificlayers of the epidermis.

4.4.4 Gene ontology (GO) enrichment analysis

GO enrichment analysis is a gene function classification system in which its purpose is to map DEG with GO terms in its database (https://www.pantherdb.org/). It is a tool categorised into three classes that include biological process, molecular function and cellular component. To annotate genes with terms from the GO database, DEG of interest (ENSEMBL ID) were imported into the "Term Enrichment Service" and was subsequently mapped to GO terms in the database. During this process, *mus musculus* is selected as mouse models were used in this study. The GO enrichment analysis will yield the number of genes in the selected DEGs dataset with the GO term. p values < 0.05 were taken as significantly enriched by DEGs. The enrichment aspect of the software shows the degree of significance of a biological function. The fold enrichment term is defined as how many more fold a biological process, molecular function or cellular compartment has occurred than would be expected randomly. For example, a fold enrichment value of 4 would indicate that a biological process, molecular function or cellular compartment has occurred four times as much than what would be expected by random chance. GO was also utilised for protein classification of DEGs.

A biological process is defined as the occurrence of molecular activities resulting in a change or a range of changes to a cell or organism (Hill et al., 2008). For example, molecular activities in an embryo resulting in the development of an arm would be stated as “limb development”. A molecular function is defined as the potential activities of a gene on a molecular level such as protein binding or catalysing. For example, the *Adh1* gene has the potential to catalyse the conversion of alcohol to an aldehyde or ketone molecule. A cellular compartment is defined as the region of the cell where a gene is located relative to a cellular structure in the organism (e.g. ribosome, golgi apparatus, cytoplasm etc.)

Each enriched biological process, molecular function and cellular compartment has a unique number of genes in the genome that are associated with each generated GO enrichment term.

4.5 Results

4.5.1 Evaluation of RNA quality and quantity

The A260/A280 ratio of all 12*R*-LOX deficient and wildtype samples have similar values and are within the "pure" RNA A260/A280 range of 1.8-2.1 as described in **Section 4.4.2** (Desjardins and Conklin, 2010). Wildtype sample 9 has the lowest A260/A280 value at 2.01, whilst 12*R*-LOX deficient samples 2 and 5 have the highest A260/A280A values. All 12*R*-LOX deficient and wildtype samples possess A260/A230 values ranging from 2.13-2.29. **Table 4.5.1** shows the lowest A260/A230 value is associated with 12*R*-LOX deficient sample 5 and the highest A260/A230 value is associated with 12*R*-LOX deficient sample 3. Sufficient quantity of RNA was obtained from all 12*R*-LOX deficient and wildtype samples required to progress to RNA-sequencing following the RNA extraction. 12*R*-LOX deficient sample 5 is found to have the lowest quantity of RNA with a value of 523.1 ng/µl, whilst wildtype sample 7 has the greatest quantity of RNA with a value of 1325.7 ng/µl.

Sample no.	Genotype	A260/A230	A260/A280	Quantity of RNA (ng/µl)
1	KO	2.24	2.03	700.1
2	KO	2.21	2.08	1124.2
3	KO	2.29	2.07	1015.4
4	KO	2.18	2.06	1315.3
5	KO	2.13	2.08	623.1
6	KO	2.23	2.04	644.8
7	WT	2.2	2.07	1325.7
8	WT	2.17	2.05	1041.3
9	WT	2.19	2.01	636.7

Table 4.5.1 Evaluation of the quantity and quality of RNA isolated from 12*R*-LOX deficient mice (n=6) and wildtype mice (n=3). A260/A230 and A260/A280 provide an assessment of RNA purity. Pure RNA is deemed to have an A260/A280 value of 1.8-2.1 and an A260/A230 value of 2.0-2.3. The standard quantity of RNA required for RNA-sequencing library construction is 100 ng – 1 µg.

4.5.2 Gene expression characteristics of 12*R*-LOX deficient and wildtype samples

Principal component analysis (PCA) as described in **Section 4.4.2** was performed on the 12*R*-LOX deficient vs wildtype dataset to assess similarities and variation in gene expression. **Figure 4.5.1** confirms that the 12*R*-LOX deficient samples 186-1, 186-2, 186-3 and 186-4 are all similar in relation to their expression profile as indicated by their close proximity. The other 12*R*-LOX deficient samples (149-1 and 149-2) are located slightly further from the cluster that includes 186-1, 186-2, 186-3 and 186-4. A possible reason for this slight variation is that 12*R*-LOX deficient samples 149-1 and 149-2 were extracted at a later date and slight variation in experimental procedure and conditions may have contributed to this. **Figure 4.5.1** shows wildtype samples 149-6 and 186-9 are clustered close together, whilst wildtype sample 149-7 is situated slightly further apart in the gene expression PCA plot. Whilst all animals were bred and treated consistently, a slight variation between samples is common.

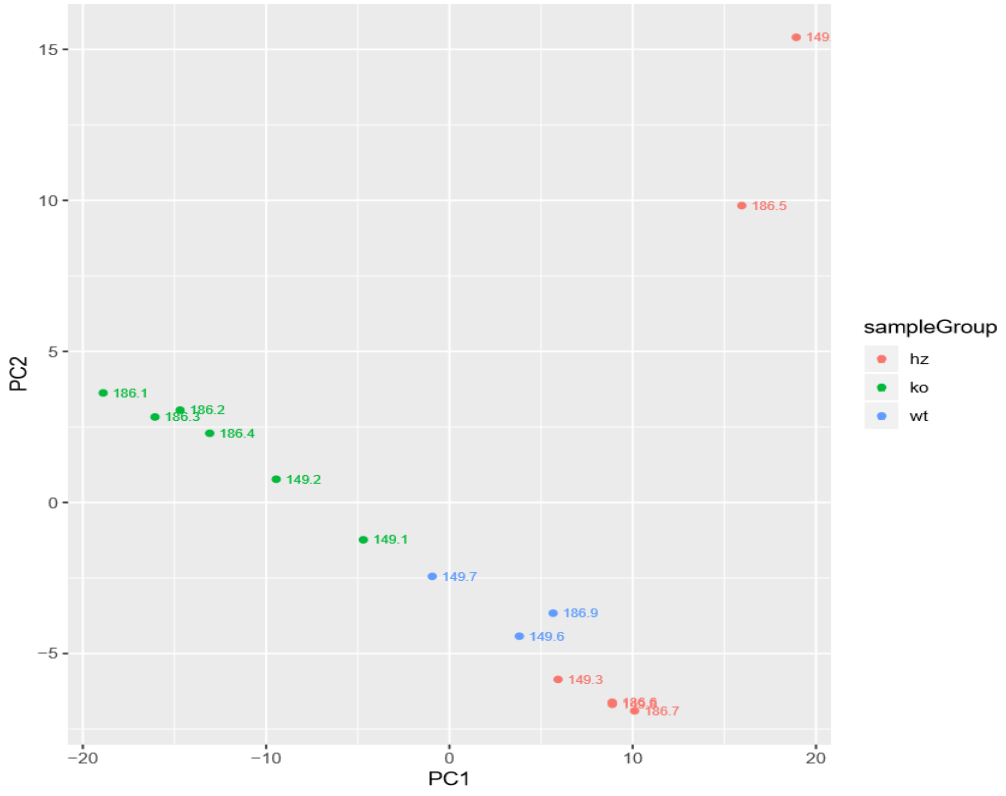

Figure 4.5.1 Evaluating similarities and variations in gene expression patterns in the 12*R*-LOX deficient dataset using principal component analysis (PCA) method. Plots were generated according to gene expression levels measured in fragments per kilobase of transcript per million mapped reads (FPKM). This PCA plot shows features of each individual sample (12*R*-LOX deficient and wildtype) which are represented as dots. Sample I.D's in GREEN = knockout; sample I.D's in BLUE = wildtype and sample I.D's in RED = Heterozygous.

4.5.3 Majority of DEGs are upregulated in response to 12*R*-LOX deficiency

A total of 193 differentially expressed genes was identified following investigation and analysis of the 12*R*-LOX deficient vs wildtype dataset. Of the 193 differentially expressed genes, 141 of these genes was identified as being upregulated (≥ 1.5-FC), whilst 52 of these genes was identified as being downregulated (≤ 1.5-FC) out of 22,048 protein coding transcripts. This equates to 0.6% of the entire genome being upregulated and 0.2% of genes in the genome being downregulated (The complete list of differentially expressed genes is provided in **Appendix 3**).

4.5.4 Upregulated genes in response to 12*R*-LOX deficiency are localised in upper layers of the epidermis

Figure 4.5.2 shows the majority of upregulated genes in the 12*R*-LOX deficient dataset are predominantly found to be expressed in the outer most layers of the epidermis, which includes the stratum granulosum and stratum corneum. 30 upregulated genes in the 12*R*-LOX deficient dataset are known to be expressed in the stratum corneum, whilst 19 of the upregulated genes are known to be expressed in the stratum granulosum and examples include small proline-rich protein 1b (*Sprr1b*), small proline-rich protein 2d (*Sprr2d*), late cornified envelope 3F (*Lce3f*), keratin 10 (*Krt10*), keratin 16 (*Krt16*), keratin 6b (*Krt6b*) and keratinocyte differentiation associated protein (*Krtdap*) (Strudwick et al., 2014; Zhang et al., 2019; Lefèvre-Utile et al., 2021). These genes are of interest as they are commonly expressed in human skin. Most upregulated differentially expressed genes that are expressed in the stratum corneum include members of the epidermal differentiation complex and keratin proteins. Keratin 24 (*Krt24*) and lymphocyte antigen 6 family member D (*Ly6d*) are two upregulated genes which are found to be expressed in the stratum spinosum region of the epidermis (Min et al., 2017; Cheng et al., 2018). Investigation into the upregulated genes with known basal layer expression revealed the presence of only one proliferative marker, keratin 14 (*Krt14*) (Sümer et al., 2019).

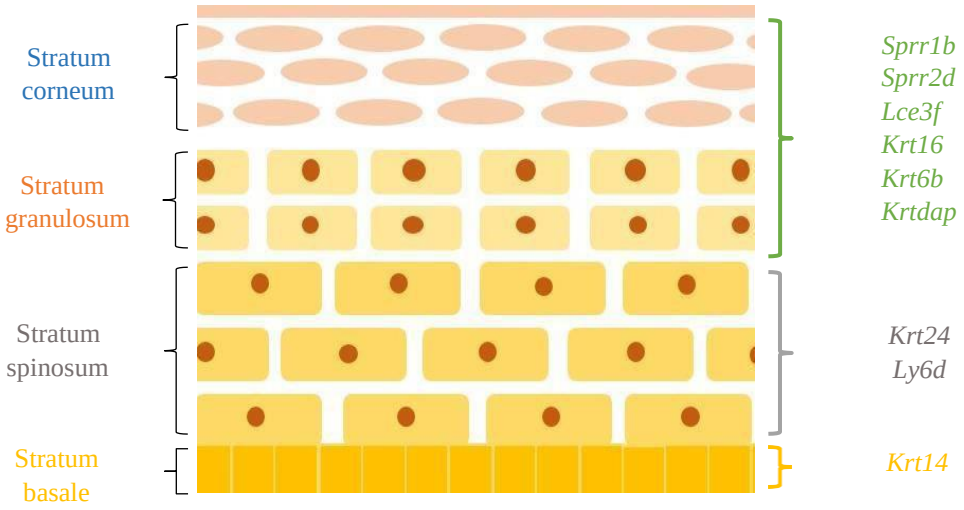

Figure 4.5.2 Epidermal layers in which upregulated genes of the 12*R*-LOX deficient dataset are known to be expressed in. Diagram of the epidermis showing the four main layers and the localisation of upregulated genes (≥1.5-fold change) of the 12*R*-LOX deficient dataset.

4.5.5 Significantly lower number of downregulated genes of the 12*R*-LOX deficient dataset are commonly found in the epidermis

Figure 4.5.3 shows stratified layers of the epidermis such as the stratum granulosum and stratum corneum having the greatest number of downregulated genes and include peroxisome proliferator-activated receptor gamma coactivator 1-alpha (*Pparγc1a*) where its expression occurs (Ramot et al., 2015). This gene is of interest as it interacts and increases the transcriptional activity of peroxisome proliferator-activated receptor gamma (*Pparγ)* which is thought to be implicated in the development of a functional epidermal barrier (PPARGC1A - Peroxisome proliferator-activated receptor gamma coactivator 1-alpha - Homo sapiens (Human) - PPARGC1A gene & protein (uniprot.org)). The downregulated *Klk1* gene is found in the stratum spinosum/stratum basale layer of the epidermis (Nauroy et al., 2020).

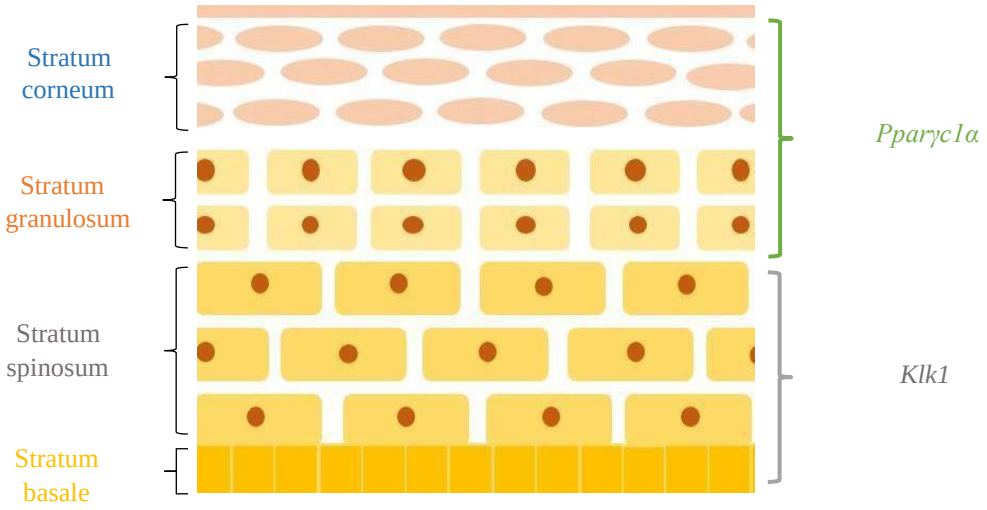

Figure 4.5.3 Epidermal layers in which downregulated genes of the 12*R*-LOX deficient dataset are known to be expressed in. Diagram of the epidermis showing the four main layers and the localisation of downregulated genes (≤1.5-fold change) of the 12*R*-LOX deficient dataset.

4.5.6 Epidermal processes associated with upregulated genes in the 12*R*-LOX deficient dataset following Gene Ontology enrichment analysis

4.5.6.1 Biological processes

A description of *biological processes* is described in **Section 4.4.5**. **Table 4.5.2** shows the top five most significantly enriched *biological processes* amongst the 141 upregulated genes include GO terms such as "cornification", "keratinization", "keratinocyte differentiation", "mononuclear cell migration" and "peptide cross-linking". Fold enrichment indicates how many more times the *biological process*, *molecular function* or *cellular component* are enriched for upregulated genes of the 12*R*-LOX deficient dataset. The *biological process* with the greatest fold enrichment for upregulated genes of the 12*R*-LOX deficient dataset is "peptide cross-linking". **Figure 4.5.4** shows the *biological process* with the greatest number of upregulated genes (≥ 1.5-FC) is "keratinocyte differentiation", whilst the "peptide cross-linking" enriched process has the fewest number of upregulated genes.

Table 4.5.3 shows at least 13% of those genes involved in "mononuclear cell migration" are upregulated (≥ 1.5-FC) in the 12*R*-LOX deficient vs wildtype dataset. This is closely followed by the "cornification" and "peptide cross-linking" processes where 12% of upregulated genes for both these processes are significantly upregulated as a result of 12*R*-LOX knockdown. **Table 4.5.3** shows the top enriched *biological process* with the greatest number of genes affected in response to 12*R*-LOX knockdown is "mononuclear cell migration", followed by "cornification" and "peptide cross-linking".

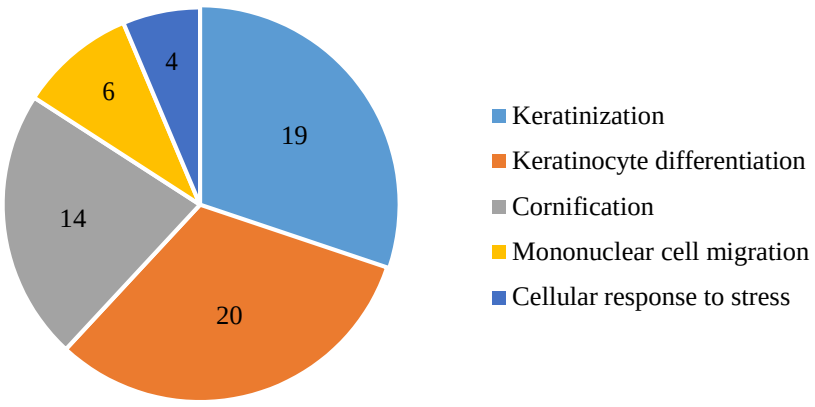

Figure 4.5.4 Gene ontology (GO) enrichment analysis summary of upregulated genes of the 12*R*-LOX deficient dataset. Number of upregulated genes associated with each enriched *biological process*.

4.5.6.2 Molecular functions

A description of *molecular function* is described in **Section 4.4.5**. **Table 4.5.2** shows that the top five enriched *molecular functions* for upregulated genes in the 12*R*-LOX deficient dataset include "receptor regulator activity", "enzyme binding", "purine ribonucleotide binding", "RNA binding" and "protein binding". **Table 4.5.3** shows the *molecular function* with the greatest fold enrichment for upregulated genes of the 12*R*-LOX deficient dataset is "receptor regulator activity". **Figure 4.5.5** shows the "protein binding" *molecular function* has the greatest number of upregulated genes out of the enriched *molecular functions*, whilst the *molecular function* with the fewest number of upregulated genes is "RNA binding".

Table 4.5.3 shows 3% of genes involved in the "receptor regulator activity" enriched *molecular function* are upregulated in response to 12*R*-LOX deficiency. **Figure 4.5.5** shows upregulated genes in the 12*R*-LOX deficient vs wildtype dataset that are associated with enriched "enzyme binding", "purine ribonucleotide binding", "RNA binding" and "protein binding" functions have a lower percentage of genes involved in these respective *molecular functions* in comparison with "receptor regulator activity". The top enriched *molecular function* term with the greatest number of significantly upregulated genes is "receptor regulator activity", followed by "protein binding" as shown in **Table 4.5.3**.

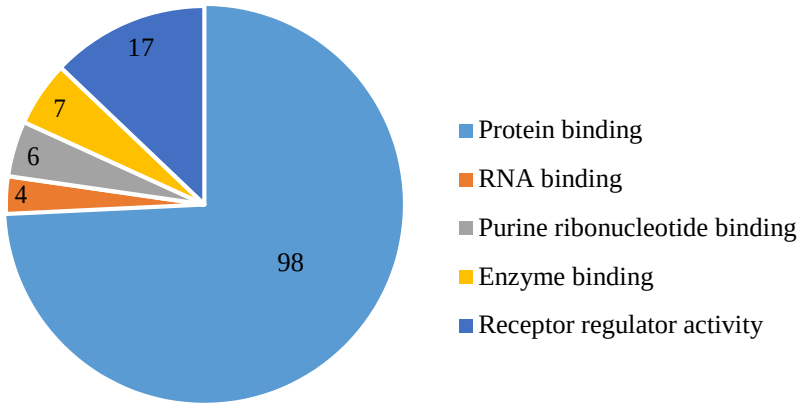

Figure 4.5.5 Gene ontology (GO) enrichment analysis summary of upregulated genes of the 12*R*-LOX deficient dataset. Number of upregulated genes associated with each *molecular function*.

4.5.6.3 Cellular compartments

A description of *cellular compartment* is described in **Section 4.4.5**. Investigation was also performed to identify the most significantly enriched *cellular compartments* using the GO enrichment analysis tool. **Table 4.5.2** shows the top five most significantly enriched terms associated with upregulated genes for *cellular compartment* is "nucleoplasm", "cornified envelope", "keratin filament", "catalytic complex" and "cytosol". **Table 4.5.3** shows the *cellular compartment* with the greatest fold enrichment for upregulated genes of the 12*R*-LOX deficient dataset is "cornified envelope". **Figure 4.5.6** shows the *cellular compartment* with the greatest number of upregulated genes is the "cytosol" compartment, whilst the "catalytic complex" has the fewest number of genes.

Table 4.5.3 shows the greatest percentage of genes affected for the enriched *cellular compartment* term is the "cornified envelope" where 18% of genes are upregulated in the 12*R*-LOX deficient dataset. The "keratin filament" enriched *cellular compartment* has a total of 7% of genes that are significantly upregulated.

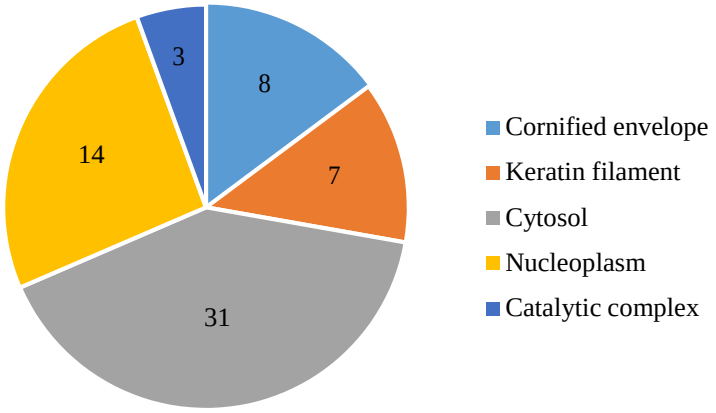

Figure 4.5.6 Gene ontology (GO) enrichment analysis summary of upregulated genes of the 12*R*-LOX deficient dataset. Number of upregulated genes (> 1.5-FC) associated with each *cellular compartment*.

GO biological process	Mapped IDs
Mononuclear cell migration	*Xcl1, Ccl20, Hist1h2ba, Sis, Ccl17, Ccl8*
Cornification	*Lipn, Rptn, Krt6b, Sprr2d, Sprr2e, Krt14, Krt16, Sprr1b, Krt10, Lce3d, Krt24, Klk14, Sprr2g, Krt1*
Keratinization	*Lipn, Rptn, Krt6b, Sprr2d, Krtap9-1, Sprr2e, Krt14, Lce3e, Krt16, Sprr1b, Krt10, Lce3d, Cnfn, Krt24, Klk14, Krtap4-8, Krtap5-4, Sprr2g, Krt1*
Keratinocyte differentiation	*Lipn, Rptn, Krt6b, Sprr2d, Krtap9-1, Sprr2e, Krt14, Lce3e, Krt16, Sprr1b, Krt10, Ereg, Lce3d, Cnfn, Krt24, Klk14, Sprr2g, Krtap4-8, Krtap5-4, Krt1*
Peptide cross-linking	*Sprr2e, Sprr1b, Krt10, Krt1*
GO molecular function	**Mapped IDs**
Protein binding	*Dnajb8, Atoh7, Xcl1, Cryba2, Kcnj4, Il5ra, Chrnb4, Smcp, Krt6b, Ccl20, Cacng2, Adm2, Spink7, Nhlh1, Themis, Myo3A, Alox12b, Myo3a, Tex19, Skor2, Cartpt, Pglyrp3, Spata32, Ccdc87, Sprr2e, Patl2, Sult2b1, Nat8, Scgb1a1, Them5, Krt14, Lce3e, Ccdc33, Mesp2, Krt16, Il1f6, Hist1h2ba, Il1f9, Sis, Htr1a, Krt10, Ccl17, Tdh, Izumo1r, Fate1, Pou1f1, Ereg, Foxh1, Defb6, Aurkc, Ccl8, Rxfp4, Pdyn, Saa1, Gpr3, Sec14l3, Sult1c2, Psca, Trim69, Bmp10, Ferd3l, Ang2, Naa11, Skor1, Mcidas, Hand1, Hmgb4, Cldn17, Mrap2, Epha10, Pkd2l1, Msmb, Oxt, Tdh, Trat1, Stra8, Grm2, Nmu, Rfx6, Catsper1, C1ql4, Akap3, Pou4f2, Prg2, Klrc1, Saxo1, Galr1, Lhfpl5, Plpp4, Cd70, Anxa10, Htr4, Serpinb12, Six3, Krt1, Tlx3, Fosl1, Gbx2, Dll3*
RNA binding	*Tex19, Patl2, Fbll1, Pabpn1l*
Purine ribonucleotide binding	*Myo3A, Acsbg2, Aurkc, Sec14l3, Epha10, Ankk1*
Enzyme binding	*Skor2, Fate1, Hand1, Trat1, Cd70, Serpinb12, Six3*
Receptor regulator activity	*Xcl1, Ccl20, Adm2, Cartpt, Il1f6, Il1f9, Sis, Ccl17, Ereg, Ccl8, Pdyn, Saa1, Bmp10, Mrap2, Oxt, Prg2, Cd70*
GO cellular compartment	**Mapped IDs**
Cornified envelope	*Rptn, Sprr2d, Sprr2e, Sprr1b, Krt10, Cnfn, Sprr2g, Krt1*
Keratin filament	*Krt6b, Krtap9-1, Krt14, Krtap4-8, Krtap4-8, Krtap5-4, Krt1*
Cytosol	*Dnajb8, Rptn, Pla2g2f, Krt6b, Cacng2, Alox12b, Sprr2d, Gsta1, Krtap9-1, Acsbg2, Sprr2e, Sult2b1, Krt14, Krt16, Sprr1b, Krt10, Tdh, Hsd17b1, Lce3d, Sult1c2, Trim69, Ang2, Naa11, Pdyn, Krt24, Gpr142, Sprr2g, Krtap4-8, Krtap5-4, Krt1, Fosl1*
Nucleoplasm	*Fbll1, Hist1h2ba, Foxh1, Uty, Tmem92, Sec14l3, Trim69, Naa11, Mcidas, Hand1, Sox3, Pou4f2, Tlx3, Fosl1*
Catalytic complex	*Tcte3, Uty, Naa11*

Table 4.5.2 Identification of upregulated genes associated with the top 5 enriched biological process, molecular function and cellular compartment.

GO biological process	# of genes in genome	Fold enrichment	% of upregulated genes involved in biological process
Keratinization	226	7.52	8
Keratinocyte differentiation	268	6.68	8
Cornification	113	11.09	12
Mononuclear cell migration	48	11.19	13
Peptide cross-linking	34	22.93	12
GO molecular function	**# of genes in genome**	**Fold enrichment**	**% of upregulated genes involved in molecular function**
Protein binding	12129	0.72	1
RNA binding	1676	0.21	<1
Purine ribonucleotide binding	1925	0.28	<1
Enzyme binding	2259	0.28	<1
Receptor regulator activity	538	2.83	3
GO cellular component	**# of genes in genome**	**Fold enrichment**	**% of upregulated genes involved in cellular compartment**
Nucleoplasm	3975	0.32	<1
Cornified envelope	45	15.91	18
Cytosol	5210	0.55	1
Catalytic complex	1382	0.19	<1
Keratin filament	101	6.2	7

Table 4.5.3 Gene Ontology (GO) enrichment analysis summary of the upregulated genes in the 12*R*-LOX deficient dataset. The results of GO analysis were classified into three distinct categories: *biological process*, *molecular function* and *cellular compartment*. % of genes in the genome that are upregulated for each *biological process*, *molecular function* and *cellular compartment* in response to 12*R*-LOX knockdown

4.5.7 *Hist1h2ba*, *Krt6b*, *Sprr2e*, *Krt14*, *Krt16*, *Krt10* and *Krt1* upregulated genes common to biological process, molecular function and cellular compartment

Figure 4.5.7 shows a total of 63 upregulated genes of the 12*R*-LOX deficient dataset are associated with enriched *biological processes*, whilst 132 and 64 upregulated genes are associated with enriched *molecular function* and *cellular compartment* respectively. The *molecular function* and *cellular compartment* categories share the most upregulated genes, whilst *biological processes* and *molecular functions* share the fewest number of upregulated genes with 16 shared between the two respectively. There are seven genes common to *biological process*, *molecular functions* and *cellular compartment*. These include histone h2b type 1-A (*Hist1h2ba*), *Krt6b*, *Sprr2e*, *Krt14*, *Krt16*, *Krt10* and *Krt1*.

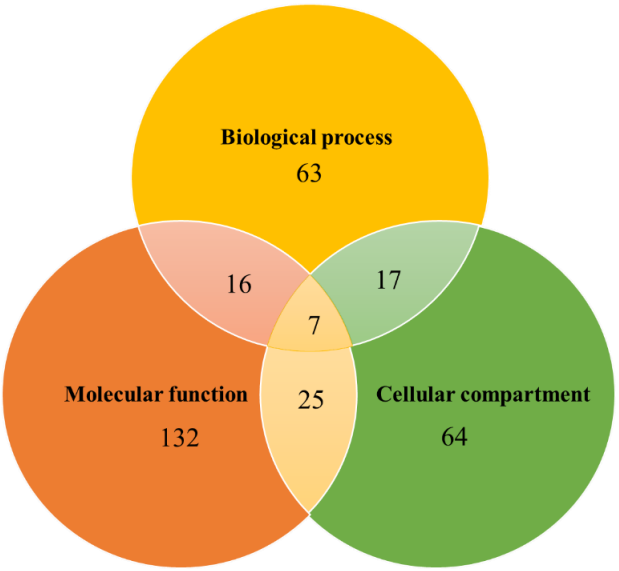

Figure 4.5.7 A Venn diagram showing the number of upregulated genes in common between biological process, molecular function and cellular compartment. The intersections show the number of genes shared between *biological process*, *molecular function* and *cellular compartment*.

Figure 4.5.8 shows a more in-depth analysis of skin relevant enriched *biological processes* where a total of 14 upregulated genes are shared between "cornification", "keratinization" and "keratinocyte differentiation". Both keratinization and keratinocyte differentiation share the greatest amount of upregulated genes with 18 for these two enriched processes. Genes enriched for all three *biological processes* include lipase family member n (*Lipn*), *Rptn*, *Krt6b*, *Sprr2d*, *Sprr2e*, *Krt14*, *Krt16*, *Sprr1b*, *Krt10*, *Lce3d*, *Krt24*, *Klk14*, *Sprr2g* and *Krt1*. Upregulated genes associated with the enriched "mononuclear cell migration" biological process are not found to be enriched for any other *biological process*. Also, of

relevance to skin biology and important in the maintenance of the epidermal barrier, is the "peptide cross-linking" biological process. Upregulated genes such as *Sprr2e*, *Sprr1b*, *Krt10* and *Krt1* proteins are also enriched for other biological processes such as "cornification" and "keratinocyte differentiation".

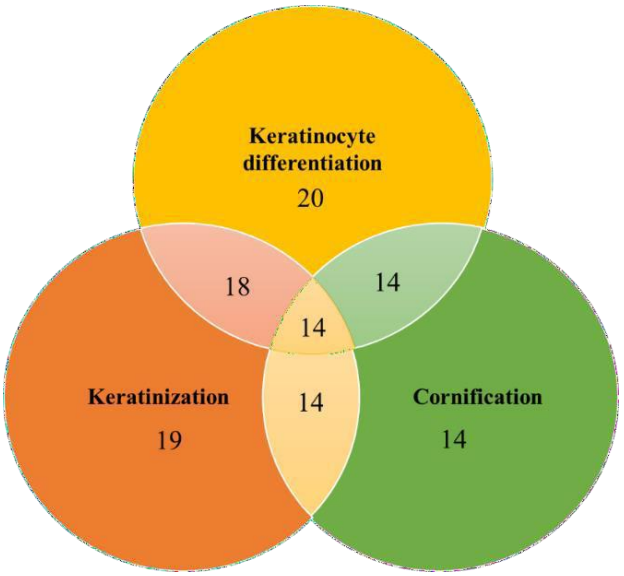

Figure 4.5.8 A Venn diagram summary of the upregulated genes in common between each enriched biological process. The enriched "cornfication" process is coloured in green with 14 upregulated genes, "keratinocyte differentiation" in yellow with 20 upregulated genes and "keratinization" in orange with 19 upregulated genes.

4.5.8 The majority of upregulated genes of the 12*R*-LOX deficient dataset associated with enriched biological processes belong to epidermal differentiation complex and keratin protein families

An investigation into the top five enriched *biological processes* reveals the majority of upregulated genes for these enriched processes belong to the epidermal differentiation complex gene cluster or keratin protein class as shown in **Figure 4.5.9**. Examples of genes that are upregulated in the 12*R*-LOX deficient dataset that belong to the epidermal differentiation complex class of proteins include all of the upregulated small proline-rich proteins and late cornified envelope proteins, along with *Rptn* and cornifelin (*Cnfn*). Other frequently observed protein classes common in the "cornification", "keratinization" and "keratinocyte differentiation" *biological processes* include lipase and serine protease protein families. The proteins attributed to these classes include *Lipn* and *Klk14*, respectively. In contrast, the histone protein family has the lowest percentage (%) share of upregulated genes.

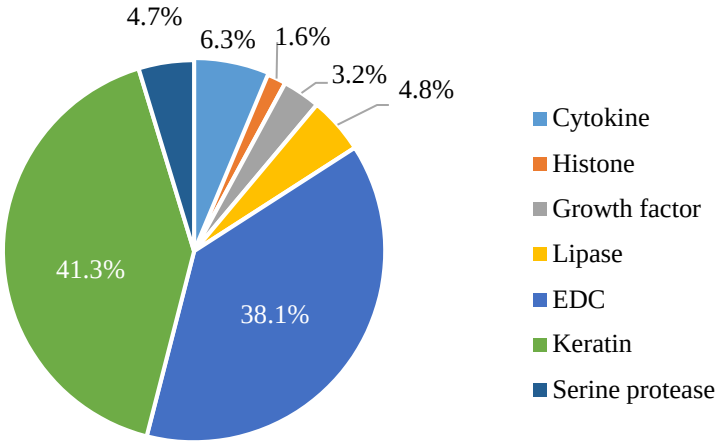

Figure 4.5.9 Protein class associated with the upregulated genes of the top five enriched biological processes. The keratin protein family has the greatest share of upregulated genes of the 12*R*-LOX deficient dataset with 41.3%, whilst the histone protein family has the lowest share of upregulated genes of the 12*R*-LOX deficient dataset with 1.6%. The different colours represent the protein classes.

The protein class of more than half of the upregulated genes for enriched *molecular functions* could not be determined and is represented as NA which can be observed in **Figure 4.5.10**. A proportion of upregulated proteins with "protein binding activity" belong to the cytokine protein class such as x-c motif chemokine ligand 1 (*Xcl1*) and c-c motif chemokine

ligand 20 (*Ccl20*). These cytokine protein class are also associated with having "receptor regulator activity" function. Other subset protein classes comprising of a smaller proportion of upregulated genes for enriched *molecular functions* include proteins belonging to "RNA processing factor", "methyltransferase" and "ligase" families.

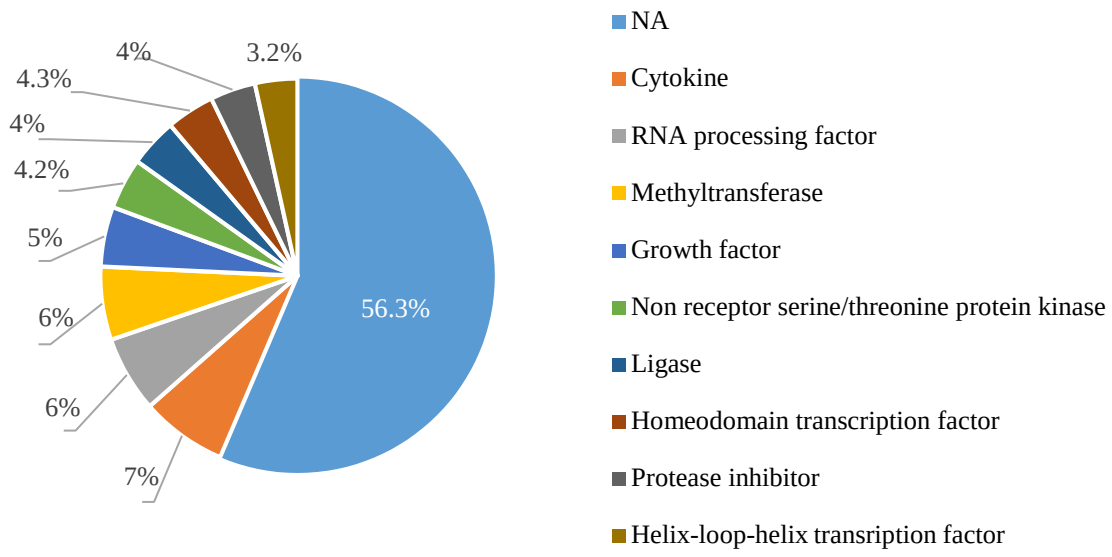

Figure 4.5.10 Protein class associated with the upregulated genes of the top five enriched molecular functions. 56.3% of upregulated genes of the 12*R*-LOX deficient dataset are regarded as NA, followed by 7% associated with the cytokine protein family. The helix-loop-helix transcription factor has the lowest share of upregulated genes of the 12*R*-LOX deficient dataset with 3.2%. The different colours represent the protein classes.

In the same way as the majority of upregulated genes for the top five enriched *biological processes* belong to the epidermal differentiation complex gene family and the keratin family of proteins, the same is true of proteins that are enriched for the top five *cellular components* as shown in **Figure 4.5.11**. For example, all proteins associated with the enriched "cornified envelope" and "keratin filament" *cellular compartments* belong to the epidermal differentiation complex, keratin and keratin associated protein class. The remaining proteins for enriched *cellular compartments* such as "nucleoplasm" and "catalytic complex" belong to other protein classes such as acetyltransferases and transcription factor families.

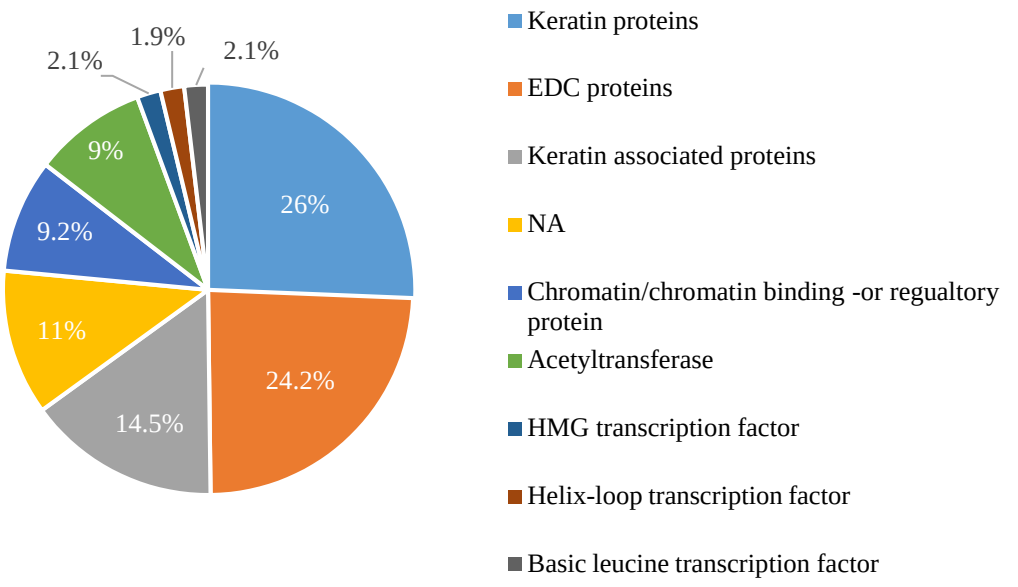

Figure 4.5.11 Protein class associated with the upregulated genes of the top five enriched cellular compartments. The keratin protein family has the greatest share of upregulated genes of the 12*R*-LOX deficient dataset with 26%, whilst the helix-loop transcription factor family has the lowest share of upregulated genes of the 12*R*-LOX deficient dataset with 1.9%. The different colours represent the protein classes.

4.5.9 Differentiation process associated with downregulated genes in the 12*R*-LOX deficient dataset

4.5.9.1 Biological processes

Identification of downregulated genes associated with each *biological process*, *molecular function* and *cellular compartment* is shown in **Table 4.5.4**. The top five significantly enriched *biological processes* amongst the 52 downregulated genes include "brown fat cell differentiation", "Positive regulation of cold-induced thermoregulation", "fat cell differentiation", "regulation of fatty acid oxidation" and "response to interleukin-6". **Table 4.5.5** shows the *biological process* with the greatest fold enrichment for downregulated genes of the 12*R*-LOX deficient dataset is "brown fat cell differentiation". Both "fat cell differentiation" and "positive regulation of cold-induced thermoregulation" have the greatest number of downregulated genes as shown in **Figure 4.5.12**. The *biological processes*, namely, "regulation of fatty acid" and "response to interleukin-6" both have the lowest number of downregulated genes as shown in **Figure 4.5.12**.

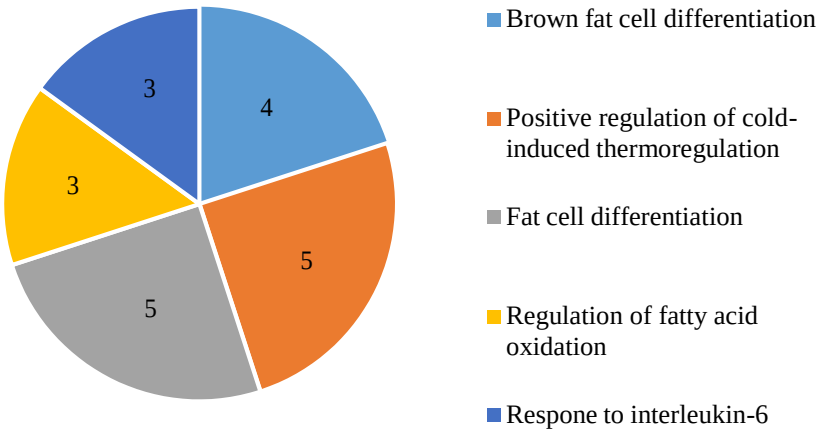

Figure 4.5.12 Gene ontology (GO) enrichment analysis summary of downregulated genes of the 12*R*-LOX deficient dataset. Number of downregulated genes associated with each enriched *biological process*.

Table 4.5.5 shows the "brown fat cell differentiation" GO term has the greatest share (%) of downregulated genes for any of the top five *biological processes*. Of the 31 genes in the genome that are directly implicated in "brown fat cell differentiation", 13% are observed to be downregulated in the 12*R*-LOX deficient vs wildtype dataset as shown in **Table 4.5.5**. These

four genes that account for the 13% include free fatty acid receptor 4 (*Ffar4*), iodothyronine deiodinase 2 (*Dio2*), peroxisome proliferator-activated receptor gamma coactivator 1-alpha (*Pparγc1α*) and uncoupling protein 1 (*Ucp1*). This is followed by the "regulation of fatty acid oxidation" biological process whereby 10% of genes involved in this process are downregulated in the 12*R*-LOX deficient vs wildtype dataset. These genes include pyruvate dehydrogenase kinase 4 (*Pdk4*), nuclear receptor subfamily 4 group A member 3 (*Nr4a3*) and *Pparγc1α*.

4.5.9.2 Molecular function

Table 4.5.4 shows the top five most significantly enriched *molecular functions* include "alpha adrenergic receptor activity", "adrenergic receptor activity", "carboxylic acid binding", "organic acid binding" and "fatty acid binding". The *molecular function* with the greatest fold enrichment for upregulated genes of the 12*R*-LOX deficient dataset is "alpha adrenergic receptor activity" as shown in **Table 4.5.5**. The GO enrichment analysis revealed that the "carboxylic acid binding" and "organic acid binding" *molecular functions* share the greatest number of downregulated genes with four genes each as shown in **Figure 4.5.13**.

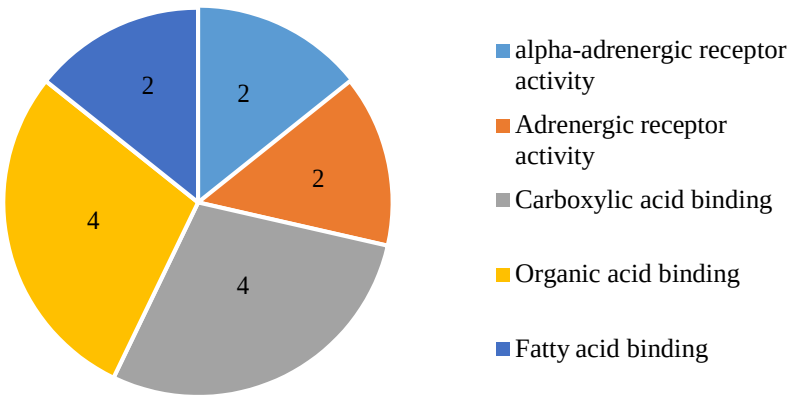

Figure 4.5.13 Gene ontology (GO) enrichment analysis summary of downregulated genes of the 12*R*-LOX deficient dataset. Number of downregulated genes associated with each enriched *molecular function*.

Table 4.5.5 shows the "alpha adrenergic receptor activity" molecular function term has a total of six genes in the genome which are specifically involved in this molecular function. Out of these six genes, 33% of these genes are found to be downregulated in the 12*R*-LOX deficient vs wildtype dataset resulting in this molecular function as having the greatest share (%) of downregulated genes out of all top five molecular functions as shown in **Table 4.5.5**. These genes include Alpha-1A adrenergic receptor (*Adra1a*) and Alpha-1D adrenergic receptor (*Adra1d*).

4.5.9.3 Cellular compartment

No statistically significant cellular compartment results could be assigned to the downregulated genes.

Biological process	Mapped IDs
Brown fat cell differentiation	*Ffar4, Dio2, Ppargc1a, Ucp1*
Positive regulation of cold-induced thermoregulation	*Ffar4, Dio2, Irf4, Ppargc1a, Ucp1*
Fat cell differentiation	*Ffar4, Nr4a3, Dio2, Ppargc1a, Ucp1*
Regulation of fatty acid oxidation	*Pdk4, Nr4a3, Ppargc1a*
Response to interleukin-6	*Cited1, Pck1, Ppargc1a*
Molecular function	**Mapped IDs**
alpha-adrenergic receptor activity	*Adra1a, Adra1d*
Adrenergic receptor activity	*Adra1a, Adra1d*
Carboxylic acid binding	*Ffar4, Susd5, Pck1, Ucp1*
Organic acid binding	*Ffar4, Susd5, Pck1, Ucp1*
Fatty acid binding	*Ffar4, Ucp1*

Table 4.5.4 Identification of downregulated genes of the 12*R*-LOX deficient dataset associated with the top five enriched biological process and molecular function.

GO biological process	# of genes in genome	Fold enrichment	% of downregulated genes involved in biological process
Brown fat cell differentiation	31	65.62	13
Positive regulation of cold-induced thermoregulation	97	26.21	5
Fat cell differentiation	108	23.54	5
Regulation of fatty acid oxidation	31	49.22	10
Response to interleukin-6	39	39.12	8
GO Molecular Function	**# of genes in genome**	**Fold enrichment**	**% of downregulated genes involved in biological process**
alpha-adrenergic receptor activity	6	> 100	33
Adrenergic receptor activity	20	50.86	10
Carboxylic acid binding	213	9.55	2
Organic acid binding	224	9.08	2
Fatty acid binding	38	26.08	5

Table 4.5.5 Gene ontology (GO) enrichment analysis summary of the downregulated genes in the 12*R*-LOX dataset. The results of GO analysis were classified into two distinct categories: *biological processes* and *molecular functions*. No statistically significant results could be generated for *cellular compartment*. Fold enrichment indicates how many more times the *biological process* and *molecular function* are enriched for downregulated genes of the 12*R*-LOX deficient dataset. % of genes in the genome that are downregulated for each *biological process* and *molecular function* in response to 12*R*-LOX knockdown.

4.5.10 *Ffar4*, *Ucp1* and *Pck1* downregulated genes common to biological process and molecular function

Figure 4.5.14 shows a total of nine downregulated genes are associated with the top five enriched *biological processes*, whilst a total of six downregulated genes are associated with enriched *molecular functions*. The downregulated genes shared between the top five enriched *biological processes* include *Ffar4*, *Dio2*, *Pparγc1α*, *Ucp1* and *Nr4a3* as shown in **Table 4.5.4**. The *Pparγc1α* gene is the only downregulated gene in the 12*R*-LOX deficient dataset that is associated with all five enriched *biological processes*. We also observe downregulated genes associated with more than one *molecular function* which include *Adra1a*, Phosphoenolpyruvate carboxykinase 1 (*Pck1*) and Sushi domain containing 5 (*Susd5*) for example. The downregulated gene *Ffar4* is associated with three enriched *molecular functions* that include "carboxylic acid binding", "organic acid binding" and "fatty acid binding". Furthermore, the downregulated genes observed in both enriched *biological processes* and enriched *molecular functions* include three genes which are *Ffar4*, *Ucp1* and *Pck1* as shown in **Figure 4.5.14**.

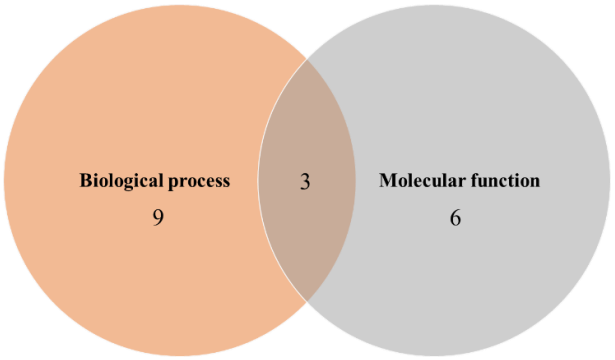

Figure 4.5.14 A Venn diagram summary of the number of downregulated genes for biological processes (Orange) and molecular functions (Grey). The intersections show the number of genes shared between *biological processes* and *molecular functions*.

4.5.11 Majority of downregulated genes of the 12*R*-LOX deficient dataset associated with enriched biological processes belong to transcription factor and non-receptor serine/threonine protein kinase family

Figure 4.5.15 shows 30% of downregulated genes associated with the top five enriched *biological processes* belong to the "transcription factor" protein class. Equally, the protein class of 30% of downregulated could not be determined according to the GO enrichment analysis software. There are a total of three protein classes with the lowest share of downregulated genes

(5%) which include “kinase”, “helix/forkhead transcription factor” and “non-receptor serine/threonine protein kinase”.

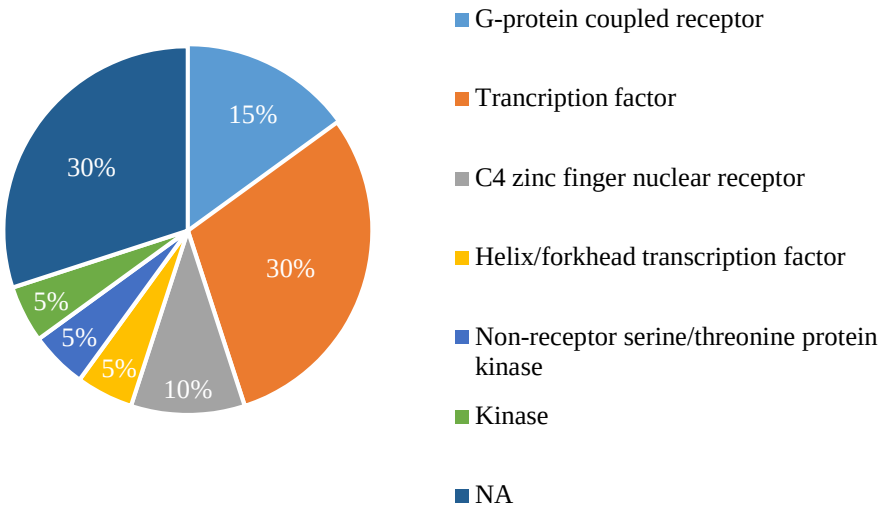

Figure 4.5.15 Pie charts summary of the protein classes associated with the downregulated genes of the top five enriched biological processes. The different colours represent the protein classes, e.g. the orange colour in pie chart represents the transcription factor protein class.

Analysis of the molecular function category shown in **Figure 4.5.16** reveals 50% of downregulated genes associated with the top five enriched *molecular functions* belong to the “G-protein coupled receptor” protein class. Approximately, 35.7% of downregulated genes could not be attributed to a protein class according to the GO enrichment analysis software. A total of 14.3% of downregulated genes associated with the top five enriched *molecular functions* belong to the “kinase” protein class.

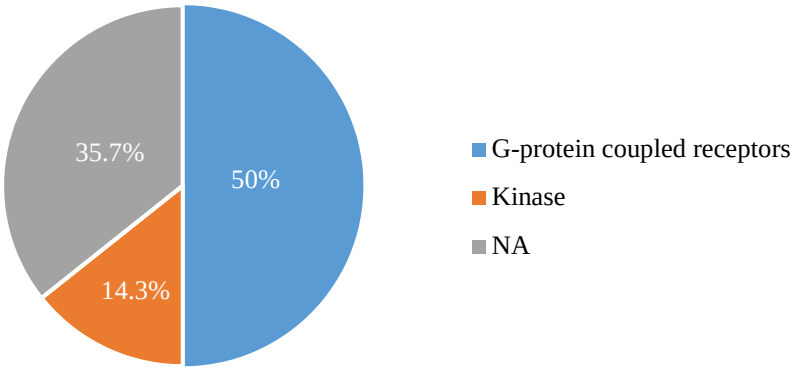

Figure 4.5.16 Pie charts showing the protein class associated with the downregulated genes of the top five enriched molecular functions. The different colours represent the protein classes, e.g. the orange colour in pie chart represents the kinase protein class.

4.6 Discussion

The detailed molecular mechanisms and processes by which 12*R*-LOX / eLOX-3 derived lipids regulate skin homeostasis is unknown and there is limited knowledge and information with regards to their role in skin diseases such as ichthyosis.

An effective RNA extraction procedure was confirmed as the majority of both upregulated and downregulated genes are known to be prevalent in skin. A total of 193 differentially expressed genes was identified with the majority of these genes being upregulated (73%) in response to 12*R*-LOX knock down which suggests that overexpression of genes would also be observed in ichthyosis rather than genes being switched off. Comparison with psoriatic and atopic dermatitis transcriptome studies also show a higher percentage of upregulated genes in comparison with downregulated genes (Elder et al., 2010; Chen et al., 2019). This similar feature in the transcriptome of 12*R*-LOX deficient models and psoriatic models demonstrate a consistency between skin disorders where abnormal and dysregulated lipid processing occurs in its pathophysiology (Pietrzak et al., 2010). However, RNA-sequencing of 12*R*-LOX deficient mouse models will also identify molecular mechanisms and biological processes that underlie skin barrier disorders such as ichthyosis, along with the possible role of 12*R*-LOX lipids in regulating skin physiology.

4.6.1 12*R*-LOX protein deficiency results in the upregulation of genes associated with epidermal biological processes such as keratinocyte differentiation, cornification and peptide cross-linking

The upregulated genes from this dataset were enriched for various ***biological processes*** known to occur within the epidermis such as “keratinocyte differentiation”, “cornification”, “keratinization”, “cell migration” and “peptide cross-linking”, all of which have an implication in the development of a functional epidermal barrier. Additionally, some upregulated genes are associated for more than one enriched *biological process* suggesting that these processes may be involved in the same pathway. Interestingly, the majority of these *biological processes* such as “cornification”, “keratinization” and “peptide cross-linking” predominantly occur in the outer most layers of the epidermis suggesting that the 12*R*-LOX protein deficiency predominantly affect suprabasal layer proteins. Ichthyosis is a skin barrier disorder characterised by abnormal thickening and scaling of the epidermis and therefore the upregulation of genes observed in the 12*R*-LOX deficient dataset may be responsible for the defective skin barrier phenotype observed in ichthyosis. Upregulation of genes such as small proline-rich proteins (*Sprrs*) which are associated with the enriched *biological processes* such

as “keratinocyte differentiation” and “cornification” are also reported to be upregulated in skin disorders such as psoriasis (Koch et al., 2000). Enriched *biological processes* such as “keratinization”, “cornification”, “keratinocyte differentiation” and “peptide cross-linking” are processes known to occur in stratified layers of the epidermis, further suggesting that 12*R*-LOX exerts its effect on *biological processes* in the outer most layers of the epidermis as shown in **Figure 4.6.1**.

The process of keratinocyte differentiation is vitally important for the maintenance of skin physiology and for the formation of the epidermal barrier (Yanagi et al., 2010). The results in this chapter may suggest that an overexpression of genes such as *Sprr1b*, *Sprr2d*, *Sprr2h*, *Rptn* which are linked with the enriched “keratinocyte differentiation” process, are compensating for an impaired keratinocyte differentiation process during the inactivation of 12*R*-LOX. These results are consistent with the biochemical abnormalities observed in ichthyosis whereby abnormal processing of differentiation markers such as keratins and Filaggrin (*Flg*) have been previously reported (Manabe et al., 1991; McLean, 2016).

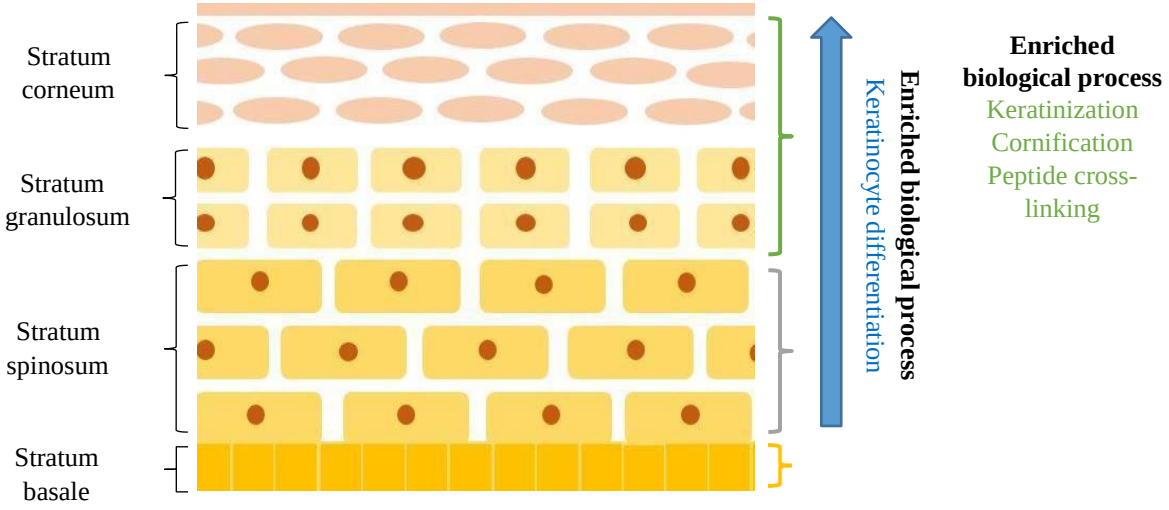

Figure 4.6.1 Schematic representation of the localisation of enriched biological processes following 12*R*-LOX deficiency. No enriched ***biological process*** for upregulated genes in the 12*R*-LOX deficient dataset are known to occur in the inner most stratum basale layer of the epidermis. Enriched ***biological processes*** highlighted in blue and green are known to occur in stratified layers of the epidermis.

4.6.2 12*R*-LOX protein deficiency upregulates epidermal serine protease enzymes and inhibitors known to be implicated in keratinocyte differentiation

The kallikrein related peptidase 14 (*Klk14*) gene shown to be upregulated in the 12*R*-LOX deficient dataset encodes a protein belonging to the serine protease enzyme family. Studies have highlighted the importance of the *Klk14* gene in the process of keratinocyte differentiation (Gouin et al., 2020). In healthy skin, the kallikrein proteins aid in homeostatic regulation through the degradation of corneodesmosome proteins leading to a "normal" level of desquamation (Kantyka et al., 2010). In skin disorders such as psoriasis and atopic dermatitis, Morizane et al., 2012 has shown that this desquamation specific enzyme is significantly upregulated which is comparable with its expression profile in 12*R*-LOX deficient mice, suggesting its upregulation is compensating for the defective differentiation process known to occur in ichthyosis. Moreover, previous studies have also confirmed increased expression of kallikrein genes in the skin of acne rosacea patients in comparison with normal, healthy skin (Yamasaki et al., 2007).

The enriched "protein binding" *molecular function* has the greatest number of upregulated genes of all enriched *molecular functions*. A number of these genes have been shown to be upregulated in other related skin disorders such as psoriasis and eczema suggesting a similar pathophysiology to that of ichthyosis including decreased differentiation. Examples of these upregulated genes include serine peptidase inhibitor kazal type 7 (*Spink7*), a member of the protease inhibitor family. It has been demonstrated that an imbalance between proteases/inhibitors and abnormal expression contributes significantly to the development of skin disorders (Weber et al., 2017). In conjunction with other findings in the 12*R*-LOX deficency analysis, the activity of these specific protease inhibitors occurs mostly in the stratified layers of the epidermis and is shown to be an important process in late stage epidermal differentiation. This is further evidence to suggest that 12*R*-LOX / eLOX-3 lipids are possible regulators/modulators of protease inhibitors.

Following deficiency of the 12*R*-LOX protein, an upregulation in protease inhibitors such as *Spink7* and Serpin family B member 12 (*Serpinb12*) is observed in the 12*R*-LOX deficient dataset, which may counteract the overexpression of serine proteases such as *Klk14*. Without the function of protease inhibitors, it has been hypothesised that protease activity would increase, resulting in an enhanced degradation of corneodesmosome proteins leading to an accumulation of broken down protein molecules (Komatsu et al., 2002). As protease enzyme activity is known to occur in the outer most layers of the epidermis, the overexpression of protease inhibitors such as *Spink7* may decrease protease activity and therefore reduce the

degradation of proteins within specific compartments of the stratum corneum. This would subsequently result in an accumulation of proteins as a result of decreased protease activity and therefore contribute to a thickening of the stratum corneum which is a clinical characteristic of ichthyosis.

4.6.3 12*R*-LOX protein deficiency upregulates lipid metabolising enzymes known to be implicated in keratinocyte differentiation

The lipase family member N (*Lipn*) gene is found to be upregulated in the 12*R*-LOX deficient dataset and is associated with the enriched "keratinocyte differentiation" *biological process*. It encodes an epidermal lipase enzyme and has been previously reported to be implicated in the development of a form of late-onset ichthyosis skin disorder (Israeli et al., 2011). As aforementioned, it is reported to play a role in latter stages of epidermal differentiation which is why it is associated with this enriched *biological process*, however, the upregulation of this gene may contribute to an abnormal differentiation process where irregular expression of differentiation markers is observed (Epp et al., 2007). Moreover, the *Lipn* gene is described as having a role in lipid metabolism in differentiated epidermal cells and could therefore be upregulated to compensate for the loss of 12*R*-LOX. Other GO enrichment term for *Lipn* is "cornification", suggesting its association with an important biological process that is reliant on the keratinocyte differentiation process.

4.6.4 12*R*-LOX protein deficiency upregulates a range of genes associated with the enriched "keratinocyte differentiation" process

The majority of upregulated genes are found to be predominantly expressed in the outer most layers of the epidermis, suggesting a possible compensatory mechanism being induced in response to 12*R*-LOX deficiency and likely loss of 12*R*-LOX derived lipids. Most upregulated genes that are expressed in the stratified layers include members of the epidermal differentiation complex, keratins and other proteins such as deoxyribonuclease 1 like 3 (*Dnase1l3*) and epiregulin (*Ereg*). The deoxyribonuclease 1 family members that include *Dnase1l3* are implicated in DNA degradation and differential expression of this gene is observed in the development of diseases including parakeratosis, cataracts and anaemia (Keyel, 2017). The upregulated *Ereg* gene is associated with the enriched "keratinocyte differentiation" *biological process* and has been previously reported to show abnormal expression during the development of atopic dermatitis (Thuong et al. 2012). Interestingly, the *Ereg* gene is also upregulated in transglutaminase 1 (*Tgm1*) deficient mice, which is another clinically relevant skin disorder mouse model shown to have impaired keratinocyte differentiation and implicated

in the ichthyosis skin disease (Haneda et al., 2016). Just as the cornifelin (*Cnfn*) gene is overexpressed when the 12*R*-LOX protein is genetically deleted, it has also been shown that overexpression of this gene is detected in psoriatic lesions (Luo et al., 2020). Moreover, it has been previously reported that an increased expression of the *Cnfn* gene subsequently alters the composition of proteins within the cornified envelope (Michibata et al., 2004). This alteration results in a defective permeability barrier suggesting that 12*R*-LOX-derived lipids may play a role in regulating the expression of cornified envelope proteins. Interestingly, these proteins are expressed in the granular or cornified layer of the epidermis, further implicating 12*R*-LOX involvement in epidermal differentiation. Furthermore, enriched *biological processes* such as "keratinocyte differentiation", "cornification", "peptide cross-linking" and "keratinization" are all biologically linked to epidermal terminal differentiation as they are processes which occur in the latter stages of keratinocyte differentiation.

4.6.5 Upregulation of migration proteins following 12*R*-LOX deficiency

Upregulated genes belonging to the chemokine ligand family of proteins that include chemokine ligand 20 (*Ccl20*), chemokine ligand 8 (*Ccl8*) and chemokine ligand 17 (*Ccl17*) are associated with the enriched "mononuclear cell migration" *biological process*. For example, it has been shown that the overexpression of *Ccl20* promotes the migration of lung cancer cells through stimulation via the interleukin-1β signal pathway (Wang et al., 2016). Without lipid products generated by LOX, this may lead to a similar pathway being activated promoting migration of cells, thus, the presence of LOX-derived lipids would regulate the normal physiological expression of *Ccl20*, resulting in controlled keratinocyte migration. Interestingly, members of the interleukin family of proteins are also found to be upregulated in the 12*R*-LOX deficient vs wildtype data, namely, interleukin 1 family member 6 (*Il-1f6*) and interleukin 1 family member 9 (*Il-1f9*). The upregulation of these genes could similarly initiate the upregulation of the *Ccl20* protein resulting in abnormal cell migration. Previous studies have reported specific cytokines such as interleukin 22 stimulating the expression of *Ccl20* in the psoriatic skin disorder (Harper et al., 2009). Fascinatingly, the overexpression of the *Ccl20* protein in psoriasis was shown to be important in facilitating the migration of leukocytes to the area of inflammation. As such, the overexpression of *Ccl20* could be linked with an inflammatory cell migration response rather than a homeostatic cell migration of keratinocytes from the basal layer to the outer most layer of the epidermis. This may suggest that 12*R*-LOX has a role in generating lipids as anti-inflammatory mediators.

In the human epidermis, cells migrating from the proliferative basal layer to the cornified layer, where corneocytes are shed, is a well-regulated and timely process in healthy skin. This complex process is believed to be accelerated in ichthyosis with an enhanced rate of basal cell proliferation and keratinocytes reaching the outer most layer in an abnormally short space of time (Williams, 1992). Interestingly, the GO enrichment analysis results suggests that 12*R*-LOX / eLOX-3 derived lipids may play a key role in regulating homeostatic cell migration and preventing the accumulation of excess skin cells that forms plaques on the surface. This is evident by the upregulation of genes involved in cell migration such as histone h2b type 1-A (*Hist1h2ba*) and a key desquamation enzyme, namely, *Klk14*.

Furthermore, the *Hist1h2ba* and *Sis* genes encode for proteins belonging to the histone and growth factor family of proteins which are attributed to a role in the enriched "mononuclear cell migration" *biological process*. We also observe these proteins associated with other *molecular functions* such as "protein binding". Previous studies have shown that the overexpression of histone proteins is characterised with an inflammatory response. Activation of inflammatory responses involving histone proteins can be directed through a different pathway such as the inflammasome pathway or toll-like receptors (Hoeksema et al., 2016). During inflammation, growth factors can be released from amassed platelets to promote leukocyte activity and increasing the expression of integrin, subsequently mediating an immune response (Wahl, 1997).

4.6.6 12*R*-LOX deficiency upregulates proteins implicated in cellular compartments of keratinocytes found in stratified layers

The enriched ***cellular components*** such as "cornified envelope" and "keratin filament" further reinforces the evidence that LOX-derived lipids predominantly have an effect on the outer most layer of the epidermis. It has previously been reported that a fragility in the cornified envelope has been observed in ichthyosis which subsequently leads to a defective barrier (Elias et al., 2012). The identification of upregulated genes associated with the enriched "cornified envelope" *cellular compartment* may be responsible for the defective scaffold of the cornified envelope observed in ichthyosis. The majority of the upregulated genes associated with the enriched "cornified envelope" also belong to the epidermal differentiation complex, suggesting that 12*R*-LOX-derived lipids are having a profound effect on a cassette of genes involved in this process.

4.6.7 Downregulation of genes associated with differentiation following 12*R*-LOX protein deficiency

A key epidermal process known as "keratinocyte differentiation" is enriched for not only upregulated genes of the 12*R*-LOX deficient dataset, but also for downregulated genes. Although downregulated genes are not specifically enriched for keratinocyte differentiation, they are however enriched for a differentiation process, in this case, "brown fat cell differentiation". This biological process involves an unspecialised cell attaining the biological properties of brown adipocytes, a tissue cell found in the dermal region of the skin and involved in the process of heat production known as thermogenesis (Sim et al., 2017). At present, there is no scientific evidence to suggest a role for 12*R*-LOX / eLOX-3 lipids in the dermal compartment.

A downregulated gene associated for the two enriched differentiation processes, "brown fat cell differentiation" and "fat cell differentiation", includes the *Ffar4* gene. This gene encodes a protein which functions as a free fatty acid receptor, binding saturated and unsaturated fatty acids. It has also been implicated in regulating the cell differentiation process (Houthuijzen, 2016). The interaction between 12*R*-LOX / eLOX-3 derived lipids and the *Ffar4* protein is unknown, however, the downregulation of such genes may be predictable in these biological circumstances due to the absence of lipids generated by LOX. As a result, the function of the *Ffar4* proteins would be redundant due to the lack of lipid produced by LOX to subsequently bind to *Ffar4* receptors. Additionally, the role of *Ffar4* in regulating differentiation may be affected due to its downregulation. In contrast, the presence of lipids would in turn increase the expression of *Ffar4* and aid in the homeostatic regulation of differentiation. This further reinforces the evidence implicating 12*R*-LOX lipids role in regulating the epidermal differentiation process.

4.6.8 Downregulation of transcription factor proteins known to play a role in keratinocyte differentiation following 12*R*-LOX protein deficiency

Downregulated genes of interest which are associated with the enriched "brown fat cell differentiation" and "fat cell differentiation" processes include the *Pparγc1α* and cbp/p300-interacting transactivator 1 genes. These downregulated genes belong to a family of transcription factors, with the peroxisome proliferator activated receptor in particular being known with having a role in key biological processes in the epidermis. As this particular family of proteins is of interest in its possible role with LOX-derived lipids, further investigation on the peroxisome proliferator activated receptor transcriptional factor family will be performed in the following chapter. It has been reported that epidermal transcription factors have been

shown to play key roles in skin health and disease. Examples of other known transcription factors having a key role in regulating epidermal proliferation and differentiation includes the activator protein 1 (*Ap1*) (Maas-Szabowski et al., 2001). Studies have shown that inactivation or suppression of this transcription factor in mouse epidermis results in an increase in epidermal proliferation and inhibits keratinocyte differentiation (Han et al., 2012). In response to the inactivation of 12*R*-LOX, we show that 30% of downregulated genes that are associated with the top five enriched *biological processes* belong to a family of transcription factors. These findings suggest that lipid products produced through 12*R*-LOX protein activity may activate transcription factors. Furthermore, if these transcription factors are involved in modulating keratinocyte differentiation, one might expect to observe the upregulated differentiation markers returning to "normal" physiological levels following the reintroduction of 12*R*-LOX-derived lipids.

4.6.9 Downregulation of receptor proteins involved in initiating differentiation following 12*R*-LOX protein deficiency

The major protein class found attributed to the top five enriched *molecular functions* associated with downregulated genes includes the G-protein coupled receptors. These proteins have been implicated in regulating pathways involving differentiation and cell self-renewal in epithelial cells (Iglesias-Bartolome et al., 2019). For example, G-protein coupled receptors are shown to play key roles in neuronal differentiation and lymphocyte differentiation. Once more, we observe a subset of downregulated genes associated with G-protein coupled receptors that are involved in the differentiation cascade. Additionally, G-protein coupled receptors detect a range of extracellular stimuli that include chemokines, hormonal peptides and more importantly, lipids (Wang and Wong., 2009). As such, lipid products released from LOX metabolism may activate G-protein coupled receptors and subsequently initiate and regulate signalling pathways associated with the differentiation of keratinocytes.

4.7 Conclusion

We report that the majority of differentially expressed genes are expressed in the granular / cornified layer of the epidermis following 12*R*-LOX protein inactivation, suggesting 12*R*-LOX / eLOX-3 derived lipids have their effect in stratified layers of the epidermis. In addition to identifying the localisation of the differentially expressed genes, the GO enrichment analysis provided strong indication that both upregulated and downregulated genes are involved in a pathway relating to cell differentiation. To elaborate, the remaining enriched *biological processes* such as "cornfication", "keratinization" and "peptide cross-linking" firmly indicate

that 12*R*-LOX / eLOX-3 derived lipids play a role in latter stages of differentiation as all three processes predominantly occur in stratified layers of the epidermis. This is further supported by the enriched *cellular compartments* which include "cornified envelope" and is a key component of terminally differentiating keratinocytes. There is minimal data from the GO enrichment analysis to suggest a direct role for 12*R*-LOX / eLOX-3 in the proliferating layers of the epidermis. For example, markers of proliferation such as *Krt5* seem to be unaffected following 12*R*-LOX protein deficiency. However, keratin proteins that are associated with differentiating keratinocytes such as *Krt10* are significantly upregulated in response to 12*R*-LOX knockdown. This further implies a role for 12*R*-LOX lipid products in regulating a feature of the differentiating process in the epidermis.

An interesting finding regarding the analysis of the downregulated genes is that a large proportion of these genes (30%) are associated with the transcriptional factor protein classification. The subsequent decrease in the expression of transcription factors such as peroxisome proliferator activated receptor and G-protein coupled receptors may indicate an agonist role for the LOX-derived lipids. The upregulated genes associated with enriched *biological processes* such as "keratinocyte differentiation" include mostly keratin proteins, late cornified envelope proteins and small proline-rich proteins. Interestingly, a majority of these proteins are members of a gene cluster known as the epidermal differentiation complex, an important cluster of genes responsible for the development of the epidermal barrier through regulating terminal differentiation and cornification. To explore this relationship further, a transcriptome investigation into the effect of 12*R*-LOX deficiency on epidermal differentiation complex and keratin genes will be explored in the next chapter. Additionally, results from the RNA-sequencing will need to be validated using analytical methods such as western blotting and Q-PCR.

Chapter 5

Transcriptome analysis of genes encoding proteins of the epidermal differentiation complex (EDC), the keratin family and peroxisome proliferator activated receptor (PPAR) Family

5.1 Introduction

The epidermal differentiation complex (EDC) consists of genes that encode for proteins involved in the essential process of keratinocyte differentiation and are found clustered on human chromosome 1q21 (Marenholz et al., 2001). This specific gene complex can be divided into three unique gene families that include the cornified envelope (CE) precursor family, the S100 family and S100 fused type protein family (SFTP) which are described in detail in **Section 1.1.7**. These genes are separated into distinct families based upon gene commonality and structures of the encoded proteins.

The expression of genes belonging to the EDC are regulated by a variety of transcription factors that up to now include *Krüppel-like* factor 4 (*Klf4*), GATA3, Grainyhead-like 3 (*Grhl3*), NRF2 and Aryl hydrocarbon receptor nuclear translocator (*Arnt*). As such, molecular evidence to date suggests genes belonging to the EDC family are regulated by a range of transcriptional factors rather than one master regulator gene. Mutations or deletions in aforementioned transcriptional regulators result in an absent or perturbed epidermal barrier causing lethality in animal models (Kypriotou et al., 2012). For example, deletion of the *Klf4* and GATA3 genes in mouse models result in death shortly after birth (Segre, 2006). Features of these animal models include defects in the cornified envelopes, aberrant lipid lamellae and abnormal differentiation and lipid synthesis. Irregular differentiation is also observed in genetic deletion studies involving *Grhl3* with an increase in the number of specialised epidermal squamous cells known as acanthosis. Furthermore, proteins found within the cornified envelope of epidermal cells are differentially expressed in comparison with wild type mice and also display varied expression in *Tgm1*. Key epidermal serine protease enzymes such as kallikreins are also affected along with tight cellular junctions (Ting et al., 2005; Yu et al., 2005).

The majority of keratin proteins are expressed in skin tissue of the human anatomy, where 80% of skin cells are comprised of the keratin protein (Herrmann et al., 2012). Furthermore, keratin intermediate filaments provide structural resistance to physical stress and help maintain cell shape. Other important functions of keratin filaments include cell adhesion and signalling (Bragulla and Homberger, 1998; Seltmann et al., 2013). In total, there are 54 functional keratin proteins in humans with the expression of different keratin proteins dependent on the stage of proliferation and differentiation (Fuchs & Green et al., 1980; Moll et al., 2008; Toivola et al., 2015; Wang et al., 2016).

Keratinocytes found in the mitotically active basal layer of the epidermis express specific keratins. These include keratin 5 (*Krt5*), keratin 14 (*Krt14*) and lesser quantities of keratin 15 (*Krt15*) (Lloyd et al., 1995; Wang et al., 2016). Once cells of the basal layer terminate cell division and migrate towards the suprabasal layers of the epidermis, keratinocytes begin to express keratin 1 (*Krt1*) and keratin 10 (*Krt10*) (Moravcová et al., 2013; Wang et al., 2016). As keratinocytes continue to differentiate and reach the upper layer of the stratum spinosum and stratum granulosum, keratin 2e (*Krt2e*) is shown to be induced and expressed (Collin et al., 1992). Abnormal expression of keratin proteins is associated with a wide range of hereditary skin disorders, from inflammatory conditions such as psoriasis to malignant skin tumours (Alameda et al., 2011; Elango et al., 2018).

Peroxisome proliferator-activated receptors (PPARs) are a family of nuclear hormone receptor proteins that have more recently been implicated in skin homeostasis along with their ligands (Sertznig et al., 2008). Studies have shown PPARs are activated by various ligands such as fatty acids and molecules derived from fatty acids. These transcriptional factor proteins are subdivided into three distinct family members that include peroxisome proliferator-activated receptor alpha (*Pparα*), peroxisome proliferator-activated receptor beta/delta (*Pparβ/δ*) and peroxisome proliferator-activated receptor gamma (*Pparγ*) and are described in detail in **Section 1.2.11**, **1.2.11.1, 1.2.11.2, 1.2.11.3** and **1.2.11.4**.

5.2 Aim

- Determine the statistically significantly differentially expressed genes (DEGs) belonging to the epidermal differentiation complex (EDC), keratin family and peroxisome proliferator-activated receptor (PPAR) family in response to 12*R*-LOX deficiency.

5.3 Objectives

- Compare fold changes of the three distinct gene families belonging to the EDC; cornified envelope precursor family, the S100 protein family and the S100 fused type protein family in the 12*R*-LOX deficient vs wildtype dataset.
- Evaluate whether a specific EDC gene family, cornified envelope precursor family, the S100 protein family or the S100 fused type protein family has a greater amount of significantly differentially expressed genes.

- Identify the most significantly upregulated and downregulated genes belonging to the EDC, keratin and PPAR gene families in the 12*R*-LOX deficient vs wildtype dataset.
- Characterise gene expression profiles of EDC, keratin and PPAR gene families in the 12*R*-LOX deficient vs wildtype dataset.
- Evaluate whether differentially expressed genes in the 12*R*-LOX deficient vs wildtype dataset are also found to be upregulated or downregulated in other skin barrier disorders.
- Investigate canonical pathways, upstream regulators, molecular and cellular functions of the genes associated with differentially expressed EDC, keratin and the PPAR gene family.

5.4 Materials and methods

Identification of differentially expressed genes (DEGs) in the 12*R*-LOX deficient vs wildtype dataset is described in **Section 2.5.5**.

5.4.1 Identification of genes belonging to the epidermal differentiation complex (EDC), keratin and PPAR family.

Biomedical and genomic information platforms such as www.genenames.org and National Centre for Biotechnology Information (NCBI) were utilised to identify all genes belonging to the EDC.

5.4.2 Ingenuity Pathway Analysis (IPA)

The Ingenuity Pathway Analysis (IPA) (Ingenuity Systems, www.ingenuity.com, Redwood City, CA) bioinformatics software was used to generate significant signalling pathways, upstream regulators and molecular networks associated with the DEGs. IPA uses an algorithm to generate a top score molecular network map according to the genes inserted into the software (Calvano et al., 2005; Thomas and Bonchev, 2010). Genes with fold change values of $\leq$ -1.5 and $\geq$ 1.5 and *p* value of < 0.05 were processed in IPA to generate pathways associated with these expression values. Genes with fold change values of $\leq$ 1.5 and $\geq$ 1.5 and adjusted *p* value of < 0.05 were used for further analysis such as determining canonical pathway enrichment, upstream regulators, biological functions and diseases in which they are biochemically active. Fisher's t-test is the statistical method employed to determine statistical significance of a network generated with $p < 0.05$ considered statistically significant.

5.4.3 Heatmap with hierarchical clustering

A commonly used hierarchical clustering heatmap tool was used known as GENE-E matrix visualization platform (https://www.software.broadinstitute.org/morpheus/) to allow grouping of genes which display similar gene expression profiles. The FPKM values for each gene were imported into the software and hierarchical clustering was performed with columns clustered. Data was then clustered with dendrogram formed to better visualize the clusters. The height of the clades between two genes indicates gene expression similarity i.e. the shorter the height of the clade between two genes indicates a similar gene expression profile, whilst the greater the height of the clade between two genes indicates a greater difference in the gene expression profile between these two genes.

5.4.4 Differentially expressed gene analysis (DEG)

R package DESeq2 was performed using the raw gene counts and the data normalized. DESeq2, a statistical tool package, generates the differential gene expression through a negative binomial distribution (Love et al., 2014). To determine differentially expressed genes that are of significance, a t-test was conducted which in turn produces *p* values for each respective gene in the dataset. The t-test is based on whether two populations (KO vs WT) are different. A p value of > 0.05 for a gene is observed when replicates within a group are not similar to each other, while a p value of < 0.05 indicates that replicates within a group are similar to each other. A p value of < 0.05 details how similar replicates are to each other and how different two populations (KO and WT) are from each other. Statistically significant DEGs was defined as a *p* value of < 0.05 included genes with a ≤ -1.5 and ≥ 1.5-fold change (FC).

5.5 Results

5.5.1 *Sprr1b*, *Sprr2d*, *Sprr2h* and *Rptn* are the most statistically significantly upregulated genes of the EDC gene family

Figure 5.5.1 shows all genes associated with the cornified envelope precursor family are upregulated with no genes found to be downregulated and nine out of the 17 genes upregulated by a fold change of over the 1.5 FC threshold. These include small proline rich protein 1b (*Sprr1b*), *Sprr2a1*, *Sprr2a2*, *Sprr2a3*, *Sprr2d*, *Sprr2e*, *Sprr2h*, *Sprr2i* and *Sprr2k*. **Figure 5.5.1** shows of all genes belonging to the cornified envelope precursor family, the *Sprr1b*, *Sprr2d* and *Sprr2h* are the most statistically significantly upregulated genes (bars highlighted in orange) ($p < 0.05$).

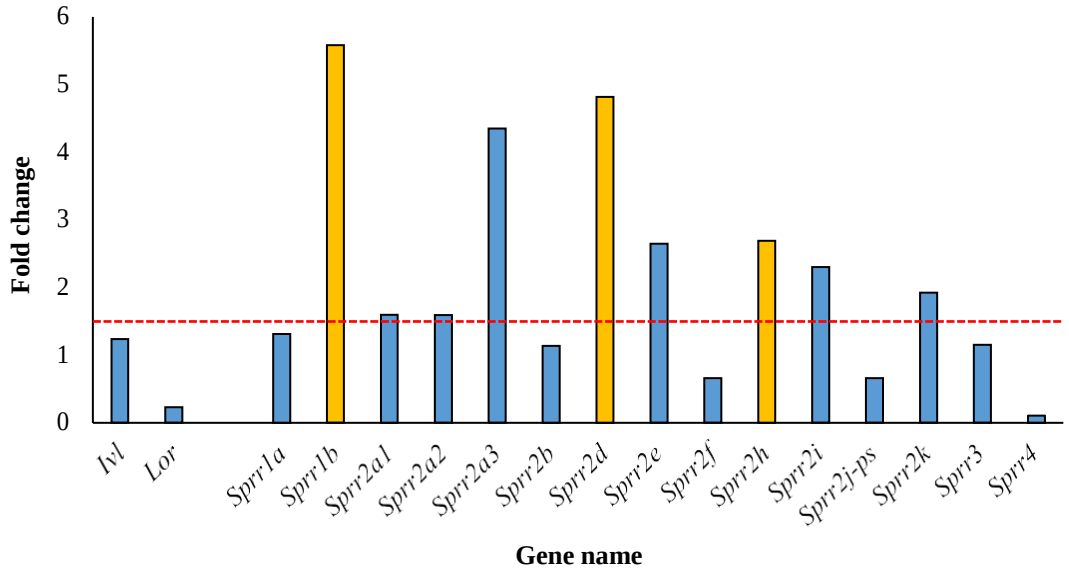

Figure 5.5.1 Protein coding genes associated with the cornified envelope precursor family showing upregulation based on fold change in 12R-LOX deficient vs wildtype dataset. The orange bars indicate statistically significant genes in the 12*R*-LOX deficient dataset ($p < 0.05$). The bars highlighted in blue indicate genes considered to be statistically non-significant in the 12*R*-LOX deficient dataset ($p > 0.05$). The dashed red line represents a fold change threshold of ≥1.5.

No genes belonging to the late cornified envelope (*Lce*) gene family are found to be statistically significantly upregulated or downregulated as shown in **Figure 5.5.2**. Of the 21 genes associated with the *Lce* protein family, only three of these genes are upregulated by a fold change of ≥ 1.5 but are not statistically significant.

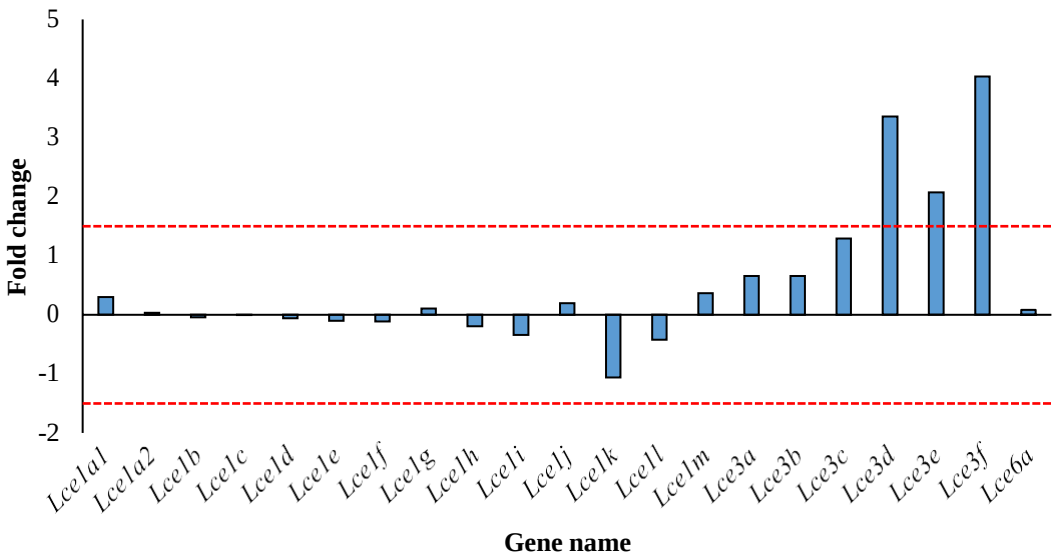

Figure 5.5.2 Protein coding genes associated with the cornified envelope precursor family showing upregulation and downregulation based on fold change in 12*R*-LOX deficient vs wildtype dataset. The absence of orange bars indicates that there are no statistically significant genes in the 12*R*-LOX deficient dataset. The bars highlighted in blue indicate genes considered to be statistically non-significant in the 12*R*-LOX deficient dataset ($p > 0.05$). The dashed red line represents a fold change threshold of ≥1.5 and ≤1.5.

Fold change analysis of genes associated with the S100 family revealed the presence of both upregulated and downregulated genes as shown in **Figure 5.5.3**. Of the 18 genes associated with the S100 family, only two genes are found to be of statistical significance, however, these S100 genes have fold change values below the -1.5 and +1.5 threshold set. These include the S100 calcium binding protein a11 (*S100a11*) and S100 calcium binding protein b (*S100b*) genes. The *S100a11* gene is upregulated with a fold change value of 0.7 whilst the *S100b* gene is downregulated with a fold change value of -0.9.

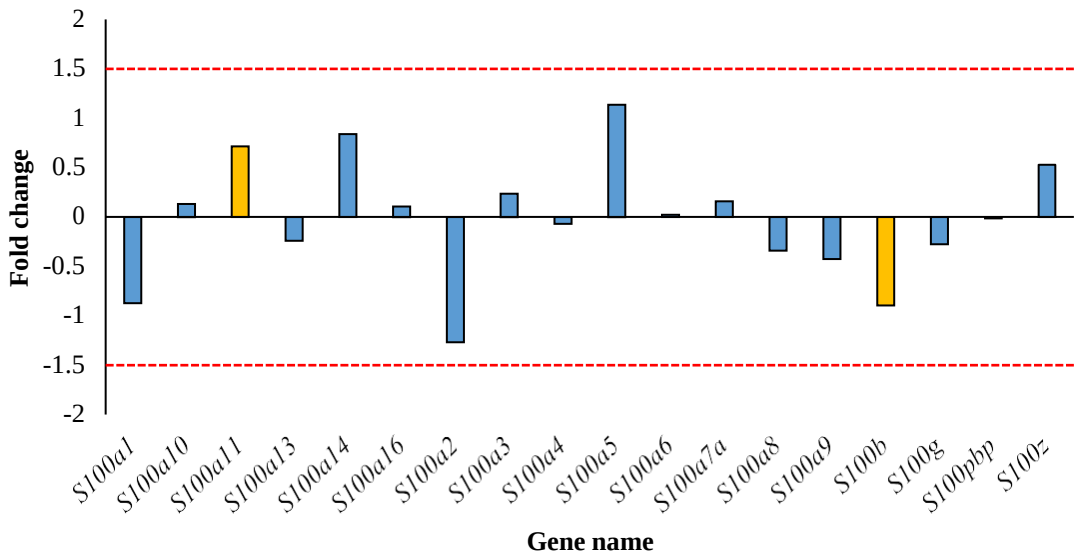

Figure 5.5.3 Protein coding genes associated with the S100 protein family showing upregulation and downregulation based on fold change in 12*R*-LOX deficient vs wildtype dataset. The orange bars indicate statistically significant genes in the 12*R*-LOX deficient dataset ($p < 0.05$). The bars highlighted in blue indicate genes considered to be statistically non-significant in the 12*R*-LOX deficient dataset ($p > 0.05$). The dashed red line represents a fold change threshold of ≥1.5 and ≤1.5.

The fold change of the remaining gene family of the EDC, the S100 fused type protein family (SFTP), was analysed with all genes in this group of EDC genes shown to be upregulated in the 12*R*-LOX deficient vs wildtype dataset as shown in **Figure 5.5.4**. The repetin (*Rptn*) gene is the most statistically significantly upregulated gene of all the SFTP family with a 2.5-fold change. The outstanding genes that include filaggrin (*Flg*), filaggrin 2 (*Flg2*), trichohyalin (*Tchh*), trichohyalin-like 1 (*Tchhl1*), cornulin (*Crnn*) and hornerin (*Hrnr*) are below the set 1.5-FC threshold.

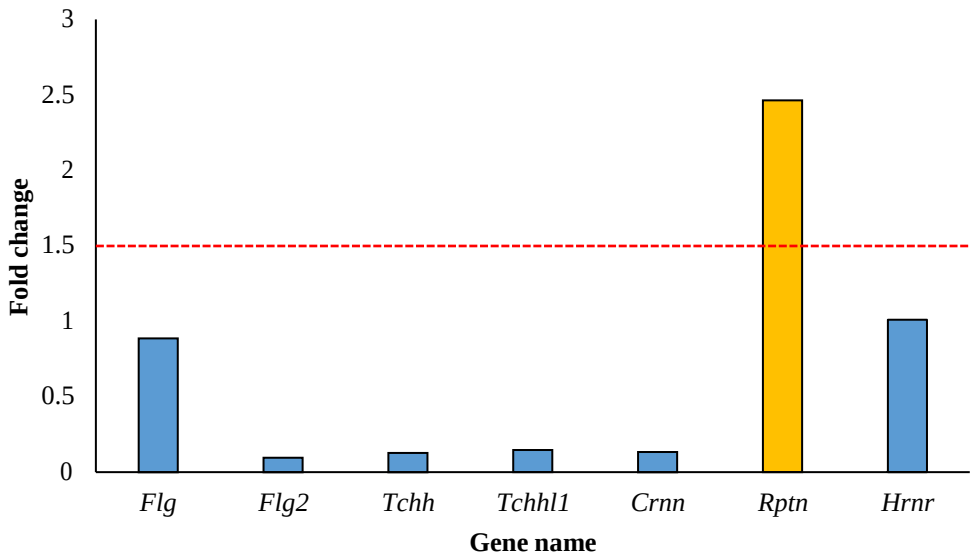

Figure 5.5.4 Protein coding genes associated with the S100 fused type protein family (SFTP) showing upregulation based on fold change in 12*R*-LOX deficient vs wildtype dataset. The orange bars indicate statistically significant genes in the 12*R*-LOX deficient dataset ($p < 0.05$). The bars highlighted in blue indicate genes considered to be statistically non-significant in the 12*R*-LOX deficient dataset ($p > 0.05$). The dashed red line represents a fold change threshold of ≥1.5.

Of all genes associated with the EDC, the *Sprr1b* is the most statistically significantly upregulated gene in response to 12*R*-LOX deficient with a 5.6-fold change. A total of three genes belonging to the cornified envelope precursor family are statistically significantly upregulated which is more than any other gene family of the EDC. The most statistically significant downregulated gene is *S100b* with 0.9-fold change. The DEGs belonging to the EDC of statistical significance ($p < 0.05$) and exceed the respective 1.5 and -1.5 FC-threshold are *Sprr1b*, *Sprr2d*, *Sprr2h* and *Rptn*.

5.5.2 *Sprr2d*, *Sprr1b*, *Sprr2h, S100a11*, *Hrnr*, *Lce3f* and *Rptn* genes identified in top cluster

Figure 5.5.5 shows a hierarchical clustering dendrogram as described in **Section 5.4.3** of genes belonging to the EDC to identify the expression profiles of this specific epidermal gene cluster. The *Sprr2a1* and *Sprr2a2* have the most similar expression profile of all genes in the EDC as demonstrated by the shortest clade height between these two genes (red highlighted circle). Trichohyalin like 1 (*Tchhl1*) and cornulin (*Crnn*) genes also have a similar expression profile as demonstrated by the short height of the clade between these genes. **Figure 5.5.5** shows a top cluster identified in purple consisting of *Sprr2d*, *Sprr1b, Sprr2h, S100a11*, hornerin (*Hrnr*), *Lce3f* and *Rptn*. A similar expression profile is observed for all of these specific EDC genes in the 12*R*-LOX deficient and wildtype samples. Interestingly, most of these EDC genes described are found to have similar expression profiles and have fold change values exceeding 1.5. The only genes with fold change values below 1.5 and found within this cluster of interest are *Hrnr* and *S100a11* genes.

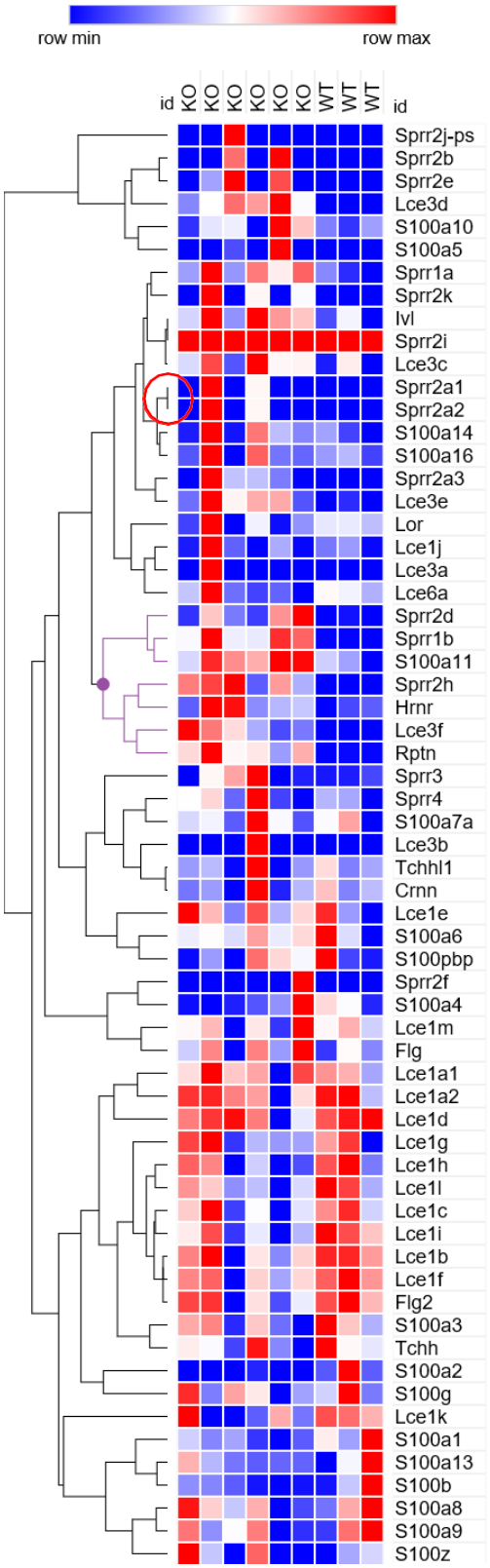

Figure 5.5.5 Hierarchical clustering analysis of the expression profiles of genes associated with the epidermal differentiation complex using GENE-E. Each column represents the FPKM values for each gene. The red blocks represent genes that are overexpressed and the blue blocks represent genes with the lowest expression. The remaining coloured bars represent relative expression levels. The minimum FPKM expression value is 0, whilst the maximum FPKM expression value is 274.6. The highlighted red circle indicates the shortest clade height.

5.5.3 *Krt1*, *Krt6b*, *Krt10, Krt16* and *Krtdap* are the most significantly upregulated genes of the keratin gene family and are expressed in suprabasal layers of the epidermis

The majority of keratin encoding genes are upregulated (82%) rather than downregulated (18%) in response to 12*R*-LOX deficiency (**Figure 5.5.6** – **Figure 5.5.12**). Of the 50 keratin encoding genes, five keratin genes exceed the 1.5-fold change threshold and are considered statistically significant (bars highlighted in orange). These include keratin 1 (*Krt1*), *Krt6b*, *Krt10*, *Krt16* and keratinocyte differentiation-associated protein (*Krtdap*) ($p < 0.05$). The *Krt16* gene has the greatest upregulation out of all keratin encoding genes with a fold change value of 2.9.

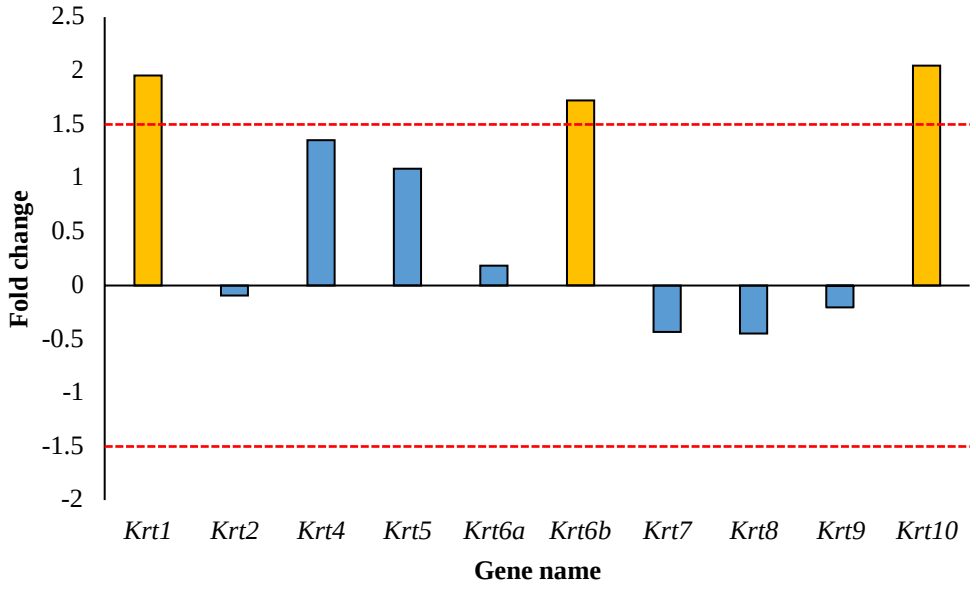

Figure 5.5.6 Protein coding genes associated with the keratin protein family (*Krt1* – *Krt10*) showing both upregulation and downregulation based on fold change in 12*R*-LOX deficient vs wildtype dataset. The orange bars indicate statistically significant genes in the 12*R*-LOX deficient dataset ($p < 0.05$). The bars highlighted in blue indicate genes considered to be statistically non-significant in the 12*R*-LOX deficient dataset ($p > 0.05$). The dashed red line represents a fold change threshold of ≥1.5 and ≤1.5.

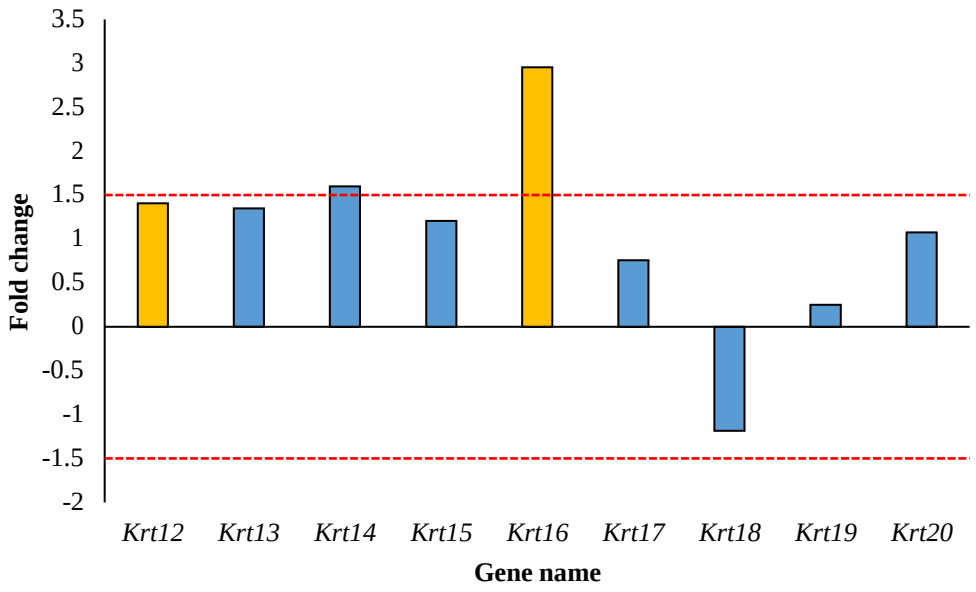

Figure 5.5.7 Protein coding genes associated with the keratin protein family (*Krt12 – Krt20*) showing both upregulation and downregulation based on fold change in 12*R*-LOX deficient vs wildtype dataset. The orange bars indicate statistically significant genes in the 12*R*-LOX deficient dataset ($p < 0.05$). The bars highlighted in blue indicate genes considered to be statistically non-significant in the 12*R*-LOX deficient dataset ($p > 0.05$). The dashed red line represents a fold change threshold of ≥1.5 and ≤1.5.

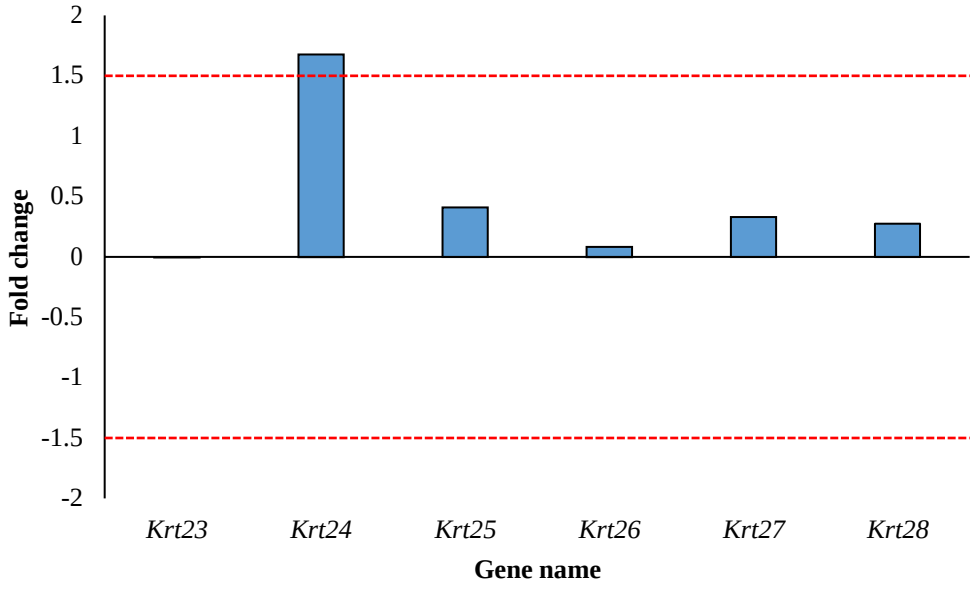

Figure 5.5.8 Protein coding genes associated with the keratin protein family (*Krt23 – Krt28)* showing upregulation based on fold change in 12*R*-LOX deficient vs wildtype dataset. The absence of orange bars indicates that there are no statistically significant genes in the 12*R*-LOX deficient dataset. The bars highlighted in blue indicate genes considered to be statistically non-significant in the 12*R*-LOX deficient dataset ($p > 0.05$). The dashed red line represents a fold change threshold of ≥1.5 and ≤1.5.

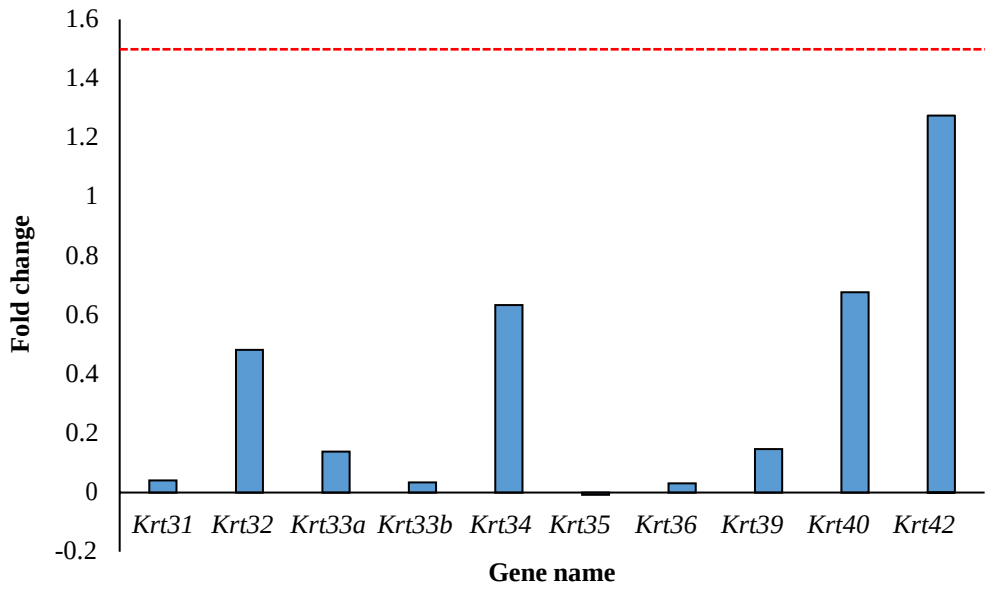

Figure 5.5.9 Protein coding genes associated with the keratin protein family (*Krt31 – Krt42)* showing upregulation based on fold change in 12*R*-LOX deficient vs wildtype dataset. The absence of orange bars indicates that there are no statistically significant genes in the 12*R*-LOX deficient dataset. The bars highlighted in blue indicate genes considered to be statistically non-significant in the 12*R*-LOX deficient dataset ($p > 0.05$). The dashed red line represents a fold change threshold of ≥1.5.

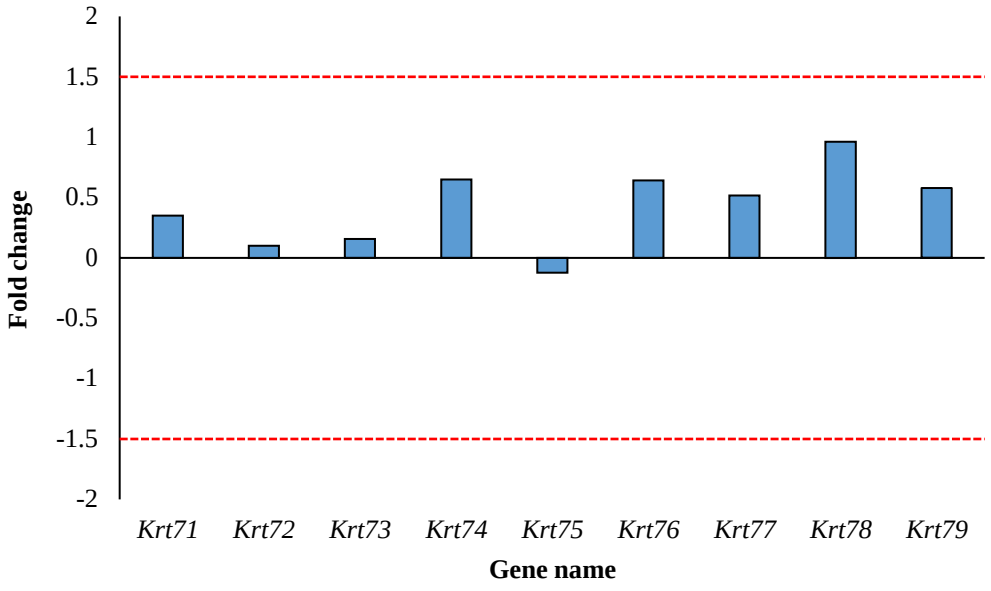

Figure 5.5.10 Protein coding genes associated with the keratin protein family (*Krt71 – Krt79)* showing both upregulation and downregulation based on fold change in 12*R*-LOX deficient vs wildtype dataset. The absence of orange bars indicates that there are no statistically significant genes in the 12*R*-LOX deficient dataset. The bars highlighted in blue indicate genes considered to be statistically non-significant in the 12*R*-LOX deficient dataset ($p > 0.05$). The dashed red line represents a fold change threshold of ≥1.5 and ≤1.5.

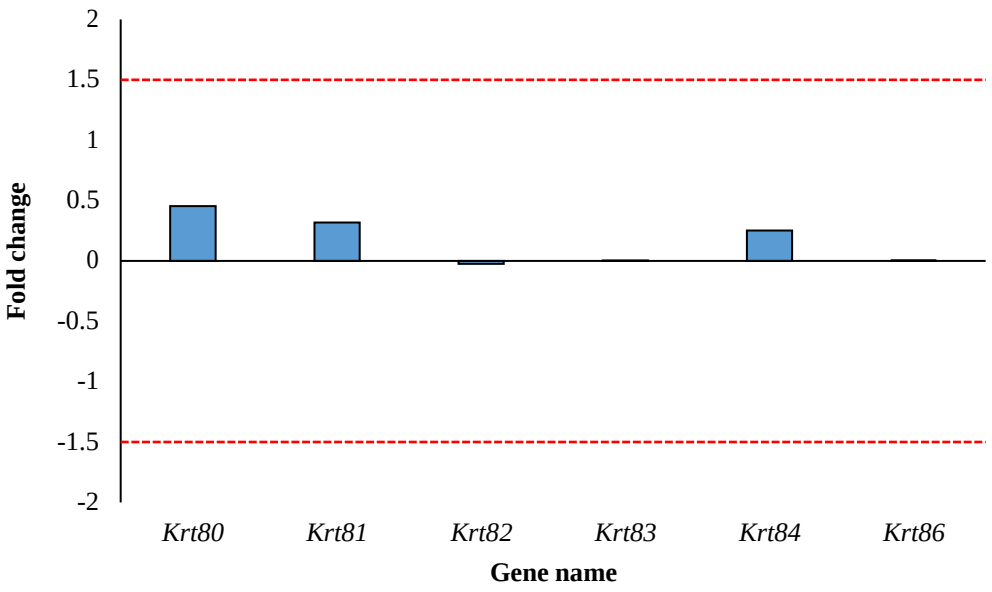

Figure 5.5.11 Protein coding genes associated with the keratin protein family (*Krt80 – Krt86)* showing both upregulation and downregulation based on fold change in 12*R*-LOX deficient vs wildtype dataset. The absence of orange bars indicates that there are no statistically significant genes in the 12*R*-LOX deficient dataset. The bars highlighted in blue indicate genes considered to be statistically non-significant in the 12*R*-LOX deficient dataset ($p > 0.05$). The dashed red line represents a fold change threshold of ≥1.5 and ≤1.5.

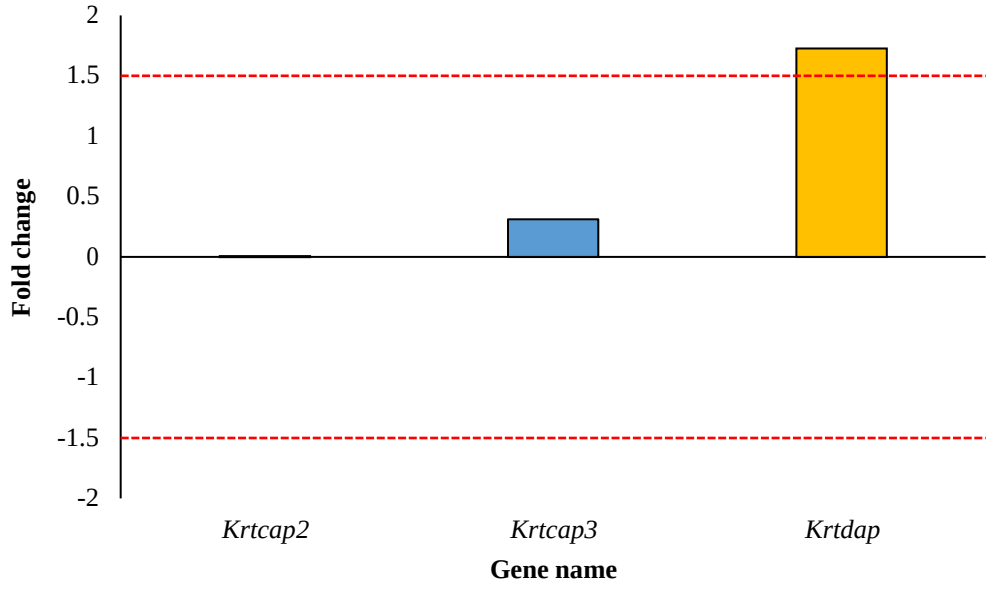

Figure 5.5.12 Protein coding genes associated with the keratin family (*Krtcap2*, *Krtcap3* and *Krtdap)* showing upregulation based on fold change in 12*R*-LOX deficient vs wildtype dataset. The orange bars indicate statistically significant genes in the 12*R*-LOX deficient dataset ($p < 0.05$). The bars highlighted in blue indicate genes considered to be statistically non-significant in the 12*R*-LOX deficient dataset ($p > 0.05$). The dashed red line represents a fold change threshold of ≥1.5 and ≤1.5.

5.5.4 *Krt1* and *Krt10* genes have the most similar expression profile of all keratin encoding genes

Hierarchical clustering was performed on the keratin encoding gene family to identify expression profiles. **Figure 5.5.14** shows the *Krt1* and *Krt10* with the most similar expression profile as demonstrated by the short height of the clade between these two genes (red highlighted circle). One of the top clusters displayed in **Figure 5.5.14** includes *Krt6b*, *Krt14*, *Krt12*, *Krt1*, *Krt10*, *Krt16* and *Krtdap* (clades highlighted in purple). We observe an overexpression of these genes in the 12*R*-LOX deficient samples, whilst lower expression of these genes are observed in the wildtype samples. The majority of other keratin encoding genes have colour variation in both deficient and wildtype samples indicating that there is no distinct difference in terms of expression pattern between 12*R*-LOX deficient and wildtype samples.

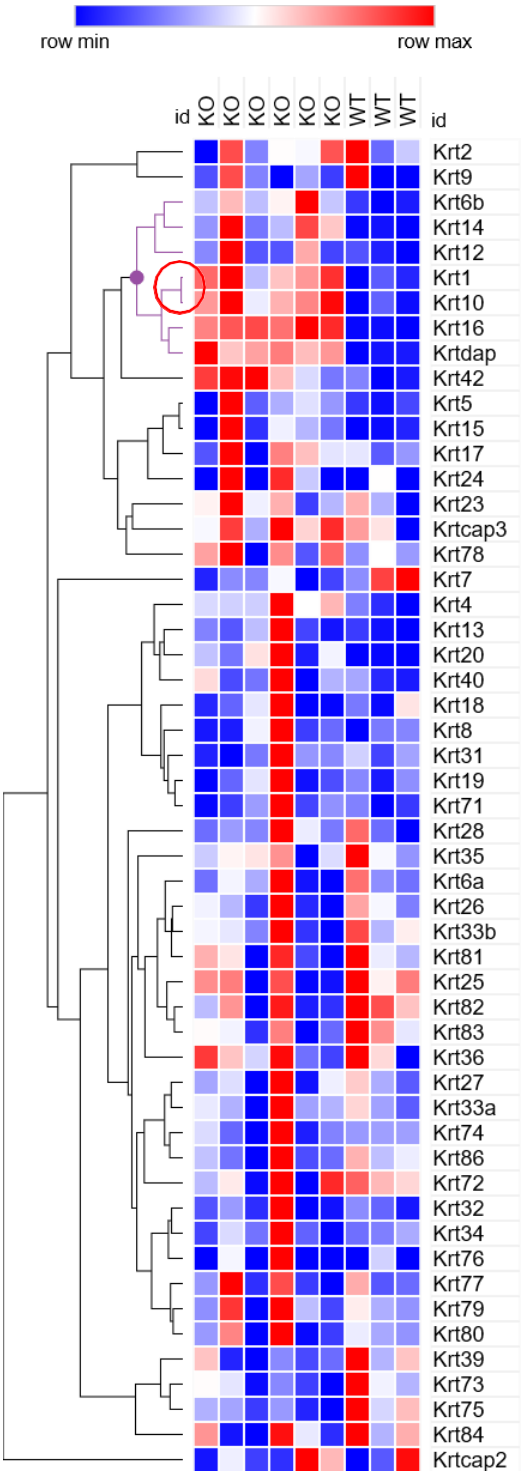

Figure 5.5.14 Hierarchical clustering analysis of the expression profiles of genes associated with the keratin encoding gene family using GENE-E. Each column represents the FPKM values for each gene. The red blocks represent genes that are overexpressed and the blue blocks represent genes with the lowest expression. The remaining coloured bars represent relative expression levels. The minimum FPKM expression value is 0, whilst the maximum FPKM expression value is 868.1. The cluster of interest is highlighted in purple.

5.5.5 *Pparγc1α* gene is the most significantly downregulated PPAR gene

Figure 5.5.15 shows all genes associated with the peroxisome proliferator-activated receptor (PPAR) family are downregulated in response to 12*R*-LOX deficiency, however, the peroxisome proliferator-activated receptor gamma coactivator 1-alpha (*Pparγc1α*) is the most statistically significantly downregulated gene with a -2.1-fold change ($p < 0.05$) (bar highlighted in yellow). The peroxisome proliferator-activated receptor gamma (*Pparγ*) is also found to be statistically significant with a -1.2-fold, falling short of the -1.5-fold change threshold.

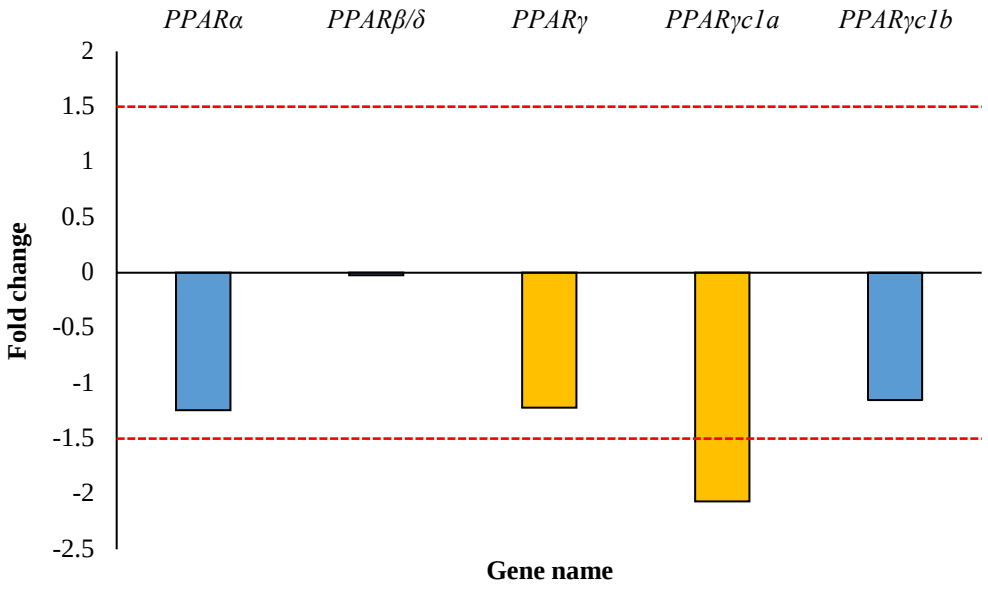

Figure 5.5.15 Protein coding genes associated with the peroxisome proliferator-activated receptor family showing downregulation based on fold change in 12*R*-LOX deficient vs wildtype dataset. The orange bars indicate statistically significant genes ($p < 0.05$). The bars highlighted in blue indicate genes considered to be statistically non-significant ($p > 0.05$). The dashed red line represents a fold change threshold of ≥1.5 and ≤1.5.

5.5.6 *Pparγc1α* and *Pparγc1b* genes have the most similar expression profile of all PPAR encoding genes

Figure 5.5.16 shows hierarchical clustering of the peroxisome proliferator-activated receptor gene family with a similar expression profile observed between the peroxisome proliferator-activated receptor gamma (*Pparγ*), peroxisome proliferator-activated receptor gamma coactivator 1a (*Pparγc1α*) and peroxisome proliferator-activated receptor gamma coactivator 1b (*Pparγc1b*) (clade highlighted in purple). The most similar expression profile exists between *Pparγc1α* and *Pparγc1b* as demonstrated by the shortest height of the clade between these two genes. The expression profile of both *Pparγc1α* and *Pparγc1b* is similar to the expression

profile of *Pparγ* as demonstrated by the clade joining these genes together. An overexpression of these genes are observed in the wildtype samples as indicated by the majority coloured red blocks whilst the expression of these genes in the 12*R*-LOX deficient samples are downregulated as demonstrated by coloured blue blocks.

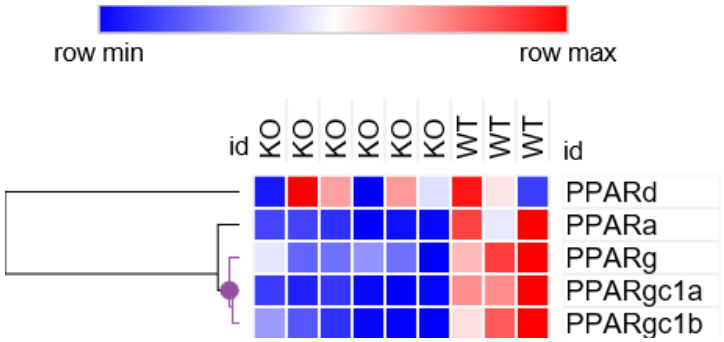

Figure 5.5.16 Hierarchical clustering heatmap showing the expression pattern of genes associated with the peroxisome proliferator-activated receptor gene family. The red blocks represent genes that are overexpressed and the blue blocks represent genes with the lowest expression. The remaining coloured bars represent relative expression levels. The minimum FPKM expression value is 0, whilst the maximum FPKM expression value is 42.2. The cluster of interest is highlighted in purple.

5.5.7 Ingenuity Pathway Analysis of EDC, keratin and the PPAR Gene Family

5.5.7.1 Glucocorticoid receptor signalling pathway identified as the top canonical pathway

Differentially expressed genes associated with EDC, keratin and the PPAR families were processed using the ingenuity pathway analysis (IPA) bioinformatics platform as described in **Section 5.4.2** to obtain signalling pathways active in the 12*R*-LOX deficient mouse models. The most significant canonical pathway associated with differentially expressed genes of the EDC, keratin and PPAR gene family is the "glucocorticoid receptor signalling pathway" (p= $3.75x10^{-6}$). A total of five differentially expressed genes belonging to the EDC, keratin and PPAR gene family in the 12*R*-LOX deficient dataset are associated with the "glucocorticoid receptor signalling pathway". These include *Krt1*, *Krt14*, *Krt16*, *Krt24* and *Krt6b*. In total, there are 462 molecules involved in the "glucocorticoid receptor signalling pathway" resulting in a 1.1% overlap of keratin differentially expressed genes.

5.5.7.2 GATA3 gene identified as top upstream regulator

The most significant upstream regulator as identified by IPA is the GATA3 gene which is a known transcriptional regulator (p= $4.43x10^{-12}$). **Figure 5.5.17** shows that GATA3 activation is predicted to be inhibited as a result of the upregulation of *Sprr1b*, *Sprr2d*, *Sprr2e*, *Sprr2h*,

Sprr2a1, *Sprr2a2*, *Lce3e* and *Krt14* observed in the 12*R*-LOX deficient vs wildtype dataset. **Figure 5.5.17** shows that the GATA3 gene has an influence on itself as demonstrated by the blue circular arrow in response to the upregulation of the aforementioned genes. Although GATA3 is not downregulated in the 12*R*-LOX deficient dataset, it possesses a low fold change value of 0.3 and is below the 1.5 threshold set in previous analysis.

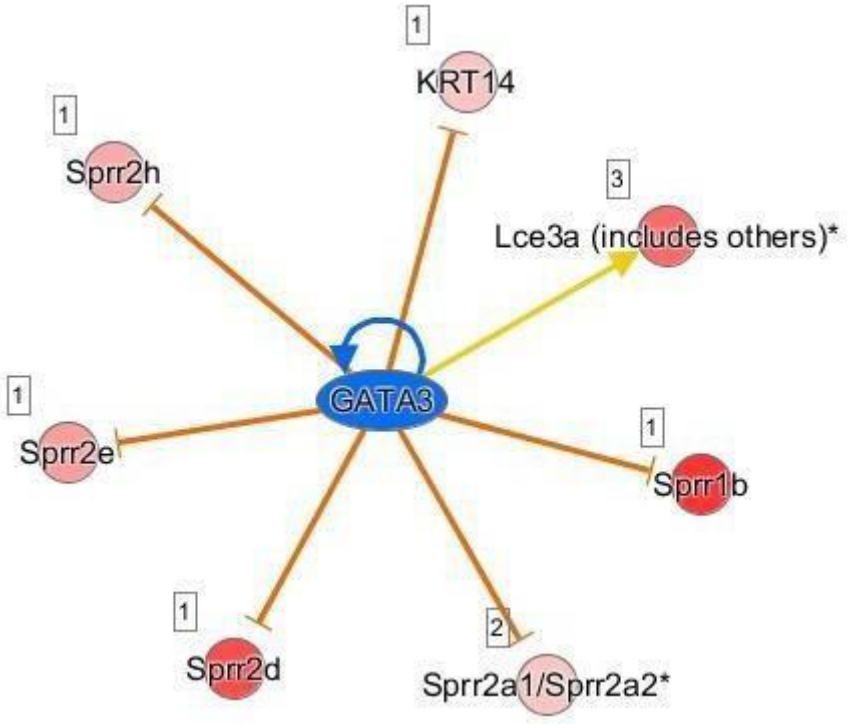

Figure 5.5.17 The top upstream regulator network associated with EDC, keratin and PPAR differentially expressed genes found in the 12*R*-LOX deficient dataset as identified by Ingenuity Pathway Analysis (IPA). Upregulated genes are coloured in red. Colour saturation of upregulated genes are correlated to fold change (High colour saturation indicates a high fold change and a low colour saturation indicates a low fold change). Predicted inhibition of genes are coloured in blue. Solid coloured lines are predicted relationships between genes. A solid orange line indicates activation of downstream genes as a result of the predicted inhibition of a gene. A solid yellow line indicates inconsistent findings with state of the downstream gene. Oval shapes represent transcriptional regulators and circles represent others in the network shape legend.

5.5.7.3 Differentially expressed genes of the 12*R*-LOX deficient dataset are associated with other dermatological diseases and conditions

The most significant disease and disorder as characterised by IPA is "dermatological diseases and conditions" (p= 4.14x10^{-2}). A total of ten differentially expressed genes belonging to the EDC, keratin and PPAR gene family in the 12*R*-LOX deficient dataset are associated with "dermatological diseases and conditions". These include *Krt1*, *Krt16*, *Krt6b*, *Krt14*, *Krt10*, *Sprr2a1*, *Sprr2a2*, *Sprr2d*, *Krtdap* and *Pparγc1a* where they are also abnormally expressed in various dermatological conditions as shown in **Table 5.5.1**.

Diseases or Functions Annotation	Molecules
Epidermolytic palmoplantar keratoderma	*Krt1,Krt16*
Autosomal dominant pachyonychia congenita	*Krt16,Krt6B*
Plaque psoriasis	*Krt1,Krt14,Krt16,Krt6B*
Benign papilloma	*Krt16,Sprr2a1,Sprr2a2,Sprr2d*
Psoriasis	*Krt1,Krt14,Krt16,Krt6B,Krtdap*
Abnormal morphology of skin	*Krt1,Krt10,Krt14,Krt6B*
Dermatitis	*Krt1,Krt14,Krt16,Pparγc1α*
Atopic dermatitis	*Krt1,Krt16,Pparγc1α*
Hyperkeratosis	*Krt1,Krt10,Krt16*
Abnormal morphology of keratinocytes	*Krt14,Krt6B*
Abnormal morphology of epidermis	*Krt1,Krt10,Krt14*
Abnormal morphology of basal layer of epidermis	*Krt10,Krt14*
Abnormality of skin morphology	*Krt1,Krt10,Krt14,Krt16*
Abnormal morphology of stratum corneum	*Krt1,Krt10*
Blister	*Krt10,Krt14*
Rupture of keratinocytes	*Krt6B*
Pachyonychia congenita 4	*Krt6B*
Naegeli syndrome	*Krt14*
Palmoplantar keratoderma striata form III	*Krt1*
Curth Macklin type ichthyosis hystrix	*Krt1*
Dermatopathia pigmentosa reticularis	*Krt14*
Late-onset epidermolytic hyperkeratosis	*Krt1*
Cyclic ichthyosis with epidermolytic hyperkeratosis	*Krt1*
Dowling-Meara type epidermolysis bullosa simplex	*Krt14*
Generalized severe epidermolysis bullosa simplex	*Krt14*
Autosomal recessive epidermolysis bullosa simplex type 1	*Krt14*
Nonepidermolytic palmoplantar keratoderma	*Krt1*
Focal nonepidermolytic palmoplantar keratoderma type 1	*Krt16*
Pachyonychia congenita 2	*Krt6B*
Ichthyosis with confetti	*Krt1*
Pachyonychia congenita 1	*Krt16*
Hypergranulosis	*Krt10*
Weber-Cockayne type dominant epidermolysis bullosa simplex	*Krt14*
Abnormal morphology of enlarged sebaceous glands	*Krt10*
Hyperplasia of epidermis	*Krt10,Krt16*
Abnormal morphology of cornified envelope	*Krt1*
Clear cell acanthoma	*Krt1*
Granulocyte colony stimulating factor-induced psoriasiform dermatitis	*Krt16*

Table 5.5.1 Top diseases and disorders associated with differentially expressed genes of the EDC, Keratin and PPAR found in the 12*R*-LOX deficient dataset as identified by Ingenuity Pathway Analysis.

5.5.7.4 The top molecular network associated with differentially expressed genes belonging to the EDC, keratin and PPAR family

The network analysis performed by IPA predicts the interaction between EDC, keratin and PPAR differentially expressed genes in the 12*R*-LOX deficient dataset and how they interact on a molecular level. **Figure 5.5.23** shows the top network as identified by IPA that are associated with differentially expressed genes belonging to the EDC, keratin and PPAR family. This network is associated with functions that include "cell morphology" and "hair and skin development and function". A total of 11 EDC, keratin and PPAR differentially expressed genes are found within this top network. These include *Krt1, Krt14, Krt16, Krt24, Krt6b, Krt10, Krtdap, Sprr2a1*, *Sprr2a2, Sprr2d*, *Rptn* and *Pparγc1a*.

The majority of upregulated keratin genes in the 12*R*-LOX dataset are directly or indirectly interacting with other keratin genes through binding or being acted upon. It is beta-defensin 4 (*Defb4*), POU class 2 homeobox 3 (*Pou2f3*) and transforming growth factor beta (*Tgfb*) that links the majority of keratin genes to other differentially expressed genes such as *Krtdap, Rptn*, *Sprr2a1*, *Sprr2a2* and *Pparγc1a*. The *Defb4* gene encodes a protein known as the hBD-2 antimicrobial peptide and is shown to be expressed in other skin disorders such as psoriasis (Bracke et al., 2004). The *Pou2f3* gene is part of a family of transcription factors and implicated in the regulation of proteins involved in epidermal differentiation (Neumann et al., 2015). *Tgfb* are a family of growth factors implicated in important biological processes such as proliferation, differentiation and apoptosis (Kubiczkova et al., 2012). *Tgfb* decreases the insertion of the methionine amino acid into *Krt1* and subsequently promotes epidermal maturation (Mansbridge and Hanawalt, 1988).

The downregulated transcriptional regulator *Pparγc1a* gene has two interactions within the network shown in **Figure 5.5.23**. These interactions are with histone h3 where its acted upon and *Tgfb* where it is indirectly acted upon. *Krt16* is shown to have an indirect effect on *Sprr2d*. Both *Krtdap* and *Rptn* are indirectly acted upon by the carbonic anhydrase 4 enzyme. The *Sprr2a1* and *Sprr2a2* differentially expressed genes indirectly acts upon histone h3 which directly effects the carbonic anhydrase 4 enzyme.

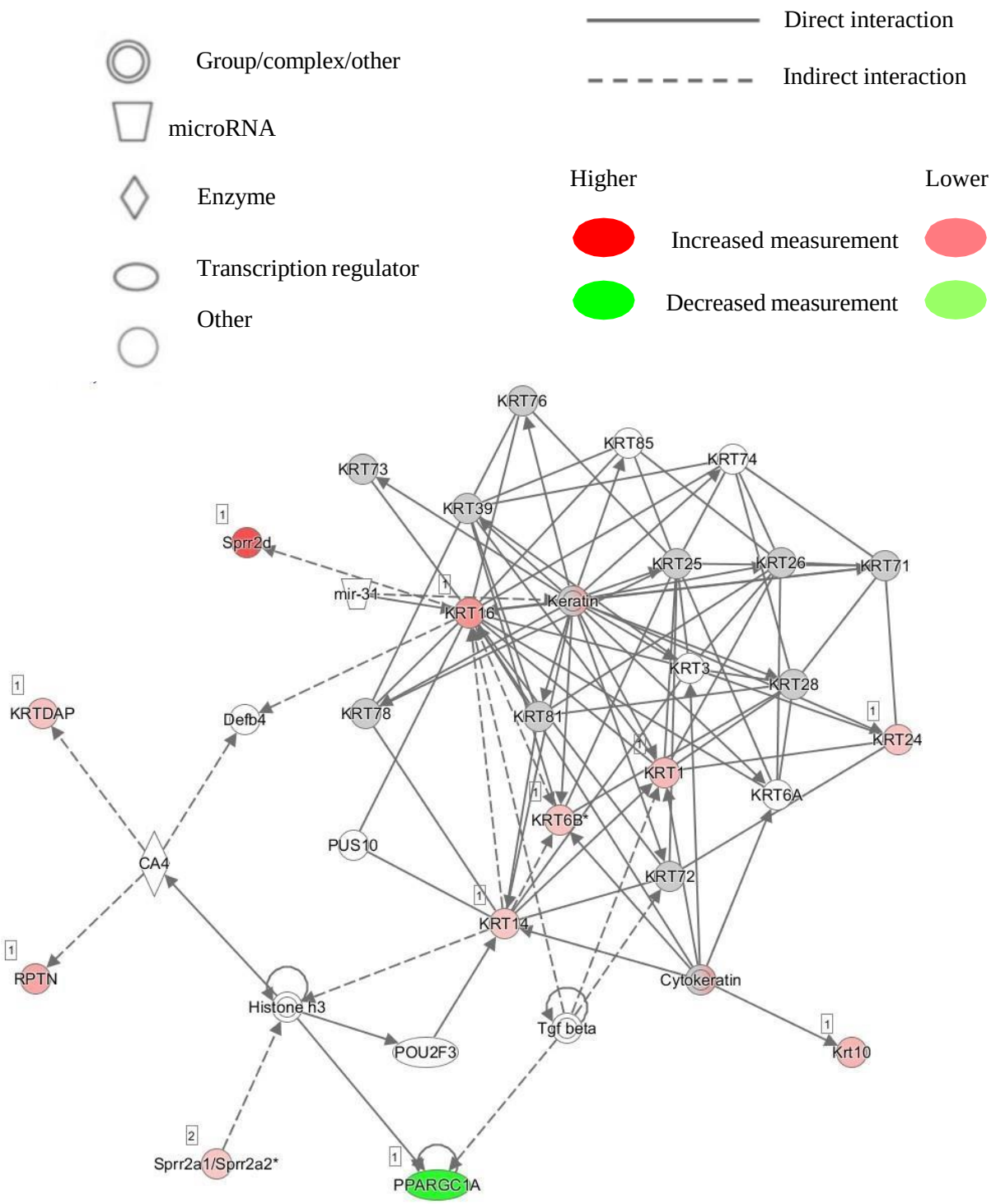

Figure 5.5.23 Top network associated with EDC, keratin and PPAR differentially expressed genes found in the 12*R*-LOX deficient dataset as identified by Ingenuity Pathway Analysis. Upregulated genes are coloured in red, whilst downregulated genes are coloured in green. Colour saturation of differentially expressed genes are correlated to fold change (High colour saturation indicates a high fold change and a low colour saturation indicates a low fold change). A solid line specifies a direct connection, whilst dotted lines indicates an indirect connection. The circular arrows indicate the gene having an effect on itself. Oval shapes represent transcriptional regulators, double circles represent a complex/groups, rhombuses represent enzymes, inverted trapezoid represent microRNA and circles represent others.

5.6 Discussion

This chapter focussed on the analysis of EDC, keratin and PPAR genes as bioinformatics analysis results from the previous chapter showed that DEGs in the 12*R*-LOX deficient vs wildtype dataset are associated with keratinization and keratinocyte differentiation processes. Furthermore, key transcriptional regulators hypothesised to be involved in regulating these processes were found to be downregulated in the 12*R*-LOX deficient vs wildtype dataset.

5.6.1 Upregulation of SPRRs in multiple skin disorders

A subset of the EDC known as the small proline-rich proteins (SPRRs) are upregulated in response to 12*R*-LOX protein deficiency according to fold change values (FC $\geq$ 1.5). Statistically significant DEGs of the SPRR family such as *Sprr1b*, *Sprr2d* and *Sprr2h* are found to be upregulated in other inflammatory skin disorders (Kartasova et al., 1996). For example, an overexpression of SPRRs are observed in a genetic skin disease known to effect the differentiation of epidermal keratin proteins, known as epidermolytic hyperkeratosis (Ishida-Yamamoto et al., 1997). Additionally, an abnormally high expression of SPPR1 proteins are observed in psoriatic lesions and in the epidermis of eczema patients in comparison with normal, healthy skin (De Heller-Milev et al., 2000; Hoffjan and Stemmler, 2007). This is similar to results found in response to the 12*R*-LOX genetic deletion in mice. Upregulation of the SPRR genes is consistent with abnormal expression of key cornified envelope constituents, leading to an impaired barrier function. A defective barrier is characteristic of the pathophysiology of ichthyosis and therefore the upregulation of SPRRs may be responsible for this specific flaw in barrier integrity. In view of this information, considerable evidence points towards high levels of SPRRs expression in multiple skin diseases and disorders.

5.6.2 Functional link between 12*R*-LOX and overexpression of SPRR proteins

It is unknown whether SPRR overexpression affects important epidermal processes such as keratinocyte proliferation and differentiation or is simply a consequence of injury or abnormality and subsequent induction of a stress response (Segre et al., 2006). Interestingly, GeneOntology analysis of 12*R*-LOX deficient differentially expressed genes such as SPRRs indicate a possible biological role in keratinocyte differentiation. As SPRRs are expressed in the most outer layers of the epidermis, this would suggest a role in the very late stages of differentiation. Furthermore, a potential role of 12*R*-LOX in cell proliferation lacks support from the overall RNA-sequencing investigative analysis, as indicated by the lack of significant DEGs associated with proliferation. For example, cell proliferation is localised to the basal layer of the epidermis, however, the number of differentially expressed genes associated with

proliferative layers is low in comparison with differentiated layers. Additionally, biological processes such as keratinization and cornification generated by GO analysis suggests SPRRs having a role in the stratified layers of the epidermis, lessening the probability of involvement in cell proliferation. To support this, Epp et al., 2007 concluded that defects in epidermal barrier formation as a result of 12*R*-LOX deficiency did not impair the proliferation process.

5.6.3 SPRR overexpression potentially linked with epidermal barrier repair

It is evident that the genetic deletion of the 12*R*-LOX protein and its subsequent effect impacts the expression of SPRRs. In line with other skin disease models, SPRRs are also shown to be overexpressed and are therefore possibly acting as stress response molecules and modulating the repair of the defected barrier (Segre et al., 2006). As a compromised epidermal barrier is a main feature of ichthyosis, this could explain the upregulation of SPRRs such as *Sprr1b*, *Sprr2d* and *Sprr2h* in the 12*R*-LOX deficient mouse models. Supporting this hypothesis is evidence from loricrin (*Lor*) deficient mice whereby upregulation of other cornified envelope genes are observed to compensate for defects in the barrier (Koch et al., 2000). Additionally, a stimulating effect on SPRRs are observed in other diseases, for example, during ischemic stress in cardiomyocytes resulting in a cardioprotective function (Pradervand et al., 2004).

5.6.4 Associated pathways and upstream regulators of DEGs in the 12*R*-LOX deficient dataset

Ingenuity Pathway Analysis (IPA) provides a valuable insight into predicted pathways and interactions with other differentially expressed genes and potential regulators in response to the 12*R*-LOX deficiency. The top upstream regulator as identified by IPA is GATA3, a transcriptional regulator with prominent expression in the stratum spinosum layer (Rácz et al., 2011). Upregulation of SPRRs such as *Sprr1b*, *Sprr2d*, *Sprr2e*, *Sprr2h*, *Sprr2a1* and *Sprr2a2* causes inhibition of GATA3 which is implicated in atopic diseases. Interestingly, GATA3 is found to have an important role in keratinocyte differentiation and is key to the formation of the epidermal barrier (Zeitvogel et al., 2017). Studies confirm a reduced expression of GATA3 in inflammatory skin conditions such as psoriasis and atopic dermatitis which is consistent with a downregulated fold change value associated with GATA3 in the 12*R*-LOX deficient dataset (Rácz et al., 2011; Zeitvogel et al., 2017). Consistent with the characteristics observed in 12*R*-LOX deficient mice, GATA3 knockout mouse models display a perturbed epidermal barrier, increased postnatal mortality and rapid water loss (de Guzman Strong et al., 2006). Numerous genes found in the EDC are affected in response to silencing of the GATA3 transcriptional factor which are similarly affected in 12*R*-LOX deficient mice. This indicates that both

knockouts have a detrimental effect on genes belonging to the EDC which are integral for the maturation of the barrier. EDC genes which are predominantly affected in GATA3 silencing studies include late cornified envelope genes, small proline-rich genes, S100 genes, trichohyalin (*Tchh*) and hornerin (*Hrnr*) (FC ≥ 1.5). Minor changes in fold change (FC ≤ 1.5) are observed in other genes belonging to the EDC such as *Ivl* and *Lor* which is also true of fold change values observed in the 12*R*-LOX deficient dataset. Although various SPRRs are upregulated in GATA3 and 12*R*-LOX deficient data, other members of the EDC such as genes associated with the S100 and late cornified envelope family were barely influenced by 12*R*-LOX deficiency as evident by the low fold change values.

5.6.5 Absence of 12*R*-LOX lipid products impacts GATA3 expression

The top upstream regulator network displayed in **Figure 5.4.16** shows 12*R*-LOX deficiency having an effect on the expression of six genes belonging to the SPRR family which are also found to be upregulated in GATA3 *in vitro* knockout studies (Zeitvogel et al., 2017). Lipid products produced via 12*R*-LOX oxygenation may act as GATA3 agonists and therefore affect the downstream expression of SPRRs. It has been shown in other studies that overexpression of GATA3 has reversed the phenotype observed in skin disorders with a perturbed epidermal barrier (Zeitvogel et al., 2017). It is possible that 12*R*-LOX generated lipids may activate GATA3 and therefore regulate the expression of SPRRs. If SPRRs are involved in compromised epidermal barriers, a regulated expression of these cross linked proteins may control their hypothesised function as stress response molecules and therefore reduce the need for rapid epidermal barrier repair.

5.6.6 Specific keratins upregulated in 12*R*-LOX deficient mice are also hallmarks of other skin diseases

Keratins have widely been recognised as providing mechanical strength and structure to the epidermis through formation of intracellular framework of various keratin proteins (Arin et al., 2010; Chamcheu et al., 2011). Keratins are important in a variety of epidermal processes which include response to a range of stress induced stimuli, cell positioning and a possible signalling role in keratinocyte differentiation (Omary et al., 2009). However, mutations in keratin genes resulting in abnormal expression are implicated in the pathogenesis of skin disorders.

Psoriatic skin lesions show elevated expression levels of specific keratins that are also highly expressed in 12*R*-LOX deficient mice (Mommers et al., 2000; Jiang et al., 2015). This study shows specific keratins (*Krt1*, *Krt6b*, *Krt10*, *Krt12*, *Krt16* and *Krtdap*) are upregulated in response to 12*R*-LOX protein deficiency. Of these specific keratins, *Krt6b* and *Krt16* are

implicated in the pathogenesis of skin disorders such as psoriasis. For example, studies have shown a role for these specific keratins in the regulation and promotion of biological processes such as proliferation and cell migration which are altered in various skin disorders (Elango et al., 2018). Indeed, it is possible that these precise keratins may be biomarkers and potential targets for a range of inflammatory skin disorders that include ichthyosis.

5.6.7 Upregulation of keratins in response to stress stimuli

Overexpression of keratins is observed in response to mechanical and proinflammatory stimuli, suggesting an essential role for keratins in managing and regulating a response. Wound healing studies have shown an overexpression of suprabasal keratins such as *Krt6a*, *Krt6b*, *Krt16* and *Krt17*. Additionally, these keratins have also shown to be induced by inflammatory cytokines and oxidative stress (Freedberg et al., 2001). Interestingly, of these specific keratins found to be upregulated in this stress stimuli, *Krt6b* and *Krt16* are found to be upregulated in response to 12*R*-LOX protein deficiency where a perturbed epidermal barrier exists.

Krt1 shown to be overexpressed in 12*R*-LOX deficient mice has been identified as a regulator of inflammasome activity (Roth et al., 2012). This in turn has a downstream effect in controlling the quantity of cytokine and antimicrobial secretions from keratinocytes. *Krt6b* and *Krt16* have been identified as alarmin molecules, giving swift and innate immune response to stress signals (Zhang et al., 2019). As a distressed and perturbed epidermal barrier is characteristic of 12*R*-LOX deficient mice, this would explain the upregulation of these specific keratins. The presence of LOX derived lipids on the other hand reverse this effect and dampen alarmin molecules that are activated in response to stimuli and are therefore implicated in a signalling network that is involved in regulating stress response molecules. As such, it is further evidence pointing towards the role of keratins in modulating an innate immune response and therefore increasing the need for epidermal barrier repair.

5.6.8 Keratin overexpression associated with epidermal barrier repair

The overexpression of keratins observed in the 12*R*-LOX deficient dataset may contribute to the formation of a “temporary” barrier to compensate for the complete barrier loss found in 12*R*-LOX deficient mice as shown in **Figure 5.6.1**. The overexpression and aggregation of *Krt1* and *Krt10* filaments result in tonofibrillar bundles which are characterised by thick, dense structures. These structures may further aid in compensating for the loss of the protective epidermal barrier and provide resistance to physical strain. Additionally, both *Krt1* and *Krt10* from an insoluble filament assembly, providing added support to a possible compensatory barrier. The overexpression of these keratins may explain the thickened stratum corneum

observed in patients with ichthyosis as has been identified with light microscopy (Ishida-Yamamoto et al., 1992). A less severe epidermal hyperkeratosis is observed in the skin of healthy patients, suggesting LOX derived lipids may contribute to the regulation of keratin expression.

As keratins provide a rigid structure and form the intermediate filament cytoskeleton of the epidermis, the upregulation and abundance of keratins would help reduce rapid water loss as well as lowering the risk of infection. *Krt1* is also shown to be upregulated in response to 12*R*-LOX deficiency and is shown to be differentially expressed during mechanical stress in other studies (Reichelt et al., 2001). *Krt1*, *Krt6a*, *Krt6b* and *Krt16* DEGs are all expressed in stratified epithelia suggesting that upper layers of the epidermis are predominantly affected in the absence of LOX derived lipids. The epidermal barrier is the first line of defence against external stimuli and therefore it is understandable that keratin proteins found in the outermost layers are induced in response to 12*R*-LOX deficiency.

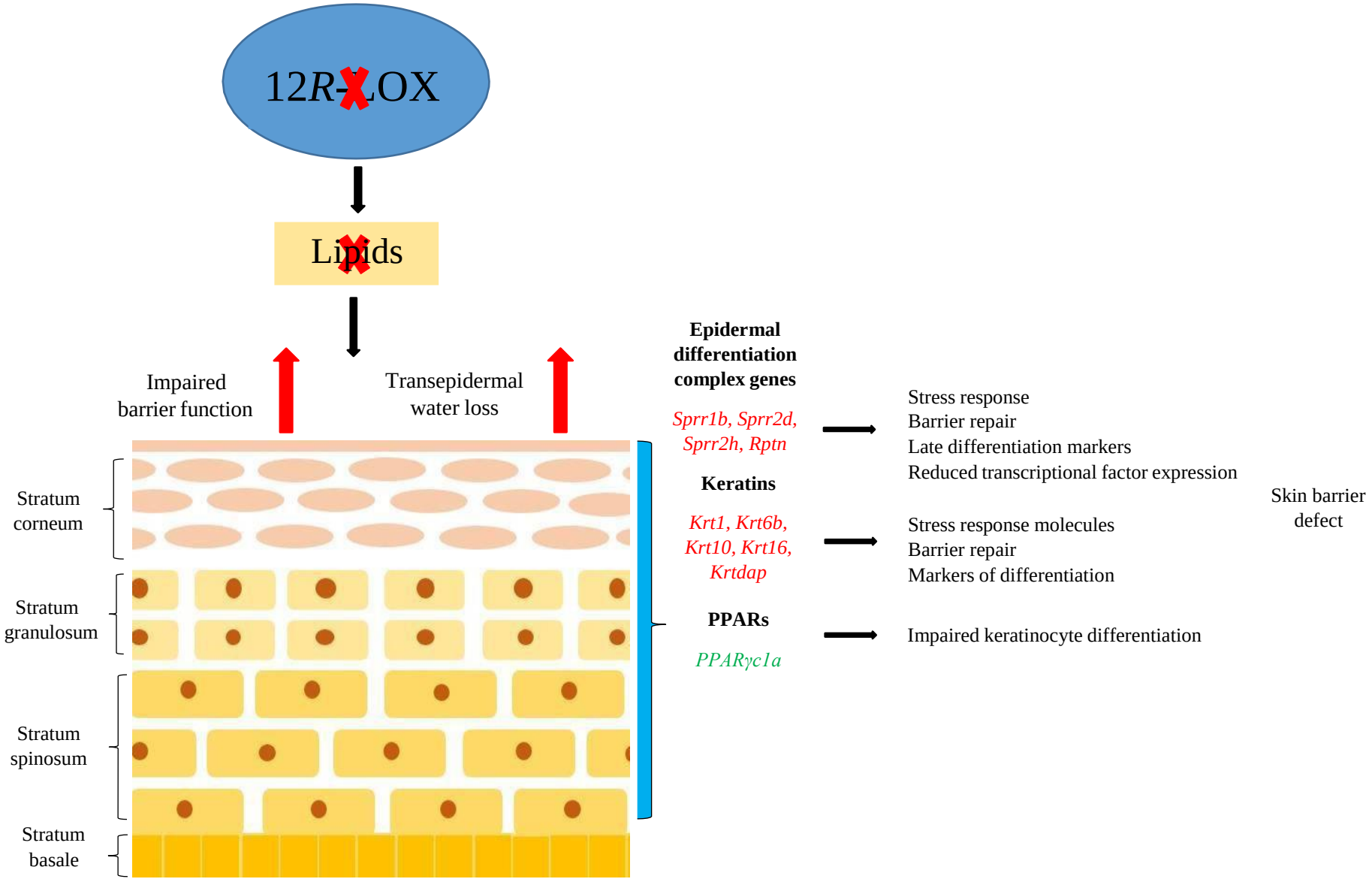

Figure 5.6.1 Schematic of the epidermis displaying localisation of DEGs in the upper layers of the epidermis and their function correlated with their expression pattern. DEGs highlighted in red represent upregulation, whilst DEGs highlighted in green represent downregulation. The right brace highlighted in blue indicates the suprabasal layer of the epidermis in which the DEGs are predominantly expressed.

5.6.9 Increased expression of specific keratins (*Krt1* and *Krt10*) associated with abnormal keratinocyte differentiation

Keratin expression occurs in a time specific sequence and is dependent on the stage of keratinocyte differentiation during epidermal development. *Krt1* and *Krt10* expression occur at an early differentiation stage suggesting that the absence of 12*R*-LOX lipids has an effect on key proteins of keratinocyte differentiation and their potential involvement in regulating differentiation. Keratins expressed in basal layers of the epidermis such as *Krt8* and *Krt18* are unaffected by 12*R*-LOX deletion as evident by their low fold change values (FC $\leq$ 1.5), suggesting that a role for lipids in the basal layers is unlikely.

Studies investigating *Krt10* expression has shown that its upregulation inhibits both cell proliferation and the cell cycle process. Aberrations in both these processes are commonly observed in multiple skin disorders. Conversely, *Krt10* overexpression stimulates terminal differentiation of keratinocytes, whereby cells become cornified and alter in shape and morphology (Paramio et al., 1999). Keratinocyte differentiation is a highly complex multi-step process and is seemingly impaired in 12*R*-LOX deficient mice as previous studies have shown (Epp et al., 2007). Terminal differentiation plays a key role in forming the insoluble and rigid barrier and therefore the overexpression of *Krt10,* known to promote terminal differentiation, may be induced to accelerate the formation of a compensatory epidermal barrier. As 12*R*-LOX deficient mice display elevated water loss which ultimately leads to early mortality, a compensatory mechanism is induced to achieve terminal differentiation and in turn compensating for the defective barrier function. This specific keratin transcript data suggest that lipids generated via 12*R*-LOX enzyme catalysis may play a key role in regulating the differentiation process and therefore modulate skin homeostasis.

To further support evidence of a direct link between 12*R*-LOX lipids and keratinocyte differentiation, an overexpression of *Krtdap* is observed in 12*R*-LOX deficient mice. This specific keratin functions in the regulation of keratinocyte differentiation and enabling epidermal maintenance. Upregulation of *Krtdap* is widely observed in suprabasal layers in lesional skin of psoriatic patients (Tsuchida et al., 2004). Its localisation along with other differentially expressed keratins in the 12*R*-LOX deficient mice suggests that LOX derived lipids mainly act upon stratified layers of the epidermis and their absence alters expression patterns of suprabasal keratins.

5.6.10 *Pparγ* and its coactivator, *Pparγc1α* are downregulated in other similar skin disorders

Whilst the fold change value of *Pparγ* falls slightly below the threshold of 1.5, it is still a gene of statistical significance. What's more, significant evidence has implicated its role in skin homeostasis and disease. Importantly, the *Pparγc1α* interacts with *Pparγ* allowing the latter to interact with other transcriptional factors and regulate biological functions such as cell differentiation, proliferation and immune response (Yun et al., 2018). Both PPARs also possess similar structural and sequence homology as described by Sertznig et al., 2011. Additionally, the *Pparγc1α* significantly increases the activity of *Pparγ* (Lin et al., 2002). The hierarchical clustering analysis shown in **Figure 5.5.16** shows that the expression profile of both *Pparγ* and *Pparγc1α* are very similar in the 12*R*-LOX deficient and wildtype samples. Due to their similar structures and interaction, it is of interest to explore the rationale behind both their downregulation in skin disorders.

Although little information is available at present regarding the expression profile of *Pparγc1α* in skin disorders, studies have conclusively shown that PPARs such as *Pparγ* are downregulated in human psoriatic skin for example (Sertznig and Reichrath, 2011). Several mouse model studies resembling hyperproliferative skin disorders have shown that an administration of *Pparγ* activators reduced the abnormally high rate of cell proliferation. *Pparγ* has been demonstrated to regulate the expression of multiple biological processes such as proliferation, differentiation and initiating an inflammatory response (Sugiyama et al., 2000; Henson, 2003). The majority of these processes are either partially abated or completely defective, thus contributing to development and progression of disease. Both PPARs found to be downregulated in the skin of 12*R*-LOX deficient mice may therefore be identified as therapeutic targets for conditions showing impairments in the aforementioned biological processes.

5.6.11 *Pparγ* and *Pparγc1α* role in keratinocyte differentiation

Pparγ performs a diverse role from modulating lipid metabolism and immune response to cell differentiation (Michalik and Wahli, 2007; Ramot et al., 2015). PPARs regulate transcription of other genes through the heterodimerization with retinoid X receptors (RXR) and the resulting complex binding to specific DNA sequence of differentiation genes known as PPAR response elements (PPRE) (Tzeng et al., 2015). This biological interaction would subsequently regulate the transcription of various genes in the presence of activators such as those involved in differentiation (Sertzing and Reichrath, 2011).

High expression of *Pparγ* is observed during adipose tissue development with a defined role in differentiation (Barak et al., 1999; Rosen et al., 2000). Whilst PPARs are hypothesised to be involved in cell differentiation in other tissue, studies are yet to confirm whether these specific PPARs, *Pparγ* and *Pparγc1α*, are key regulators of keratinocyte differentiation. If these select PPARs are implicated in differentiation, their downregulation has a downstream effect on genes involved in differentiation and differentially expressed in 12*R*-LOX deficient mice. This would suggest that *Pparγ* and *Pparγc1α* are implicated or have a direct role in regulating keratinocyte differentiation. These differentiation proteins include members of the EDC family such as *Sprr1b, Sprr2d, Sprr2h* and *Rptn*. Additional proteins linked with the epidermal differentiation program and are found to be differentially expressed in the 12*R*-LOX deficient mice include members of the keratin family such as *Krtdap, Krt1, Krt10, Krt6b* and *Krt16*. However, as both *Pparγ* and *Pparγc1a* are downregulated, one might expect the differentially expressed proteins of the EDC and keratin differentiation markers to be downregulated in the same way. Other EDC proteins are shown to be downregulated such as members of the S100 family, however, they fail to reach the 1.5-fold change threshold and are not of statistical significance ($p > 0.05$). Furthermore, genes which encode proteins that are differentially expressed in the 12*R*-LOX deficient dataset may be induced to compensate for the impaired differentiation programme incurred in 12*R*-LOX deficient mice. A compensatory differentiation mechanism that does not involve the downregulated PPARs may be induced to accelerate the formation of a barrier.

In accordance, *Pparγ* and its coactivator, *Pparγc1α*, are found to be expressed in the granular layer of the epidermis where keratinocytes have undergone differentiation (Mao-Qiang et al., 2004). This is consistent with the localisation and activity of the 12*R*-LOX protein, further suggesting that 12*R*-LOX / eLOX-3 derived lipids impact processes and proteins found in the upper layers which consist of differentiated keratinocytes.

PPARs are also known to induce a key enzyme, transglutaminase 1 (*Tgm1*), which is involved in cross linking proteins of the cornified envelope to form an insoluble barrier component. This protein acts mainly in the granular and cornified layers of the epidermis and therefore confined to a role in differentiated keratinocytes (Westergaard et al., 2001). A fold change value of 1 for *Tgm1* in 12*R*-LOX deficient mice indicates an upregulation. Transglutaminase 2 (*Tgm2*) on the other hand is found to be downregulated slightly, having a fold change of -0.5 ($p > 0.05$) in response to deletion of 12*R*-LOX, suggesting a possible link between PPAR downregulation and a key enzyme involved in the latter stages of

differentiation. Moreover, *Tgm1* may be overexpressed to repair and rebuild the compromised barrier observed in 12*R*-LOX mice.

5.6.12 12*R*-LOX lipids activate/induce the expression of transcriptional regulators *Pparγ* and *Pparγc1α*

Absence of 12*R*-LOX lipids results in reduced *Pparγ* and *Pparγc1α* expression. This may suggest that lipid products generated through 12*R*-LOX oxidation of polyunsaturated fatty acids activate or induce the expression of both *Pparγ* and *Pparγc1α*. Its activation may then trigger downstream effects such as inducing the homeostatic regulation of vital processes such as differentiation. Interestingly, previous studies involving PPAR activation show a wide range of long-chain fatty acids that are capable of activating the transcriptional regulator (Ramot et al., 2015). For example, *Pparα* is activated by substrates that include palmitic acid, oleic acid and linoleic acid (Popeijus et al., 2014; Kamata et al., 2020).

Known *Pparγ* and *Pparγc1α* endogenous agonists include polyunsaturated fatty acids such as docosahexaenoic acid, eicosapentaenoic acid, low density lipoproteins and long chain monounsaturated fatty acids (Grygiel-Górniak, 2014). Exogenous agonists developed as treatment for inflammatory conditions and which target the activation of both *Pparγ* and *Pparγc1α* include a group of oral anti-diabetic drugs known as thiazolidinediones (TZDs). These include compounds such as rosiglitazone, pioglitazone, ciglitazone and troglitazone (Ramot et al., 2015). It is currently unknown whether LOX derived lipids such as 9R,10R,13R-TriHOME activate or induce expression of the downregulated *Pparγ* and *Pparγc1α* found in 12*R*-LOX deficient skin.

Fascinatingly, 12*R*-LOX deficiency results suggests that lipid products may act as specific *Pparγ* ligands, resulting in its conformational change. Its coactivator, *Pparγc1a*, is thereby recruited in response to the conformational change of *Pparγ*. This also indicates the importance of LOX derived lipids in the recruitment of coactivators to allow for effective function of *Pparγ*. The interaction between *Pparγ* and *Pparγc1α* consequently allows regulation of gene clusters such as the EDC. This in turn, activates or inactivates the effect of PPAR on biological processes such as proliferation and differentiation.

Significantly, *ex vivo* studies show high expression of *Pparγ* during epidermal differentiation (Adachi et al., 2013). This is further evidence to support LOX derived lipids role in regulating keratinocyte differentiation. To support LOX derived lipids role in controlling differentiation, both *in vitro* and *in vivo* studies show the importance of *Pparγ* in maintaining the epidermal permeability barrier. Ligands known to upregulate *Pparγ* has been

shown to inhibit cell proliferation and stimulate terminal differentiation process which is found to be impaired in skin disorders such as ichthyosis (Demerjian et al., 2006; Schmuth et al., 2014).

5.7 Conclusion

The majority of DEGs found in 12*R*-LOX deficient skin are also found to be differentially expressed in other skin disorders such as psoriasis and atopic dermatitis (Henson et al., 2003; Hoffjan and Stemmler 2007; Jiang et al., 2015). The upregulation of genes such as members of the EDC and keratins found in 12*R*-LOX deficient skin suggest a possible compensatory mechanism at work. The loss of the epidermal barrier as observed in 12*R*-LOX deficient mice may induce alternative mechanisms to repair the compromised barrier. Consistent with this is the localisation of the DEGs, where their expression is predominantly found in differentiated layers of the epidermis. This analysis also supports 12*R*-LOX / eLOX-3 lipids role in affecting stratified proteins rather than proliferative proteins, ruling out its role in basal layers of the epidermis. Compensatory mechanisms have been observed in other epidermal gene knockout studies involving loricrin, a key structural protein (Koch et al., 2000). The overexpression of *Sprr1b, Sprr2d, Sprr2h, Rptn* and keratin proteins found in the outer most layers of the epidermis may be responsible and contribute to the thickening of the epidermis observed in lesional skin of ichthyosis patients.

Analysis of specific DEGs reveals a role for 12*R*-LOX / eLOX-3 in the process of keratinocyte differentiation. GeneOntology analysis performed in **Chapter 4** indicated that DEGs of the 12*R*-LOX deficient dataset are implicated in “keratinocyte differentiation”, “keratinization”, “peptide cross-linking” and “cornification”. To investigate further, analysis performed on an important epidermal gene complex, known as the EDC, revealed differential expression of several members of this gene cluster in response to 12*R*-LOX protein deficiency. The DEGs belonging to the EDC include *Sprr1b, Sprr2d, Sprr2h* and *Rptn*, all of which are expressed in late stages of differentiation. The absence of 12*R*-LOX clearly impacts the expression of these late stage differentiation marks, suggesting that the presence of LOX derived lipids may modulate latter stages of keratinocyte differentiation. To further support LOXs role in differentiation, the majority of differentially expressed keratins such as *Krt1, Krt6b, Krt10, Krt16* and *Krtdap* are predominantly expressed in differentiated layers. Their overexpression might indicate an uncontrolled regulation of the differentiation process in the absence of LOX lipids. Instead, the lack of lipids products may induce compensatory

differentiation mechanism/process involving the DEGs that are overexpressed in the 12*R*-LOX deficient vs wildtype dataset.

Additional evidence to support 12*R*-LOX / eLOX-3 role in keratinocyte differentiation includes the downregulation of *Pparγ* and *Pparγc1α*. As both are thought to be associated with the promotion of epidermal differentiation (Ramot et al., 2015), their downregulation observed in 12*R*-LOX deficient skin may inhibit or impair this key epidermal process entirely. It's possible that 12*R*-LOX / eLOX-3 derived lipids may activate these specific transcriptional factors and promote the keratinocyte differentiation process as a downstream effect. Both *Pparγ* and *Pparγc1α* activation by 12*R*-LOX lipid products can be explored using *in vitro* systems such as skin cell models. Moreover, PPARs role in promoting differentiation may also be investigated through analysing key differentiation markers in response to their activation. As such, a PPAR mediated differentiation signalling pathway may be able to be elucidated from these studies. It would also be of interest to determine the expression levels of DEGs associated with differentiation in 12*R*-LOX deficient skin in response to PPAR activation by LOX products. The majority of the DEGs are expressed in the granular/cornified layers and are late differentiation markers that include *Sprr1b*, *Sprr2d*, *Sprr2h* and *Rptn*. The localisation and expression stage of these differentiation markers suggest that the terminal differentiation step is impacted in response to 12*R*-LOX deficiency and that lipids may have a role in this stage of differentiation.

Chapter 6

The effect of the terminal product of the 12*R*-LOX / eLOX-3 pathway, 9R,10R,13R-TriHOME on cell proliferation, apoptosis, migration and differentiation

6.1 Introduction

Mutations in the *ALOX12B* gene which encodes for the 12*R*-LOX protein results in the development of the ichthyosis skin disorders which is characterised by hyperproliferation, abnormal keratinocyte differentiation and increased sensitivity to apoptosis (Fleckman et al., 1997; Marukian and Choate, 2016). The previous chapters have focussed on the *ALOX12B* gene knockout and its apparent effect on the expression of a range of epidermal associated genes known to be vital in the development of the epidermal barrier. This chapter will focus on the effect of the terminal product of the 12*R*-LOX / eLOX-3 pathway, 9R,10R,13R-TriHOME on a variety of fundamental epidermal processes that include, proliferation, differentiation, migration and apoptosis. The structure

6.1.1 Alterations in keratinocyte proliferation lead to epidermal disease

Cells undergo the mitotic cycle which involves a number of sequential steps, allowing for cell division to occur (McIntosh, 2016). The development of the cell cycle in epidermal cells is down to growth factor and growth inhibitor equilibrium, differentiation of keratinocytes and adhesion to basement membrane. Proliferative cells in the epidermis are subdivided into two cell types which include stem cells and the progeny of these cells known as transit amplifying cells. The rate of cellular proliferation is determined by transit amplifying cells in normal epidermis which undergo multiple stages of mitosis, eventually exiting the mitotic cycle and differentiating (Gniadecki, 1998). The specific molecular mechanisms responsible for regulating keratinocyte proliferation are yet to be fully elucidated.

Irregularities in keratinocyte proliferation underly the pathophysiology of many inflammatory skin disorders. Keratinocytes likely undergo proliferative pathomechanisms responsible for the development of skin conditions such as psoriasis. Expression of specific keratins such as keratin 6 (*Krt6*) and keratin 16 (*Krt16*) are indicative of hyperproliferative keratinocytes found in various skin conditions (Jiang et al., 1993). Interestingly, these precise keratins are also found to be overexpressed in 12*R*-LOX deficient skin, suggesting a possible role for LOX in regulating keratinocyte proliferation. The expression of *Krt6* and *Krt16* replace the expression of keratin 5 (*Krt5*) and keratin 14 (*Krt14*) that would normally be observed in healthy skin (Mazzalupo et al., 2003; Zhang et al., 2019). The upregulation of keratin 6 and keratin 16 in mouse models display a phenotype resembling the physiology of psoriasis. The overexpression of both hyperproliferative keratin biomarkers in psoriasis and 12*R*-LOX deficient mouse skin indicates that these skin disorders may share a common pathological mechanism leading to the proliferative phenotype observed in these diseases.

6.1.2 Importance of epidermal cell migration in defective skin barrier

Epidermal cell migration is an important biological process that contributes to skin homeostasis. The process is best described as keratinocytes exiting the mitotic cycle and moving laterally to suprabasal layers and subsequently differentiating into becoming cells with specialised function (Lü et al., 2013; Woodley et al., 2015). These processes are all tightly regulated and rely upon one another for the development of a robust skin barrier. Alterations in these biological processes result in the clinical manifestation of dry, thick and scaly skin phenotype associated with various skin disorders (Lopez-Pajares et al., 2013). Molecular evidence obtained from the RNA-sequencing analysis of 12*R*-LOX deficient mice suggest a possible role or implication for 12*R*-LOX in the regulation of these processes. These include the differential expression of EDC proteins associated with differentiation along with the overexpression of proliferative biomarkers such as *Krt6* and *Krt16*. It is therefore of interest to investigate the effect of 12*R*-LOX lipids on key biological processes that are known to be impaired or altered in 12*R*-LOX deficient skin.

6.1.3 Abnormal keratinocyte differentiation results in skin barrier disease

As basal proliferative cells exit the cell cycle they then commit to the highly complex program of epidermal differentiation. Early differentiation markers are expressed as soon as cells migrate from the basal layer to suprabasal layers. Early differentiation biomarkers such as *Krt10* are expressed in the stratum spinosum, followed by the expression of various other differentiation biomarkers specific to granular and cornified layers. Examples of granular differentiation biomarkers include involucrin (*Ivl*), whilst cornified layers express biomarkers such as filaggrin (*Flg*) and loricrin (*Lor*) (ter Horst et al., 2018). Each epidermal layer uniquely expresses specific proteins required for progression of the differentiation process (Eckert et al., 2002). Additionally, the production of various other molecules such as cytokines, interleukins and growth factors are produced as a result of keratinocyte differentiation (Eller et al., 1995; Jiang et al., 2020).

The process of keratinocyte differentiation is thought to be influenced by several factors which have been investigated in both *in vitro* and *in vivo* models. To date, substances known to play a role in this essential epidermal process include calcium, retinoic acid and vitamin D (Pillai et al., 1988; Gibbs et al., 1996). Of these three factors, calcium has been utilised significantly in the initiation of keratinocyte differentiation to study mechanisms and pathways associated with this biological process.

The genetic knockout of *Alox12b* gene which encodes 12*R*-LOX has shown to impact EDC proteins that include several SPRRs along with repetin (*Rptn*). Additionally, the

keratinocyte differentiation-associated protein (*Krtdap*) is also differentially expressed, suggesting a role for 12*R*-LOX in modulating parts of the differentiation process. A disruption in keratinocyte differentiation is associated with over a 100 genetic skin diseases. Many of the genes responsible for aberrant differentiation are thought to participate in various biological pathways, thus providing researchers with molecular targets in the investigation of these skin disorders (Lopez-Pajares et al., 2013). During the terminal differentiation stage of epidermal development, cells in the stratum corneum become enclosed by lipid species, forming the cornified lipid envelope (Elias et al., 2014). Keratinocytes residing within the granular layer secrete specialised secretory organelles known as lamellar bodies. Lipid metabolising enzymes convert secreted contents of the lamellar bodies into various lipid molecules that include free fatty acids and ceramides. This process occurs in the latter stages of differentiation and aids in the formation of an effective permeability barrier (Fehrenschild et al., 2012; Lopez-Pajares et al., 2013).

6.1.4 Importance of apoptosis in maintaining skin barrier

Additional epidermal processes required to maintain skin homeostasis and contribute to terminal differentiation is the program of cell death known as apoptosis. The balance between the processes of proliferation, migration, differentiation and apoptosis is vital for maintaining epidermal integrity and skin barrier function. The apoptotic process specifically controls keratinocyte proliferation occurring within the epidermis, thus maintaining stratum corneum thickness and aiding in the construction of the epidermal barrier. An abnormal apoptotic process contributes to the development of multiple skin disorders as seen in psoriasis (Raj et al., 2006).

Numerous studies have been performed in several cell lines to understand the effect of LOX derived lipids on biological processes mentioned. For example, in cancerous cells found in colorectal tissue, specific metabolites of *ALOX15* have been shown to induce apoptosis, suggesting that LOX products could have anti-cancer properties (Shureiqi et al., 2003). Investigations performed by Shureiqi et al., 2003 has shown that LOX metabolites interact with PPAR-δ, subsequently promoting apoptosis. In hepatocellular cells, *in vitro* and *in vivo* studies have shown that the activity of 12-LOX results in an anti-apoptotic effect (Xu et al., 2012).

6.2 Aim

- Determine the effect of the terminal product of the 12*R*-LOX / eLOX-3 pathway, 9R,10R,13R-TriHOME on cell proliferation, migration, differentiation and apoptosis in the hTERT keratinocyte cell line.

6.3 Objectives

- Explore whether different concentrations of 9R,10R,13R-TriHOME increases, decreases or yields no effect on cell proliferation when compared against control treatments.
- Evaluate cell confluence to determine the rate at which 9R,10R,13R-TriHOME treated cells reach 100% confluence.
- Evaluate whether different concentrations of 9R,10R,13R-TriHOME increases, decreases or has no effect on the rate in which a scratch wound area closes.
- Assess the effect of the 9R,10R,13R-TriHOME on the expression of selected epidermal differentiation protein biomarkers. These biomarkers of differentiation include *Krt10* and *Ivl*.
- Assess whether the 9R,10R,13R-TriHOME has any effect on cornified envelope formation.
- Assess the effect of the 9R,10R,13R-TriHOME on the expression of apoptotic biomarkers (Caspase-3 and cleaved PARP).
- Determine the number of live/dead cells following treatment with 9R,10R,13R-TriHOME, providing more evidence of the role of 12*R*-LOX lipids in apoptosis.

6.4 Materials and methods

Materials, equipment and routine cell culture of the hTERT immortalized human keratinocyte cell line are described in **Section 2.1.3** and **2.1.4** respectively. The 9R,10R,13R-TriHOME was kindly received from Dr Christopher Thomas (School of Pharmacy and Pharmaceutical Sciences, Cardiff University) (Cayman Chemical). Linoleic acid was purchased from Cayman Chemicals (#90150) and ethanol absolute ≥99.8% molecular biology grade DNase/RNase-free was purchased from VWR, UK (#437433T).

6.4.1 WST-1 assay to assess cell proliferation in response to treatment with 9R,10R,13R-TriHOME

hTERT immortalized human keratinocyte cells were harvested by trypsinization and resuspended in KGM^{TM} Gold Keratinocyte Growth Medium BulletKit^{TM} that excluded the vial with 2.00 mL BPE (Bovine Pituitary Extract) as it is known to contain lipid species (Sawada et al., 2002). The hTERT immortalized human keratinocyte cells were plated at a density of 2500 cells per well in a 96-well plate in 100 µl of medium and incubated overnight in a humidified atmosphere at 37ºC and at 5% CO_2. The medium was removed and washed twice with 1 mL sterile PBS at RT. The 9R,10R,13R-TriHOME suspended in ethanol was added to three wells (n = 3) containing hTERT cells at concentrations of 2 and 20 µM and incubated for 24 hours. The controls included three replicates of linoleic acid (2 and 20 µM), EtOH 20 µM (vehicle control), without bovine pituitary extract, -BPE (Control 2) and containing bovine pituitary extract, +BPE (Control 3). Cell proliferation was assessed using the WST-1 Cell Proliferation Reagent (Abcam, UK #ab155902). WST-1 reagent (10 µl) was added into each well and incubated for 2 hours in a humidified atmosphere at 37ºC and at 5% CO_2. The 96-well plate was then placed onto an orbital shaker for 1 minute. The absorbance of samples was measured at 450 nm using the Infinite 200 PRO plate reader. The reference wavelength was set at 650 nm. Readings for each sample was averaged from each replicate and the culture medium background was subtracted from the sample readings. The absorbance value obtained is proportional to cell number. A number of colorimetric assays are widely utilised in the investigation of cell proliferation, including WST-1, XTT and MTT assays. The biochemistry of these assays are based on the formation of a water insoluble compound known as formazan. The amount of formazan dye produced as a consequence of mitochondrial dehydrogenase activity is directly proportional to the number of viable cells. The colour intensity produced from the formazan is quantified and measured using a microplate reader (Yin et al., 2013). These assays differ in the time taken for the intense colour of formazan to be produced. The WST-1 proliferation assay is deemed more sensitive than the XTT and MTT assays due to the high solubility of the formazan product produced in the WST-1 assay (Ishiyama et al., 1993; Tominaga et al., 1999). As such, the WST-1 assay was the preferred method for determining the effect of the 9R,10R,13R-TriHOME on cell proliferation. Other conventional methods of assessing cell proliferation include cell counting using a haemocytometer and measuring the percentage of surface area in which cells have covered over a period of time, known as cell confluence. These in vitro techniques were used in conjunction with the WST-1 assay to assess cell proliferation following treatment.

6.4.2 Assessing cell confluence in response to treatment with 9R,10R,13R-TriHOME

The hTERT immortalized human keratinocyte cells were plated at a density of 500,000 cells per well in a 24-well plate in 1 mL of medium and incubated overnight in a humidified atmosphere at 37ºC and at 5% CO_2. The medium was removed after overnight incubation and washed twice with 1 mL sterile PBS at RT. The 9R,10R,13R-TriHOME suspended in ethanol was added to three wells (n = 3) containing hTERT cells at concentrations of 2 and 20 µM and incubated for 48 hours in a humidified atmosphere at 37ºC and at 5% CO_2. The controls included three replicates of linoleic acid (2 and 20 µM), EtOH 20 µM (vehicle control), without bovine pituitary extract, -BPE (Control 2) and containing bovine pituitary extract, +BPE (Control 3). To ensure reproducibility, a circle was drawn on the 24-well plate lid and images taken in the exact same area each time. Images were taken on an inverted phase contrast microscope (Olympus BX50 fluorescence microscope) at 0, 3, 16, 24 and 48 hours. ImageJ software was used to determine cell confluence through Image > Adjust > Threshold > Manually selecting the threshold to cover the entire area of cells > Analyze > Set measurement > Analyze > Measure.

6.4.3 Assessing cell count, viability and trypan blue stained cells in response to treatment with 9R,10R,13R-TriHOME

The hTERT immortalized human keratinocyte cells were plated at a density of 500,000 cells per well in a 24-well plate in 1 mL of medium and incubated overnight in a humidified atmosphere at 37ºC and at 5% CO_2. The medium was removed after overnight incubation and washed twice with 500 µl sterile PBS at RT. The 9R,10R,13R-TriHOME was added to three wells (n = 3) containing hTERT cells at concentrations of 2 and 20 µM and incubated for 48 hours in a humidified atmosphere at 37ºC and at 5% CO_2. The controls included three replicates of linoleic acid (2 and 20 µM), EtOH 20 µM (vehicle control), without bovine pituitary extract, -BPE (Control 2) and containing bovine pituitary extract, +BPE (Control 3). After 48 hours, the medium containing the different conditions was removed and incubated with 500 µl of 0.05% trypsin for 5 minutes to detach cells from the surface of the 24-well plate. Following detachment of cells from the surface, cells were resuspended in 10 mL of pre-warmed KGM™ Gold Keratinocyte Growth Medium BulletKit™ medium. Trypan blue solution (10 µl), 0.4% (Thermo Fisher Scientific, UK #15250061) was added to a 0.5 mL Eppendorf tube and mixed with 10 µl of sample. Trypan blue solution is used to stain for dead cells. This mixture (10 µl) was then added to a haemocytometer and the cell count, viability and the number of trypan blue stained cells was measured. Three measurements were taken for each condition.

6.4.4 Cell migration/wound healing assay to assess the effect of 9R,10R,13R-TriHOME on keratinocyte migration

hTERT immortalized human keratinocyte cells were seeded at a density of 500,000 cells in a 24-well plate and incubated in a humidified atmosphere at 37ºC and at 5% CO_2 for 24 hours to reach 90% confluence. The medium was removed after overnight incubation and washed twice with 500 µl sterile PBS at RT. A sterile 20–200 µl pipette tip was used to scratch a vertical line down each well. The detached cells were removed by washing twice with 500 µl sterile PBS and a gentle shake for 10 seconds. The 9R,10R,13R-TriHOME was added to three wells (n = 3) containing hTERT cells at concentrations of 2 and 20 µM and incubated for 48 hours. The controls included three replicates of linoleic acid (2 and 20 µM), EtOH 20 µM (vehicle control), without bovine pituitary extract, -BPE (Control 2) and containing bovine pituitary extract, +BPE (Control 3). Images were captured at 10x magnification using the inverted phase contrast microscope equipped with a Nikon digital camera at 0, 3, 16, 24 and 48 hours. ImageJ software was used to measure the wound closure after the scratch was made.

6.4.5 Growth of hTERT immortalized human keratinocyte cells to determine the effect of 9R,10R,13R-TriHOME on involucrin and keratin 10

The hTERT immortalized human keratinocyte cells were seeded at a density of 1.0 x 10^6 cells in a T25 cm^2 flask in 5 ml of KGM™ Gold Keratinocyte Growth Medium BulletKit™ that excluded the vial with 2.00 mL BPE and incubated overnight in a humidified atmosphere at 37ºC and at 5% CO_2. Once cells reached a 30-40% confluence, the medium was removed and washed twice with 1 ml of sterile PBS. The 9R,10R,13R-TriHOME was added to three separate T25 cm^2 flasks (n = 3) at concentrations of 2 and 20 µM and incubated for 48 hours in a humidified atmosphere at 37ºC and at 5% CO_2. The controls included three flasks of each of linoleic acid (2 and 20 µM), EtOH 20 µM (vehicle control), without bovine pituitary extract, -BPE (Control 2) and containing bovine pituitary extract +BPE (Control 3).

6.4.6 Protein extraction and quantification of hTERT keratinocyte cells treated with 9R,10R,13R-TriHOME and controls

hTERT immortalized keratinocyte cells treated with 9R,10R,13R-TriHOME (2 and 20 µM) were harvested after 48 incubations along with the controls. Protein extraction and quantification of hTERT immortalized keratinocyte cells is described in **Section 2.2**.

6.4.7 Antibodies used for investigating involucrin, keratin 10 and caspase-3 expression

The primary antibodies used here include rabbit polyclonal IgG anti-involucrin (1:500) (Abcam, UK #53112), rabbit polyclonal IgG anti-cytokeratin 10 (1:500) (Abcam, UK

#111447), rabbit polyclonal IgG anti-caspase-3 (1:500) (Abcam, UK #13847) and rabbit polyclonal IgG anti-β-actin (1:1000) (Abcam, UK #ab8227). Secondary antibodies used were goat anti-rabbit IgG (HRP) (1:2000) (Abcam, UK #ab6721).

6.4.8 Western blot analysis for the detection of involucrin, keratin 10 and caspase-3 protein expression

The western blot protocol for investigating involucrin, keratin 10 and caspase-3 protein expression in the hTERT immortalized keratinocyte cells is described in **Section 2.3**.

6.4.9 Determining the percentage (%) of cells forming cornified envelopes following treatment with 9R,10R,13R-TriHOME

hTERT immortalized human keratinocyte cells were seeded at a density of 500,000 cells in a 24-well plate and incubated in a humidified atmosphere at 37ºC and at 5% CO_2 overnight. The medium was removed after overnight incubation and washed twice with 500 µl sterile PBS at RT. The 9R,10R,13R-TriHOME was added to three wells (n = 3) containing hTERT cells at concentrations of 2 and 20 µM and incubated for 48 hours in a humidified atmosphere at 37ºC and at 5% CO_2. The controls included three replicates of linoleic acid (2 and 20 µM), EtOH 20 µM (vehicle control), without bovine pituitary extract, -BPE (Control 2) and containing bovine pituitary extract, +BPE (Control 3). Cells were trypsinized and counted in 10 mL of medium. Cells were then centrifuged for 5 minutes at 2000 g and resuspended in a 10 mL solution containing 2% SDS and 5 mM β-mercaptoethanol. This was then boiled at a 100ºC for 15 minutes and vortexed for 5 minutes. Following treatment of cells with these conditions, cells with cornified envelopes survive whilst cells that have not formed cornified envelopes are solubilized. Cells that formed cornified envelopes were counted using a haemocytometer under a light microscope and divided by the number of cells counted originally x 100 (Jeon et al., 1998).

6.4.10 Statistical analysis

All experiments were carried out three times (triplicate wells and flasks) and data are expressed as the mean ± SD. Statistical significance between treatments was determined using Student's t-test when three independent biological repeats were performed with three technical repeats per biological replicate. $p < 0.05$ was considered of statistical significance and is represented with an asterisk. Statistical analysis was done using GraphPad Prism 9.0 software (GraphPad Software Inc., San Diego, CA, USA) and Microsoft Excel software.

6.5 Results

6.5.1 No significant effect of 9R,10R,13R-TriHOME on cell proliferation

Figure 6.5.1 shows no significant difference in cell proliferation between hTERT cells treated with 9R,10R,13R-TriHOME (2 µM) and linoleic acid (2 µM), vehicle control (EtOH, 20µM), -BPE and +BPE as indicated by the similar absorbance values. Interestingly, cells treated with linoleic acid (20 µM) produced the lowest absorbance value of all conditions, indicating that linoleic acid (20 µM) likely had a toxic effect on hTERT immortalized keratinocytes. hTERT cells treated with a higher concentration of 9R,10R,13R-TriHOME (20 µM) shows a difference in cell proliferation when compared with hTERT cells treated with the same concentration of linoleic acid. However, no statistically significant difference in cell proliferation is observed between hTERT cells treated with 9R,10R,13R-TriHOME (20 µM) and vehicle control (EtOH,20 µM), -BPE and +BPE.

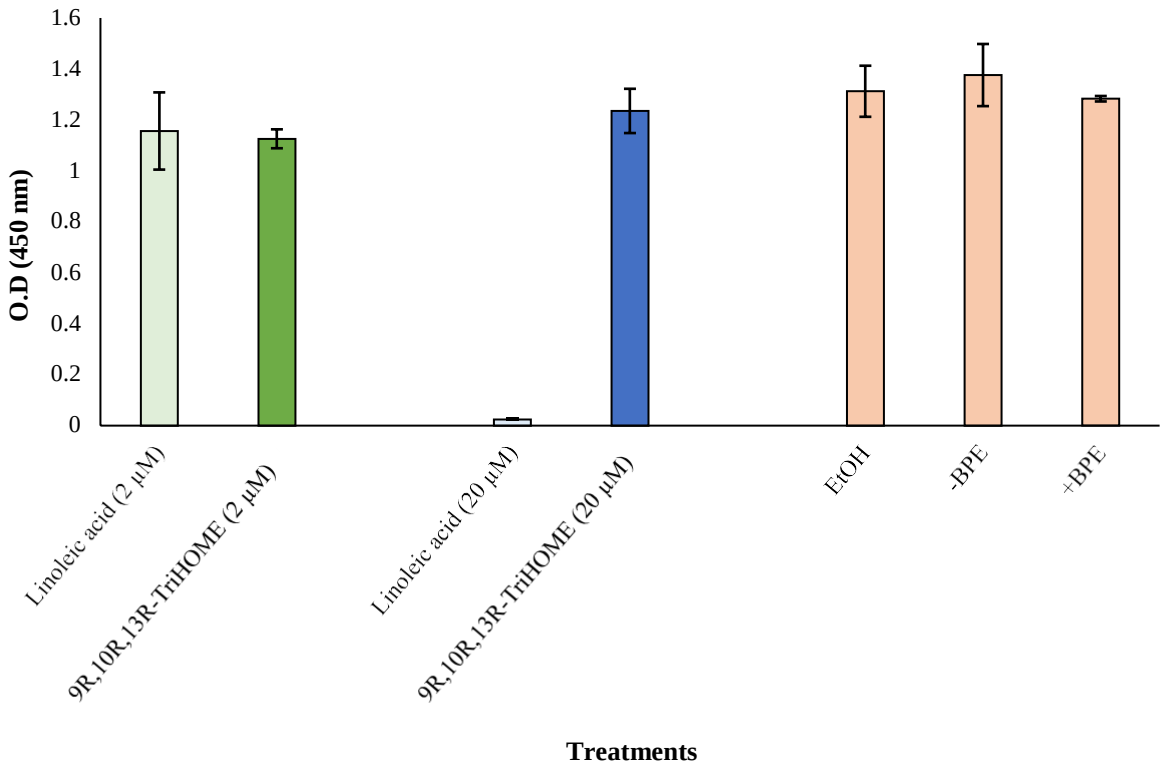

Figure 6.5.1 Effect of 9R,10R,13R-TriHOME product of 12*R*-LOX / eLOX-3 pathway on hTERT primary keratinocyte cell proliferation. Proliferation was determined by the WST-1 Quick Cell Proliferation Assay kit II (Abcam) by measuring absorbance at 450 nm following a 24-hour treatment with linoleic acid (2 µM), 9R,10R,13R-TriHOME (2 µM), linoleic acid (20 µM), 9R,10R,13R-TriHOME (20 µM), vehicle control (EtOH, 20 µM), -BPE and +BPE. Data presented as mean absorbance values calculated from nine replicates for each condition (n = 9) and the experiment performed three times. Data obtained using a microplate reader, 450 nm, ± SD.

6.5.2 9R,10R,13R-TriHOME does not significantly effect cell confluence

The cell growth of hTERT immortalized keratinocyte cells was then investigated following 48 hours' treatment with different concentrations of the 9R,10R,13R-TriHOME. **Figure 6.5.2** shows no significant difference in cell growth after 3 hours between any of the conditions and controls. After 16 hours, hTERT cells treated with linoleic acid (2 µM) shows an increase in cell growth in comparison with the conditions and controls. The mean cell growth value for cells treated with linoleic acid (2 µM) at 16 hours is 23.1%, whereas cell growth for other conditions and controls at 16 hours, range from 4.3% to 11.7%. At 24 hours, cells treated with linoleic acid (2 µM) has the most significant growth of all conditions and controls with a mean growth value of 28.9%. Relatively similar growth rates are observed up to 24 hours between cells treated with 9R,10R,13R-TriHOME (2 µM) and 9R,10R,13R-TriHOME (20 µM). At 48 hours, a significant difference in cell growth is observed between cells treated with 9R,10R,13R-TriHOME (2 µM) and 9R,10R,13R-TriHOME (20 µM). However, cells treated with 9R,10R,13R-TriHOME (20 µM) has a significantly lower growth than cells treated with 9R,10R,13R-TriHOME (2 µM) at 48 hours. Cells treated with linoleic acid (20 µM) has the smallest growth of all conditions and control after 24 hours once again, indicating the toxicity of linoleic acid at this concentration.

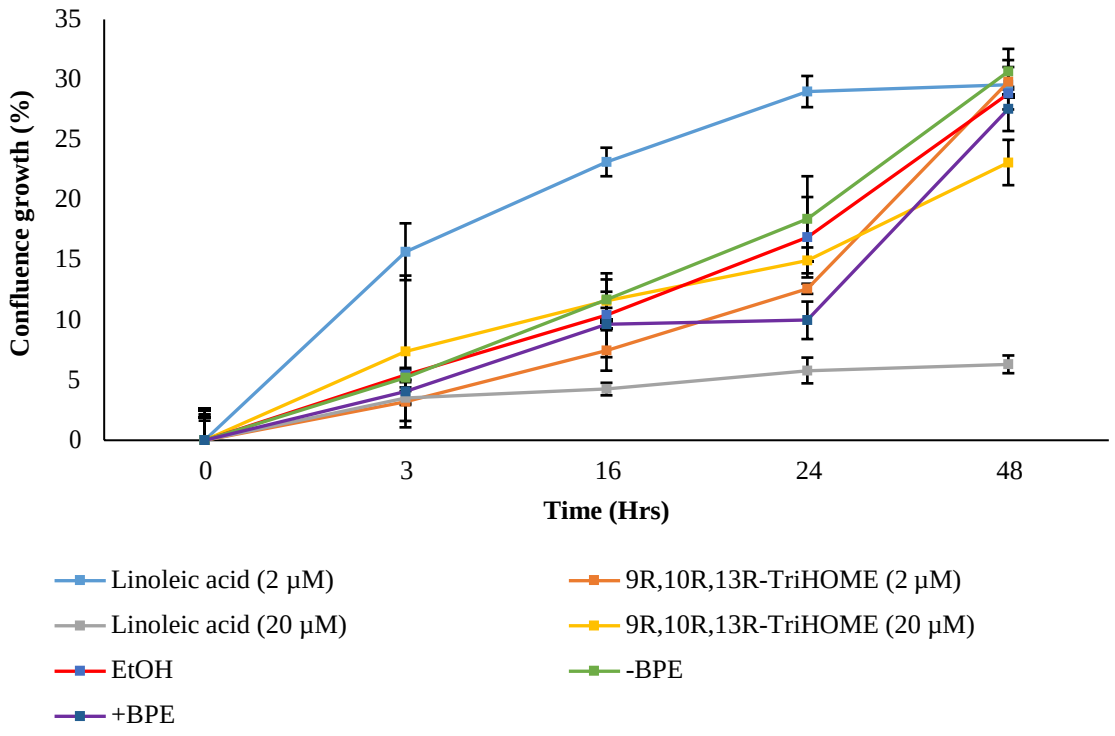

Figure 6.5.2 Effect of 9R,10R,13R-TriHOME product of the 12*R*-LOX / eLOX-3 pathway on growth rate of hTERT cells over 48 hours. Rate of growth was quantified by ImageJ software following treatment with linoleic acid (2 µM), 9R,10R,13R-TriHOME (2 µM), linoleic acid (20 µM), 9R,10R,13R- TriHOME (20 µM), vehicle control (EtOH, 20 µM), -BPE, +BPE. Data is presented as mean cell growth values, which are calculated from nine replicates for each time point and 3 different experiments performed. Images obtained for each time point (0, 3, 16, 24 and 48 hours), ± SD (*n* = 9).

6.5.3 9R,10R,13R-TriHOME does not have a significant effect on the cell count

To accompany cell growth experiments, the effect of the 9R,10R,13R-TriHOME on cell viability was assessed using trypan blue staining. **Figure 6.5.3** shows that after 48 hours of exposure to lipids, a significantly lower number of viable cells is observed when cells are treated with 9R,10R,13R-TriHOME (2 µM and 20 µM) when compared with +BPE. No statistical significance in the mean number of viable cells is observed when comparing cells treated with 9R,10R,13R-TriHOME (2 µM & 20 µM) and linoleic acid (2 µM). Moreover, no significant difference in the mean number of viable cells is observed when comparing hTERT cells treated with 9R,10R,13R-TriHOME (2 µM & 20 µM) and the vehicle control (EtOH) and -BPE. All other conditions have over a million mean number of viable cells, hTERT cells treated with linoleic acid (20 µM) has a mean cell viablity value of 683,333. This data further implies toxicity at higher concentrations of linoleic acid. Concerning the 9R,10R,13R-TriHOME product of the 12*R*-LOX / eLOX-3 pathway, no significant change in the mean number of viable cells is observed following the different concentrations used.

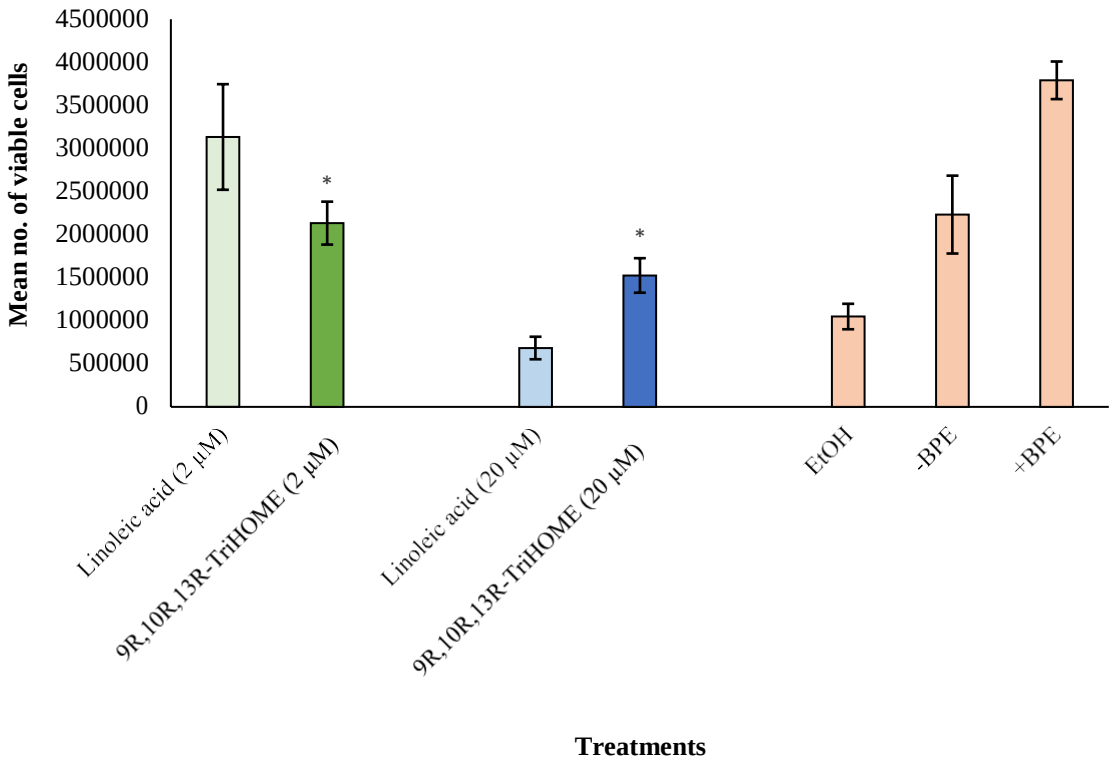

Figure 6.5.3 Effect of the 9R,10R,13R-TriHOME product of the 12*R*-LOX / eLOX-3 pathway on cell count after 48 hours. Viability of hTERT cells measured by trypan blue staining following treatment with linoleic acid (2 µM), 9R,10R,13R-TriHOME (2 µM), linoleic acid (20 µM) 9R,10R,13R-TriHOME (20 µM), vehicle control (EtOH), -BPE and +BPE. Data is presented as the mean cell viability ± SD (*n*= 3). Nine replicates for each condition (*n* = 9) and three different experiments were performed.* *P* <0.05 when compared with +BPE.

6.5.4 9R,10R,13R-TriHOME does not significantly effect cell migration/wound healing

Figure 6.5.4 and **Figure 6.5.5** shows no significant difference in the wound area remaining in any of the conditions or controls from 0 hours to 24 hours, suggesting minimal changes in migration of cells caused by the lipid treatment. From 0 hours to 24 hours, the scratch/wound remaining for all conditions and controls ranges from 98.2% to 82.3%. At least 90% of the scratch/wound area remains at 48 hours from treatment of cells with linoleic acid (20 µM), 9R,10R,13R-TriHOME (2 µM) and 9R,10R,13R-TriHOME (20 µM). However, the mean wound area remaining at 48 hours from treatment of cells with linoleic acid (2 µM) is 70.4%, suggesting that cells treated with the linoleic acid (2 µM) has the greatest migration out of all conditions. This wound area value is significantly lower when compared with any other condition and control. The wound area after 48 hours in 9R,10R,13R-TriHOME (2 µM) and 9R,10R,13R-TriHOME (20 µM) is similar throughout as indicated by **Figure 6.5.5**.

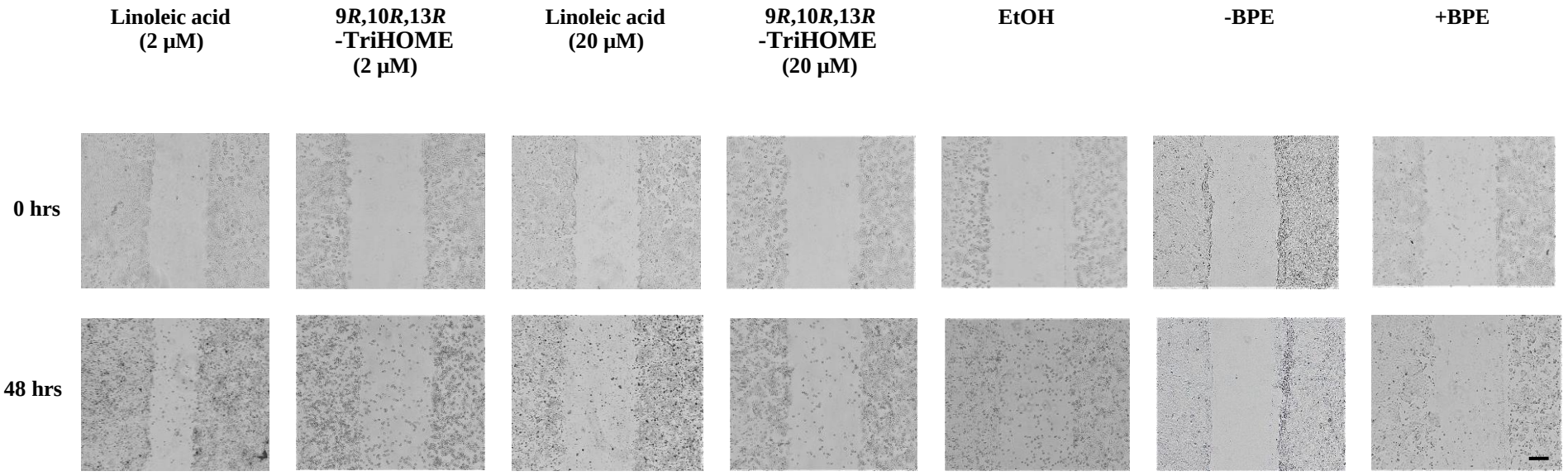

Figure 6.5.4 Representative images displaying the effect of the 9R,10R,13R-TriHOME product of the 12*R*-LOX / eLOX-3 pathway on wound closure. Images showing original scratch/wound at 0 hours and final image taken at 48 hours for hTERT cells treated with 9R,10R,13R-TriHOME (2 µM and 20 µM), linoleic acid (2 µM and 20 µM), vehicle control (EtOH, 20 µM), -BPE, +BPE. Images taken at 10x magnification and scale bar denotes 500 µm.

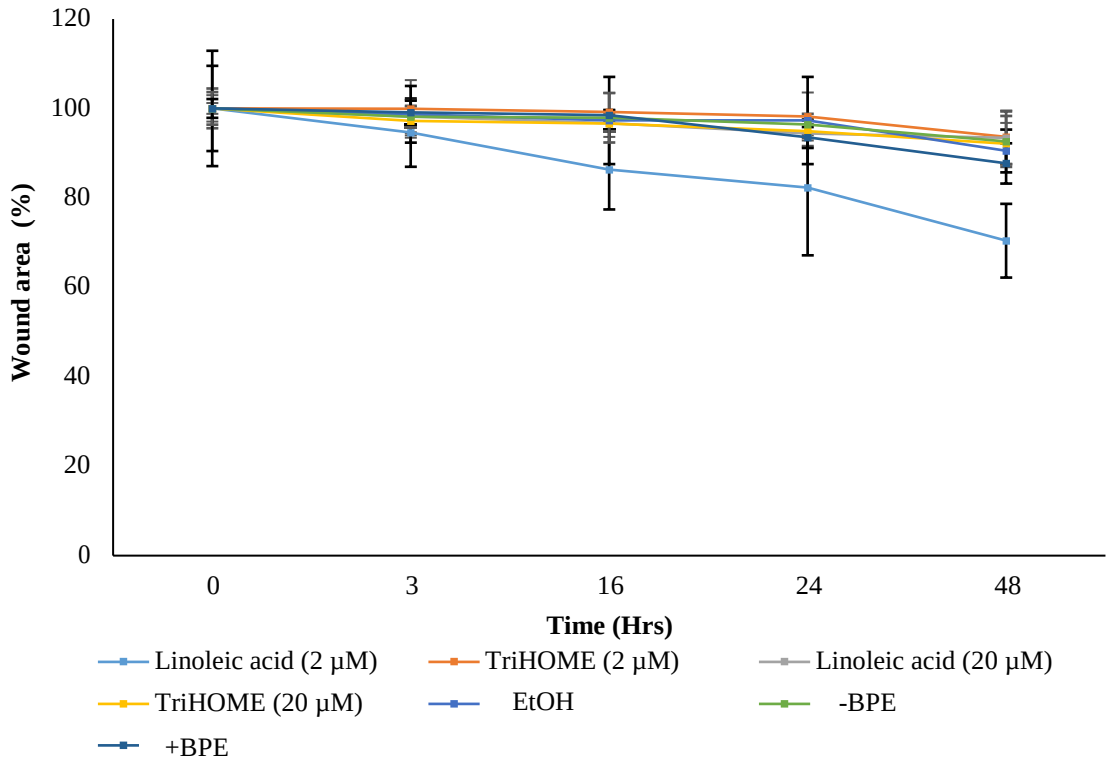

Figure 6.5.5 Effect of the 9R,10R,13R-TriHOME product of the 12*R*-LOX / eLOX-3 pathway on wound area closure over 48 hours. Quantitative analysis of wound area closure using the ImageJ software following treatment of hTERT cells with linoleic acid (2 µM), 9R,10R,13R-TriHOME (2 µM), linoleic acid (20 µM) 9R,10R,13R-TriHOME (20 µM), vehicle control (EtOH), -BPE and +BPE as a function of time. Mean wound area shown was determined as the wound area at the specified time relative to the original wound area at 0 hours. Data is presented as the mean wound area ± SD (n = 3).

6.5.5 9R,10R,13R-TriHOME significantly increases the relative protein level of involucrin (*Ivl*)

Figure 6.5.7 shows treatment of hTERT cells with 9R,10R,13R-TriHOME (20 µM) for 48 hours significantly increases the relative protein level of *Ivl* when compared with hTERT cells treated with vehicle control (EtOH), -BPE and +BPE. Following treatment of hTERT cells with 9R,10R,13R-TriHOME (2 µM), a significantly lower relative protein level of *Ivl* is observed when compared with hTERT cells treated with linoleic acid (2 µM). However, no statistically significant difference is observed when comparing cells treated with 9R,10R,13R-TriHOME (2 µM) and vehicle control (EtOH), -BPE and +BPE when analysing the relative protein level of *Ivl*. Increasing the concentration of 9R,10R,13R-TriHOME significantly increases the relative protein level of *Ivl* (**Figure 6.5.7**). **Figure 6.5.6** shows a dense band for the presence of *Ivl* in control 4 (protein lysate from skin sample) as expected due its known expression in skin. This is also supported by the relative protein level for control 4 shown in **Figure 6.5.7**.

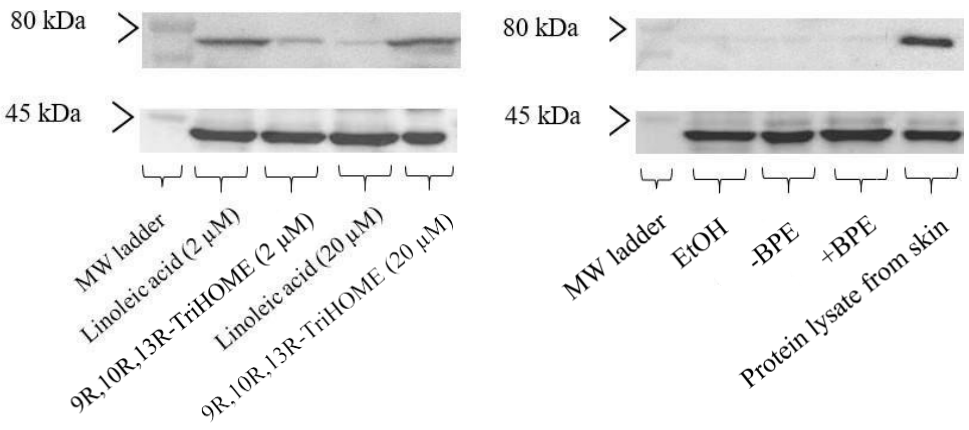

Figure 6.5.6 Representative images of western blots in the detection of involucrin (*Ivl*). 20 µg of protein extract from hTERT cells treated with various conditions were separated through SDS-PAGE and transferred onto a PVDF membrane. A band corresponding to *Ivl* and β-actin was detected at the predicted molecular weight of 68 kDa and 42 kDa respectively.

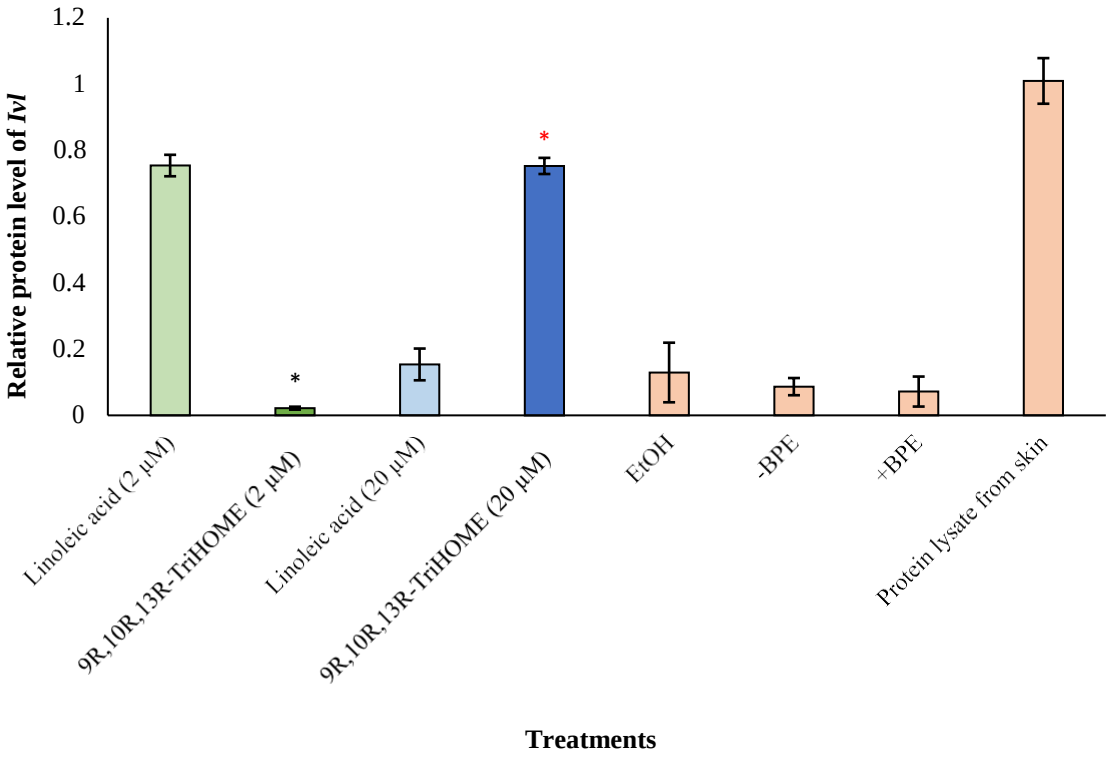

Figure 6.5.7 Effect of the 9R,10R,13R-TriHOME product of the 12*R*-LOX / eLOX-3 pathway on the relative protein level of involucrin (*Ivl*). Western blot quantification of protein level of *Ivl* following treatment of hTERT cells with linoleic acid (2 µM), 9R,10R,13R-TriHOME (2 µM), linoleic acid (20 µM), 9R,10R,13R-TriHOME (20 µM), vehicle control (EtOH), -BPE, +BPE and protein lysate from skin for 48 hours. The relative protein level of *Ivl* was quantified using the ImageJ software. Relative protein levels are represented as mean protein values normalized to β-actin, ± SD. Six replicates for each condition (n = 6) and three different experiments were performed. * $P < 0.05$ when compared with linoleic acid (2 µM). * $P < 0.05$ when compared with vehicle control (EtOH), -BPE and +BPE.

6.5.6 9R,10R,13R-TriHOME significantly increases the relative protein level of keratin 10 (*Krt10*)

Figure 6.5.8 and **Figure 6.5.9** shows that the treatment of hTERT cells with 9R,10R,13R-TriHOME (20 µM) has a significant impact on the mean relative protein level of *Krt10*, an early keratinocyte differentiation marker. **Figure 6.5.9** indicates that the mean relative protein level value of *Krt10* following treatment with 9R,10R,13R-TriHOME (20 µM) is 1.1 which is significantly greater than hTERT cells treated with vehicle control (EtOH), -BPE and +BPE, where the mean relative protein level value ranges from 0.2 – 0.85. **Figure 6.5.8** shows a dense band is observed in control 4 (protein lysate from skin sample) for *Krt10* as would be expected due to its known expression in skin. Determining the effect of 2 µM of both linoleic acid and 9R,10R,13R-TriHOME on the protein expression of *Krt10* was not possible due to insufficient quantities of both these components.

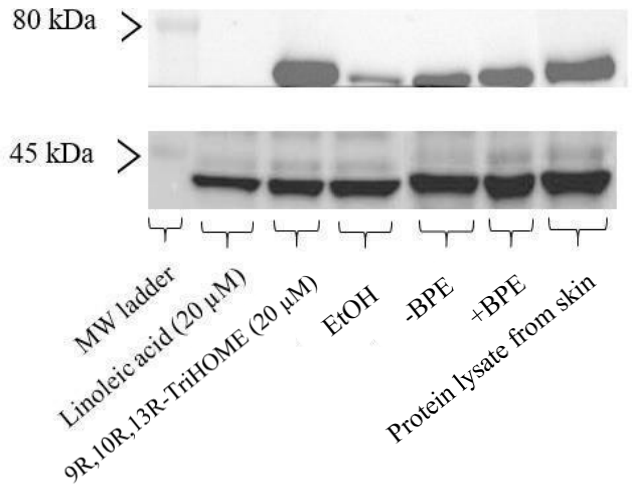

Figure 6.5.8 Representative images of western blots in the detection of keratin 10 (*Krt10*). 20 µg of protein extract from hTERT cells treated with various conditions were separated through SDS-PAGE and transferred onto a PVDF membrane. A band corresponding to *Krt10* and β-actin was detected at the predicted molecular weight of 60 kDa and 42 kDa respectively.

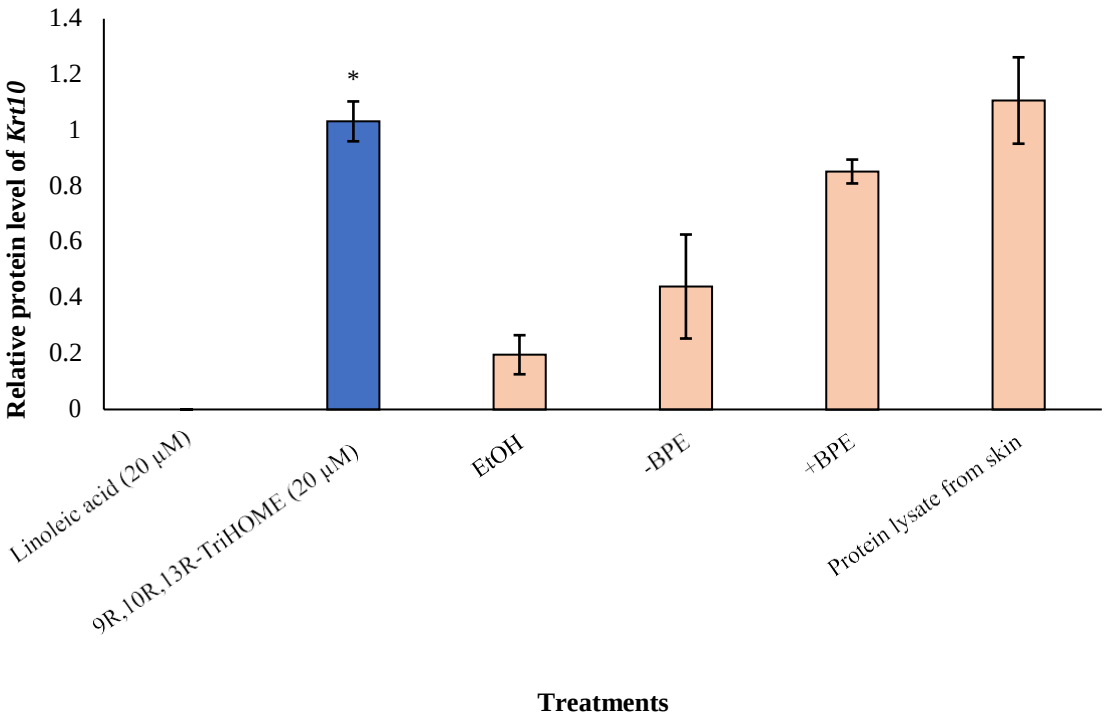

Figure 6.5.9 Effect of the 9R,10R,13R-TriHOME product of the 12*R*-LOX / eLOX-3 pathway on relative protein level of keratin 10 (*Krt10*). Western blot quantification of the protein level of *Krt10* following treatment of hTERT cells with linoleic acid (20 µM), 9R,10R,13R-TriHOME (20 µM), vehicle control (EtOH), -BPE, +BPE and protein lysate from skin sample for 48 hours. The relative protein level of *Krt10* was quantified using the ImageJ software. Relative protein levels are represented as mean protein values normalized to β-actin, ± SD. Six replicates for each condition (n = 6) and 3 different experiments were performed. * $P < 0.05$ when compared with vehicle control (EtOH), -BPE and +BPE.

6.5.7 9R,10R,13R-TriHOME significantly increases the percentage (%) of cells forming a cornified envelope

Determining the percentage (%) of cells forming a cornified envelope is described in **Section 6.4.9**. After treatment of hTERT cells with 9R,10R,13R-TriHOME (2 µM), no significant difference in % of cells forming cornified envelopes can be observed when compared with linoleic acid (2 µM). Moreover, no statistically significant difference in the % of cells forming cornified envelopes is observed between hTERT cells treated with 9R,10R,13R-TriHOME (2 µM) and controls 1-4 as shown in **Figure 6.5.10**. **Figure 6.5.10** shows a statistically significant difference in the % of cells forming cornified envelopes following treatment of cells with 9R,10R,13R-TriHOME (20 µM) when compared with vehicle control (EtOH), -BPE and +BPE. A mean value of 58.2% of cornified envelope formation is observed following treatment with 9R,10R,13R-TriHOME (2 µM), showing no statistical significance when compared with linoleic acid (2 µM) and other controls. The mean % of cornified envelope formation in hTERT cells treated with 9R,10R,13R-TriHOME (20 µM) is

83.2%, whilst cells treated with linoleic acid (20 µM) showed no detectable formation of cornified envelopes, that is likely due to toxicity. Increasing the concentration of 9R,10R,13R-TriHOME from 2 µM to 20 µM significantly increases the formation of cornified envelopes by 25%. The mean % cornified envelope formation for vehicle control (EtOH), -BPE and +BPE ranges from 51.8% - 56.8%.

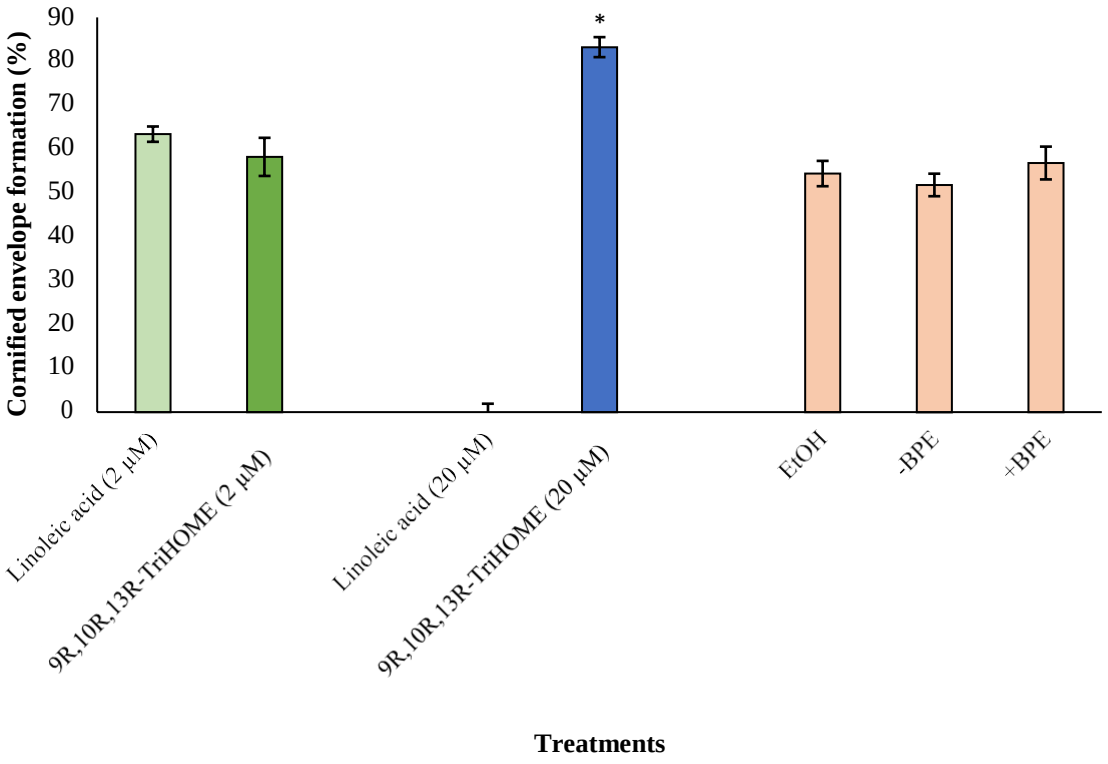

Figure 6.5.10 Effect of the 9R,10R,13R-TriHOME product of the 12*R*-LOX / eLOX-3 pathway on cornified envelope formation in hTERT cells. Cornified envelope formation was quantified using a haemocytometer under phase contrast microscopy following treatment of hTERT cells with linoleic acid (2 µM), 9R,10R,13R-TriHOME (2 µM), linoleic acid (20 µM) 9R,10R,13R-TriHOME (20 µM), vehicle control (EtOH), -BPE and +BPE for 48 hours. Cells were harvested and the cornified envelope was extracted by boiling in 2% SDS and 20 mM DTT at 100ºC. Data is presented as mean values obtained from three independent experiments ±SD. Six replicates for each condition (n = 6) and three different experiments were performed. * $P < 0.05$ when compared with vehicle control (EtOH), -BPE and +BPE.

6.5.8 Reduced relative protein level of caspase-3 following treatment with 9R,10R,13R-TriHOME

Figure 6.5.12 shows a significantly lower relative protein level of caspase-3 (*Casp3*) is observed following treatment of hTERT cells with 9R,10R,13R-TriHOME (2 µM), when compared with vehicle control (EtOH) and linoleic acid (2 µM). A statically significant difference in relative protein level of *Casp3* can be observed when comparing the 9R,10R,13R-TriHOME (20 µM) with vehicle control (EtOH) and linoleic acid (20 µM). Interestingly,

treatment of hTERT cells with linoleic acid (2 µM and 20 µM) has a greater mean relative protein levels of *Casp3* when compared with other controls as demonstrated by the dense bands shown in **Figure 6.5.11**. Moreover, treatment of hTERT cells with linoleic acid at both concentrations (2 µM and 20 µM) has similar *Casp3* protein levels, with mean protein level values at 0.73 and 0.84 respectively. hTERT cells treated with 2 µM and 20 µM of linoleic acid show higher *Casp3* protein levels when compared with hTERT cells treated with the two different concentrations of 9R,10R,13R-TriHOME, reinforcing its possible toxic effect on cells. The mean relative protein level of *Casp3* following treatment with the four controls utilised inthis experiment ranges from 0.03 – 0.51.

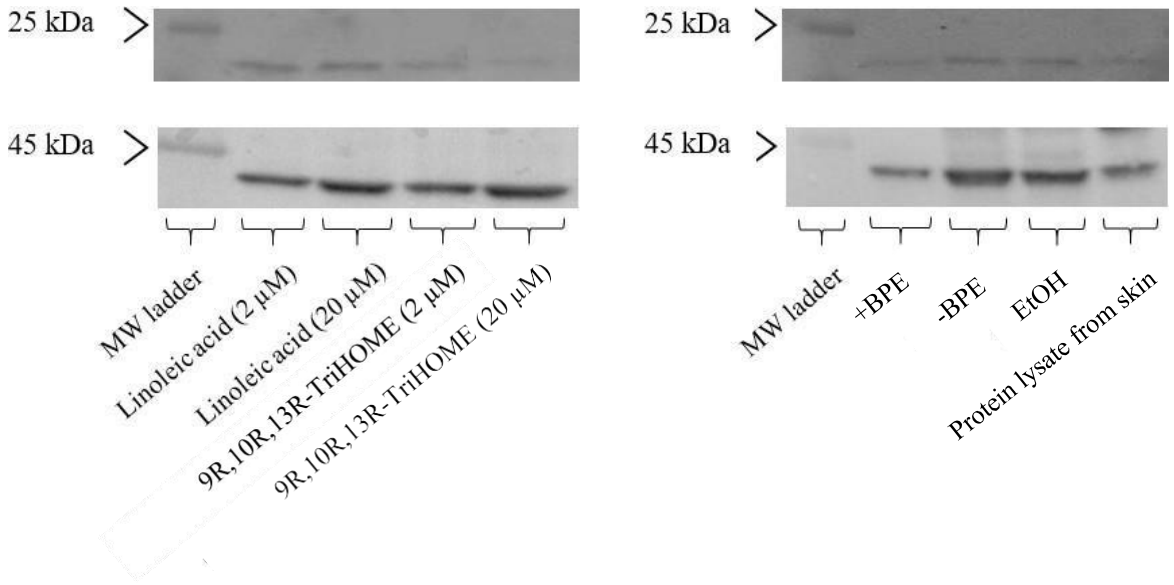

Figure 6.5.11 Representative images of western blots in the detection of the caspase-3 (*Casp3*) apoptotic biomarker. 20 µg of protein extract from hTERT cells treated with various conditions were separated through SDS-PAGE and transferred onto a PVDF membrane. A band corresponding to *Casp3* and β-actin was detected at the predicted molecular weight of 17 kDa and 42 kDa respectively.

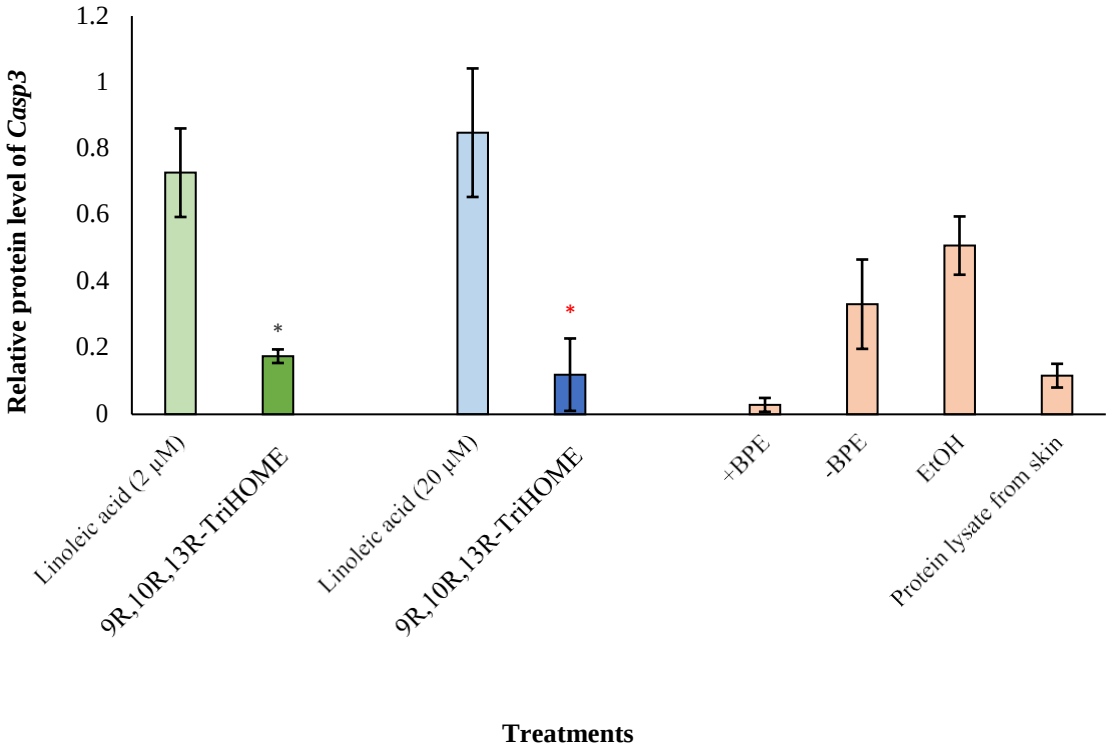

Figure 6.5.12 Effect of the 9R,10R,13R-TriHOME product of the 12*R*-LOX / eLOX-3 pathway on relative protein level of caspase-3 (*Casp3*). Western blot quantification of the protein level of *Casp3* following treatment of hTERT cells with linoleic acid (2 µM), 9R,10R,13R-TriHOME (2 µM), linoleic acid (20 µM), 9R,10R,13R-TriHOME (20 µM), +BPE, -BPE, vehicle control (EtOH) and protein lysate from skin sample for 48 hours. The relative protein level was quantified using the ImageJ software. Relative protein levels are represented as mean protein values normalized to β-actin, ± SD. Six replicates for each condition (n = 6) and three different experiments were performed. * P < 0.05 when compared with vehicle control (EtOH). * P < 0.05 when compared with vehicle control (EtOH) and linoleic acid (2 µM).

6.5.9 9R,10R,13R-TriHOME does not have a significant effect on the number of trypan blue stained cells

As additional evidence to understand the role of 12*R*-LOX lipids in the process of apoptosis, the mean number of trypan blue stained cells were analysed as per methods **Section 6.4.3** following treatment of hTERT cells with the 9R,10R,13R-TriHOME product of the 12*R*-LOX / eLOX-3 pathway. **Figure 6.5.13** shows no difference between the mean number of trypan blue stained cells following treatment of hTERT cells with 9R,10R,13R-TriHOME and the linoleic acid at both concentrations (2 µM and 20 µM). Moreover, no statistically significant difference is observed between the 9R,10R,13R-TriHOME at both concentrations and the controls utilised in this experiment. The mean number of trypan blue stained cells following treatment with 9R,10R,13R-TriHOME (2 µM) for a period of 48 hours is 1.2 million, whilst hTERT cells treated with a higher concentration of 9R,10R,13R-TriHOME (20 µM) results in a slightly lower mean number of dead cells with a value of 800,000, but no statistically significant difference.

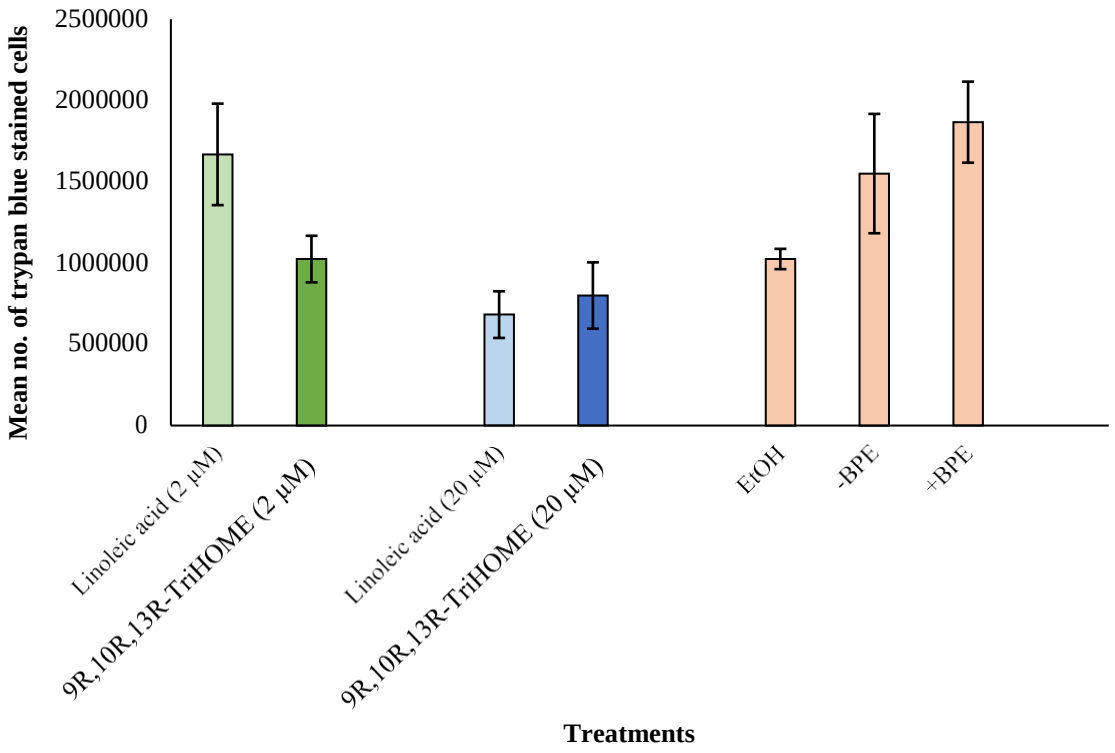

Figure 6.5.13 Effect of the 9R,10R,13R-TriHOME product of the 12*R*-LOX / eLOX-3 pathway on the mean number of trypan blue stained hTERT cells after 48 hours. Mean number of dead cells measured by trypan blue staining following treatment with linoleic acid (2 µM), 9R,10R,13R-TriHOME (2 µM), linoleic acid (20 µM) 9R,10R,13R-TriHOME (20 µM), vehicle control (EtOH), -BPE, +BPE for 48 hours. Data is presented as mean dead cells ± SD. Six replicates for each condition (n = 6) and threedifferent experiments were performed. No statistically significant results are observed.

6.6 Discussion

6.6.1 Both concentrations of 9R,10R,13R-TriHOME has no significant effect on cell proliferation

Treatment of hTERT cells with terminal product of the 12*R*-LOX / eLOX-3 pathway 9R,10R,13R-TriHOME at both concentrations (2 µM and 20 µM) did not have a significant effect on cell proliferation as indicated by WST-1 assay results and also observations. Studies performed by Epp et al., 2007 has shown that cell proliferation is unaffected in mice possessing a defective barrier function because of 12*R*-LOX deficiency. Epp et al., 2007 confirmed this by staining of epidermal proliferative markers such as keratin 6, whereby its expression was unaltered, suggesting that keratinocyte proliferation is unaffected in response to 12*R*-LOX protein deficiency. Other similar studies involving cell treatment with various other fatty acids such as oleic acid have also shown little or no effects on the proliferation process (Finstad et al., 1998).

Comparison of the hTERT cell growth rate shows no significant difference between the two 9R,10R,13R-TriHOME concentrations up to a time point of 24 hours, suggesting an unlikely role of 9R,10R,13R-TriHOME in epidermal proliferation. Interestingly, the growth rate of hTERT cells in response to treatment with 2 µM of linoleic acid is significantly greater at 16 and 24 hours. Various *in vitro* studies have shown that treatment with linoleic acid and other n-6 polyunsaturated fatty acids for 24 hours can promote cell proliferation through specific biological pathways such as the phosphatidylinositol 3-kinase (PI3K) pathway (Hardy et al., 2000). Studies have determined that the presence of double bonds within the chemical structure of polyunsaturated fatty acids may prove significant in the stimulation of proliferation in muscle cells (Lee et al., 2009). Beyond 24 hours however, the rate of cell growth following treatment with 2 µM of linoleic acid begins to plateau. A statistically significantly lower mean cell viability is observed when comparing the 9R,10R,13R-TriHOME (2 µM and 20 µM) with +BPE. BPE consists of multiple growth factors and hormones known to enhance cell proliferation in other cell types (Kent and Bomser, 2003; Xu et al., 2013).

Overall, it can be concluded that the 9R,10R,13R-TriHOME has no significant impact on cell proliferation, rate of cell growth nor cell viability. Moreover, a lower concentration of linoleic acid has a similar effect on proliferation and cell viability as both concentrations of the 9R,10R,13R-TriHOME. hTERT cells were treated with the 9R,10R,13R-TriHOME and controls at 50-60% confluence, as to ensure enough cells to perform the WST-1 proliferation assay. At this confluence, cells still exhibit proliferative properties and therefore the addition of lipids for 48 might be overridden by cells naturally proliferating. The results obtained from the WST-1 cell proliferation assay suggests that 9R,10R,13R-TriHOME used at these specific concentrations do not affect cell proliferation in the basal layer of the epidermis.

6.6.2 Linoleic acid (20 µM) significantly inhibits cell proliferation

Whilst no significant difference is observed in cell proliferation following treatment of hTERT cells with different concentration of the 9R,10R,13R-TriHOME, increasing the concentration of linoleic acid dose dependently from 2 µM to 20 µM significantly inhibits cell proliferation. This is further confirmed by the rate of cell growth observed in **Figure 6.5.2** in response to treatment with 20 µM of linoleic acid. A concentration of 20 µM linoleic acid was used for comparison purposes with 20 µM 9R,10R,13R-TriHOME. Although previous studies have not determined the effect of linoleic acid on epithelial cell models, *in vitro* studies using smooth muscle and lymphocyte cells have revealed anti-proliferative properties of linoleic acid when used at higher concentrations (> 10 µM) (Belal et al., 2018). Moreover, it has been documetated

that high concentrations of fatty acids (20-100 µM) such as linoleic acid significantly inhibit cell proliferation in human adipocyte cell lines and prevent growth of cancerous tumours (Maurin et al., 2002; van Beelen et al., 2007; Lu et al., 2010).

The biological mechanism by which linoleic acid inhibits cell proliferation in these various cell models has not been fully elucidated. An interesting hypothesis proposed to explain the anti-proliferative effects of linoleic acid includes its incorporation into the cell membrane and thus altering cell permeability and fluidity. Fatty acid incorporation into the cell membrane results in changes to cell behaviour which may lead to the inhibition of cell proliferation. Other possible mechanisms by which linoleic acid may inhibit proliferation is through the activation of the p53 gene, known to be involved in the regulation of cell proliferation (Wawryk-Gawda et al., 2014). It has also been reported that the processing of fatty acids such as linoleic acid into metabolites may specifically interact and activate a family of nuclear receptors known as the peroxisome proliferator-activated receptor (PPAR) family. Interestingly, the activation of PPAR has been shown to be associated with the regulation of cell proliferation (Yu et al., 1995; Forman et al., 1997). If 12*R*-LOX is present and active in hTERT cells, the linoleic acid (20 µM) may undergo 12*R*-LOX oxidation and thereby generating eicosanoids which may trigger a downstream inhibitory effect on the proliferation process. More specifically, the formation of products such as 9R,10R,13R-TriHOME through the 12*R*-LOX and eLOX-3 pathway may activate PPAR and subsequently inhibit cell proliferation. However, the 9R,10R,13R-TriHOME had no effect on cell proliferation. Free linoleic acid was used in this experiment, whilst in human skin, linoleic acid is esterified in a hydroxyl-ceramide. It is therefore unlikely that the free linoleic acid inhibits cell proliferation through the 12*R*-LOX pathway as the 9R,10R,13R- TriHOME would also be expected to show the same result. Further studies are required to elucidate the exact biological mechanism and pathways by which a high concentration of linoleic acid inhibits proliferation in epidermal cells.

The addition of higher concentrations of linoleic acid (20 µM) might resemble the abundance of unoxidized linoleic acid observed in 12*R*-LOX deficient skin as an accumulation of linoleic acid is found as a consequence of 12*R*-LOX being unable to oxygenate the substrate. As such, the accumulation and abundance of unoxidized linoleic acid may contribute and trigger abnormal cell proliferation as a result of its inhibition. Moreover, this may possibly contribute towards the pathophysiology of ichthyosis. A high concentration and accumulation of lipids in various other tissue such as in blood vessels are associated with vascular function failure, suggesting that higher concentration of lipid can lead to the development of disease (Velagaleti et al., 2013).

6.6.3 Both concentrations of 9R,10R,13R-TriHOME have no effect on cell migration/wound area after 48 hours

The migration of cells from the basal layer to the suprabasal layers of the epidermis is essential for skin homeostasis as keratinocyte migration enables the process of differentiation and desquamation to occur (Kirfel and Hirzog, 2004). Limited studies have been performed to determine the effect of LOX lipids on cell migration. Of the literature available, the disruption of other LOXs such as *ALOX15* seemingly impairs cell migration of *in vitro* smooth muscle cell lines. On the other hand, certain eicosanoids such as the 12-hydroxyeicosatetraenoic acid (12-HETE) has shown to promote cell migration in rat aortic muscle cells (Nakao et al., 1982). Further evidence of 5-LOX metabolites in stimulating the migration and invasion of macrophages has been demonstrated in studies performed by Wen et al., 2014.

Previous studies have demonstrated increased migration in HaCaT cells following treatment with linoleic acid (Manosalva et al., 2020). Furthermore, studies performed in murine models have demonstrated the promotion of wound closure in response to treatment with linoleic acid (Magalhães et al., 2008). An enhanced cell migration as a result of linoleic acid (2 μM) treatment may not necessarily yield an effective skin barrier function and further studies would be required to confirm whether an increased keratinocyte migration aids in skin barrier functionality. On the other hand, in an injury inflicted site of the skin, cell migration is essential to repair the damage and reform the epidermal barrier.

6.6.4 A higher concentration of 9R,10R,13R-TriHOME significantly increases the protein level of involucrin (*Ivl*) and keratin 10 (*Krt10*)

Analysis of the 12*R*-LOX deficient RNA-sequencing data in **Chapter 4** revealed strong links to processes associated with terminal differentiation such as keratinization, cornification and cross-linking of peptides. Other indications of links to differentiation include the downregulation of PPAR which is hypothesised to play a role in the regulation of keratinocyte differentiation. Here, investigation into the expression of *Ivl* following treatment with the 9R,10R,13R-TriHOME was performed.

Ivl is a soluble precursor protein that is cross-linked to other proteins and subsequently forming a protein scaffold in the stratified layer of the epidermis (Watt, 1983). The resulting cross-linked envelope is essential for providing resistance to external stress stimuli and invasion of pathogens that may subsequently compromise epidermal integrity (Djian et al., 2000). Mice deficient in *Ivl* show severe defects in the epidermal barrier as a result of an impaired desquamation process (Sevilla et al., 2007). Due to its expression, localisation and importance in upholding the integrity of the epidermal barrier, it is deemed as an important

late-stage differentiation biomarker. As such, it was an appropriate and relevant biomarker to determine the effects of 9R,10R,13R-TriHOME on late stage keratinocyte differentiation.

Whilst 9R,10R,13R-TriHOME is hypothesised to be involved in maintenance of the epidermal barrier, their precise biological role in human skin is unknown. Several studies have suggested a variety of roles for 12*R*-LOX derived lipids, from having a structural role to regulating epidermal processes such as keratinocyte proliferation and differentiation (Muñoz-Garcia et al., 2013). In healthy skin, 12*R*-LOX metabolites and products such as 12-HETE, 9-HODE, 13-HODE and hepoxilins are found in abundance, unlike in 12*R*-LOX deficient skin (Tyrrell et al., 2021).

During complete inactivation of the 12*R*-LOX protein, studies have shown ultrastructural abnormalities in differentiated layers of the epidermis (Epp et al., 2007). Of course, the epidermis of 12*R*-LOX deficient mice shows a much reduced level of the 9R,10R,13R-TriHOME in comparison with the wild type as a result of decreased lipid processing. As *Ivl* is a structural protein found in the cornified envelope, it is of interest to investigate the effect of the 9R,10R,13R-TriHOME on an important epidermal protein found in differentiated granular layers. Furthermore, studies performed by Epp et al., 2007 showed an increased fragility of the cornified envelope in 12*R*-LOX deficient mice, where *Ivl* is a known component. As 9R,10R,13R-TriHOME would be reduced or absent in 12*R*-LOX deficient mice models, this might suggest that normal functioning of the 12*R*-LOX protein and production of 9R,10R,13R-TriHOME may contribute to a robust cornified envelope through increasing the expression of *Ivl*. Interestingly, the lower concentration of 9R,10R,13R-TriHOME (2 µM) has no effect on the protein level of *Ivl* as shown in **Figure 6.5.7**.

9R,10R,13R-TriHOME released from epidermal ceramides has been hypothesised to play a key role in activating PPAR (Muñoz-Garcia et al., 2013). Whilst metabolites of arachidonic acid have been shown to activate a specific subtype of the PPAR family, the effect of products formed from linoleate oxidation by 12*R*-LOX on PPAR has yet to be explored. As PPAR is hypothesised to be involved in keratinocyte differentiation, it's possible that the 9R,10R,13R-TriHOME may activate the PPAR nuclear receptor hormone and subsequently regulate the expression of *Ivl* through a PPAR mediated pathway. Interestingly, *Pparγc1α* is shown to be statistically significantly downregulated following 12*R*-LOX protein deficiency. The absence or reduced quantity of 9R,10R,13R-TriHOME in 12*R*-LOX deficient skin may result in the downregulation of PPAR as can observed in the 12*R*-LOX deficient vs wildtype RNA-sequencing data (**Chapter 5**). Studies performed by Hanley and Feingold have shown that PPARα regulates the expression of transglutaminase, a key enzyme involved in the cross-

linking of proteins of the cornified envelope such as *Ivl*. If transglutaminase and PPAR are both involved in the same biological signalling pathway, it would be of interest to investigate the protein levels of the transglutaminase enzyme following treatment with 9R,10R,13R-TriHOME. This may provide concise mechanistic details as to how 12*R*-LOX derived lipids regulate skinphysiology.

Relative protein levels of *Krt10* shown in **Figure 6.5.9** are consistent with results observed in **Figure 6.5.6** and **Figure 6.5.7**, that is, the 9R,10R,13R-TriHOME (20 µM) significantly increasing the protein level of a marker of epidermal differentiation. *Krt10* is found to be expressed at both early stage and late stage keratinocyte differentiation (Strudwick et al., 2015). As such, its expression profile makes it an ideal biomarker candidate to investigate the effect of 9R,10R,13R-TriHOME on a protein expressed throughout the keratinocyte differentiation process. The statistically significant effect of 9R,10R,13R-TriHOME (20 µM) on *Krt10* suggests that the 9R,10R,13R-TriHOME increases the expression of a keratin protein associated with keratinocyte differentiation, indicating that 12*R*-LOX lipids are directly involved in the differentiation process. Interestingly, the keratinization process is a top five enriched biological process following GO analysis of the DEGs in the 12*R*-LOX deficient vs wildtype dataset shown in **Chapter 4**.

Experimental results in this chapter however shows an increase in *Krt10* expression following treatment with 9R,10R,13R-TriHOME (20 µM). Of course, the quantities of 9R,10R,13R-TriHOME (20 µM) in 12*R*-LOX deficient mice models have been shown to be severely reduced. This information suggests that the 9R,10R,13R-TriHOME may regulate the expression of a key differentiation marker. The regulation of *Krt10* expression by 9R,10R,13R-TriHOME may result in a normal degree of keratinization observed in healthy skin, whilst the genetic deletion of 12*R*-LOX protein which evidently results in an upregulation of *Krt10* gives rise to an abnormal degree of keratinization.

6.6.5 9R,10R,13R-TriHOME significantly increases the percentage (%) of cornified envelope formation

In conjunction with differentiation experiments, treatment of hTERT cells with 9R,10R,13R-TriHOME (20 µM) shows a significantly higher percentage of cornified envelope formation when compared with vehicle control (EtOH), -BPE and +BPE. Similar to the effect of 9R,10R,13R-TriHOME on *Ivl* and *Krt10* expression, a higher 9R,10R,13R-TriHOME concentration (20 µM) is more effective in forming a greater percentage of cornified envelopes. This suggests that 9R,10R,13R-TriHOME plays a key role in formation of a robust cornified

envelope through increasing the expression of key envelope proteins such as *Ivl* and *Krt10*. Moreover, as formation of the cornified envelope occurs in upper layers of the epidermis, this suggests that the 9*R*,10*R*,13*R*-triHOME has an effect on terminal keratinocyte differentiation. This is consistent with the localisation of the 12*R*-LOX protein, where its expression is hypothesised to be in the stratified layers of the epidermis.

The peptide cross-linking term is enriched for upregulated DEGs in the 12*R*-LOX deficient vs wildtype RNA-sequencing dataset, possibly suggesting that the overexpression of specific DEGs are compensating for the loss of the epidermal barrier and fragility of the cornified envelope which is shown to be observed in 12*R*-LOX deficient mouse models. Although 9R,10R,13R-TriHOME is reduced in 12*R*-LOX deficient skin, alternative pathways may be induced which involve the cross-linking of cornified envelope proteins to compensate for barrier loss. The cross linking of cornified envelope proteins occurring to compensate for the loss of the epidermal barrier may be responsible for the high degree of scaling and thickening of the stratum corneum commonly found in the skin of patients with ichthyosis. It's possible that the 9R,10R,13R-TriHOME may regulate the expression of cross linking proteins of the cornified envelope such as *Ivl* through specific pathways and thus contributing to the formation of functional cornified envelopes. This would be further evidence that the 9R,10R,13R-TriHOME is involved in terminal differentiation of keratinocytes.

6.6.6 Caspase-3 expression is increased following treatment with linoleic acid whilst a reduced Caspase-3 expression is observed following treatment with 9R,10R,13R-TriHOME

The balance between cell proliferation and apoptosis in the epidermis is regulated to maintain thickness of the epidermis and subsequently contribute to skin homeostasis. Currently, the literature surrounding the role of 12*R*-LOX lipids in apoptosis is relatively limited, however, a dysfunction in the apoptotic process which controls cell proliferation can result in the development of skin diseases such as psoriasis (Raj et al., 2006). Without an effective apoptotic process, skin development is impaired and results in the inadequate removal of keratinocytes. This in turn result in an impaired epidermal barrier function (Raj et al., 2006). In skin diseases such as psoriasis, clinical studies have shown that the apoptosis process is decreased as correlated by the expression of an apoptosis inhibitor known as Bcl-xL, along with reduced levels of caspase protease enzymes (Raj et al., 2006). Most skin diseases that are characterised by hyperkeratosis and hyperplasia are associated with a decrease in epidermal apoptosis (Bowen et al., 2004

Further evidence of linoleic acid' apoptosis promoting effect is shown in hepatoma cells through the hypothesised cytochrome c biological pathway (Zhang et al., 2012). However, the mechanisms of linoleic acid involvement in apoptosis is yet to be fully understood. The two double bonds found in the chemical structure of linoleic acid means it can be easily oxidized into products with cytotoxic properties that are highly active under intracellular conditions. For example, products from enzymatic transformation include hydroperoxides and aldehydes. *In vitro* studies involving lymphocytes and THP-1 cells show increased sensitivity to apoptosis following treatment with native polyunsaturated fatty acids, without their enzymatic transformation to various other products (Iuchi et al., 2019).

Whilst it was free unoxidized linoleic acid that was used in these experiments and not bound linoleic acid, higher physiological concentration of linoleic acid is found in the skin of 12*R*-LOX deficient mice, where the phenotype is described as a thick scaling of the epidermis. It's possible that the accumulation of linoleic acid as a result of the incapability of 12*R*-LOX enzymatic catalysis is contributing to an increased apoptotic effect which may disrupt formation of an effective epidermal barrier. Interestingly, studies have confirmed that excessive linoleic acid promotes the expression of proinflammatory molecules in rat models, which in turn are capable of inducing apoptosis (Bruewer et al., 2003; Marchix et al., 2015). Moreover, high doses of polyunsaturated fatty acids such as linoleic acid have been shown to induce apoptosis through downstream production of ROS (Cury-Boaventura et al., 2006). It is possible that the high concentration of linoleic acid alone is responsible for inducing apoptosis, as shown by the increased expression of the *Casp3* biomarker. On the other hand, lipoxygenase enzymes such as 15-LOX are also found in epidermal cells and are able to convert linoleic acid into 13-HODE and 9-HODE metabolites. Moreover, the 13-HODE metabolite exerts an anti-proliferative effect on cells (Ziboh et al., 2000). As such, it is possible that linoleic acid metabolites produced from other LOX enzymes could be responsible for significantly reducing cell proliferation. Possible future studies would be to investigate oxidized metabolites in samples. However, as the 9R,10R,13R-TriHOME is a significantly oxidized product of 12*R*-LOX processing and has no effect on cell proliferation nor apoptosis, it is likely that the reduced proliferation and increased apoptosis following treatment with linoleic acid is due to its toxic effect.

6.7 Conclusion

Results gathered in this chapter demonstrates that higher concentrations of the terminal product of 12*R*-LOX / eLOX-3, 9R,10R,13R-TriHOME is effective in increasing the expression of

epidermal differentiation biomarkers, whilst not significantly having an effect on cell proliferation, apoptosis nor cell migration/wound healing. To emphasise 12*R*-LOX derived lipids potential role in keratinocyte differentiation, the relative protein level of *Ivl* and *Krt10* is significantly increased following treatment with 9R,10R,13R-TriHOME. *Ivl* is an important constituent of the cornified envelope and is one of many proteins which are cross-linked to form a scaffold structure (Robinson et al., 1996). *Krt10* is expressed from early keratinocyte differentiation to late differentiation and is essential for effective epidermal barrier formation, suggesting that the 9R,10R,13R-TriHOME has an effect on the entire keratinocyte differentiation process.

In conclusion, the effect of 9R,10R,13R-TriHOME on differentiation is of most interest and promise as several articles have highlighted the possible roles of lipids formed from 12*R*- LOX processing in the differentiation process (Epp et al., 2007; Fürstenberger et al., 2007). Results obtained in this chapter strongly implicate 12*R*-LOX lipids in inducing epidermal differentiation as suggested by the significant increase in protein levels of differentiation markers such as *Ivl* and *Krt10*. Moreover, the cornified envelope formation data indicate that higher concentrations of 9R,10R,13R-TriHOME increases the percentage of cornified envelopes at a higher concentration. Hypothesised to interact with 12*R*-LOX lipids is the PPAR nuclear receptor hormone involved in regulating the expression of genes. As PPAR is thought to be associated with keratinocyte differentiation, it would be of most interest to investigate whether the 9R,10R,13R-TriHOME activates this specific transcriptional regulator. The activation of PPARγ and PPARγc1α by the 9R,10R,13R-TriHOME may provide further evidence of 12*R*-LOX lipids involvement in epidermal differentiation and yield novel pathways by which LOX regulates skin physiology.

Together with the significantly reduced proliferation, lower cell viability, lowest growth rate and increased expression of the caspase-3 apoptotic biomarker, this indicates that a higher concentration of linoleic acid may be cytotoxic to cells. This study also established that apoptosis was likely to be induced as a result of an excessive build-up of lipid species in the intracellular compartment of cells, and not strictly as a result of the number of double bonds within the structure of the fatty acid. Linoleic acid has only two double bonds and considerably less in comparison with other common fatty acids such as arachidonic acid and therefore it is likely that the higher concentration is the reason for possibly inducing cytotoxicity rather than the number of double bonds. In the epidermis, linoleic acid is esterified to a very long chain fatty acid and may therefore yield different results in comparison with the free linoleic acid used in these experiments.

Chapter 7

Determining the effect of the terminal product of the 12*R*-LOX / eLOX-3 pathway, 9R,10R,13R-TriHOME on peroxisome proliferator-activated receptor γ coactivator 1 α (PPARγc1α) activation

7.1 Introduction

Previous studies have demonstrated the effect of PPAR agonists on important epidermal processes such as keratinocyte proliferation, differentiation, apoptosis, wound healing an inflammation (Sertznig and Reichrath, 2011; Gupta et al., 2015). Corroborating this was the study by Kim et al., 2005 that showed the GW0742 PPARβ agonist promotes the expression of key terminal differentiation markers including involucrin and small proline-rich proteins, whilst selectively inhibiting keratinocyte proliferation. Both PPARγ agonists, ciglitazone and rosiglitazone stimulated an enhanced expression of epidermal differentiation markers including loricrin, involucrin and filaggrin in wildtype mouse models, whilst epidermal morphological characteristics remained the same (Mao-Qiang et al., 2004). The addition of PPARγ agonists to PPARγ deficient mice showed no significant effect on the differentiation markers, suggesting that the promotion of these markers is mediated through the PPARγ pathway. An increase in the expression of late differentiation markers such as loricrin, filaggrin and small proline-rich protein 1a (SPRR1a) are observed following PPARβ/δ activation by the GW0742, further suggesting the essential role of PPARs in promoting epidermal differentiation (Kim et al., 2005). The activation of PPARα in mouse models significantly increases keratinocyte differentiation, resulting in the formation of a robust skin barrier with minimal epidermal abnormalities (Yang et al., 2006).

The PPARβ/δ agonist, GW1515, improved epidermal barrier function following topical treatment of mice, whilst also improving the effects of detergent and solvent exposure (Schmuth et al., 2004). *In vivo* mouse studies suggest that activators of all PPAR subtypes increase the expression of lipid metabolising genes such as lipoprotein lipase and lipid molecules including cholesterol and ceramide species found in stratified layers of the epidermis (Man et al., 2006). In particular, treatment of skin equivalents with the Wy 14,643 PPARα agonist increased the presence of ceramides and cholesterol species within the epidermis, strengthening the role of PPARs in keratinocyte lipid processing (Rivier et al., 2000). Moreover, an increase in the membrane coating granules responsible for processing lipids of the cornified layer was also observed following extended exposure to Wy 14,643, whilst the lipid composition in the stratum corneum was also found to be significantly elevated with an enhanced synthesis of key epidermal ceramides, cholesterol sulfate, cholesteryl esters and triglycerides.

Specific PUFA such as docosahexaenoic acid (DHA) and eicosapentaenoic acid (EPA) are natural ligands of PPARγ. Activation of PPARγ by DHA has been shown to inhibit the

growth of human lung cancerous cells, highlighting PPARs as therapeutic targets in the treatment of diseases (Trombetta et al., 2007). Long chain monounsaturated fatty acids are also shown to increase the expression of PPARγ, resulting in the reduced expression of inflammatory proteins in white adipose tissue (Yang et al., 2013). Omega n-3 PUFA are considered natural agonists of PPARα and studies performed in endothelial cells have demonstrated that oxidized EPA has a greater effect on PPARα activation than unoxidized (Volker et al., 2000; Grygiel-Górniak, 2014). In addition, oxidized low density lipoprotein (LDL) is more effective in activating PPARα, whilst unoxidized LDL does not have any effect in activating this PPAR isoform (Sethi et al., 2002). These studies suggest that oxidized lipid species are crucial in the activation of PPARs.

The exposure of atopic dermatitis and psoriasis mouse models to PPARα agonists such as clofibrate re-establishes epidermal function following its topical application (Komuves et al., 2000). Additionally, an overexpression of PPARα following ligand activation is shown to inhibit hyperproliferation and therefore reducing a build-up of cells (Yang et al., 2006). The troglitazone compound known to activate PPARγ alleviates psoriasis symptoms through improving morphology and reducing skin hyperplasia (Ellis et al., 2000). Moreover, in hyperproliferative mouse models, exposure to PPARα agonists partially recovers the functioning of the epidermis (Demerjian et al., 2006).

7.1.1 Potential interaction of the 9R,10R,13R-TriHOME terminal product of 12*R*-LOX / eLOX-3 pathway with epidermal PPARs

Interestingly, PPARγ and PPARγc1a are both downregulated in response to 12*R*-LOX protein deficiency. Previous studies have reported PPARγc1a involvement in mediating the differentiation of mesenchymal stem cells to brown adipose cells. Moreover, it has been demonstrated that mice deficient in PPARγc1a revealed abnormal brown fat tissue morphology and irregular lipid droplet formation (Wong et al., 2011). PPARγc1a interacts with PPARγ, allowing its interaction with a range of proteins. PPARγ is associated with regulating and promoting keratinocyte differentiation and its coactivation by PPARγc1a may be required to perform this important function (Mao-Qiang et al., 2004). One possible mechanism by which 12*R*-LOX derived lipids regulate skin physiology is through interaction and subsequent activation of PPARs. To date, LOX derived metabolites such as the 8R-hydroxy-11R,12R-epoxyeicosa-5Z,9E,14Z-trienoic acid activates PPARα (Yu et al., 1995). Moreover, endogenous lipid molecules produced via 12-LOX metabolism are shown to activate PPARγ which in turn stimulates the differentiation of adipocytes (Harsløf et al., 2010). The PPARγ

and PPARγc1a subtypes were found to be downregulated in 12*R*-LOX deficient mice models, suggesting that 12*R*-LOX derived lipids may have a role in regulating expression of these specific PPARs. Interestingly, PPARγ is shown to be upregulated during keratinocyte differentiation, adding further evidence that 12*R*-LOX lipids have a role to play in epidermal differentiation (Muga et al., 2000). The effect of 9R,10R,13R-TriHOME on PPAR activation has yet to be fully investigated. Binding of PPARγc1a to PPARγ increases its activity and permits interaction with other proteins. PPARs are thought to contribute to epidermal homeostasis through possible regulation of key epidermal processes such as proliferation, differentiation and lipid metabolism (Sertznig et al., 2008; Ramot et al., 2015). As such, the downregulation of both PPARγc1a and PPARγ observed in 12*R*-LOX deficient mouse skin may therefore result in aberrant epidermal processes and leading to a defective epidermal barrier.

PPARs have also been linked to maintaining epidermal barrier function through regulating the transcription of a key cornified envelope cross-linking enzyme (Hanley et al., 1998). This suggests that PPARs would contribute to latter stages of epidermal differentiation as cornified envelope formation occurs towards the end of the keratinocyte differentiation process. Interestingly, significant evidence from the RNA-sequencing analysis suggested that 12*R*-LOX deficiency predominantly effects proteins found in late keratinocyte differentiation. This is further emphasised by enriched terms for differentially expressed genes in the 12*R*-LOX deficient dataset such as cornification, keratinization and peptide cross-linking. Significant evidence point towards PPARs role in regulating terminal keratinocyte differentiation and lipid processing (Elias, 2005). The transglutaminase enzyme catalyses the formation of isopeptide bonds between various proteins to form the cornified envelope (Eckert et al., 2005). Whilst the transglutaminase enzyme is not significantly downregulated in 12*R*-LOX deficient mice, cross-linking proteins such as SPRRs are found to be differentially expressed. With the evidence that 12*R*-LOX products may effect PPAR gene expression, this chapter explores whether the 9R,10R,13R-TriHome terminal product of the 12*R*-LOX / eLOX-3 pathway could also act as agonists to these same PPAR transcription factors.

7.2 Aim

- Determine the effect of the 9R,10R,13R-TriHOME terminal product of the 12*R*-LOX /eLOX-3 pathway on PPARγc1α activation in the A549 cell line.

7.3 Objectives

- Purify PPARγc1α and PPAR response element (PPRE) plasmids in preparation for transfection.
- Verify and confirm the presence of the PPARγc1α DNA plasmid after purification procedure using restriction enzymes and gel electrophoresis.
- Explore the possible agonist effects of the 9R,10R,13R-TriHOME terminal product ofthe 12*R*-LOX / eLOX-3 pathway on PPARγc1α using a reporter gene assay.

7.4 Materials and methods

Materials, equipment and routine cell culture of the A549 cancer cell line are described in **Section 2.1.6** and **2.1.7** respectively. Other materials used in this chapter include Opti-MEM® Reduced Serum Medium (Thermo Fisher Scientific, UK #31985062), Lipofectamine™ 2000 transfection reagent (Thermo Fisher Scientific, UK #11668019), pGL3 basic vector (Promega, UK #E1751), pRL–TK renilla luciferase control reporter vector (Promega, UK #E2241), Dual-Glo® luciferase assay system (Promega, UK #E2920), rCutSmart™ buffer 10 X (New England Biolabs #B6004S), gel loading dye, purple (6X) (New England Biolabs #B7024A), Rosiglitazone (Abcam, UK #ab120762), ethanol absolute ≥99.8% molecular biology grade DNase/RNase-free (VWR, UK #437433T) and DMSO molecular biology grade (VWR, UK #76177-938). The plasmids used include pcDNA-f:PGC1 (*Pparγc1a*) (Addgene plasmid #1026 ;http://n2t.net/addgene:1026 ; RRID:Addgene_1026) and PPRE X3-TK-luc (Addgene plasmid #1015 ;http://n2t.net/addgene:1015 ; RRID:Addgene_1015) which were received as a gift from Bruce Spiegelman. Restriction enzymes used included *AvrII* (New England Biolabs #RO174S) and *XhoI* (New England Biolabs #RO146S). Lipids used include 9R,10R,13R-TriHOME which was kindly received from Dr Christopher Thomas (School of Pharmacy and Pharmaceutical Sciences, Cardiff University) and Linoleic acid (Cayman Chemicals, UK #90150).

7.4.1 Inoculating an overnight bacterial liquid culture containing the PPARγc1α and PPAR response element (PPRE) plasmids

Luria broth (LB) (4g NaCl, 4g tryptone, 2g yeast extract and 400 mL of distilled water) was prepared in a 500 mL glass bottle. For Miniprep purification, 2 mL of LB was added to a 50

mL falcon tube containing 100 µg/mL ampicillin. For Maxiprep purification, 1 L of LB was added to a 2 L Erlenmeyer flask containing 100 µg/mL ampicillin. A separate sterile 200 µl pipette tip was used to select a single colony from an LB agar plate containing the pcDNA-f:PGC1 plasmid and PPRE X3-TK-luc plasmid respectively and was placed into a tube/flask and swirled for 5 minutes. The bacterial culture was then incubated at 37ºC overnight in a shaking incubator.

7.4.2 Purification of PPARγc1α and PPRE plasmids

Qiagen Plasmid Mini Kit (Qiagen, UK #12123) was used for PPARγc1α and PPRE plasmid DNA Miniprep purification as per manufacturer's instructions. PureLink™ HiPure Plasmid Maxiprep kit (Thermo Fisher Scientific, UK #K21007) was also used for PPARγc1α and PPRE plasmid DNA Maxiprep purification as per manufacturer's instructions. Following PPARγc1α and PPRE plasmid DNA purification, 2 µl of PPARγc1α and PPRE plasmid DNA was taken for DNA concentration and purity measurement using the NanoDrop™ One/One^{C} Microvolume UV-Vis Spectrophotometer. A260/A280 values are a measurement of DNA purity with values between 1.80-2.00 deemed as a "good" purity range. "Pure" DNA has an A260/A230 value of 2.0-2.2 (Lucena-Aguilar et al., 2016).

7.4.3 Restriction digestion of PPARγc1α and PPRE plasmid DNA

Digestion of the PPARγc1α plasmid was performed with the *AvrII* restriction enzyme, whilst digestion of the PPRE plasmid was performed with the *XhoI* restriction enzyme. *Pparγc1a* and PPRE plasmid DNA (1 µg) were added to separate 1.5 mL tubes with 1 µl of each respective restriction digestion enzyme, 3 µl of rCutSmart™ buffer 10 X and 43 µl of dH_2O with gentle pipette mixing. Each mixture was incubated at 37ºC for 1 hour.

7.4.4 Gel electrophoresis and verification of PPARγc1α and PPRE plasmids

To prepare 1% agarose gel, 1g of agarose was mixed with 100 mL of 1 X tris-acetate-EDTA (TAE) in a 50 mL conical flask. The conical flask was placed in a microwave for 1 minute, swirling and then placed back in the microwave for an additional 2 minutes. The agarose solution was then cooled for 5-10 minutes at RT and 2 µl of ethidium bromide was added to a final concentration of 0.2 µg/mL. The 1% agarose gel was slowly poured into a gel tray containing the comb and was left to solidify for 30 minutes at RT. Gel loading buffer (7 µl) was added to the PPARγc1α and PPRE DNA samples respectively. The 1% agarose gel was carefully placed into an electrophoresis chamber and filled with 1 X TAE buffer to completely cover the gel. The PPARγc1α, PPRE DNA sample and molecular weight ladder were loaded

into wells using a gel loading pipette tip. Gel electrophoresis was run at 100 V for 1 hour and DNA fragments corresponding to PPARγc1α and PPRE plasmid DNA were visualized using the G:BOX Chemi XX6/XX9 detection system.

7.4.5 Transfection and reporter gene assay to determine whether a PPARγc1α stimulating effect is observed in response to treatment with the 9R,10R,13R-TriHOME terminal product of 12*R*-LOX / eLOX-3

A549 cancer cells were plated at a density of 1.0 x 10^6 cells per well in a 24-well plate in 1 mL of medium and incubated overnight in a humidified atmosphere at 37ºC and at 5% CO_2 to reach 70-80% confluence. Per well, 3 µl of Lipofectamine™ 2000 transfection reagent was diluted in 50 µl Opti-MEM® medium. Plasmid DNA (1 µg) consisting of the luciferase gene which is under the control of PPAR response elements (PPRE X3-TK-luc), 500 ng of pcDNA-f:PGC1 plasmid DNA and 0.5 µg of pGL3 basic vector was diluted in 250 µl of Opti-MEM® medium. Diluted DNA (50 µl) was added to 50 µl of the diluted Lipofectamine™ 2000 transfection reagent and incubated at RT for 5 minutes. A549 cells were then serum deprived and treated with 9R,10R,13R-TriHOME to three wells (n = 3) at concentrations of 2 and 20 µM and incubated for 24 hours in a humidified atmosphere at 37ºC and at 5% CO_2. Rosiglitazone is a known PPARγ agonist and was used as a positive control, linoleic acid control (2 and 20 µM), EtOH (2 and 20 µM) (Control 1), DMEM media (Control 2) and DMSO (Control 3).

7.4.6 Statistical analysis

PPAR activation experiments was repeated three times which were performed in triplicate and data are expressed as the mean ± SD. Statistical significance between treatments was determined using Student's *t*-test with $p < 0.05$ considered of statistical significance and is represented with an asterisk. Statistical analysis was done using GraphPad Prism 9.0 software (GraphPad Software Inc., San Diego, CA, USA) and Microsoft Excel software.

7.5 Results

7.5.1 Determining the most effective method for PPAR and PPRE plasmid DNA purification

Initially, a Miniprep purification of PPARγc1α and PPAR response element (PPRE) plasmid DNA was performed. **Table 7.5.1** shows a concentration of 428.4 ng/µl was obtained for the PPARγc1a DNA plasmid using the Miniprep purification method. The A260/A280 value obtained for the PPARγc1a DNA plasmid following Miniprep purification was 1.85, whilst the A260/A230 value was 2.25. A significantly lower concentration of 178.7 ng/µl was obtained for the PPRE DNA plasmid in comparison with the PPARγc1α plasmid DNA following the

Miniprep purification method. The A260/A280 value obtained for the PPRE plasmid DNA following Miniprep purification was 1.86, whilst the A260/A230 value was 2.01. The A260/A280 and A260/A230 values for the PPARγc1α DNA plasmid are within the expected "purity" range. Whilst the A260/A280 value obtained for the PPRE DNA plasmid are within the expected "purity" range, the A260/A230 value of 2.26 indicates possible contamination. Likely sources of contamination include residual phenol or guanidine which are used during Miniprep purification procedures.

Miniprep purification			
Plasmid DNA	**Concentration (ng/µl)**	**A260/A280**	**A260/A230**
PPARγc1a	428.4	1.87	2.26
PPRE	178.7	1.86	2.26
Maxiprep purification			
Plasmid DNA	**Concentration (ng/µl)**	**A260/A280**	**A260/A230**
PPARγc1a	1236.1	1.85	2.25
PPRE	827.4	1.86	2.01

Table 7.5.1 Comparison of PPARγc1α and PPRE plasmid DNA quantity and quality using Miniprep and Maxiprep purification methods and measured using the NanoDrop One/One^{C} Microvolume UV-Vis Spectrophotometer. The A260/A280 and A260/A230 ratios are a measure of nucleic acid purity. A260/A280 value range of 1.85-1.88 and A260/A230 value range of 2.0-2.2 are indicative of pure DNA.

Due to the significantly lower concentration of plasmid DNA observed for PPRE and the optimisation likely required for the transfection experiments, a Maxiprep purification was also performed which yielded a significantly higher plasmid DNA concentration of 1236.1 ng/µl. Following Miniprep purification of the PPARγc1α plasmid DNA, the A260/A280 was calculated to be 1.87, whilst the A260/A230 value was calculated to be 2.26. An A260/A280 value of 1.85 was obtained for the PPRE plasmid DNA following Maxiprep purification, whilst the A260/A230 value was calculated to be 2.25.

7.5.2 Verification of PPARγc1a and PPRE plasmid DNA

Prior to commencing transfection and functional studies, the purified PPARγc1a and PPRE plasmid DNA required verification utilising restriction enzymes. The total size of the PPARγc1a and PPRE plasmid DNA are 7904 base pairs and 6763 base pairs respectively. **Figure 7.5.1** shows that the digestion of the PPARγc1α plasmid with the *Avrll* enzyme resulted in a single band of 4291 base pairs, whilst digestion of the PPRE plasmid with the *Xhol* enzyme

resulted in a single band of 6726 base pairs. The resulting gel shown in **Figure 7.5.1** correspond to the predicted sizes of the digested PPARγc1α and PPRE plasmid DNA with the respective enzymes.

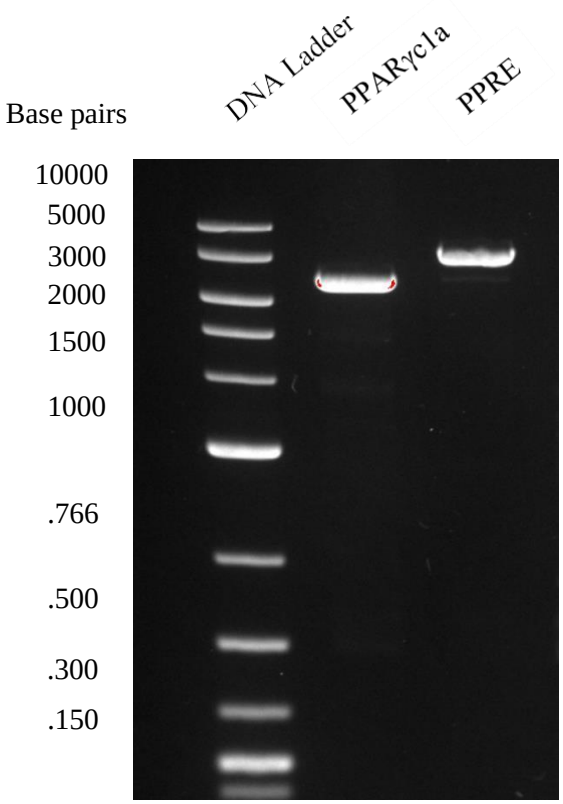

Figure 7.5.1 Verification of the PPARγc1α and PPRE plasmid DNA. The 0.8% agarose gel (110V, 1hr) displays a DNA molecular weight ladder and two bands that represent the PPARγc1α (4291 base pairs) and PPRE (6726 base pairs) plasmid DNA after digestion with *AvrII* and *XhoI* enzymes respectively.

7.5.3 A lower concentration (2 μM) of the 9R,10R,13R-TriHOME terminal product of 12*R*-LOX / eLOX-3 pathway is significantly more effective in activating PPARγc1α than at a higher concentration (20 μM)

The PPRE-reporter assay consisting of co-transfection with PPARγc1α performed in A549 cells showed activation of PPARγc1α in response to treatment with 2 μM of 9R,10R,13R-TriHOME. **Figure 7.5.2** shows that the mean PPRE-luciferase activity value of 0.5 in response to treatment with 2 μM of 9R,10R,13R-TriHOME is significantly greater when compared with vehicle control (EtOH). The mean PPRE-luciferase activity is close to that of the rosiglitazone positive control, known for its PPARγc1α activation. An equivalent concentration (2 μM) of linoleic acid had no effect in in activating PPARγc1α as evident by a mean PPRE-luciferase activity value of 0.06.

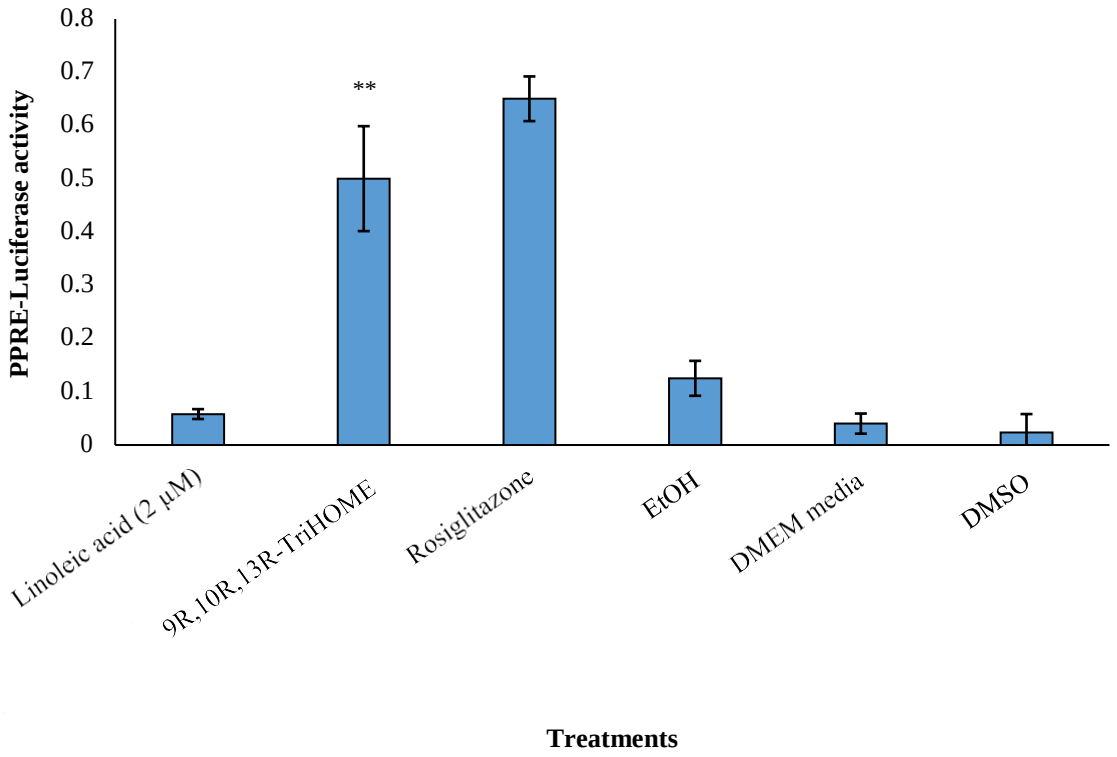

Figure 7.5.2 PPARγc1α stimulating effect of the 9R,10R,13R-TriHOME product of the 12*R*-LOX / eLOX-3 pathway (2 µM). The A549 cells were transfected with 1µg 3X PPRE TK-luciferase in pGL3 basic vector and 500 ng of pcDNA-Flag-PPARγc1α using Lipofectamine 2000 for 24 hrs. The A549 cells were serum deprived (0% BPE) and treated with the 9R,10R,13R-TriHOME for 24 hrs. Rosiglitazone (2 µM) was used as a positive control and linoleic acid was used as an unoxidized lipid control (*n*=3, ± SD). Data represents mean ± SEM of three independent experiments performed in triplicate. ** p<0.01 vs vehicle control (EtOH).

A greater PPRE-luciferase activity (2.4) is observed following treatment of A549 cells with a higher concentration of 9R,10R,13R-TriHOME (20 µM), however, **Figure 7.5.3** shows that, in this experiment, it did not significantly activate PPARγc1α when compared with the vehicle control (EtOH). A clearer, significant effect of the 9R,10R,13R-TriHOME on PPARγc1α activation can be observed at a lower concentration (2 µM) than at a higher 9R,10R,13R-TriHOME concentration (20 µM). The rosiglitazone shown in both **Figure 7.5.2** and **Figure 7.5.3** served as a positive control.

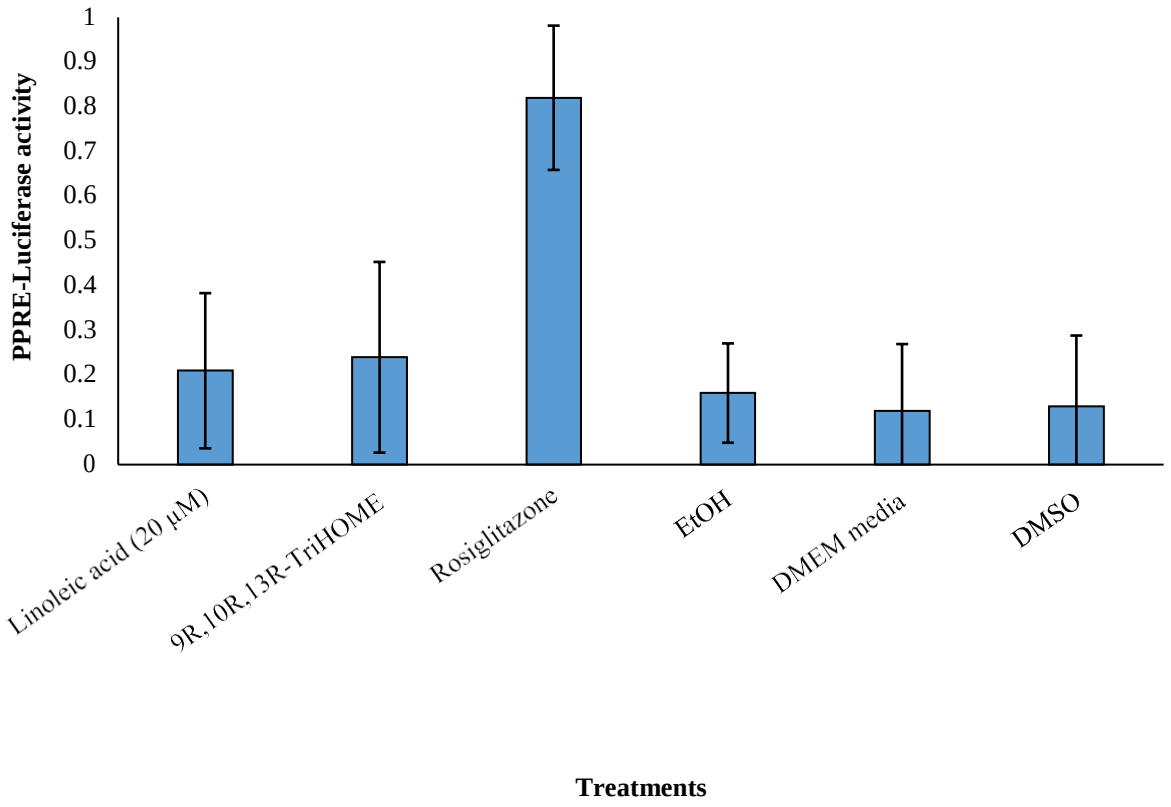

Figure 7.5.3 PPARγc1a stimulating effect of the 9R,10R,13R-TriHOME product of the 12*R*-LOX / eLOX-3 pathway (20 µM). The A549 cells were transfected with 1µg 3X PPRE TK-luciferase in pGL3 basic vector and 500 ng of pcDNA-Flag-PPARγc1a using Lipofectamine 2000 for 24 hrs. The A549 cells were serum deprived (0% BPE) and treated with the 9R,10R,13R-TriHOME for 24 hrs. Data represents mean ± SEM of three independent experiments performed in triplicate. Rosiglitazone (20 µM) was used as a positive control and linoleic acid was used as an unoxidized lipid control (*n*=3, ± SD).

7.6 Discussion

Various PPAR isoforms are shown to be expressed in human skin and may contribute to the formation of the epidermal barrier (Schmuth et al., 2008). Of the three main PPAR isoforms, the PPARγ and its co-activator, PPARγc1α, are of most interest for this thesis due to their significant downregulation in response to 12*R*-LOX deletion in mouse models discussed in **Chapter 5**. Moreover, the PPARγc1α gene is believed to have play an important role in cell differentiation (Zhang et al., 2018). PPARγ and PPARγc1α is expressed in a variety of tissue, from kidney and spleen tissue to skeletal muscle and the skin (Grygiel-Górniak et al., 2014; Ramot et al., 2015). Humans show elevated levels of PPARγ in healthy skin whilst reduced expression is observed in skin barrier disorders such as psoriasis and atopic dermatitis (Sertznig and Reichrath, 2011; Sobolev et al., 2020). It is evident from the RNA-sequencing analysis of 12*R*-LOX deficient mice in this thesis that the PPARγc1α subtype is significantly downregulated. Interestingly, a reduction in inflammatory molecules are observed in skin

barrier disease animal models following PPAR activation (Heming et al., 2018). Due to their wide range of stimulating effects on key epidermal processes and anti-inflammatory promoting properties, PPARs have become potential targets in the treatment of disorders involving a compromised skin barrier. RNA-sequencing analysis of 12*R*-LOX deficient mice dataset shown in **Chapter 5** showed PPARγc1α downregulation and DEGs belonging to the EDC. As such, investigation into 9R,10R,13R-TriHOME activation of PPARγc1α was performed. PPARγc1α is a member of a group of transcription coactivator proteins which interacts and enhances PPARγ activity, allowing its interaction with various other proteins (Liang and Ward, 2006). Gene Ontology enrichment analysis performed in **Chapter 4** also revealed terms associated with keratinocyte differentiation such as "cornification", "peptide cross-linking", "cornified envelope" and "keratinization". Interestingly, the differentiation process is altered in skin disorders such as ichthyosis, known to be associated with an impaired epidermal barrier function. Moreover, 9R,10R,13R-TriHOME terminal product of the 12*R*-LOX / eLOX-3 pathway is shown to induce the expression of key epidermal differentiation markers such as keratin 10 and showed an increase in the number of cornified envelope as shown in **Chapter 6**.

7.6.1 9R,10R,13R-TriHOME terminal product of 12*R*-LOX / eLOX-3 pathway stimulates the activation of PPARγc1a

Treatment of A549 cells with 2 μM of 9R,10R,13R-TriHOME for 24 hours significantly activates PPARγc1a with an almost similar mean PPRE-luciferase value to cells treated with the rosiglitazone positive control. In other similar studies, PPARα and PPARβ are also shown to be activated by lower concentrations of phthalate esters (Bility et al., 2004). High concentrations of alpha-hydroxy acids found in skin greatly reduces corneocyte adhesion, which in turn results in epidermal disruption and skin irritation, suggesting higher concentrations of lipids may not be preferable for a functional epidermal barrier (Tang and Yang, 2018). However, *in vivo* studies have also confirmed PPAR activation at higher concentrations (100 μM) using EFA and eicosanoids (Plutzky, 2000; Varga et al., 2011). Significant *in vitro* and *in vivo* evidence points towards PPARγ involvement in regulating and maintaining the skin permeability barrier through promoting keratinocyte differentiation (Adachi et al., 2013). It has previously been shown that ligands which activate specific PPARs such as PPARα also stimulate the expression of epidermal differentiation markers (Hanley et al., 1997). As shown in **Chapter 6**, the relative expression levels of key epidermal differentiation markers such as involucrin and keratin 10 are increased following exposure to

9R,10R,13R-TriHOME. Combining the data from **Chapter 6** and **7**, a lower concentration of 9R,10R,13R-TriHOME (2 μM) is shown to stimulate the activation of PPARγc1α, whilst a higher concentration of the 9R,10R,13R-TriHOME (20 μM) is more effective in enhancing the expression of involucrin and keratin 10. The 9R,10R,13R-TriHOME terminal product of 12*R*- LOX and eLOX-3 pathway evidently has an effect on the PPARγ coactivator, PPARγc1α, which coordinates the activity of PPARγ (Stenmark and Tuder, 2018). Its interaction and coactivation of PPARγ would in turn effect the expression of epidermal differentiation markersand therefore play a role in keratinocyte differentiation.

7.6.2 Activation of PPARγ and PPARγc1α are associated with promoting important epidermal processes

PPARs are particularly sensitive to lipid molecules which have previously been shown to induce the activation of this family of nuclear receptor hormones. **Figure 7.5.2** clearly demonstrates that the 9R,10R,13R-TriHOME terminal product of the 12*R*-LOX / eLOX-3 pathway has an activating effect on the PPARγc1α subtype, adding to the body of evidence that lipid molecules are potent activators.

In healthy skin, the abundance of lipid species in stratified layers of the epidermis may activate PPAR and therefore promoting the expression of keratinocyte differentiation markers such as involucrin and keratin 10, thus having a role in keratinocyte differentiation. Some lipid species are esterified to long chain ceramides and their release by an unknown enzyme may be key in regulating the concentration available to act on expression of PPAR and also as PPAR agonists. An increase in the expression of both these differentiation markers are observed following exposure to the 9R,10R,13R-TriHOME, suggesting that the increased protein levels of these differentiation markers may possibly be mediated through a PPAR pathway. The activation of PPARα results in a significantly reduced epidermal thickness due to suppression of cell proliferation. A thickened epidermis is a clinical manifestation observed in ichthyosis and the activation of PPARγc1α by 9R,10R,13R-TriHOME may contribute to the maintenance of normal epidermal thickness through stimulating the expression of epidermal differentiation proteins. As the 9R,10R,13R-TriHOME is shown to increase the expression of keratinocyte differentiation markers, it's possible that lipids such as 9R,10R,13R-TriHOME can become ameliorative candidates for treatment of skin diseases with a perturbed epidermal barrier. Whilst previous studies and experimental results shown here establish a strong possibility that the 9R,10R,13R-TriHOME and PPARγc1α contribute to

epidermal barrier restoration and possible role in effective barrier function, the exact biological mechanism by which this occurs remains unsolved.

PPARγ and PPARγc1α are predominantly expressed in the outer differentiated layers of the epidermis. Interestingly, a majority of DEGs following 12*R*-LOX protein deficiency are expressed in suprabasal regions of the epidermis and to a lesser extent in proliferative layers of the epidermis as shown in **Chapter 4**. Studies have demonstrated the role of PPARγ in regulating differentiation in the adipocyte cell line, suggesting the potential to also regulate differentiation in other cell lines such as keratinocytes (Siersbaek et al., 2010). PPARγc1α has been shown to mediate the transformation of mesenchymal stem cell into adipocytes through increasing the expression of genes which are implicated in brown fat cell differentiation (Wong et al., 2011). Interestingly, an increase in the relative protein level of involucrin following the treatment of the hTERT keratinocyte cell line with the 9R,10R,13R-TriHOME is observed in **Chapter 6**. Involucrin is a protein found cross-linked by transglutaminase in the cornified envelope (Nemes et al., 1999). Activation and expression of PPARγc1α may result in fully functional skin barrier through stimulating keratinocyte differentiation. In addition to promoting keratinocyte differentiation, controlled keratinocyte proliferation is also observed during the expression of PPARγ (Adachi et al., 2013). Enhanced keratinocyte proliferation is a key pathophysiological trait associated with multiple skin barrier disorders such as psoriasis (Franssen et al., 2004). Therefore, the activation of PPARγc1α may not only stimulate the expression of important differentiation markers but also regulate epidermal proliferation. Whilst the exact mechanism of PPAR regulation of proliferation is yet to be fully elucidated, similar results have been observed in studies involving PPARα, where its activation by clofibrate and Wy-14,643 promotes the expression of key differentiation markers and suppresses irregular keratinocyte proliferation (Kömüves et al., 2000). Furthermore, ligand activation of PPARβ/δ inhibits cell proliferation in mouse keratinocytes, human HaCaT cells and endothelial cells (Müller-Brüsselbach et al., 2007; Borland et al., 2008).

The administration of PPARα specific ligands resulted in an increase in the expression of proteins found in stratified layers of the epidermis such as loricrin and filaggrin (Kömüves et al., 2000). Their expression is essential for formation of the cornified envelope and keratohyalin granules which are found only in differentiated layers of the epidermis (Fuchs, 1990). Interestingly, studies involving PPARα deficient mice showed a reduction in involucrin and loricrin expression, suggesting PPAR is implicated in regulating key epidermal differentiation proteins (Kömüves et al., 2000).

7.7 Conclusion

To conclude, this chapter demonstrates that the 9R,10R,13R-TriHOME terminal product of the 12*R*-LOX / eLOX-3 pathway activates PPARγc1α. The expression of PPARγc1α coordinates the coactivation of PPARγ and thus permitting its interaction and possible transcriptional regulation of epidermal proteins such as involucrin and keratin 10. This specific PPAR subtype was selected for investigation due to its observed downregulation following 12*R*-LOX protein deficiency shown in **Chapter 5** and its importance in regulating a range of key epidermal processes. Localisation analysis in **Chapter 4** showed most DEGs were expressed in stratified layers of the epidermis. A body of evidence has implicated other PPAR subtypes such as PPARα in maintaining barrier homeostasis through stimulating keratinocyte differentiation and suppressing uncontrollable proliferation (Mao-Qiang et al., 2004; Schmuth et al., 2008). Regulation of these epidermal processes results in the development of a functional epidermal barrier, thus reducing transepidermal water loss and the development of skin disorders such as ichthyosis. Previous studies have shown that the activation of PPAR by specific ligands resulted in barrier recovery in patients with severe atopic dermatitis (Sertznig and Reichrath, 2011). As such, PPAR represent biological targets for the treatment of skin disorders such as ichthyosis. In healthy skin, the 9R,10R,13R-TriHOME may contribute and maintain skin homeostasis through a PPARγc1α mediated pathway. More specifically, the 9R,10R,13R-TriHOME is shown to significantly increase the relative protein level of involucrin and keratin 10 in **Chapter 6**, suggesting a role in keratinocyte differentiation. As aberrant keratinocyte differentiation is a characteristic of 12*R*-LOX deficient mice, the activation of PPARγc1a following treatment with 9R,10R,13R-TriHOME may be beneficial in aiding barrier recovery through stimulating the expression of key differentiation proteins. Current PPARγ agonists that include TZDs such as pioglitazone show reduced specificity and therefore the 9R,10R,13R-TriHOME may represent an alternative natural ligand for the treatment of inflammatory skin disorders such as ichthyosis.

Chapter 8

General discussion and future studies

8.1 Transcriptome analysis of 12*R*-LOX deficient mice reveals a possible role in keratinocyte differentiation

A thorough analysis of the RNA-sequencing data of 12*R*-LOX deficient mice shown in **Chapter 4** demonstrated that the majority of upregulated differentially expressed genes (DEGs) were predominantly expressed in stratified layers of the epidermis. This suggested that deletion of the *Alox12b* gene that encodes the 12*R*-LOX protein affects differentiated layers of the epidermis rather than proliferative layers such as the stratum basale. Furthermore, a similar trend is observed in localisation analysis of downregulated DEGs, with the majority of these genes found to be expressed in the outer layer of the epidermis. In addition to determining localisation of DEGs, Gene Ontology enrichment analysis, a bioinformatics analytical tool, was used to identify the top biological processes associated with differentially expressed genes (DEGs). Examples of these biological processes associated with upregulated genes following 12*R*-LOX deficiency includes keratinocyte differentiation, cornification, keratinization and peptide cross-linking. These upregulated genes associated with these processes included repetin (*Rptn*), small proline-rich protein 1b (*Sprr1b*), small proline-rich protein 2d (*Sprr2d*), keratin 1 (*Krt1*), keratin 6b (*Krt6b*) and keratin 10 (*Krt10*). Cornification and keratinization occur only during terminal keratinocyte differentiation, further suggesting that the 12*R*-LOX protein is implicated or partly responsible for regulating the differentiation process. Moreover, cellular components enriched for upregulated genes include cornified envelope and keratin filament, indicating that 12*R*-LOX deletion significantly impacts cellular constituents only found to be associated with keratinocyte differentiation. It's possible that 12*R*-LOX deletion induces a compensatory mechanism to repair the compromised permeability barrier function. The activation of compensatory mechanisms are common occurrences following gene knockouts. For example, the knockout of myoglobin in mouse model studies in the investigation of cardiac function reported activation of compensatory mechanisms including steepening of the PO2 gradient to alleviate the effects of myoglobin loss (Gödecke et al., 1999). Additionally, keratin 7 (*Krt7*) deficient mice induce compensatory mechanisms as demonstrated by the upregulation of keratin 8 (*Krt8*) and keratin 20 (*Krt20*). The expression of keratin 8 is known to overlap with the expression of *Krt7* (Moll et al., 1982; Sandilands et al., 2013). Other examples include the upregulation of ribosomal protein L22 like 1 that compensates for the loss of ribosomal protein L22, leading to normal conversion of genetic information into proteins (O'Leary et al., 2013). As such, the biological processes and cellular compartments associated with the DEGs are therefore enriched in an attempt to restore the barrier function of the epidermis, thus preventing transepidermal water loss and infection.

These processes and compartments are characteristic of terminally differentiated keratinocytes which are localised in the outermost layer of the epidermis and serving as the first line of a skin defence barrier. This initial data suggested that the 12*R*-LOX protein contributes to formation of the epidermal barrier through regulating processes occurring in latter stages of keratinocyte differentiation.

A total of 20 upregulated DEGs are associated with the enriched keratinocyte differentiation process. Examples of these DEGs include *Rptn, Sprr1b, Sprr2d, Krt1* and *Krt6b,* all of which belong to an epidermal gene cluster known as the epidermal differentiation complex (EDC). The EDC plays an important role in the maturation and maintenance of the epidermis by regulating the expression of various proteins via unique epidermal signalling pathways (Marenholz et al., 2001). A protein class analysis revealed that the majority of upregulated DEGs (79.4%) are associated with either the EDC or keratin protein family. In healthy skin, *Rptn* is essential for the formation of the cornified envelope through cross linking with other proteins such as *Sprr1b* and *Sprr2d* proteins and therefore providing an effective epidermal barrier function (Eckert et al., 2004; Huber et al., 2005). As the permeability barrier is impaired in 12*R*-LOX deficient mice, overexpression of proteins may compensate for loss of barrier functionality and may therefore be responsible for the enriched keratinization and cornification processes observed following GO enrichment analysis. Morphological analysis of ichthyosis shows abnormal thickening and scaling of the skin (Craiglow, 2013). Interestingly, upregulated DEGs observed in 12*R*-LOX deficient mice such as *Rptn* and *Sprr1b* proteins are also found to be overexpressed in skin disorders such psoriasis and atopic dermatitis (Trzeciak et al., 2020). Moreover, observed overexpression of keratins found in 12*R*-LOX deficient mice such as *Krt1, Krt14* and *Krt6b* are associated with abnormal morphology of keratinocytes and of the cornified envelope as demonstrated by the ingenuity pathway analysis (IPA). Deficiency of the 12*R*-LOX protein significantly impacts the expression of a keratin protein hypothesised to function as a regulator of keratinocyte differentiation known as the keratinocyte differentiation associated protein (*Krtdap*). *Krtdap* is also shown to be overexpressed in lesional psoriatic skin, suggesting its overexpression is linked with skin disorders having impaired differentiation (Tsuchida et al., 2004). Interestingly, 12*R*-LOX derived lipids are also increased in human psoriatic lesions (Tyrrell et al., 2021). 12*R*-LOX derived lipids may therefore play a role in regulating and normalizing the expression of these proteins and therefore contribute to the development of a functional epidermal barrier.

Further evidence of 12*R*-LOX hypothesised role in keratinocyte differentiation includes the overexpression of the lipase family member N (*Lipn*) gene. In healthy skin, its expression

is specifically observed during keratinocyte differentiation and is implicated in the lipid metabolism process in differentiated keratinocytes and may therefore be upregulated to compensate for the loss of the 12*R*-LOX (Israeli et al., 2011).

8.2 Downregulation of *Pparγ* and *Pparγc1a* following 12*R*-LOX deficiency – hypothesised regulator of keratinocyte differentiation

The peroxisome proliferator activated receptor gamma coactivator 1a (*Pparγc1a*) was a clear target of interest as demonstrated by its downregulation in the RNA-sequencing data, along with other papers reporting PPARs involvement in the differentiation process (Hanley et al., 1998; Rivier et al., 1998; Mao-Qiang et al., 2004; Kim et al., 2005). Analysis of the RNA-sequencing data following 12*R*-LOX protein deficiency showed that the *Pparγc1a* is most significantly affected out of all PPAR subtypes and therefore was pursued further in lipid activation experiments in **Chapter 7**. To date, experimental evidence has demonstrated *Pparγc1a* involvement in mediating mesenchymal differentiation, suggesting its potential in regulating the differentiation process in other cell types (Huang et al., 2011). Abnormal differentiation of brown adipocytes and fibroblasts are a consequence of *Pparγc1a* downregulation as shown in the IPA in **Chapter 5**. Interestingly, in other inflammatory skin disorders such as psoriasis, reduced expression of *Pparγ* is observed (Sobolev et al., 2020). Ingenuity pathway analysis (IPA) performed in **Chapter 5** demonstrates *Pparγc1a* downregulation in dermatitis. This specific transcriptional coactivator interacts with *Pparγ* and possibly regulating and coactivating proteins involved in differentiation such as involucrin (*Ivl*) and *Sprr1b*. Stimulation of key markers of keratinocyte differentiation such as loricrin (*Lor*) and *Ivl* results in the improvement of epidermal barrier function (Westergaard et al., 2001; Mao-Qiang et al., 2004). Moreover, *ex vivo* studies has demonstrated high levels of *Pparγ* expression during keratinocyte differentiation (Adachi et al., 2013).

Subsequent activation of *Pparγc1a* by 12*R*-LOX lipids may possibly stimulate the expression of important keratinocyte differentiation markers and therefore contribute to epidermal barrier homeostasis. Examples of molecules known to activate PPAR with similar structural features to fatty acid derived molecules include eicosanoids, endocannabinoids and oxidised fatty acids (Hostetler et al., 2005; Itoh et al., 2008). 15-deoxy-delta 12, 14-prostaglandin J2 derived from the metabolism of polyunsaturated fatty acids show high binding

affinity and preference for specific PPAR subtypes as demonstrated in previous studies (Forman et al., 1995; Muga et al., 2000).

8.3 9R,10R,13R-TriHOME terminal product of 12*R*-LOX / eLOX-3 pathway stimulates the activation of *Pparγc1a* and increases the relative protein level of keratinocyte differentiation markers but has no effect on proliferation, migration or apoptosis

As Pparγc1a is hypothesised to play a role in keratinocyte differentiation and because of its downregulation following 12*R*-LOX deficiency, an experiment was performed to determine whether the 9R,10R,13R-TriHOME terminal product of the 12*R*-LOX / eLOX-3 pathway activates this specific PPAR subtype. Activation of *Pparγc1a* was demonstrated following exposure to the 9R,10R,13R-TriHOME. As discussed, a body of *in vitro* and *in vivo* evidence demonstrate PPARs function in promoting skin homeostasis through stimulating the expression of differentiation markers. Moreover, activation and expression of *PPARγc1a* is consistent with an increase in expression of differentiation markers (Adachi et al., 2013). Genetic deletion studies involving PPAR deficient mice have also shown weak expression of key keratinocyte differentiation markers, further establishing the link between PPAR expression and epidermal differentiation (Hanley et al., 1998; Schmuth et al., 2004).

In parallel with the localisation of 12*R*-LOX expression, PPARγ and PPARγc1a are strongly expressed during keratinocyte differentiation in humans (Mao-Qiang et al., 2004). Lipid species such as ceramides are found in the granular layer of the epidermis and therefore the enzymatic processing of lipids by 12*R*-LOX and eLOX-3 to produce 9R,10R,13R-TriHOME may activate PPAR, thereby promoting the expression of epidermal differentiation markers such as *Ivl* and *Krt10*. This is possibly one of numerous processes that occur during epidermal differentiation. In **Chapter 7**, following treatment of A549 cells with 9R,10R,13R-TriHOME, an increase in the relative protein level of *Ivl* and *Krt10* is observed. In combination with the activation of *Pparγc1a*, this suggests that the 9R,10R,13R-TriHOME may stimulate the expression of keratinocyte differentiation markers through a PPAR mediated pathway. Furthermore, an increase in the relative protein level of *Ivl* and *Krt10* is accompanied by an increase in the number of cornified envelope formation observed in **Chapter 6**, further implicating the 9R,10R,13R-TriHOME terminal product in the process of terminal keratinocytedifferentiation.

Activation of *Pparγc1a* by 9R,10R,13R-TriHOME may subsequently regulate the expression of cornified envelope proteins and therefore contribute to a rigid and mechanically robust epidermal barrier. For example, the overexpression of cornified envelope proteins such

as *Rptn*, *Sprr1b*, *Sprr2d*, *Sprr2h Krt1*, *Krt6b*, *Krt10*, *Krt16* and *Krtdap* following 12*R*-LOX deficiency may be the consequence of a compromised epidermal barrier which is observed in 12*R*-LOX deficient skin. As such, their upregulation may be part of a compensatory mechanism to restore barrier integrity and prevent excessive water and essential ion loss. A consequence of the overexpression of structural proteins such as *Rptn*, *Sprr1b*, *Sprr2h* and *Sprr2d* may be leading to a thickening of the epidermis, normally characterised with skin barrier disorders such as ichthyosis. Previous studies in lesional atopic dermatitis skin models have demonstrated that the activation of PPARα significantly reduces epidermal thickness due to a suppressing effect on keratinocyte proliferation (Demerjian et al., 2009). Further investigation would be required to determine whether a similar effect is observed following 9R,10R,13R-TriHOME activation of *Pparγc1a*. hTERT cells treated with the terminal product of the 12*R*-LOX / eLOX-3 pathway, 9R,10R,13R-TriHOME did not have a significant effect on cell proliferation, migration nor apoptosis as shown by experiments performed in **Chapter 6**.

8.4 Conclusion

RNA-sequencing analysis of 12*R*-LOX deficient mouse skin shown in **Chapter 4** and **5** provided an invaluable insight into biological pathways and processes by which 12*R*-LOX may regulate skin physiology. Moreover, analysis of the 12*R*-LOX transcriptome identified a number of genes of interest and opened avenues for further investigation into the effects of 12*R*-LOX lipids. Initial analysis of the 12*R*-LOX deficient vs wildtype dataset confirmed that the majority of DEGs were localised in upper layers of the epidermis. Gene Ontology analysis aimed to identify biological processes, molecular functions and cellular compartments that are affected in the 12*R*-LOX deficient mouse model. Utilising this approach identified enriched terms such as keratinization, cornification and peptide cross-linking. These processes are all associated with terminal keratinocyte differentiation and more interestingly, the keratinocyte differentiation is a process enriched for the differentially expressed genes (DEGs) of the 12*R*-LOX deficient model.

An examination of DEGs associated with these processes included many belonging to the epidermal differentiation complex (EDC), suggesting 12*R*-LOX lipids possible role involvement in this epidermal process. Abnormal expression of proteins belonging to the EDC have previously been implicated in a range of skin disorders such as atopic dermatitis and psoriasis (Hoffjan et al., 2007). Moreover, deficiency of the 12*R*-LOX protein impacted cellular components associated with keratinocyte differentiation such as cornified envelope and keratin filaments. A downregulated gene of interest, hypothesised to regulate the expression of

important proteins involved in keratinocyte differentiation includes the *Pparγc1a*. A reduced expression of *Pparγc1a* has also been observed in other skin disorders, where aberrant keratinocyte differentiation is demonstrated (Ramot et al., 2015; Sobolev et al., 2020). Furthermore, *Pparγc1a* has been demonstrated to mediate the differentiation of adipocytes, suggesting its involvement in differentiation of other cell types.

Following the observed downregulation of *Pparγc1a* in the 12*R*-LOX deficient vs wildtype dataset, a transfection and reporter gene assay experiment demonstrated that the 9R,10R,13R-TriHOME terminal product of 12*R*-LOX / eLOX-3 pathway activates *Pparγc1a*. Previous studies have shown that the activation and expression of PPARs have been demonstrated to improve epidermal barrier homeostasis through promoting expression of key differentiation proteins (Mao-Qiang et al., 2014; Yan et al., 2015). An increase in epidermal differentiation markers such as *Ivl* and *Krt10* is also observed following exposure to 9R,10R,13R-TriHOME, indicating its stimulating effect on key differentiation markers. To support this, an increase in the number of cornified envelope formation is observed as a result of exposure to 9R,10R,13R-TriHOME for 48 hours. Evidence of a role for 9R,10R,13R-TriHOME in potentially regulating keratinocyte proliferation, migration and apoptosis is limited, with no significant effect on these processes shown in **Chapter 6**. Taken together, the 9R,10R,13R-TriHOME evidential effect on keratinocyte differentiation may be mediated through activation of *Pparγc1a*. Both bioinformatics data and biochemical data suggests a possible role for 12*R*-LOX lipids in regulating the keratinocyte differentiation process which is essential for epidermal barrier integrity. These observations raise the possibility of utilising the 9R,10R,13R-TriHOME as treatment for skin disorders with an impaired epidermal barrier function.

8.5 Study limitations and future studies

Global screening of the 12*R*-LOX deficient mouse skin transcriptome generated a significant amount of interesting observations which could be investigated further by utilising other bioinformatics platforms available. Whilst identification of several genes of interest have been discovered in the transcriptomic analysis, additional work to develop a complete mechanism by which 12*R*-LOX regulates skin homeostasis would be of most benefit. To date, investigative analysis of differentially expressed genes identified the overexpression of several EDC genes such as members of the SPRR family, as well as the upregulation of specific keratin proteins. Previous studies have demonstrated increased SPRR1 and SPRR2 expression in inflammatory skin disorders (De Heller-Milev et al., 2000). Moreover, the upregulation of *Krt6*b and *Krt16*

observed following 12*R*-LOX protein deficiency are also considered as hallmarks of psoriasis (Zhang et al., 2019). Determining the effect of 9R,10R,13R-TriHOME on the aforementioned overexpressed proteins such as *Sprr1b*, *Sprr2d*, *Sprr2h*, *Rptn* and *Krtdap* using PCR and western blotting would demonstrate whether 12*R*-LOX regulates the expression of these proteins known to be implicated in various skin disorders. Only the 9R,10R,13R-TriHOME was used to determine the effect on various epidermal processes. Additional LOX derived lipids such as 9-HODE and 13-HODE are also produced during the enzymatic conversion of the linoleate substrate and their effect on specific proteins shown to be differentially expressed following 12*R*-LOX deficiency would be of most interest.

Whilst the 9R,10R,13R-TriHOME is shown to activate *Pparγc1a*, experiments to determine the effect of other 12*R*-LOX derived lipids on PPAR activation would provide more evidence of an activating effect of 12*R*-LOX metabolites and products on the PPAR transcriptional factor. As PPARs are hypothesised to promote keratinocyte differentiation, the effect of additional lipids such as HODEs on terminal differentiation markers would further demonstrate LOXs role in stimulating an essential epidermal process.

The 12*R*-LOX protein deficient vs wildtype RNA-sequencing data has also not been fully validated using analytical methods such as PCR and western blotting and is therefore a limitation in this study. As the RNA-sequencing dataset is derived from 12*R*-LOX deficient mouse models, the transcriptome may not be fully representative of what would be observed in human epidermal 12*R*-LOX deficiency and is therefore a study limitation. A global screening approach of human 12*R*-LOX deficient skin would represent a more accurate transcriptome model of ichthyosis and would be of more clinical relevance. This could be achieved through utilising microneedles containing siRNA for delivery into an *ex vivo* human skin explant model to silence the 12*R*-LOX protein. Changes in gene expression and how these are mediated can then be determined as performed in earlier chapters of this thesis. Downregulation of 12*R*-LOX in human skin may result in the identification of additional differentially expressed genes related to the EDC or other epidermal proteins. Following successful silencing of 12*R*-LOX, specific lipid species would then be reintroduced to further identify networks by which the 12*R*-LOX regulates skin physiology. In conjunction with this, time course experiments of 12*R*-LOX derived lipid upregulation or downregulation of genes could be performed. This experiment would subsequently identify the most effective lipid in positively regulating important proteins required for skin homeostasis which could have comprehensive clinical benefit.

References

Abdo, J., Sopko, N. and Milner, S., (2020). "The applied anatomy of human skin: A model for regeneration." *Wound Medicine*, **28**, p.100179.

Adabi, S., Hosseinzadeh, M., Noei, S., Conforto, S., Daveluy, S., Clayton, A., Mehregan, D. and Nasiriavanaki, M., (2017). "Universal in vivo Textural Model for Human Skin based on Optical Coherence Tomograms." *Scientific Reports*, **7**(1).

Adachi, Y., Hatano, Y., Sakai, T. and Fujiwara, S., (2013). "Expressions of peroxisome proliferator-activated receptors (PPARs) are directly influenced by permeability barrier abrogation and inflammatory cytokines and depressed PPARα modulates expressions of chemokines and epidermal differentiation-related molecule." *Experimental Dermatology*, **22**(9), pp.606-608.

Ahmadian, M., Suh, J., Hah, N., Liddle, C., Atkins, A., Downes, M. and Evans, R., (2013). "PPARγ signaling and metabolism: the good, the bad and the future." *Nature Medicine*, **19**(5), pp.557-566.

Akagi A, Kitoh A, Moniaga CS, Fujimoto A, Fujikawa H, Shimomura Y, et al. Case of Netherton syndrome with an elevated serum thymus and activation-regulated chemokine level. *J Dermatol* 2013; 40:752–3.

Akiyama, M., Sawamura, D. and Shimizu, H., (2003). "The clinical spectrum of nonbullous congenital ichthyosiform erythroderma and lamellar ichthyosis." *Clinical and Experimental Dermatology*, **28**(3), pp.235-240.

Akiyama, T., Meinke, P. and Berger, J., (2005). "PPAR ligands: Potential therapies for metabolic syndrome." *Current Diabetes Reports*, **5**(1), pp.45-52.

Akiyama, M., (2017). "Corneocyte lipid envelope (CLE), the key structure for skin barrier function and ichthyosis pathogenesis." *Journal of Dermatological Science*, **88**(1), pp.3-9.

Alameda, J., Fernández-Aceñero, M., Moreno-Maldonado, R., Navarro, M., Quintana, R., Page, A., Ramírez, A., Bravo, A. and Casanova, M., (2011). "CYLD regulates keratinocyte differentiation and skin cancer progression in humans." *Cell Death & Disease*, **2**(9), pp. e208-e208.

Al-Naamani, A., Al-Waily, A., Al-Kindi, M., Al-Awadi, M. and Al-Yahyaee, S., (2013). "Transglutaminase-1 Mutations in Omani Families with Lamellar Ichthyosis." *Medical Principles and Practice*, **22**(5), pp.438-443.

Amisten, S., Neville, M., Hawkes, R., Persaud, S., Karpe, F. and Salehi, A., (2015). "An atlas of G-protein coupled receptor expression and function in human subcutaneous adipose tissue." *Pharmacology & Therapeutics*, **146**, pp.61-93.

Ananthapadmanabhan, K., Mukherjee, S. and Chandar, P., (2013). "Stratum corneum fatty acids: their critical role in preserving barrier integrity during cleansing." *International Journal of Cosmetic Science*, **35**(4), pp.337-345.

Anders, S. and Huber, W., (2010). "Differential expression analysis for sequence count data." *Genome Biology*, **11**(10).

Arin, M., Grimberg, G., Schumann, H., De Almeida Jr, H., Chang, Y., Tadini, G., Kohlhase, J., Krieg, T., Bruckner-Tuderman, L. and Has, C., (2010). "Identification of novel and known KRT5 and KRT14 mutations in 53 patients with epidermolysis bullosa simplex: correlation between genotype and phenotype." *British Journal of Dermatology*, **162**(6), pp.1365-1369.

Bang JO, Dyberg J (1985): "Fish oil consumption and mortality from coronary heart disease." *N Engl J Med*, **313**: 822-823.

Barak, Y., Nelson, M., Ong, E., Jones, Y., Ruiz-Lozano, P., Chien, K., Koder, A. and Evans, R., (1999). "PPARγ Is Required for Placental, Cardiac, and Adipose Tissue Development." *Molecular Cell*, **4**(4), pp.585-595.

Barish, G., (2006). "PPAR: a dagger in the heart of the metabolic syndrome." *Journal of Clinical Investigation*, **116**(3), pp.590-597.

Bata-Csorgo, Z., Hammerberg, C., Voorhees, J. and Cooper, K., (1995). "Kinetics and regulation of human keratinocyte stem cell growth in short-term primary ex vivo culture. Cooperative growth factors from psoriatic lesional T lymphocytes stimulate proliferation among psoriatic uninvolved, but not normal, stem keratinocytes." *Journal of Clinical Investigation*, **95**(1), pp.317-327.

Bazzi, H., Fantauzzo, K., Richardson, G., Jahoda, C. and Christiano, A., (2007). "Transcriptional profiling of developing mouse epidermis reveals novel patterns of coordinated gene expression." *Developmental Dynamics*, **236**(4), pp.961-970.

Behne, M., Uchida, Y., Seki, T., de Montellano, P., Elias, P. and Holleran, W., (2000). "Omega-Hydroxyceramides are Required for Corneocyte Lipid Envelope (CLE) Formation and Normal Epidermal Permeability Barrier Function." *Journal of Investigative Dermatology*, **114**(1), pp.185-192.

Belal, S., Sivakumar, A., Kang, D., Cho, S., Choe, H. and Shim, K., (2018). "Modulatory effect of linoleic and oleic acid on cell proliferation and lipid metabolism gene expressions in primary bovine satellite cells." *Animal Cells and Systems*, **22**(5), pp.324-333.

Benhadou, F., Mintoff, D. and del Marmol, V., (2018). "Psoriasis: Keratinocytes or Immune Cells – Which Is the Trigger?." *Dermatology*, **235**(2), pp.91-100.

Berger, J., Akiyama, T. and Meinke, P., (2005). "PPARs: therapeutic targets for metabolic disease." *Trends in Pharmacological Sciences*, **26**(5), pp.244-251.

Bility, M., Thompson, J., McKee, R., David, R., Butala, J., Vanden Heuvel, J. and Peters, J., (2004). "Activation of Mouse and Human Peroxisome Proliferator-Activated Receptors (PPARs) by Phthalate Monoesters." *Toxicological Sciences*, **82**(1), pp.170-182.

Bligh, E. and Dyer, W., (1959). "A Rapid Method of Total Lipid Extraction and Purification." *Canadian Journal of Biochemistry and Physiology*, **37**(1), pp.911-917.

Boeglin, W., Kim, R. and Brash, A., 1998. A 12R-lipoxygenase in human skin: Mechanistic evidence, molecular cloning, and expression. *Proceedings of the National Academy of Sciences*, 95(12), pp.6744-6749.

Boer, M., Duchnik, E., Maleszka, R. and Marchlewicz, M., (2016). "Structural and biophysical characteristics of human skin in maintaining proper epidermal barrier function." *Advances in Dermatology and Allergology*, **1**, pp.1-5.

Bongartz, T., Coras, B., Vogt, T., Schölmerich, J. and Müller-Ladner, U., (2005). "Treatment of active psoriatic arthritis with the PPAR ligand pioglitazone: an open-label pilot study." *Rheumatology*, **44**(1), pp.126-129.

Borland, M., Foreman, J., Girroir, E., Zolfaghari, R., Sharma, A., Amin, S., Gonzalez, F., Ross, A. and Peters, J., (2008). "Ligand Activation of Peroxisome Proliferator-Activated Receptor-β/δ Inhibits Cell Proliferation in Human HaCaT Keratinocytes." *Molecular Pharmacology*, **74**(5), pp.1429-1442.

Borowiec, A., Delcourt, P., Dewailly, E. and Bidaux, G., (2013). "Optimal Differentiation of In Vitro Keratinocytes Requires Multifactorial External Control." *PLoS ONE*, **8**(10), p. e77507.

Boukamp, P., Petrussevska, R., Breitkreutz, D., Hornung, J., Markham, A. and Fusenig, N., (1988). "Normal keratinization in a spontaneously immortalized aneuploid human keratinocyte cell line." *The Journal of Cell Biology*, **106**(3), pp.761-771.

Bouwens, M., Afman, L. and Müller, M., (2007). "Fasting induces changes in peripheral blood mononuclear cell gene expression profiles related to increases in fatty acid β-oxidation: functional role of peroxisome proliferator–activated receptor α in human peripheral blood mononuclear cells." *The American Journal of Clinical Nutrition*, **86**(5), pp.1515-1523.

Bowen, A., Hanks, A., Murphy, K., Florell, S. and Grossman, D., (2004). "Proliferation, Apoptosis, and Survivin Expression in Keratinocytic Neoplasms and Hyperplasias." *The American Journal of Dermatopathology*, **26**(3), pp.177-181.

Bouwstra, J., Gooris, G., van der Spek, J. and Bras, W., (1991). "Structural Investigations of Human Stratum Corneum by Small-Angle X-Ray Scattering." *Journal of Investigative Dermatology*, **97**(6), pp.1005-1012.

Bouwstra, J., Gooris, G., Dubbelaar, F., Weerheim, A., IJzerman, A. and Ponec, M., (1998). "Role of ceramide 1 in the molecular organization of the stratum corneum lipids." *Journal of Lipid Research*, **39**(1), pp.186-196.

Bouwstra, J., Dubbelaar, F., Gooris, G. and Ponec, M., (2000). "The Lipid Organisation in the Skin Barrier." *Acta Dermato-Venereologica*, **80**(0), pp.23-30.

Bracke, S., Carretero, M., Guerrero-Aspizua, S., Desmet, E., Illera, N., Navarro, M., Lambert, J. and Del Rio, M., (2014). "Targeted silencing of DEFB4 in a bioengineered skin-humanized mouse model for psoriasis: development of siRNA SECosome-based novel therapies." *Experimental Dermatology*, **23**(3), pp.199-201.

Bragulla, H. and Homberger, D., (2009). "Structure and functions of keratin proteins in simple, stratified, keratinized and cornified epithelia." *Journal of Anatomy*, **214**(4), pp.516-559.

Brash, A., (1999). "Lipoxygenases: Occurrence, Functions, Catalysis, and Acquisition of Substrate." *Journal of Biological Chemistry*, **274**(34), pp.23679-23682.

Brenner, M. and Hearing, V., (2007). “The Protective Role of Melanin Against UV Damage in Human Skin.” *Photochemistry and Photobiology*, **84**(3), pp.539-549.

Bruewer, M., Luegering, A., Kucharzik, T., Parkos, C., Madara, J., Hopkins, A. and Nusrat, A., (2003). “Proinflammatory Cytokines Disrupt Epithelial Barrier Function by Apoptosis-Independent Mechanisms.” *The Journal of Immunology*, **171**(11), pp.6164-6172.

Bryniarski, K., Biedron, R., Jakubowski, A., Chlopicki, S. and Marcinkiewicz, J., (2008). “Anti-inflammatory effect of 1-methylnicotinamide in contact hypersensitivity to oxazolone in mice; involvement of prostacyclin.” *European Journal of Pharmacology*, **578**(2-3), pp.332-338.

Burek, C., Roth, J., Koch, H., Harzer, K., Los, M. and Schulze-Osthoff, K., (2001). “The role of ceramide in receptor- and stress-induced apoptosis studied in acidic ceramidase-deficient Farber disease cells.” *Oncogene*, **20**(45), pp.6493-6502.

Burr, G. and Burr, M., (1930). “ON THE NATURE AND RÔLE OF THE FATTY ACIDS ESSENTIAL IN NUTRITION.” *Journal of Biological Chemistry*, **86**(2), pp.587-621.

Calvano, S., Xiao, W., Richards, D., Felciano, R., Baker, H., Cho, R., Chen, R., Brownstein, B., Cobb, J., Tschoeke, S., Miller-Graziano, C., Moldawer, L., Mindrinos, M., Davis, R., Tompkins, R. and Lowry, S., (2005). “A network-based analysis of systemic inflammation in humans.” *Nature*, **437**(7061), pp.1032-1037.

Caputo, R. and Peluchetti, D., (1977). “The junctions of normal human epidermis.” *Journal of Ultrastructure Research*, **61**(1), pp.44-61.

Cerqueira, N., Oliveira, E., Gesto, D., Santos-Martins, D., Moreira, C., Moorthy, H., Ramos, M. and Fernandes, P., (2016). “Cholesterol Biosynthesis: A Mechanistic Overview.” *Biochemistry*, **55**(39), pp.5483-5506.

Chambers, E. and Vukmanovic-Stejic, M., (2019). “Skin barrier immunity and ageing.” *Immunology*, **160**(2), pp.116-125.

Chapkin, R. and Ziboh, V., (1984). “Inability of skin enzyme preparations to biosynthesize arachidonic acid from linoleic acid.” *Biochemical and Biophysical Research Communications*, **124**(3), pp.784-792.

Chapkin, R., Ziboh, V., Marcelo, C. and Voorhees, J., (1986). “Metabolism of essential fatty acids by human epidermal enzyme preparations: evidence of chain elongation.” *Journal of Lipid Research*, **27**(9), pp.945-954.

Cheng, J., Sedgewick, A., Finnegan, A., Harirchian, P., Lee, J., Kwon, S., Fassett, M., Golovato, J., Gray, M., Ghadially, R., Liao, W., Perez White, B., Mauro, T., Mully, T., Kim, E., Sbitany, H., Neuhaus, I., Grekin, R., Yu, S., Gray, J., Purdom, E., Paus, R., Vaske, C., Benz, S., Song, J. and Cho, R., (2018). “Transcriptional Programming of Normal and Inflamed Human Epidermis at Single-Cell Resolution.” *Cell Reports*, **25**(4), pp.871-883.

Chieosilapatham, P., Kiatsurayanon, C., Umehara, Y., Trujillo-Paez, J., Peng, G., Yue, H., Nguyen, L. and Niyonsaba, F., (2021). “Keratinocytes: innate immune cells in atopic dermatitis.” *Clinical and Experimental Immunology*, **204**(3), pp.296-309.

Choi, M. and Maibach, H., (2005). "Role of Ceramides in Barrier Function of Healthy and Diseased Skin." *American Journal of Clinical Dermatology*, **6**(4), pp.215-223.

Coderch, L., López, O., de la Maza, A. and Parra, J., (2003). "Ceramides and Skin Function." *American Journal of Clinical Dermatology*, **4**(2), pp.107-129.

Collin, C., Ouhayoun, J., Grund, C. and Franke, W., (1992). "Suprabasal marker proteins distinguishing keratinizing squamous epithelia: Cytokeratin 2 polypeptides of oral masticatory epithelium and epidermis are different." *Differentiation*, **51**(2), pp.137-148.

Colombe, L., Vindrios, A., Michelet, J. and Bernard, B., (2007). "Prostaglandin metabolism in human hair follicle." *Experimental Dermatology*, **16**(9), pp.762-769.

Colombo, I., Sangiovanni, E., Maggio, R., Mattozzi, C., Zava, S., Corbett, Y., Fumagalli, M., Carlino, C., Corsetto, P., Scaccabarozzi, D., Calvieri, S., Gismondi, A., Taramelli, D. and Dell'Agli, M., (2017). "HaCaT Cells as a Reliable In Vitro Differentiation Model to Dissect the Inflammatory/Repair Response of Human Keratinocytes." *Mediators of Inflammation*, **2017**, pp.1-12.

Craiglow, B., (2013). "Ichthyosis in the newborn." *Seminars in Perinatology*, **37**(1), pp.26-31.

Cruz, P., Mo, H., McConathy, W., Sabnis, N. and Lacko, A., (2013). "The role of cholesterol metabolism and cholesterol transport in carcinogenesis: a review of scientific findings, relevant to future cancer therapeutics." *Frontiers in Pharmacology*, **4**.

Cury-Boaventura, M., Gorjão, R., de Lima, T., Newsholme, P. and Curi, R., (2006). "Comparative toxicity of oleic and linoleic acid on human lymphocytes." *Life Sciences*, **78**(13), pp.1448-1456.

Dalman, M., Deeter, A., Nimishakavi, G. and Duan, Z., (2012). "Fold change and p-value cutoffs significantly alter microarray interpretations." *BMC Bioinformatics*, **13**(S2).

Darragh, J., Hunter, M., Pohler, E., Nelson, L., Dillon, J., Nenutil, R., Vojtesek, B., Ross, P., Kernohan, N. and Hupp, T., (2006). "The calcium-binding domain of the stress protein SEP53 is required for survival in response to deoxycholic acid-mediated injury." *FEBS Journal*, **273**(9), pp.1930-1947.

Deeg, M. and Tan, M., (2008). "Pioglitazone versus Rosiglitazone: Effects on Lipids, Lipoproteins, and Apolipoproteins in Head-to-Head Randomized Clinical Studies." *PPAR Research*, **2008**, pp.1-6.

Demerjian, M., Choi, E., Man, M., Chang, S., Elias, P. and Feingold, K., (2009). "Activators of PPARs and LXR decrease the adverse effects of exogenous glucocorticoids on the epidermis." *Experimental Dermatology*, **18**(7), pp.643-649.

Dennis, E., Cao, J., Hsu, Y., Magrioti, V. and Kokotos, G., (2011). "Phospholipase A2 Enzymes: Physical Structure, Biological Function, Disease Implication, Chemical Inhibition, and Therapeutic Intervention." *Chemical Reviews*, **111**(10), pp.6130-6185.

Desjardins, P. and Conklin, D., (2010). "NanoDrop Microvolume Quantitation of Nucleic Acids." *Journal of Visualized Experiments*, (-1).

Deyrieux, A. and Wilson, V., (2007). “In vitro culture conditions to study keratinocyte differentiation using the HaCaT cell line.” *Cytotechnology*, **54**(2), pp.77-83.

de Guzman Strong, C., Wertz, P., Wang, C., Yang, F., Meltzer, P., Andl, T., Millar, S., Ho, I., Pai, S. and Segre, J., (2006). “Lipid defect underlies selective skin barrier impairment of an epidermal-specific deletion of Gata-3.” *Journal of Cell Biology*, **175**(4), pp.661-670.

De Heller-Milev, M., Huber, M., Panizzon, R. and Hohl, D., (2000). “Expression of small proline rich proteins in neoplastic and inflammatory skin diseases.” *British Journal of Dermatology*, **143**(4), pp.733-740.

de Jager, M., Groenink, W., van der Spek, J., Janmaat, C., Gooris, G., Ponec, M. and Bouwstra, J., (2006). “Preparation and characterization of a stratum corneum substitute for in vitro percutaneous penetration studies.” *Biochimica et Biophysica Acta (BBA) - Biomembranes*, **1758**(5), pp.636-644.

de Juanes, S., Epp, N., Latzko, S., Neumann, M., Fürstenberger, G., Hausser, I., Stark, H. and Krieg, P., (2009). “Development of an Ichthyosiform Phenotype in Alox12b-Deficient Mouse Skin Transplants.” *Journal of Investigative Dermatology*, **129**(6), pp.1429-1436.

Dickson, M., Hahn, W., Ino, Y., Ronfard, V., Wu, J., Weinberg, R., Louis, D., Li, F. and Rheinwald, J., (2000). “Human Keratinocytes That Express hTERT and Also Bypass a p16 INK4a -Enforced Mechanism That Limits Life Span Become Immortal Yet Retain Normal Growth and Differentiation Characteristics.” *Molecular and Cellular Biology*, **20**(4), pp.1436-1447.

DiGiovanna, J. and Robinson-Bostom, L., (2003). “Ichthyosis.” *American Journal of Clinical Dermatology*, **4**(2), pp.81-95.

Di Nardo, A., Wertz, P., Giannetti, A. and Seidenari, S., (1998). “Ceramide and cholesterol composition of the skin of patients with atopic dermatitis.” *Acta Dermato-Venereologica*, **78**(1), pp.27-30.

Djian, P., Easley, K. and Green, H., (2000). “Targeted Ablation of the Murine Involucrin Gene.” *Journal of Cell Biology*, **151**(2), pp.381-388.

Donato, R., R. Cannon, B., Sorci, G., Riuzzi, F., Hsu, K., J. Weber, D. and L. Geczy, C., (2012). “Functions of S100 Proteins.” *Current Molecular Medicine*, **13**(1), pp.24-57.

Dorris, S. and Peebles, R., (2012). “PGI2 as a Regulator of Inflammatory Diseases.” *Mediators of Inflammation*, **2012**, p.9 pages.

Driskell, R., Jahoda, C., Chuong, C., Watt, F. and Horsley, V., (2014). “Defining dermal adipose tissue.” *Experimental Dermatology*, **23**(9), pp.629-631.

Dubrac, S., Stoitzner, P., Pirkebner, D., Elentner, A., Schoonjans, K., Auwerx, J., Saeland, S., Hengster, P., Fritsch, P., Romani, N. and Schmuth, M., (2007). “Peroxisome Proliferator-Activated Receptor-α Activation Inhibits Langerhans Cell Function.” *The Journal of Immunology*, **178**(7), pp.4362-4372.

Dumasia, R., Eagle, K., Kline-Rogers, E., May, N., Cho, L. and Mukherjee, D., (2005). “Role of PPAR-Gamma; Agonist Thiazolidinediones in Treatment of Pre-Diabetic and Diabetic

Individuals: A Cardiovascular Perspective." *Current Drug Target -Cardiovascular & Hematological Disorders*, 5(5), pp.377-386.

Eckert, R., Efimova, T., Dashti, S., Balasubramanian, S., Deucher, A., Crish, J., Sturniolo, M. and Bone, F., (2002). "Keratinocyte Survival, Differentiation, and Death: Many Roads Lead to Mitogen-Activated Protein Kinase." *Journal of Investigative Dermatology Symposium Proceedings*, **7**(1), pp.36-40.

Eckert, R., Broome, A., Ruse, M., Robinson, N., Ryan, D. and Lee, K., (2004). "S100 Proteins in the Epidermis." *Journal of Investigative Dermatology*, **123**(1), pp.23-33.

Eckert, R., Sturniolo, M., Broome, A., Ruse, M. and Rorke, E., (2005). "Transglutaminase Function in Epidermis." *Journal of Investigative Dermatology*, **124**(3), pp.481-492.

Eckhart, L., Declercq, W., Ban, J., Rendl, M., Lengauer, B., Mayer, C., Lippens, S., Vandenabeele, P. and Tschachler, E., (2000). "Terminal Differentiation of Human Keratinocytes and Stratum Corneum Formation is Associated with Caspase-14 Activation." *Journal of Investigative Dermatology*, **115**(6), pp.1148-1151.

Eckl, K., Krieg, P., Küster, W., Traupe, H., André, F., Wittstruck, N., Fürstenberger, G. and Hennies, H., (2005). "Mutation spectrum and functional analysis of epidermis-type lipoxygenases in patients with autosomal recessive congenital ichthyosis." *Human Mutation*, **26**(4), pp.351-361.

Eckl, K., de Juanes, S., Kurtenbach, J., Nätebus, M., Lugassy, J., Oji, V., Traupe, H., Preil, M., Martínez, F., Smolle, J., Harel, A., Krieg, P., Sprecher, E. and Hennies, H., (2009). "Molecular Analysis of 250 Patients with Autosomal Recessive Congenital Ichthyosis: Evidence for Mutation Hotspots in ALOXE3 and Allelic Heterogeneity in ALOX12B." *Journal of Investigative Dermatology*, **129**(6), pp.1421-1428.

Elango, T., Sun, J., Zhu, C., Zhou, F., Zhang, Y., Sun, L., Yang, S. and Zhang, X., (2018). "Mutational analysis of epidermal and hyperproliferative type I keratins in mild and moderate psoriasis vulgaris patients: a possible role in the pathogenesis of psoriasis along with disease severity." *Human Genomics*, **12**(1).

Elder, J., Bruce, A., Gudjonsson, J., Johnston, A., Stuart, P., Tejasvi, T., Voorhees, J., Abecasis, G. and Nair, R., (2010). "Molecular Dissection of Psoriasis: Integrating Genetics and Biology." *Journal of Investigative Dermatology*, **130**(5), pp.1213-1226.

Elias, P. and Friend, D., (1975). "The permeability barrier in mammalian epidermis." *Journal of Cell Biology*, **65**(1), pp.180-191.

Elias, P., (2005). "Stratum Corneum Defensive Functions: An Integrated View." *Journal of Investigative Dermatology*, **125**(2), pp.183-200.

Elias, P., Williams, M. and Feingold, K., (2012). "Abnormal barrier function in the pathogenesis of ichthyosis: Therapeutic implications for lipid metabolic disorders." *Clinics in Dermatology*, **30**(3), pp.311-322.

Elias, P., Gruber, R., Crumrine, D., Menon, G., Williams, M., Wakefield, J., Holleran, W. and Uchida, Y., (2014). "Formation and functions of the corneocyte lipid envelope

(CLE).” *Biochimica et Biophysica Acta (BBA) - Molecular and Cell Biology of Lipids*, **1841**(3), pp.314-318.

Elias, P. and Wakefield, J., (2014). “Mechanisms of abnormal lamellar body secretion and the dysfunctional skin barrier in patients with atopic dermatitis.” *Journal of Allergy and Clinical Immunology*, **134**(4), pp.781-791.e1.

Elias, P., Williams, M., Choi, E. and Feingold, K., (2014). “Role of cholesterol sulfate in epidermal structure and function: Lessons from X-linked ichthyosis.” *Biochimica et Biophysica Acta (BBA) - Molecular and Cell Biology of Lipids*, **1841**(3), pp.353-361.

Eller, M., Yaar, M., Ostrom, K., Harkness, D. and Gilchrest, B., (1995). “A role for interleukin-1 in epidermal differentiation: regulation by expression of functional versus decoy receptors.” *Journal of Cell Science*, **108**(8), pp.2741-2746.

Ellis, C., Varani, J., Fisher, G., Zeigler, M., Pershadsingh, H., Benson, S., Chi, Y. and Kurtz, T., (2000). “Troglitazone Improves Psoriasis and Normalizes Models of Proliferative Skin Disease.” *Archives of Dermatology*, **136**(5).

Epp, N., Fürstenberger, G., Müller, K., de Juanes, S., Leitges, M., Hausser, I., Thieme, F., Liebisch, G., Schmitz, G. and Krieg, P., (2007). “12R-lipoxygenase deficiency disrupts epidermal barrier function.” *Journal of Cell Biology*, **177**(1), pp.173-182.

Fairley, J., (1991). “Calcium metabolism and the pathogenesis of dermatological disease.” *Seminars in Dermatology*, **10**(3):225-31.

Fehrenschild, D., Galli, U., Breiden, B., Bloch, W., Schettina, P., Brodesser, S., Michels, C., Günschmann, C., Sandhoff, K., Niessen, C. and Niemann, C., (2012). “TCF/Lef1-Mediated Control of Lipid Metabolism Regulates Skin Barrier Function.” *Journal of Investigative Dermatology*, **132**(2), pp.337-345.

Feige, J., Gelman, L., Tudor, C., Engelborghs, Y., Wahli, W. and Desvergne, B., (2005). “Fluorescence Imaging Reveals the Nuclear Behavior of Peroxisome Proliferator-activated Receptor/Retinoid X Receptor Heterodimers in the Absence and Presence of Ligand*♦.” *Journal of Biological Chemistry*, **280**(18), pp.17880-17890.

Feingold, K., (2007). “Thematic review series: Skin Lipids. The role of epidermal lipids in cutaneous permeability barrier homeostasis.” *Journal of Lipid Research*, **48**(12), pp.2531-2546.

Feingold, K., Schmuth, M. and Elias, P., (2007). “The Regulation of Permeability Barrier Homeostasis.” *Journal of Investigative Dermatology*, **127**(7), pp.1574-1576.

Feingold, K., (2009). “The outer frontier: the importance of lipid metabolism in the skin.” *Journal of Lipid Research*, **50**, pp. S417-S422.

Feingold, K. and Jiang, Y., (2011). “The mechanisms by which lipids coordinately regulate the formation of the protein and lipid domains of the stratum corneum.” *Dermato-Endocrinology*, **3**(2), pp.113-118.

Feingold, K. and Denda, M., (2012). “Regulation of permeability barrier homeostasis.” *Clinics in Dermatology*, **30**(3), pp.263-268.

Ferre, P., (2004). “The Biology of Peroxisome Proliferator-Activated Receptors: Relationship with Lipid Metabolism and Insulin Sensitivity.” *Diabetes*, **53**(Supplement 1), pp. S43-S50.

Finstad, H., Drevon, C., Kulseth, M., Synstad, A., Knudsen, E. and Kolset, S., (1998). “Cell proliferation, apoptosis and accumulation of lipid droplets in U937-1 cells incubated with eicosapentaenoic acid.” *Biochemical Journal*, **336**(2), pp.451-459.

Fischer, J., (2009). “Autosomal Recessive Congenital Ichthyosis.” *Journal of Investigative Dermatology*, **129**(6), pp.1319-1321.

Fleckman, P., Hager, B. and Dale, B., (1997). “Harlequin Ichthyosis Keratinocytes in Lifted Culture Differentiate Poorly by Morphologic and Biochemical Criteria.” *Journal of Investigative Dermatology*, **109**(1), pp.36-38.

Fluhr, J., Kao, J., Ahn, S., Feingold, K., Elias, P. and Jain, M., (2001). “Generation of Free Fatty Acids from Phospholipids Regulates Stratum Corneum Acidification and Integrity.” *Journal of Investigative Dermatology*, **117**(1), pp.44-51.

Fogh, K., Herlin, T. and Kragballe, K., (1989). “Eicosanoids in skin of patients with atopic dermatitis: Prostaglandin E and leukotriene B are present in biologically active concentrations.” *Journal of Allergy and Clinical Immunology*, **83**(2), pp.450-455.

Fontao, L., Laffitte, E., Briot, A., Kaya, G., Roux-Lombard, P., Fraitag, S., Hovnanian, A. and Saurat, J., (2011). “Infliximab Infusions for Netherton Syndrome: Sustained Clinical Improvement Correlates with a Reduction of Thymic Stromal Lymphopoietin Levels in the Skin.” *Journal of Investigative Dermatology*, **131**(9), pp.1947-1950.

Forman, B., Tontonoz, P., Chen, J., Brun, R., Spiegelman, B. and Evans, R., (1995). “15-Deoxy-Δ12,14-Prostaglandin J2 is a ligand for the adipocyte determination factor PPARγ.” *Cell*, **83**(5), pp.803-812.

Forman, B., Chen, J. and Evans, R., (1997). “Hypolipidemic drugs, polyunsaturated fatty acids, and eicosanoids are ligands for peroxisome proliferator-activated receptors α and δ.” *Proceedings of the National Academy of Sciences*, **94**(9), pp.4312-4317.

Fuchs, E. and Green, H., (1980). “Changes in keratin gene expression during terminal differentiation of the keratinocyte.” *Cell*, **19**(4), pp.1033-1042.

Fuchs, E., (1990). “Epidermal differentiation: the bare essentials.” *Journal of Cell Biology*, **111**(6), pp.2807-2814.

Furuse, M., Hata, M., Furuse, K., Yoshida, Y., Haratake, A., Sugitani, Y., Noda, T., Kubo, A. and Tsukita, S., (2002). “Claudin-based tight junctions are crucial for the mammalian epidermal barrier.” *Journal of Cell Biology*, **156**(6), pp.1099-1111.

Gagna, C., Chan, N., Farnsworth, P., Kuo, H., Kanthala, T., Patel, A., Patel, N., Law, A., Patel, P., Richards, S., Yam, T., Nici, A. and Lambert, W., (2009). “Localization and quantification of intact, undamaged right-handed double-stranded B-DNA, and denatured single-stranded DNA in normal human epidermis and its effects on apoptosis and terminal differentiation (denucleation).” *Archives of Dermatological Research*, **301**(9), pp.659-672.

Geilen, C., Wieder, T. and Orfanos, C., (1997). “Ceramide signalling: regulatory role in cell proliferation, differentiation and apoptosis in human epidermis.” *Archives of Dermatological Research,* **289**(10), pp.559-566.

Georgiadi, A. and Kersten, S., (2012). “Mechanisms of Gene Regulation by Fatty Acids.” *Advances in Nutrition,* **3**(2), pp.127-134.

Gibbs, S., Backendorf, C. and Ponec, M., (1996). “Regulation of keratinocyte proliferation and differentiation by all-trans-retinoic acid, 9-cis-retinoic acid and 1,25-dihydroxy vitamin D3.” *Archives of Dermatological Research,* **288**(12), pp.729-738.

Girroir, E., Hollingshead, H., He, P., Zhu, B., Perdew, G. and Peters, J., (2008). “Quantitative expression patterns of peroxisome proliferator-activated receptor-β/δ (PPARβ/δ) protein in mice.” *Biochemical and Biophysical Research Communications,* **371**(3), pp.456-461.

Gniadecki, R., (1998). “Regulation of Keratinocyte Proliferation.” *General Pharmacology: The Vascular System*, **30**(5), pp.619-622.

Gouin, O., Barbieux, C., Leturcq, F., Bonnet des Claustres, M., Petrova, E. and Hovnanian, A., (2020). “Transgenic Kallikrein 14 Mice Display Major Hair Shaft Defects Associated with Desmoglein 3 and 4 Degradation, Abnormal Epidermal Differentiation, and IL-36 Signature.” *Journal of Investigative Dermatology*, **140**(6), pp.1184-1194.

Graham, T., Mookherjee, C., Suckling, K., A. Palmer, C. and Patel, L., (2005). “The PPARδ agonist GW0742X reduces atherosclerosis in LDLR−/− mice.” *Atherosclerosis*, **181**(1), pp.29-37.

Grall, A., Guaguère, E., Planchais, S., Grond, S., Bourrat, E., Hausser, I., Hitte, C., Le Gallo, M., Derbois, C., Kim, G., Lagoutte, L., Degorce-Rubiales, F., Radner, F., Thomas, A., Küry, S., Bensignor, E., Fontaine, J., Pin, D., Zimmermann, R., Zechner, R., Lathrop, M., Galibert, F., André, C. and Fischer, J., (2012). “PNPLA1 mutations cause autosomal recessive congenital ichthyosis in golden retriever dogs and humans.” *Nature Genetics*, **44**(2), pp.140-147.

Greco, M., Lorand, L., Lane, W., Baden, H., Parameswaran, K. and Kvedar, J., (1995). “The Pancornulins: A Group of Small Proline Rich-Related Cornified Envelope Precursors with Bifunctional Capabilities in Isopeptide Bond Formation.” *Journal of Investigative Dermatology*, **104**(2), pp.204-210.

Green, E., Mansfield, J., Bell, J. and Winlove, C., (2014). “The structure and micromechanics of elastic tissue.” *Interface Focus,* **4**(2), p.20130058.

Gregus, A., Dumlao, D., Wei, S., Norris, P., Catella, L., Meyerstein, F., Buczynski, M., Steinauer, J., Fitzsimmons, B., Yaksh, T. and Dennis, E., (2013). “Systematic analysis of rat 12/15-lipoxygenase enzymes reveals critical role for spinal eLOX3 hepoxilin synthase activity in inflammatory hyperalgesia.” *The FASEB Journal,* **27**(5), pp.1939-1949.

Grygiel-Górniak, B., (2014). “Peroxisome proliferator-activated receptors and their ligands: nutritional and clinical implications - a review.” *Nutrition Journal,* **13**(1).

Guimberteau, J., Delage, J., McGrouther, D. and Wong, J., (2010). “The microvacuolar system: how connective tissue sliding works.” *Journal of Hand Surgery (European Volume)*, **35**(8), pp.614-622.

Gupta, M., Mahajan, V., Mehta, K., Chauhan, P. and Rawat, R., (2015). “Peroxisome proliferator-activated receptors (PPARs) and PPAR agonists: the ‘future’ in dermatology therapeutics?.” *Archives of Dermatological Research*, **307**(9), pp.767-780.

Haftek, M., (2014). “Epidermal barrier disorders and corneodesmosome defects.” *Cell and Tissue Research*, **360**(3), pp.483-490.

Halata, Z., Grim, M. and Baumann, K., (2010). “Current understanding of Merkel cells, touch reception and the skin.” *Expert Review of Dermatology*, **5**(1), pp.109-116.

Hallenborg, P., Jørgensen, C., Petersen, R., Feddersen, S., Araujo, P., Markt, P., Langer, T., Furstenberger, G., Krieg, P., Koppen, A., Kalkhoven, E., Madsen, L. and Kristiansen, K., (2010). “Epidermis-Type Lipoxygenase 3 Regulates Adipocyte Differentiation and Peroxisome Proliferator-Activated Receptor γ Activity.” *Molecular and Cellular Biology*, **30**(16), pp.4077-4091.

HALPRIN, K., (1972). “EPIDERMAL "TURNOVER TIME"—A RE-EXAMINATION.” *British Journal of Dermatology*, **86**(1), pp.14-19.

Hammarstrom, S., Hamberg, M., Samuelsson, B., Duell, E., Stawiski, M. and Voorhees, J., (1975). “Increased concentrations of nonesterified arachidonic acid, 12L-hydroxy-5,8,10,14-eicosatetraenoic acid, prostaglandin E2, and prostaglandin F2alpha in epidermis of psoriasis.” *Proceedings of the National Academy of Sciences*, **72**(12), pp.5130-5134.

Han, B., Rorke, E., Adhikary, G., Chew, Y., Xu, W. and Eckert, R., (2012). “Suppression of AP1 Transcription Factor Function in Keratinocyte Suppresses Differentiation.” *PLoS ONE*, **7**(5), p.e36941.

Haneda, T., Imai, Y., Uchiyama, R., Jitsukawa, O. and Yamanishi, K., (2016). “Activation of Molecular Signatures for Antimicrobial and Innate Defense Responses in Skin with Transglutaminase 1 Deficiency.” *PLOS ONE*, **11**(7), p. e0159673.

Hanley, K., Jiang, Y., Crumrine, D., Bass, N., Appel, R., Elias, P., Williams, M. and Feingold, K., (1997). “Activators of the nuclear hormone receptors PPARalpha and FXR accelerate the development of the fetal epidermal permeability barrier.” *Journal of Clinical Investigation*, **100**(3), pp.705-712.

Hanley, K., Jiang, Y., Shan He, S., Friedman, M., Elias, P., Bikle, D., Williams, M. and Feingold, K., (1998). “Keratinocyte Differentiation is Stimulated by Activators of the Nuclear Hormone Receptor PPARα.” *Journal of Investigative Dermatology*, **110**(4), pp.368-375.

Hanley, K., Ng, D., He, S., Lau, P., Min, K., Elias, P., Bikle, D., Mangelsdorf, D., Williams, M. and Feingold, K., (2000). “Oxysterols Induce Differentiation in Human Keratinocytes and Increase Ap-1-Dependent Involucrin Transcription.” *Journal of Investigative Dermatology*, **114**(3), pp.545-553.

Hansen, H. and Jensen, B., (1985). “Essential function of linoleic acid esterified in acylglucosylceramide and acylceramide in maintaining the epidermal water permeability

barrier. Evidence from feeding studies with oleate, linoleate, arachidonate, columbinate and α-linolenate." *Biochimica et Biophysica Acta (BBA) - Lipids and Lipid Metabolism*, **834**(3), pp.357-363.

Hardy S, Langelier Y, Prentki M., (2000). "Oleate activates phosphatidylinositol 3-kinase and promotes proliferation and reduces apoptosis of MDA-MB-231 breast cancer cells, whereas palmitate has opposite effects." *Cancer Res*. **60**:6353–6358.

Harizi, H., Corcuff, J. and Gualde, N., (2008). "Arachidonic-acid-derived eicosanoids: roles in biology and immunopathology." *Trends in Molecular Medicine*, **14**(10), pp.461-469.

Harper, E., Guo, C., Rizzo, H., Lillis, J., Kurtz, S., Skorcheva, I., Purdy, D., Fitch, E., Iordanov, M. and Blauvelt, A., (2009). "Th17 Cytokines Stimulate CCL20 Expression in Keratinocytes In Vitro and In Vivo: Implications for Psoriasis Pathogenesis." *Journal of Investigative Dermatology*, **129**(9), pp.2175-2183.

Harris, S., Padilla, J., Koumas, L., Ray, D. and Phipps, R., (2002). "Prostaglandins as modulators of immunity." *Trends in Immunology*, **23**(3), pp.144-150.

Harsløf, T., Husted, L., Nyegaard, M., Carstens, M., Stenkjær, L., Brixen, K., Eiken, P., Jensen, J., Børglum, A., Mosekilde, L., Rejnmark, L. and Langdahl, B., (2010). "Polymorphisms in the ALOX12 gene and osteoporosis." *Osteoporosis International*, **22**(8), pp.2249-2259.

Heidt, M., Fürstenberger, G., Vogel, S., Marks, F. and Krieg, P., (2000). "Diversity of mouse lipoxygenases: Identification of a subfamily of epidermal isozymes exhibiting a differentiation-dependent mRNA expression pattern." *Lipids*, **35**(7), pp.701-707.

Heming, M., Gran, S., Jauch, S., Fischer-Riepe, L., Russo, A., Klotz, L., Hermann, S., Schäfers, M., Roth, J. and Barczyk-Kahlert, K., (2018). "Peroxisome Proliferator-Activated Receptor-γ Modulates the Response of Macrophages to Lipopolysaccharide and Glucocorticoids." *Frontiers in Immunology*, **9**.

Hennings, H., Michael, D., Cheng, C., Steinert, P., Holbrook, K. and Yuspa, S., (1980). "Calcium regulation of growth and differentiation of mouse epidermal cells in culture." *Cell*, **19**(1), pp.245-254.

Henry, J., Hsu, C., Haftek, M., Nachat, R., Koning, H., Gardinal-Galera, I., Hitomi, K., Balica, S., Jean-Decoster, C., Schmitt, A., Paul, C., Serre, G. and Simon, M., (2011). "Hornerin is a component of the epidermal cornified cell envelopes." *The FASEB Journal*, **25**(5), pp.1567-1576.

Henson, P., (2003). "Suppression of macrophage inflammatory responses by PPARs." *Proceedings of the National Academy of Sciences*, **100**(11), pp.6295-6296.

Herman, M., Farasat, S., Steinbach, P., Wei, M., Toure, O., Fleckman, P., Blake, P., Bale, S. and Toro, J., (2009). "Transglutaminase-1 gene mutations in autosomal recessive congenital ichthyosis: Summary of mutations (including 23 novel) and modeling of TGase-1." *Human Mutation*, **30**(4), pp.537-547.

Herrmann, H., Wedig, T., Porter, R., Lane, E. and Aebi, U., (2002). "Characterization of Early Assembly Intermediates of Recombinant Human Keratins." *Journal of Structural Biology*, **137**(1-2), pp.82-96.

Hill, D., Smith, B., McAndrews-Hill, M. and Blake, J., (2008). "Gene Ontology annotations: what they mean and where they come from." *BMC Bioinformatics*, **9**(S5).

Hoeksema, M., van Eijk, M., Haagsman, H. and Hartshorn, K., (2016). "Histones as mediators of host defense, inflammation and thrombosis." *Future Microbiology*, **11**(3), pp.441-453.

Hoffjan, S. and Stemmler, S., (2007). "On the role of the epidermal differentiation complex in ichthyosis vulgaris, atopic dermatitis and psoriasis". *British Journal of Dermatology*, **157**(3), pp.441-449.

Hohl, D., Mehrel, T., Lichti, U., Turner, M., Roop, D. and Steinert, P., (1991). "Characterization of human loricrin. Structure and function of a new class of epidermal cell envelope proteins." *Journal of Biological Chemistry*, **266**(10), pp.6626-6636.

Hohl, D., (2005). "Formation of the cornified envelope." *Experimental Dermatology*, **14**(10), pp.777-780.

Holleran, W., Man, M., Gao, W., Menon, G., Elias, P. and Feingold, K., (1991). "Sphingolipids are required for mammalian epidermal barrier function. Inhibition of sphingolipid synthesis delays barrier recovery after acute perturbation." *Journal of Clinical Investigation*, **88**(4), pp.1338-1345.

Honda, H., Suzuki, H., Hosaka, N., Hirai, Y., Sanada, D., Nakamura, M., Nagai, H., Ashikaga, E., Matsumoto, K., Mukai, M., Watanabe, M. and Akizawa, T., (2009). "Ultrapure Dialysate Influences Serum Myeloperoxidase Levels and Lipid Metabolism." *Blood Purification*, **28**(1), pp.29-39.

Hostetler, H., Petrescu, A., Kier, A. and Schroeder, F., (2005). "Peroxisome Proliferator-activated Receptor α Interacts with High Affinity and Is Conformationally Responsive to Endogenous Ligands." *Journal of Biological Chemistry*, **280**(19), pp.18667-18682.

Hotz, A., Bourrat, E., Küsel, J., Oji, V., Alter, S., Hake, L., Korbi, M., Ott, H., Hausser, I., Zimmer, A. and Fischer, J., (2018). "Mutation update for CYP4F22 variants associated with autosomal recessive congenital ichthyosis." *Human Mutation*, **39**(10), pp.1305-1313.

Houthuijzen, J., (2016). "For Better or Worse: FFAR1 and FFAR4 Signaling in Cancer and Diabetes." *Molecular Pharmacology*, **90**(6), pp.738-743.

Hrdlickova, R., Toloue, M. and Tian, B., (2016). "RNA -Seq methods for transcriptome analysis." *WIREs RNA*, **8**(1).

Huang, P., Chen, Y., Chen, L., Juan, C., Ku, H., Wang, S., Chiou, S., Chiou, G., Chi, C., Hsu, C., Lee, H., Chen, L. and Kao, C., (2011). "PGC-1α Mediates Differentiation of Mesenchymal Stem Cells to Brown Adipose Cells". *Journal of Atherosclerosis and Thrombosis*, **18**(11), pp.966-980.

Huber, M., Siegenthaler, G., Mirancea, N., Marenholz, I., Nizetic, D., Breitkreutz, D., Mischke, D. and Hohl, D., (2005). "Isolation and Characterization of Human Repetin, a Member of the Fused Gene Family of the Epidermal Differentiation Complex." *Journal of Investigative Dermatology*, **124**(5), pp.998-1007.

Iglesias-Bartolome, R., Uchiyama, A., Molinolo, A., Abusleme, L., Brooks, S., Callejas-Valera, J., Edwards, D., Doci, C., Asselin-Labat, M., Onaitis, M., Moutsopoulos, N., Silvio Gutkind, J. and Morasso, M., (2018). "Transcriptional signature primes human oral mucosa for rapid wound healing." *Science Translational Medicine*, **10**(451).

Ikai, K. and Imamura, S., (1988). "Prostaglandin D2 in the skin." *International Journal of Dermatology*, **27**(3), pp.141-9.

Ipponjima, S., Umino, Y., Nagayama, M. and Denda, M., (2020). "Live imaging of alterations in cellular morphology and organelles during cornification using an epidermal equivalent model." *Scientific Reports*, **10**(1).

Ishibashi, M., Arikawa, J., Okamoto, R., Kawashima, M., Takagi, Y., Ohguchi, K. and Imokawa, G., (2003). "Abnormal Expression of the Novel Epidermal Enzyme, Glucosylceramide Deacylase, and the Accumulation of its Enzymatic Reaction Product, Glucosylsphingosine, in the Skin of Patients with Atopic Dermatitis." *Laboratory Investigation*, **83**(3), pp.397-408.

Ishida-Yamamoto, A., McGrath, J., Judge, M., Leigh, I., Lane, E. and Eady, R., (1992). "Selective Involvement of Keratins K1 and K10 in the Cytoskeletal Abnormality of Epidermolytic Hyperkeratosis (Bullous Congenital Ichthyosiform Erythroderma)." *Journal of Investigative Dermatology*, **99**(1), pp.19-26.

Ishida-Yamamoto, A. and Iizuka, H., (1998). "Structural organization of cornified cell envelopes and alterations in inherited skin disorders." *Experimental Dermatology*, **7**(1), pp.1-10.

Ishida-Yamamoto, A., Kartasova, T., Matsuo, S., Kuroki, T. and Iizuka, H., (1997). "Involucrin and SPRR Are Synthesized Sequentially in Differentiating Cultured Epidermal Cells." *Journal of Investigative Dermatology*, **108**(1), pp.12-16.

Ishiyama, M., Shiga, M., Sasamoto, K., Mizoguchi, M. and HE, P., (1993). "A New Sulfonated Tetrazolium Salt That Produces a Highly Water-Soluble Formazan Dye." *Chemical and Pharmaceutical Bulletin*, **41**(6), pp.1118-1122.

Israeli, S., Khamaysi, Z., Fuchs-Telem, D., Nousbeck, J., Bergman, R., Sarig, O. and Sprecher, E., (2011). "A Mutation in LIPN, Encoding Epidermal Lipase N, Causes a Late-Onset Form of Autosomal-Recessive Congenital Ichthyosis." *The American Journal of Human Genetics*, **88**(4), pp.482-487.

Itoh, T., Fairall, L., Amin, K., Inaba, Y., Szanto, A., Balint, B., Nagy, L., Yamamoto, K. and Schwabe, J., (2008). "Structural basis for the activation of PPARγ by oxidized fatty acids." *Nature Structural & Molecular Biology*, **15**(9), pp.924-931.

Iuchi, K., Ema, M., Suzuki, M., Yokoyama, C. and Hisatomi, H., (2019). "Oxidized unsaturated fatty acids induce apoptotic cell death in cultured cells." *Molecular Medicine Reports*, **19**(4), pp.2767-2773.

James, W.D., Berger, T.G., & Elston, D.M. (2006). *Andrews' diseases of the skin: Clinical dermatology* (10th ed.). Philadelphia: Elsevier Saunders.

Janes, K., (2015). “An analysis of critical factors for quantitative immunoblotting.” *Science Signaling*, **8**(371).

Janssen-Timmen, U., Vickers, P., Wittig, U., Lehmann, W., Stark, H., Fusenig, N., Rosenbach, T., Radmark, O., Samuelsson, B. and Habenicht, A., (1995). “Expression of 5-lipoxygenase in differentiating human skin keratinocytes.” *Proceedings of the National Academy of Sciences*, **92**(15), pp.6966-6970.

Jacques, C., Perdu, E., Jamin, E., Cravedi, J., Mavon, A., Duplan, H. and Zalko, D., (2014). “Effect of Skin Metabolism on Dermal Delivery of Testosterone: Qualitative Assessment using a New Short-Term Skin Model.” *Skin Pharmacology and Physiology*, **27**(4), pp.188-188.

Jay, M. and Ren, J., (2007). “Peroxisome Proliferator-Activated Receptor (PPAR) in Metabolic Syndrome and Type 2 Diabetes Mellitus.” *Current Diabetes Reviews*, **3**(1), pp.33-39.

Jennemann, R., Sandhoff, R., Langbein, L., Kaden, S., Rothermel, U., Gallala, H., Sandhoff, K., Wiegandt, H. and Gröne, H., (2007). “Integrity and Barrier Function of the Epidermis Critically Depend on Glucosylceramide Synthesis.” *Journal of Biological Chemistry*, **282**(5), pp.3083-3094.

Jeon, S., Djian, P. and Green, H., (1998). “Inability of keratinocytes lacking their specific transglutaminase to form cross-linked envelopes: Absence of envelopes as a simple diagnostic test for lamellar ichthyosis.” *Proceedings of the National Academy of Sciences*, **95**(2), pp.687-690.

Jiang, C., Magnaldo, T., Ohtsuki, M., Freedberg, I., Bernerd, F. and Blumenberg, M., (1993). “Epidermal growth factor and transforming growth factor alpha specifically induce the activation- and hyperproliferation-associated keratins 6 and 16.” *Proceedings of the National Academy of Sciences*, **90**(14), pp.6786-6790.

Jiang, S., Hinchliffe, T. and Wu, T., (2015). “Biomarkers of An Autoimmune Skin Disease—Psoriasis.” *Genomics, Proteomics & Bioinformatics*, **13**(4), pp.224-233.

Jiang, Y., Tsoi, L., Billi, A., Ward, N., Harms, P., Zeng, C., Maverakis, E., Kahlenberg, J. and Gudjonsson, J., (2020). “Cytokinocytes: the diverse contribution of keratinocytes to immune responses in skin.” *JCI Insight*, **5**(20).

Jin, K., Higaki, Y., Takagi, Y., Higuchi, K., Yada, Y., Kawashima, M. and Imokawa, G., (1994). “Analysis of beta-glucocerebrosidase and ceramidase activities in atopic and aged dry skin.” *Acta dermato-venereologica*, **74**(5), pp.40-337.

Jobard, F., Lefévre, C., Karaduman, A., Blanchet-Bardon, C., Emre, S., Weissenbach, J., Özgüc, M., Lathrop, M., Prud'Homme, J. and Fischer, J., (2002). “Lipoxygenase-3 (ALOXE3) and 12(R)-lipoxygenase (ALOX12B) are mutated in non-bullous congenital ichthyosiform erythroderma (NCIE) linked to chromosome 17p13.1.” *Human Molecular Genetics*, **11**(1), pp.107-113.

Johansen, C., (2017). “Generation and Culturing of Primary Human Keratinocytes from Adult Skin.” *Journal of Visualized Experiments*, (**130**).

Kabashima, K. and Miyachi, Y., (2004). “Prostanoids in the cutaneous immune response.” *Journal of Dermatological Science*, **34**(3), pp.177-184.

Kaboord, B., Smith, S., Patel, B. and Meier, S., (2015). “Enrichment of low-abundant protein targets by immunoprecipitation upstream of mass spectrometry.” *Methods in molecular biology*, **1295**, pp.51-135.

Kamata, S., Oyama, T., Saito, K., Honda, A., Yamamoto, Y., Suda, K., Ishikawa, R., Itoh, T., Watanabe, Y., Shibata, T., Uchida, K., Suematsu, M. and Ishii, I., (2020). “PPARα Ligand-Binding Domain Structures with Endogenous Fatty Acids and Fibrates.” *iScience*, **23**(11), p.101727.

Kanitakis, J. (2002). “Anatomy, histology and immunohistochemistry of normal human skin.” *European Journal of Dermatology*, **12**(4), 390–401.

Kantyka, T., Fischer, J., Wu, Z., Declercq, W., Reiss, K., Schröder, J. and Meyer-Hoffert, U., (2011). “Inhibition of kallikrein-related peptidases by the serine protease inhibitor of Kazal-type 6.” *Peptides*, **32**(6), pp.1187-1192.

Kartasova, T., Darwiche, N., Kohno, Y., Koizumi, H., Osada, S., Huh, N., Lichti, U., Steinert, P. and Kuroki, T., (1996). “Sequence and Expression Patterns of Mouse SPR1: Correlation of Expression with Epithelial Function.” *Journal of Investigative Dermatology*, **106**(2), pp.294-304.

Kaur, N., Chugh, V. and Gupta, A., (2012). “Essential fatty acids as functional components of foods- a review.” *Journal of Food Science and Technology*, **51**(10), pp.2289-2303.

Kehrer, J., Biswal, S., La, E., Thuillier, P., Datta, K., Fischer, S. and Vander Heuvel, J., (2001). “Inhibition of peroxisome-proliferator-activated receptor (PPAR)α by MK886.” *Biochemical Journal*, **356**(3), pp.899-906.

Kendall, A., Kiezel-Tsugunova, M., Brownbridge, L., Harwood, J. and Nicolaou, A., (2017). “Lipid functions in skin: Differential effects of n-3 polyunsaturated fatty acids on cutaneous ceramides, in a human skin organ culture model.” *Biochimica et Biophysica Acta (BBA) - Biomembranes*, **1859**(9), pp.1679-1689.

Kent, K. and Bomser, J., (2003). “Bovine pituitary extract provides remarkable protection against oxidative stress in human prostate epithelial cells.” *In Vitro Cellular and Developmental Biology--Animal*, **39**(8-9), pp.94-388.

Kersten, S., (2008). “Peroxisome Proliferator Activated Receptors and Lipoprotein Metabolism.” *PPAR Research*, **2008**, pp.1-11.

Keyel, P., (2017). “Dnases in health and disease.” *Developmental Biology*, **429**(1), pp.1-11.

Khanapure, S., Garvey, D., Janero, D. and Gordon Letts, L., (2007). “Eicosanoids in Inflammation: Biosynthesis, Pharmacology, and Therapeutic Frontiers.” *Current Topics in Medicinal Chemistry*, **7**(3), pp.311-340.

Khnykin, D., Miner, J. and Jahnsen, F., (2011). “Role of fatty acid transporters in epidermis.” *Dermato-Endocrinology*, **3**(2), pp.53-61.

Kim, D., Murray, I., Burns, A., Gonzalez, F., Perdew, G. and Peters, J., (2005). “Peroxisome Proliferator-activated Receptor-β/δ Inhibits Epidermal Cell Proliferation by Down-regulation of Kinase Activity.” *Journal of Biological Chemistry*, **280**(10), pp.9519-9527.

Kim, H., Kim, M., Im, S. and Fang, S., (2018). “Mouse Cre-LoxP system: general principles to determine tissue-specific roles of target genes.” *Laboratory Animal Research*, **34**(4), p.147.

Kirfel, J., Magin, T. and Reichelt, J., (2003). “Keratins: a structural scaffold with emerging functions.” *Cellular and Molecular Life Sciences (CMLS)*, **60**(1), pp.56-71.

Kirfel, G. and Herzog, V., (2004). “Migration of epidermal keratinocytes: mechanisms, regulation, and biological significance.” *Protoplasma*, **223**(2-4).

Kleiner, S., Nguyen-Tran, V., Baré, O., Huang, X., Spiegelman, B. and Wu, Z., (2009). “PPARδ Agonism Activates Fatty Acid Oxidation via PGC-1α but Does Not Increase Mitochondrial Gene Expression and Function.” *Journal of Biological Chemistry*, **284**(28), pp.18624-18633.

Kliewer, S., Sundseth, S., Jones, S., Brown, P., Wisely, G., Koble, C., Devchand, P., Wahli, W., Willson, T., Lenhard, J. and Lehmann, J., (1997). “Fatty acids and eicosanoids regulate gene expression through direct interactions with peroxisome proliferator-activated receptors α and γ.” *Proceedings of the National Academy of Sciences*, **94**(9), pp.4318-4323.

Kobayashi, T. and Narumiya, S., (2002). “Function of prostanoid receptors: studies on knockout mice.” *Prostaglandins & Other Lipid Mediators*, 68-69, pp.557-573.

Koch, P., de Viragh, P., Scharer, E., Bundman, D., Longley, M., Bickenbach, J., Kawachi, Y., Suga, Y., Zhou, Z., Huber, M., Hohl, D., Kartasova, T., Jarnik, M., Steven, A. and Roop, D., (2000). “Lessons from loricrin-deficient mice: compensatory mechanisms maintaining skin barrier function in the absence of a major cornified envelope protein.” *The Journal of Cell Biology*, **151**(2), pp.389-400.

Komatsu, N., Takata, M., Otsuki, N., Ohka, R., Amano, O., Takehara, K. and Saijoh, K., (2002). “Elevated Stratum Corneum Hydrolytic Activity in Netherton Syndrome Suggests an Inhibitory Regulation of Desquamation by SPINK5-Derived Peptides.” *Journal of Investigative Dermatology*, **118**(3), pp.436-443.

Kömüves, L., Hanley, K., Jiang, Y., Elias, P., Williams, M. and Feingold, K., (1998). “Ligands and Activators of Nuclear Hormone Receptors Regulate Epidermal Differentiation During Fetal Rat Skin Development.” *Journal of Investigative Dermatology*, **111**(3), pp.429-433.

Kömüves, L., Hanley, K., Man, M., Elias, P., Williams, M. and Feingold, K., (2000). “Keratinocyte Differentiation in Hyperproliferative Epidermis: Topical Application of PPARα Activators Restores Tissue Homeostasis.” *Journal of Investigative Dermatology*, **115**(3), pp.361-367.

Konger, R., Malaviya, R. and Pentland, A., (1998). “Growth regulation of primary human keratinocytes by prostaglandin E receptor EP2 and EP3 subtypes.” *Biochimica et Biophysica Acta (BBA) - Molecular Cell Research*, **1401**(2), pp.221-234.

Koster, M., (2009). “Making an Epidermis.” *Annals of the New York Academy of Sciences*, **1170**(1), pp.7-10.

Kragballe, K., Duell, E. and Voorhees, J., (1986). “Selective decrease of 15-hydroxyeicosatetraenoic acid (15-HETE) formation in uninvolved psoriatic dermis.” *Archives of Dermatology*, **122**(8), pp.877-880.

Krieg, P., Marks, F. and Fürstenberger, G., (2001). "A Gene Cluster Encoding Human Epidermis-type Lipoxygenases at Chromosome 17p13.1: Cloning, Physical Mapping, and Expression." *Genomics*, **73**(3), pp.323-330.

Krieg, P., Rosenberger, S., de Juanes, S., Latzko, S., Hou, J., Dick, A., Kloz, U., van der Hoeven, F., Hausser, I., Esposito, I., Rauh, M. and Schneider, H., (2013). "Aloxe3 Knockout Mice Reveal a Function of Epidermal Lipoxygenase-3 as Hepoxilin Synthase and Its Pivotal Role in Barrier Formation." *Journal of Investigative Dermatology*, **133**(1), pp.172-180.

Krieg, P. and Fürstenberger, G., (2014). "The role of lipoxygenases in epidermis." *Biochimica et Biophysica Acta (BBA) - Molecular and Cell Biology of Lipids*, **1841**(3), pp.390-400.

Kruit, J., Groen, A., van Berkel, T. and Kuipers, F., (2006). "Emerging roles of the intestine in control of cholesterol metabolism." *World Journal of Gastroenterology*, **12**(40), p.6429.

Kubiczkova, L., Sedlarikova, L., Hajek, R. and Sevcikova, S., (2012). "TGF-β – an excellent servant but a bad master." *Journal of Translational Medicine*, **10**(1).

Kukurba, K. and Montgomery, S., (2015). "RNA Sequencing and Analysis." *Cold Spring Harbor Protocols*, **2015**(11), pp.69-951.

Kypriotou, M., Huber, M. and Hohl, D., (2012). "The human epidermal differentiation complex: cornified envelope precursors, S100 proteins and the 'fused genes' family." *Experimental Dermatology*, **21**(9), pp.643-649.

Lai, J. and Pittelkow, M., (2004). "Culture confluence regulates gene expression of normal human keratinocytes." *Wound Repair and Regeneration*, **12**(6), pp.613-617.

Lands, W., Libelt, B., Morris, A., Kramer, N., Prewitt, T., Bowen, P., Schmeisser, D., Davidson, M. and Burns, J., (1992). "Maintenance of lower proportions of (n − 6) eicosanoid precursors in phospholipids of human plasma in response to added dietary (n − 3) fatty acids." *Biochimica et Biophysica Acta (BBA) - Molecular Basis of Disease*, **1180**(2), pp.147-162.

Lee, Jee-Bum Lee, Jae-Jeong Seo, Yo, S., (1999). "Expression of Trichohyalin in Dermatological Disorders: a Comparative Study with Involucrin and Filaggrin by Immunohistochemical Staining." *Acta Dermato-Venereologica*, **79**(2), pp.122-126.

Lee, S., Jeong, S. and Ahn, S., (2006). "An Update of the Defensive Barrier Function of Skin." *Yonsei Medical Journal*, **47**(3), p.293.

Lee, E., Xia, Y., Kim, W., Kim, M., Kim, T., Kim, K., Park, B. and Sung, J., (2009). "Hypoxia-enhanced wound-healing function of adipose-derived stem cells: Increase in stem cell proliferation and up-regulation of VEGF and bFGF." *Wound Repair and Regeneration*, **17**(4), pp.540-547.

Lefebvre, P., Chinetti, G., Fruchart, J. and Staels, B., (2006). "Sorting out the roles of PPAR in energy metabolism and vascular homeostasis." *Journal of Clinical Investigation*, **116**(3), pp.571-580.

Lefèvre, C., Bouadjar, B., Karaduman, A., Jobard, F., Saker, S., Özguc, M., Lathrop, M., Prud'homme, J. and Fischer, J., (2004). "Mutations in ichthyin a new gene on chromosome

5q33 in a new form of autosomal recessive congenital ichthyosis." *Human Molecular Genetics*, **13**(20), pp.2473-2482.

Lefèvre-Utile, A., Braun, C., Haftek, M. and Aubin, F., (2021). "Five Functional Aspects of the Epidermal Barrier." *International Journal of Molecular Sciences*, **22**(21), p.11676.

Lehmann, J., Moore, L., Smith-Oliver, T., Wilkison, W., Willson, T. and Kliewer, S., (1995). "An Antidiabetic Thiazolidinedione Is a High Affinity Ligand for Peroxisome Proliferator-activated Receptor γ (PPARγ)." *Journal of Biological Chemistry*, **270**(22), pp.12953-12956.

Lehrke, M. and Lazar, M., (2005). "The many faces of PPARgamma." *Cell*, **123**(6), pp.9-993.

Lei, H., Li, X., Jing, B., Xu, H. and Wu, Y., (2017). "Human S100A7 Induces Mature Interleukin1α Expression by RAGE-p38 MAPK-Calpain1 Pathway in Psoriasis." *PLOS ONE*, **12**(1), p. e0169788.

Li, S., Gallup, M., Chen, Y. and McNamara, N., (2010). "Molecular Mechanism of Proinflammatory Cytokine-Mediated Squamous Metaplasia in Human Corneal Epithelial Cells." *Investigative Opthalmology & Visual Science*, **51**(5), p.2466.

Li, H., Loriè, E., Fischer, J., Vahlquist, A. and Törmä, H., (2012). "The Expression of Epidermal Lipoxygenases and Transglutaminase-1 Is Perturbed by NIPAL4 Mutations: Indications of a Common Metabolic Pathway Essential for Skin Barrier Homeostasis." *Journal of Investigative Dermatology*, **132**(10), pp.2368-2375.

Li, H., Vahlquist, A. and Törmä, H., (2013). "Interactions between FATP4 and ichthyin in epidermal lipid processing may provide clues to the pathogenesis of autosomal recessive congenital ichthyosis." *Journal of Dermatological Science*, **69**(3), pp.195-201.

Liang, H. and Ward, W., (2006). "PGC-1α: a key regulator of energy metabolism." *Advances in Physiology Education*, **30**(4), pp.145-151.

Lin, J., Wu, H., Tarr, P., Zhang, C., Wu, Z., Boss, O., Michael, L., Puigserver, P., Isotani, E., Olson, E., Lowell, B., Bassel-Duby, R. and Spiegelman, B., (2002). "Transcriptional co-activator PGC-1α drives the formation of slow-twitch muscle fibres." *Nature*, **418**(6899), pp.797-801.

Lloyd, C., Yu, Q., Cheng, J., Turksen, K., Degenstein, L., Hutton, E. and Fuchs, E., (1995). "The basal keratin network of stratified squamous epithelia: defining K15 function in the absence of K14." *Journal of Cell Biology*, **129**(5), pp.1329-1344.

Lopez-Pajares, V., Yan, K., Zarnegar, B., Jameson, K. and Khavari, P., (2013). "Genetic pathways in disorders of epidermal differentiation." *Trends in Genetics*, **29**(1), pp.31-40.

Lu, X., Yu, H., Ma, Q., Shen, S. and Das, U., (2010). "Linoleic acid suppresses colorectal cancer cell growth by inducing oxidant stress and mitochondrial dysfunction." *Lipids in Health and Disease*, **9**(1).

Lucena-Aguilar, G., Sánchez-López, A., Barberán-Aceituno, C., Carrillo-Ávila, J., López-Guerrero, J. and Aguilar-Quesada, R., (2016). "DNA Source Selection for Downstream Applications Based on DNA Quality Indicators Analysis." *Biopreservation and Biobanking*, **14**(4), pp.264-270.

Luo, Y., Luo, Y., Chang, J., Xiao, Z. and Zhou, B., (2020). "Identification of candidate biomarkers and pathways associated with psoriasis using bioinformatics analysis." *Hereditas*, **157**(1).

Ma, X., Wang, D., Zhao, W. and Xu, L., (2018). "Deciphering the Roles of PPARγ in Adipocytes via Dynamic Change of Transcription Complex." *Frontiers in Endocrinology*, **9**.

Maas-Szabowski, N., Szabowski, A., Andrecht, S., Kolbus, A., Schorpp-Kistner, M., Angel, P., Stark, H. and Fusenig, N., (2001). "Organotypic Cocultures with Genetically Modified Mouse Fibroblasts as a Tool to Dissect Molecular Mechanisms Regulating Keratinocyte Growth and Differentiation." *Journal of Investigative Dermatology*, **116**(5), pp.816-820.

Madison, K., Sando, G., Howard, E., True, C., Gilbert, D., Swartzendruber, D. and Wertz, P., (1998). "Lamellar Granule Biogenesis: A Role for Ceramide Glucosyltransferase, Lysosomal Enzyme Transport, and the Golgi." *Journal of Investigative Dermatology Symposium Proceedings*, **3**(2), pp.80-86.

Magalhães, M., Fechine, F., Macedo, R., Monteiro, D., Oliveira, C., Brito, G., Moraes, M. and Moraes, M., (2008). "Effect of a combination of medium chain triglycerides, linoleic acid, soy lecithin and vitamins A and E on wound healing in rats." *Acta Cirurgica Brasileira*, **23**(3), pp.262-269.

Majewski, G., Craw, J. and Falla, T., (2021). "Accelerated Barrier Repair in Human Skin Explants Induced with a Plant-Derived PPAR-α Activating Complex via Cooperative Interactions." *Clinical, Cosmetic and Investigational Dermatology*, Volume **14**, pp.1271-1293.

Mak, M., Spill, F., Kamm, R. and Zaman, M., (2016). "Single-Cell Migration in Complex Microenvironments: Mechanics and Signaling Dynamics." *Journal of Biomechanical Engineering*, **138**(2).

Makino, T., Takaishi, M., Morohashi, M. and Huh, N., (2001). "Hornerin, a Novel Profilaggrin-like Protein and Differentiation-specific Marker Isolated from Mouse Skin." *Journal of Biological Chemistry*, **276**(50), pp.47445-47452.

Malik, K., He, H., Huynh, T., Tran, G., Mueller, K., Doytcheva, K., Renert-Yuval, Y., Czarnowicki, T., Magidi, S., Chou, M., Estrada, Y., Wen, H., Peng, X., Xu, H., Zheng, X., Krueger, J., Paller, A. and Guttman-Yassky, E., (2019). "Ichthyosis molecular fingerprinting shows profound TH17 skewing and a unique barrier genomic signature." *Journal of Allergy and Clinical Immunology*, **143**(2), pp.604-618.

Man, M., Choi, E., Schmuth, M., Crumrine, D., Uchida, Y., Elias, P., Holleran, W. and Feingold, K., (2006). "Basis for Improved Permeability Barrier Homeostasis Induced by PPAR and LXR Activators: Liposensors Stimulate Lipid Synthesis, Lamellar Body Secretion, and Post-Secretory Lipid Processing." *Journal of Investigative Dermatology*, **126**(2), pp.386-392.

Manabe, M., Sanchez, M., Sun, T. and Dale, B., (1991). "Interaction of filaggrin with keratin filaments during advanced stages of normal human epidermal differentiation and in Ichthyosis vulgaris." *Differentiation*, **48**(1), pp.43-50.

Manosalva, C., Alarcón, P., González, K., Soto, J., Igor, K., Peña, F., Medina, G., Burgos, R. and Hidalgo, M., (2020). "Free Fatty Acid Receptor 1 Signaling Contributes to Migration,

MMP-9 Activity, and Expression of IL-8 Induced by Linoleic Acid in HaCaT Cells." *Frontiers in Pharmacology,* **11**(595).

Mansbridge, J. and Hanawalt, P., (1988). "Role of Transforming Growth Factor Beta in the Maturation of Human Epidermal Keratinocytes." *Journal of Investigative Dermatology*, **90**(3), pp.336-341.

Mao-Qiang, M., Fowler, A., Schmuth, M., Lau, P., Chang, S., Brown, B., Moser, A., Michalik, L., Desvergne, B., Wahli, W., Li, M., Metzger, D., Chambon, P., Elias, P. and Feingold, K., (2004). "Peroxisome-Proliferator-Activated Receptor (PPAR)-γ Activation Stimulates Keratinocyte Differentiation." *Journal of Investigative Dermatology*, **123**(2), pp.305-312.

Marchix, J., Choque, B., Kouba, M., Fautrel, A., Catheline, D. and Legrand, P., (2015). "Excessive dietary linoleic acid induces proinflammatory markers in rats." *The Journal of Nutritional Biochemistry,* **26**(12), pp.1434-1441.

Marenholz, I., Zirra, M., Fischer, D., Backendorf, C., Ziegler, A. and Mischke, D., (2001). "Identification of Human Epidermal Differentiation Complex (EDC)-Encoded Genes by Subtractive Hybridization of Entire YACs to a Gridded Keratinocyte cDNA Library." *Genome Research,* **11**(3), pp.341-355.

Marshall, D., Hardman, M., Nield, K. and Byrne, C., (2001). "Differentially expressed late constituents of the epidermal cornified envelope." *Proceedings of the National Academy of Sciences,* **98**(23), pp.13031-13036.

Marukian, N. and Choate, K., (2016). "Recent advances in understanding ichthyosis pathogenesis." *F1000Research*, **5**, p.1497.

Masoodi, M., Nicolaou, A., Gledhill, K., Rhodes, L., Tobin, D. and Thody, A., (2009). "Prostaglandin D2 production in FM55 melanoma cells is regulated by α-melanocyte-stimulating hormone and is not related to melanin production." *Experimental Dermatology,* **19**(8), pp.751-753.

Matsui, T. and Amagai, M., (2015). "Dissecting the formation, structure and barrier function of the stratum corneum." *International Immunology*, **27**(6), pp.269-280.

Matsumoto, Naoka Umemoto, Hisashi S, M., (1999). "Difference in Ceramide Composition between "Dry" and "Normal" Skin in Patients with Atopic Dermatitis." *Acta Dermato-Venereologica*, **79**(3), pp.246-247.

Maurin, A., Chavassieux, P., Vericel, E. and Meunier, P., (2002). "Role of polyunsaturated fatty acids in the inhibitory effect of human adipocytes on osteoblastic proliferation." *Bone*, **31**(1), pp.260-266.

Mayer, B., Rauter, L., Zenzmaier, E., Gleispach, H. and Esterbauer, H., (1984). "Characterization of lipoxygenase metabolites of arachidonic acid in cultured human skin fibroblasts." *Biochimica et Biophysica Acta (BBA) - Lipids and Lipid Metabolism*, **795**(1), pp.151-161.

Mazzalupo, S., Wong, P., Martin, P. and Coulombe, P., (2003). "Role for keratins 6 and 17 during wound closure in embryonic mouse skin." *Developmental Dynamics,* **226**(2), pp.356-365.

McCarthy, D., Chen, Y. and Smyth, G., (2012). “Differential expression analysis of multifactor RNA-Seq experiments with respect to biological variation.” *Nucleic Acids Research*, **40**(10), pp.4288-4297.

McCusker, M. and Grant-Kels, J., (2010). “Healing fats of the skin: the structural and immunologic roles of the ω-6 and ω-3 fatty acids.” *Clinics in Dermatology*, **28**(4), pp.440-451.

McIntosh, T., (2003). “Organization of Skin Stratum Corneum Extracellular Lamellae: Diffraction Evidence for Asymmetric Distribution of Cholesterol.” *Biophysical Journal*, **85**(3), pp.1675-1681.

McIntosh, J. and Hays, T., (2016). “A Brief History of Research on Mitotic Mechanisms.” *Biology*, **5**(4), p.55.

McLean, W., (2016). “Filaggrin failure - from ichthyosis vulgaris to atopic eczema and beyond.” *British Journal of Dermatology*, **175**, pp.4-7.

Medina-Gomez, G., Gray, S., Yetukuri, L., Shimomura, K., Virtue, S., Campbell, M., Curtis, R., Jimenez-Linan, M., Blount, M., Yeo, G., Lopez, M., Seppänen-Laakso, T., Ashcroft, F., Orešič, M. and Vidal-Puig, A., (2007). “PPAR gamma 2 Prevents Lipotoxicity by Controlling Adipose Tissue Expandability and Peripheral Lipid Metabolism.” *PLoS Genetics*, **3**(4), p.e64.

Menon, G., Grayson, S. and Elias, P., (1985). “Ionic Calcium Reservoirs in Mammalian Epidermis: Ultrastructural Localization by Ion-Capture Cytochemistry.” *Journal of Investigative Dermatology*, **84**(6), pp.508-512.

Menon, G., Cleary, G. and Lane, M., (2012). “The structure and function of the stratum corneum.” *International Journal of Pharmaceutics*, **435**(1), pp.3-9.

Menon, G., Lee, S. and Lee, S., (2018). “An overview of epidermal lamellar bodies: Novel roles in biological adaptations and secondary barriers.” *Journal of Dermatological Science*, **92**(1), pp.10-17.

Micallef, L., Belaubre, F., Pinon, A., Jayat-Vignoles, C., Delage, C., Charveron, M. and Simon, A., (2009). “Effects of extracellular calcium on the growth-differentiation switch in immortalized keratinocyte HaCaT cells compared with normal human keratinocytes.” *Experimental Dermatology*, **18**(2), pp.143-151.

Michalik, L., Desvergne, B., Dreyer, C., Gavillet, M., Laurini, R. and Wahli, W., (2002). “PPAR expression and function during vertebrate development.” *The International Journal of Developmental Biology*, **46**(1), pp.14-105.

Michalik, L., Desvergne, B. and Wahli, W., (2004). “Peroxisome-proliferator-activated receptors and cancers: complex stories.” *Nature Reviews Cancer*, **4**(1), pp.61-70.

Michalik, L. and Wahli, W., (2007). “Peroxisome proliferator-activated receptors (PPARs) in skin health, repair and disease.” *Biochimica et Biophysica Acta (BBA) - Molecular and Cell Biology of Lipids*, **1771**(8), pp.991-998.

Michibata, H., Chiba, H., Wakimoto, K., Seishima, M., Kawasaki, S., Okubo, K., Mitsui, H., Torii, H. and Imai, Y., (2004). “Identification and characterization of a novel component of the

cornified envelope, cornifelin." *Biochemical and Biophysical Research Communications*, **318**(4), pp.803-813.

Min, M., Chen, X., Wang, P., Landeck, L., Chen, J., Li, W., Cai, S., Zheng, M. and Man, X., (2017). "Role of keratin 24 in human epidermal keratinocytes." *PLOS ONE*, **12**(3), p. e0174626.

Mirza, R., Hayasaka, S., Takagishi, Y., Kambe, F., Ohmori, S., Maki, K., Yamamoto, M., Murakami, K., Kaji, T., Zadworny, D., Murata, Y. and Seo, H., (2006). "DHCR24 Gene Knockout Mice Demonstrate Lethal Dermopathy with Differentiation and Maturation Defects in the Epidermis." *Journal of Investigative Dermatology*, **126**(3), pp.638-647.

Mishra, A., Chaudhary, A. and Sethi, S., (2004). "Oxidized Omega-3 Fatty Acids Inhibit NF-κB Activation Via a PPARα-Dependent Pathway." *Arteriosclerosis, Thrombosis, and Vascular Biology*, **24**(9), pp.1621-1627.

Mishra, K., Jandial, A., Gupta, K., Prakash, G. and Malhotra, P., (2018). "Ichthyosis: A Harbinger of Lymphoma." *BMJ Case Reports*, pp.bcr-**2018**-224229.

Mittal, B., (2019). "Subcutaneous adipose tissue & visceral adipose tissue." *Indian Journal of Medical Research*, **149**(5), p.571.

Miyai, M., Hamada, M., Moriguchi, T., Hiruma, J., Kamitani-Kawamoto, A., Watanabe, H., Hara-Chikuma, M., Takahashi, K., Takahashi, S. and Kataoka, K., (2016). "Transcription Factor MafB Coordinates Epidermal Keratinocyte Differentiation." *Journal of Investigative Dermatology*, **136**(9), pp.1848-1857.

Miyazaki, M., Dobrzyn, A., Elias, P. and Ntambi, J., (2005). "Stearoyl-CoA desaturase-2 gene expression is required for lipid synthesis during early skin and liver development." *Proceedings of the National Academy of Sciences*, **102**(35), pp.12501-12506.

Moran, J., Qiu, H., Turbe-Doan, A., Yun, Y., Boeglin, W., Brash, A. and Beier, D., (2007). "A Mouse Mutation in the 12R-Lipoxygenase, Alox12b, Disrupts Formation of the Epidermal Permeability Barrier." *Journal of Investigative Dermatology*, **127**(8), pp.1893-1897.

Moll, R., Franke, W., Schiller, D., Geiger, B. and Krepler, R., (1982). "The catalog of human cytokeratins: Patterns of expression in normal epithelia, tumors and cultured cells." *Cell*, **31**(1), pp.11-24.

Moll, R., Divo, M. and Langbein, L., (2008). "The human keratins: biology and pathology." *Histochemistry and Cell Biology*, **129**(6).

Mommers, J., van Rossum, M., van Erp, P. and van de Kerkhof, P., (2000). "Changes in Keratin 6 and Keratin 10 (Co-)Expression in Lesional and Symptomless Skin of Spreading Psoriasis." *Dermatology*, **201**(1), pp.15-20.

Moravcová, M., Libra, A., Dvořáková, J., Víšková, A., Muthný, T., Velebný, V. and Kubala, L., (2013). "Modulation of keratin 1, 10 and involucrin expression as part of the complex response of the human keratinocyte cell line HaCaT to ultraviolet radiation." *Interdisciplinary Toxicology*, **6**(4), pp.203-208.

Moreno, S., Farioli-Vecchioli, S. and Cerù, M., (2004). “Immunolocalization of peroxisome proliferator-activated receptors and retinoid x receptors in the adult rat CNS.” *Neuroscience*, **123**(1), pp.131-145.

Moukachar, A., (2021). “Developing a 3D bio-printed human skin model.” PhD thesis, Cardiff University, Cardiff.

Muga, S., Thuillier, P., Pavone, A., Rundhaug, J., Boeglin, W., Jisaka, M., Brash, A. and Fischer, S., (2000). “8S-lipoxygenase products activate peroxisome proliferator-activated receptor alpha and induce differentiation in murine keratinocytes.” *Cell Growth and Differentiation*, **11**(8), pp.54-447.

Muñoz-Garcia, A., Thomas, C., Keeney, D., Zheng, Y. and Brash, A., (2013). “The importance of the lipoxygenase-hepoxilin pathway in the mammalian epidermal barrier.” *Biochimica et Biophysica Acta (BBA) - Molecular and Cell Biology of Lipids*, **1841**(3), pp.401-408.

Murphy M, Reid K, Dutton R et al. (1997) “Neural stem cells.” *J Investig Dermatol Symp Proc* **2**:8–13

Murthy, S., (2019). “Approaches for Delivery of Drugs Topically.” *AAPS PharmSciTech*, **21**(1).

Nagalakshmi, U., Wang, Z., Waern, K., Shou, C., Raha, D., Gerstein, M. and Snyder, M., (2008). “The Transcriptional Landscape of the Yeast Genome Defined by RNA Sequencing.” *Science*, **320**(5881), pp.1344-1349.

Nagasawa, T., Inada, Y., Nakano, S., Tamura, T., Takahashi, T., Maruyama, K., Yamazaki, Y., Kuroda, J. and Shibata, N., (2006). “Effects of bezafibrate, PPAR pan-agonist, and GW501516, PPARδ agonist, on development of steatohepatitis in mice fed a methionine- and choline-deficient diet.” *European Journal of Pharmacology*, **536**(1-2), pp.182-191.

Nair, R. and Maseeh, A., (2012). “Vitamin D: The "sunshine" vitamin.” *Journal of Pharmacology & Pharmacotherapeutics*, **3**(2), pp.26-118.

Nakao, J., Ooyama, T., Ito, H., Chang, W. and Murota, S., (1982). “Comparative effect of lipoxygenase products of arachidonic acid on rat aortic smooth muscle cell migration.” *Atherosclerosis*, **44**(3), pp.339-342.

Nauroy, P. and Nyström, A., (2020). “Kallikreins: Essential epidermal messengers for regulation of the skin microenvironment during homeostasis, repair and disease.” *Matrix Biology Plus*, **6-7**, p.100019.

Nemes, Z., Marekov, L. and Steinert, P., (1999). “Involucrin Cross-linking by Transglutaminase 1.” *Journal of Biological Chemistry*, **274**(16), pp.11013-11021.

Neschen, S., Morino, K., Dong, J., Wang-Fischer, Y., Cline, G., Romanelli, A., Rossbacher, J., Moore, I., Regittnig, W., Munoz, D., Kim, J. and Shulman, G., (2007). “n-3 Fatty Acids Preserve Insulin Sensitivity In Vivo in a Peroxisome Proliferator-Activated Receptor- -Dependent Manner.” *Diabetes*, **56**(4), pp.1034-1041.

Neumann, C., Bigliardi-Qi, M., Widmann, C. and Bigliardi, P., (2015). "The δ-Opioid Receptor Affects Epidermal Homeostasis via ERK-Dependent Inhibition of Transcription Factor POU2F3." *Journal of Investigative Dermatology*, **135**(2), pp.471-480.

Nguyen, A. and Soulika, A., (2019). "The Dynamics of the Skin's Immune System." *International Journal of Molecular Sciences*, **20**(8), p.1811.

Nicolaou, A. and Harwood, J., (2016). "Skin lipids in health and disease." *Lipid Technology*, **28**(2), pp.36-39.

Nicolaou, A., (2013). "Eicosanoids in skin inflammation." *Prostaglandins, Leukotrienes and Essential Fatty Acids*, **88**(1), pp.131-138.

Oji, V. and Traupe, H., (2006). "Ichthyoses: differential diagnosis and molecular genetics." *European Journal of Dermatology*, **16**(4), pp.59-349.

Oji, V., Tadini, G., Akiyama, M., Blanchet Bardon, C., Bodemer, C., Bourrat, E., Coudiere, P., DiGiovanna, J., Elias, P., Fischer, J., Fleckman, P., Gina, M., Harper, J., Hashimoto, T., Hausser, I., Hennies, H., Hohl, D., Hovnanian, A., Ishida-Yamamoto, A., Jacyk, W., Leachman, S., Leigh, I., Mazereeuw-Hautier, J., Milstone, L., Morice-Picard, F., Paller, A., Richard, G., Schmuth, M., Shimizu, H., Sprecher, E., Van Steensel, M., Taïeb, A., Toro, J., Vabres, P., Vahlquist, A., Williams, M. and Traupe, H., (2010). "Revised nomenclature and classification of inherited ichthyoses: Results of the First Ichthyosis Consensus Conference in Sorèze 2009." *Journal of the American Academy of Dermatology*, **63**(4), pp.607-641.

Oliveira, A., Bertollo, C., Rocha, L., Nascimento, E., Costa, K. and Coelho, M., (2007). "Antinociceptive and antiedematogenic activities of fenofibrate, an agonist of PPAR alpha, and pioglitazone, an agonist of PPAR gamma." *European Journal of Pharmacology*, **561**(1-3), pp.194-201.

Olsen, B., Schlesinger, P. and Baker, N., (2009). "Perturbations of Membrane Structure by Cholesterol and Cholesterol Derivatives Are Determined by Sterol Orientation." *Journal of the American Chemical Society*, 131(13), pp.4854-4865.

Omary, M., Ku, N., Strnad, P. and Hanada, S., (2009). "Toward unraveling the complexity of simple epithelial keratins in human disease." *Journal of Clinical Investigation*, **119**(7), pp.1794-1805.

Pappas, A., (2009). "Epidermal surface lipids." *Dermato-Endocrinology*, **1**(2), pp.72-76.

Paramio, J., Casanova, M., Segrelles, C., Mittnacht, S., Lane, E. and Jorcano, J., (1999). "Modulation of Cell Proliferation by Cytokeratins K10 and K16." *Molecular and Cellular Biology*, **19**(4), pp.3086-3094.

Patro, N., Panda, M. and Mohanty, P., (2019). "Congenital ichthyosiform erythroderma: A rare neonatal dermatoses responding to acitretin." *Indian Journal of Pharmacology*, **51**(5), p.343.

Pchelintsev, N., Adams, P. and Nelson, D., (2016). "Critical Parameters for Efficient Sonication and Improved Chromatin Immunoprecipitation of High Molecular Weight Proteins." *PLOS ONE*, **11**(1), p.e0148023.

Pedro, M., Salinas Parra, N., Gutkind, J. and Iglesias-Bartolome, R., (2020). "Activation of G-Protein Coupled Receptor–Gαi Signaling Increases Keratinocyte Proliferation and Reduces Differentiation, Leading to Epidermal Hyperplasia." *Journal of Investigative Dermatology*, **140**(6), pp.1195-1203.e3.

Pentland, A. and Needleman, P., (1986). "Modulation of keratinocyte proliferation in vitro by endogenous prostaglandin synthesis." *Journal of Clinical Investigation*, **77**(1), pp.246-251.

Picard, F. and Auwerx, J., (2002). "PPAR(gamma) and glucose homeostasis." *Annual Review of Nutrition*, **22**, pp.97-167.

Picardo, M., Ottaviani, M., Camera, E. and Mastrofrancesco, A., (2009). "Sebaceous gland lipids." *Dermato-Endocrinology*, **1**(2), pp.68-71.

Pilgram, G., Vissers, D., van der Meulen, H., Koerten, H., Pavel, S., Lavrijsen, S. and Bouwstra, J., (2001). "Aberrant Lipid Organization in Stratum Corneum of Patients with Atopic Dermatitis and Lamellar Ichthyosis." *Journal of Investigative Dermatology*, **117**(3), pp.710-717.

Pillai, S., Bikle, D. and Elias, P., (1988). "1,25-Dihydroxyvitamin D production and receptor binding in human keratinocytes varies with differentiation." *Journal of Biological Chemistry*, **263**(11), pp.5390-5395.

Pietrzak, A., Michalak-Stoma, A., Chodorowska, G. and Szepietowski, J., (2010). "Lipid Disturbances in Psoriasis: An Update." *Mediators of Inflammation*, **2010**, pp.1-13.

Plutzky, J., (2000). "Peroxisome proliferator-activated receptors in vascular biology and atherosclerosis: Emerging insights for evolving paradigms." *Current Atherosclerosis Reports*, **2**(4), pp.327-335.

Popeijus, H., van Otterdijk, S., van der Krieken, S., Konings, M., Serbonij, K., Plat, J. and Mensink, R., (2014). "Fatty acid chain length and saturation influences PPARα transcriptional activation and repression in HepG2 cells." *Molecular Nutrition & Food Research*, **58**(12), pp.2342-2349.

Poumay, Y. and Pittelkow, M., (1995). "Cell Density and Culture Factors Regulate Keratinocyte Commitment to Differentiation and Expression of Suprabasal K1/K10 Keratins." *Journal of Investigative Dermatology*, **104**(2), pp.271-276.

Pradervand, S., Yasukawa, H., Muller, O., Kjekshus, H., Nakamura, T., St Amand, T., Yajima, T., Matsumura, K., Duplain, H., Iwatate, M., Woodard, S., Pedrazzini, T., Ross, J., Firsov, D., Rossier, B., Hoshijima, M. and Chien, K., (2004). "Small proline-rich protein 1A is a gp130 pathway- and stress-inducible cardioprotective protein." *The EMBO Journal*, **23**(22), pp.4517-4525.

Presland, R., Boggess, D., Patrick Lewis, S., Hull, C., Fleckman, P. and Sundberg, J., (2000). "Loss of Normal Profilaggrin and Filaggrin in Flaky Tail (ft/ft) Mice: an Animal Model for the Filaggrin-Deficient Skin Disease Ichthyosis Vulgaris." *Journal of Investigative Dermatology*, **115**(6), pp.1072-1081.

Proksch, E., Holleran, W., Menon, G., Elias, P. and Feingold, K., (1993). “Barrier function regulates epidermal lipid and DNA synthesis.” *British Journal of Dermatology*, **128**(5), pp.473-482.

Prost-Squarcioni, C., Fraitag, S., Heller, M. and Boehm, N., (2008). “Functional histology of dermis.” *Annales de Dermatologie et de Venereologie*, **135**(1 Pt 2), pp.1S5-20.

Rácz, E., Kurek, D., Kant, M., Baerveldt, E., Florencia, E., Mourits, S., de Ridder, D., Laman, J., van der Fits, L. and Prens, E., (2011). “GATA3 Expression Is Decreased in Psoriasis and during Epidermal Regeneration; Induction by Narrow-Band UVB and IL-4.” *PLoS ONE*, **6**(5), p.e19806.

Raj, D., Brash, D. and Grossman, D., (2006). “Keratinocyte Apoptosis in Epidermal Development and Disease.” *Journal of Investigative Dermatology*, **126**(2), pp.243-257.

Ramot, Y., Mastrofrancesco, A., Camera, E., Desreumaux, P., Paus, R. and Picardo, M., (2015). “The role of PPARγ-mediated signalling in skin biology and pathology: new targets and opportunities for clinical dermatology.” *Experimental Dermatology*, **24**(4), pp.245-251.

Rassner, U., Feingold, K., Crumrine, D. and Elias, P., (1999). “Coordinate assembly of lipids and enzyme proteins into epidermal lamellar bodies.” *Tissue and Cell*, **31**(5), pp.489-498.

Raymond, A., de Peredo, A., Stella, A., Ishida-Yamamoto, A., Bouyssie, D., Serre, G., Monsarrat, B. and Simon, M., (2008). “Lamellar Bodies of Human Epidermis.” *Molecular & Cellular Proteomics*, **7**(11), pp.2151-2175.

Reichelt, J., Büssow, H., Grund, C. and Magin, T., (2001). “Formation of a Normal Epidermis Supported by Increased Stability of Keratins 5 and 14 in Keratin 10 Null Mice.” *Molecular Biology of the Cell*, **12**(6), pp.1557-1568.

Rhodes, L., Gledhill, K., Masoodi, M., Haylett, A., Brownrigg, M., Thody, A., Tobin, D. and Nicolaou, A., (2009). “The sunburn response in human skin is characterized by sequential eicosanoid profiles that may mediate its early and late phases.” *The FASEB Journal*, **23**(11), pp.3947-3956.

Rivier, M., Safonova, I., Lebrun, P., Griffiths, C., Ailhaud, G. and Michel, S., (1998). “Differential expression of peroxisome proliferator-activated receptor subtypes during the differentiation of human keratinocytes.” *Journal of Dermatological Science*, **16**, p.S137.

Rivier, M., Safonova, I., Michel, S., Castiel, I. and Ailhaud, G., (2000). “Peroxisome Proliferator-Activated Receptor-α Enhances Lipid Metabolism in a Skin Equivalent Model.” *Journal of Investigative Dermatology*, **114**(4), pp.681-687.

Robinson, N., LaCelle, P. and Eckert, R., (1996). “Involucrin Is a Covalently Crosslinked Constituent of Highly Purified Epidermal Corneocytes: Evidence for a Common Pattern of Involucrin Crosslinking in Vivo and in Vitro.” *Journal of Investigative Dermatology*, **107**(1), pp.101-107.

Robinson, M., McCarthy, D. and Smyth, G., (2009). “edgeR: a Bioconductor package for differential expression analysis of digital gene expression data.” *Bioinformatics*, **26**(1), pp.139-140.

Rogue, A., Spire, C., Claude, N. and Guillouzo, A., (2010). "Comparative changes in gene expression profiles induced by PPARγ AND PPARα/γ agonists in primary human hepatocytes and HepaRG cells." *Toxicology Letters*, **196**, p.S209.

Rosen, E., Walkey, C., Puigserver, P. and Spiegelman, B., (2000). "Transcriptional regulation of adipogenesis." *Genes & Development*, **14**(11), pp.1293-1307.

Roth, W., Kumar, V., Beer, H., Richter, M., Wohlenberg, C., Reuter, U., Thiering, S., Staratschek-Jox, A., Hofmann, A., Kreusch, F., Schultze, J., Vogl, T., Roth, J., Hausser, I. and Magin, T., (2012). "Keratin 1 maintains skin integrity and participates in an inflammatory network in skin via interleukin-18." *Journal of Cell Science*, **125**(Pt 22), pp.79-5269.

Rothnagel, J., Seki, T., Ogo, M., Longley, M., Wojcik, S., Bundman, D., Bickenbach, J. and Roop, D., (1999). "The mouse keratin 6 isoforms are differentially expressed in the hair follicle, footpad, tongue and activated epidermis." *Differentiation*, **65**(2), pp.119-130.

Rout, D., Nair, A., Gupta, A. and Kumar, P., (2019). "Epidermolytic hyperkeratosis: clinical update." *Clinical, Cosmetic and Investigational Dermatology*, **12**, pp.333-344.

Ruchusatsawat, K., Wongpiyabovorn, J., Protjaroen, P., Chaipipat, M., Shuangshoti, S., Thorner, P. and Mutirangura, A., (2011). "Parakeratosis in skin is associated with loss of inhibitor of differentiation 4 via promoter methylation." *Human Pathology*, **42**(12), pp.1878-1887.

Sampath, H. and Ntambi, J., (2011). "The role of fatty acid desaturases in epidermal metabolism." *Dermato-Endocrinology*, **3**(2), pp.62-64.

Sandilands, A., Sutherland, C., Irvine, A. and McLean, W., (2009). "Filaggrin in the frontline: role in skin barrier function and disease." *Journal of Cell Science*, **122**(9), pp.1285-1294.

Sandilands, A., Smith, F., Lunny, D., Campbell, L., Davidson, K., MacCallum, S., Corden, L., Christie, L., Fleming, S., Lane, E. and McLean, W., (2013). "Generation and Characterisation of Keratin 7 (K7) Knockout Mice." *PLoS ONE*, **8**(5), p.e64404.

Sarhangi, N., Sharifi, F., Hashemian, L., Hassani Doabsari, M., Heshmatzad, K., Rahbaran, M., Jamaldini, S., Aghaei Meybodi, H. and Hasanzad, M., (2020). "PPARG (Pro12Ala) genetic variant and risk of T2DM: a systematic review and meta-analysis." *Scientific Reports*, **10**(1).

Sawada, Y., Yuan, C. and Huang, A., (2002). "Lipid Supplements Support the Growth of Corneal and Epidermal Epithelial Cells in Serum-Free Culture System." *Investigative Ophthalmology & Visual Science*, **43**(13), p.137.

Scarpulla, R., (2002). "Transcriptional activators and coactivators in the nuclear control of mitochondrial function in mammalian cells." *Gene*, **286**(1), pp.81-89.

Schäfer, M. and Werner, S., (2011). "The Cornified Envelope: A First Line of Defense against Reactive Oxygen Species." *Journal of Investigative Dermatology*, **131**(7), pp.1409-1411.

Schmuth, M., Haqq, C., Cairns, W., Holder, J., Dorsam, S., Chang, S., Lau, P., Fowler, A., Chuang, G., Moser, A., Brown, B., Mao-Qiang, M., Uchida, Y., Schoonjans, K., Auwerx, J., Chambon, P., Willson, T., Elias, P. and Feingold, K., (2004). "Peroxisome Proliferator-

Activated Receptor (PPAR)-β/δ Stimulates Differentiation and Lipid Accumulation in Keratinocytes." *Journal of Investigative Dermatology*, **122**(4), pp.971-983.

Schmuth, M., Jiang, Y., Dubrac, S., Elias, P. and Feingold, K., (2008). "Thematic Review Series: Skin Lipids. Peroxisome proliferator-activated receptors and liver X receptors in epidermal biology." *Journal of Lipid Research*, **49**(3), pp.499-509.

Schmuth, M., Martinz, V., Janecke, A., Fauth, C., Schossig, A., Zschocke, J. and Gruber, R., (2012). "Inherited ichthyoses/generalized Mendelian disorders of cornification." *European Journal of Human Genetics*, **21**(2), pp.123-133.

Schneider, C., Keeney, D., Boeglin, W. and Brash, A., (2001). "Detection and Cellular Localization of 12R-Lipoxygenase in Human Tonsils." *Archives of Biochemistry and Biophysics*, **386**(2), pp.268-274.

Schurer, N., Kohne, A., Schliep, V., Barlag, K. and Goerz, G., (1993). "Lipid composition and synthesis of HaCaT cells, an immortalized human keratinocyte line, in comparison with normal human adult keratinocytes." *Experimental Dermatology*, **2**(4), pp.179-185.

Scott, G., Leopardi, S., Printup, S., Malhi, N., Seiberg, M. and LaPoint, R., (2004). "Proteinase-Activated Receptor-2 Stimulates Prostaglandin Production in Keratinocytes: Analysis of Prostaglandin Receptors on Human Melanocytes and Effects of PGE2 and PGF2α on Melanocyte Dendricity." *Journal of Investigative Dermatology*, **122**(5), pp.1214-1224.

Seeger, M. and Paller, A., (2015). "The Roles of Growth Factors in Keratinocyte Migration." *Advances in Wound Care*, **4**(4), pp.213-224.

Segre, J. A., Bauer, C., and Fuchs, E. (1999). "Klf4 is a transcription factor required for establishing the barrier function of the skin." *Nat. Genet.* **22**, pp.356–360.

Segre, J., (2006). "Epidermal barrier formation and recovery in skin disorders." *Journal of Clinical Investigation*, **116**(5), pp.1150-1158.

Seltmann, K., Fritsch, A., Kas, J. and Magin, T., (2013). "Keratins significantly contribute to cell stiffness and impact invasive behavior." *Proceedings of the National Academy of Sciences*, **110**(46), pp.18507-18512.

Seo, E., Namkung, J., Lee, K., Lee, W., Im, M., Kee, S., Tae Park, G., Yang, J., Seo, Y., Park, J., Deok Kim, C. and Lee, J., (2005). "Analysis of calcium-inducible genes in keratinocytes using suppression subtractive hybridization and cDNA microarray." *Genomics*, **86**(5), pp.528-538.

Seo, M., Kang, T., Lee, C., Lee, A. and Noh, M., (2012). "HaCaT Keratinocytes and Primary Epidermal Keratinocytes Have Different Transcriptional Profiles of Cornified Envelope-Associated Genes to T Helper Cell Cytokines." *Biomolecules and Therapeutics*, **20**(2), pp.171-176.

Serhan, C. and Chiang, N., (2008). "Endogenous pro-resolving and anti-inflammatory lipid mediators: a new pharmacologic genus." *British Journal of Pharmacology*, **153**(S1), pp.S200-S215.

Sertznig, P., Seifert, M., Tilgen, W. and Reichrath, J., (2007). "Present concepts and future outlook: Function of peroxisome proliferator-activated receptors (PPARs) for pathogenesis, progression, and therapy of cancer." *Journal of Cellular Physiology*, **212**(1), pp.1-12.

Sertznig, P., Seifert, M., Tilgen, W. and Reichrath, J., (2008). "Peroxisome Proliferator-Activated Receptors (PPARs) and the Human Skin." *American Journal of Clinical Dermatology*, **9**(1), pp.15-31.

Sertznig, P. and Reichrath, J., (2011). "Peroxisome proliferator-activated receptors (PPARs) in dermatology." *Dermato-Endocrinology*, **3**(3), pp.130-135.

Sethi, S., Ziouzenkova, O., Ni, H., Wagner, D., Plutzky, J. and Mayadas, T., (2002). "Oxidized omega-3 fatty acids in fish oil inhibit leukocyte-endothelial interactions through activation of PPARα." *Blood*, **100**(4), pp.1340-1346.

Sethu C., Sethu A.U., (2016). "Glomus tumour." *Ann. R. Coll. Surg. Engl*, **98**(1): e1–e2.

Sevilla, L., Nachat, R., Groot, K., Klement, J., Uitto, J., Djian, P., Määttä, A. and Watt, F., (2007). "Mice deficient in involucrin, envoplakin, and periplakin have a defective epidermal barrier." *Journal of Cell Biology*, **179**(7), pp.1599-1612.

Sheng, R., Chen, Y., Yung Gee, H., Stec, E., Melowic, H., Blatner, N., Tun, M., Kim, Y., Källberg, M., Fujiwara, T., Hye Hong, J., Pyo Kim, K., Lu, H., Kusumi, A., Goo Lee, M. and Cho, W., (2012). "Cholesterol modulates cell signaling and protein networking by specifically interacting with PDZ domain-containing scaffold proteins." *Nature Communications*, **3**(1).

Sheu, S., Kaya, T., Waxman, D. and Vajda, S., (2004). "Exploring the Binding Site Structure of the PPARγ Ligand-Binding Domain by Computational Solvent Mapping." *Biochemistry*, **44**(4), pp.1193-1209.

Shipton, E., (2013). "Skin Matters: Identifying Pain Mechanisms and Predicting Treatment Outcomes." *Neurology Research International*, **2013**, pp.1-7.

Shirakata, Y., (2010). "Regulation of epidermal keratinocytes by growth factors." *Journal of Dermatological Science*, **59**(2), pp.73-80.

Shruthi, B., Nilgar, B., Dalal, A. and Limbani, N., (2017). "Harlequin ichthyosis: A rare case." *Journal of Turkish Society of Obstetric and Gynecology*, **14**(2), pp.138-140.

Shureiqi, I., Jiang, W., Zuo, X., Wu, Y., Stimmel, J., Leesnitzer, L., Morris, J., Fan, H., Fischer, S. and Lippman, S., (2003). "The 15-lipoxygenase-1 product 13-S-hydroxyoctadecadienoic acid down-regulates PPAR- to induce apoptosis in colorectal cancer cells." *Proceedings of the National Academy of Sciences*, **100**(17), pp.9968-9973.

Siebert, M., Krieg, P., Lehmann, W., Marks, F. and Fürstenberger, G., (2001). "Enzymic characterization of epidermis-derived 12-lipoxygenase isoenzymes." *Biochemical Journal*, **355**(1), pp.97-104.

Siersbaek, R., Nielsen, R. and Mandrup, S., (2010). "PPARγ in adipocyte differentiation and metabolism - Novel insights from genome-wide studies." *FEBS Letters*, **584**(15), pp.3242-3249.

Sim, C., Kim, S., Brunmeir, R., Zhang, Q., Li, H., Dharmasegaran, D., Leong, C., Lim, Y., Han, W. and Xu, F., (2017). "Regulation of white and brown adipocyte differentiation by RhoGAP DLC1." *PLOS ONE*, **12**(3), p.e0174761.

Simard-Bisson, C., Parent, L., Moulin, V. and Fruteau de Laclos, B., (2018). "Characterization of Epidermal Lipoxygenase Expression in Normal Human Skin and Tissue-Engineered Skin Substitutes." *Journal of Histochemistry & Cytochemistry*, **66**(11), pp.813-824.

Sims, D., Sudbery, I., Ilott, N., Heger, A. and Ponting, C., (2014). "Sequencing depth and coverage: key considerations in genomic analyses." *Nature Reviews Genetics*, **15**(2), pp.121-132.

Sivamani, R., (2014). "Eicosanoids and Keratinocytes in Wound Healing." *Advances in Wound Care*, **3**(7), pp.476-481.

Sjövall, P., Skedung, L., Gregoire, S., Biganska, O., Clément, F. and Luengo, G., (2018). "Imaging the distribution of skin lipids and topically applied compounds in human skin using mass spectrometry." *Scientific Reports*, **8**(1).

Sjursen, W., Brekke, O. and Johansen, B., (2000). "Secretory and cytosolic phospholipase A(2)regulate the long-term cytokine-induced eicosanoid production in human keratinocytes." *Cytokine*, **12**(8), pp.1189-1194.

Slotte, J., (2013). "Biological functions of sphingomyelins." *Progress in Lipid Research*, **52**(4), pp.424-437.

Smith, W. and Langenbach, R., (2001). "Why there are two cyclooxygenase isozymes." *Journal of Clinical Investigation*, **107**(12), pp.1491-1495.

Smith, W., Urade, Y. and Jakobsson, P., (2011). "Enzymes of the Cyclooxygenase Pathways of Prostanoid Biosynthesis." *Chemical Reviews*, **111**(10), pp.5821-5865.

Smits, J., Niehues, H., Rikken, G., van Vlijmen-Willems, I., van de Zande, G., Zeeuwen, P., Schalkwijk, J. and van den Bogaard, E., (2017). "Immortalized N/TERT keratinocytes as an alternative cell source in 3D human epidermal models." *Scientific Reports*, **7**(1).

Smyth, E., Grosser, T., Wang, M., Yu, Y. and FitzGerald, G., (2009). "Prostanoids in health and disease." *Journal of Lipid Research*, **50**, pp.S423-S428.

Sobolev, V., Nesterova, A., Soboleva, A., Dvoriankova, E., Piruzyan, A., Mildzikhova, D., Korsunskaya, I. and Svitich, O., (2020). "The Model of PPARγ-Downregulated Signaling in Psoriasis." *PPAR Research*, **2020**, pp.1-11.

Spector, A. and Kim, H., (2015). "Discovery of essential fatty acids." *Journal of Lipid Research*, **56**(1), pp.11-21.

Stark, R., Grzelak, M. and Hadfield, J., (2019). "RNA sequencing: the teenage years." *Nature Reviews Genetics*, **20**(11), pp.631-656.

Steensel, M., (2007). "Emerging drugs for ichthyosis." *Expert Opinion on Emerging Drugs*, **12**(4), pp.647-656.

Steinert, P., Chung, S. and Kim, S., (1996). “Inactive Zymogen and Highly Active Proteolytically Processed Membrane-Bound Forms of the Transglutaminase 1 Enzyme in Human Epidermal Keratinocytes.” *Biochemical and Biophysical Research Communications*, **221**(1), pp.101-106.

Steinert, P., Parry, D. and Marekov, L., (2003). “Trichohyalin Mechanically Strengthens the Hair Follicle.” *Journal of Biological Chemistry*, **278**(42), pp.41409-41419.

Stenmark, K. and Tuder, R., (2018). “Peroxisome Proliferator-activated Receptor γ and Mitochondria: Drivers or Passengers on the Road to Pulmonary Hypertension?.” *American Journal of Respiratory Cell and Molecular Biology*, **58**(5), pp.555-557.

Stephen, R., Gustafsson, M., Jarvis, M., Tatoud, R., Marshall, B., Knight, D., Ehrenborg, E., Harris, A., Wolf, C. and Palmer, C., (2004). “Activation of Peroxisome Proliferator-Activated Receptor δ Stimulates the Proliferation of Human Breast and Prostate Cancer Cell Lines.” *Cancer Research*, **64**(9), pp.3162-3170.

Strachan, L. and Ghadially, R., (2008). “Tiers of Clonal Organization in the Epidermis: The Epidermal Proliferation Unit Revisited.” *Stem Cell Reviews*, **4**(3), pp.149-157.

Straus, D. and Glass, C., (2001). “Cyclopentenone prostaglandins: New insights on biological activities and cellular targets.” *Medicinal Research Reviews*, **21**(3), pp.185-210.

Strudwick, X., Lang, D., Smith, L. and Cowin, A., (2015). “Combination of Low Calcium with Y-27632 Rock Inhibitor Increases the Proliferative Capacity, Expansion Potential and Lifespan of Primary Human Keratinocytes while Retaining Their Capacity to Differentiate into Stratified Epidermis in a 3D Skin Model.” *PLOS ONE*, **10**(4), p.e0123651.

Sugimoto, M., Arai, I., Futaki, N., Hashimoto, Y., Honma, Y. and Nakaike, S., (2006). “Role of COX-1 and COX-2 on skin PGs biosynthesis by mechanical scratching in mice.” *Prostaglandins, Leukotrienes and Essential Fatty Acids*, **75**(1), pp.1-8.

Sugiyama, H., Nonaka, T., Kishimoto, T., Komoriya, K., Tsuji, K. and Nakahata, T., (2000). “Peroxisome proliferator-activated receptors are expressed in human cultured mast cells: a possible role of these receptors in negative regulation of mast cell activation.” *European Journal of Immunology*, **30**(12), pp.3363-3370.

Sümer, C., Bozer, A. and Dincer, T., 2019. Keratin 14 is a novel interaction partner of keratinocyte differentiation regulator: receptor-interacting protein kinase 4. *TURKISH JOURNAL OF BIOLOGY*, 43(4), pp.225-234.

Sunshine, H. and Iruela-Arispe, M., (2017). “Membrane lipids and cell signaling.” *Current Opinion in Lipidology*, **28**(5), pp.408-413.

Taherzadeh-Fard, E., Saft, C., Akkad, D., Wieczorek, S., Haghikia, A., Chan, A., Epplen, J. and Arning, L., (2011). “PGC-1alpha downstream transcription factors NRF-1 and TFAM are genetic modifiers of Huntington disease.” *Molecular Neurodegeneration*, **6**(1).

Taichman, L. and Prokop, C., (1982). “Synthesis of Keratin Proteins during Maturation of Cultured Human Keratinocytes.” *Journal of Investigative Dermatology*, **78**(6), pp.464-467.

Takaishi, M., Makino, T., Morohashi, M. and Huh, N., (2005). “Identification of Human Hornerin and Its Expression in Regenerating and Psoriatic Skin.” *Journal of Biological Chemistry*, **280**(6), pp.4696-4703.

Tan, N., Michalik, L., Noy, N., Yasmin, R., Pacot, C., Heim, M., Flühmann, B., Desvergne, B. and Wahli, W., (2001). “Critical roles of PPARβ/δ in keratinocyte response to inflammation.” *Genes & Development*, **15**(24), pp.3263-3277.

Tang, S. and Yang, J., (2018). “Dual Effects of Alpha-Hydroxy Acids on the Skin.” *Molecules*, **23**(4), p.863.

Tarcsa, E., Marekov, L., Andreoli, J., Idler, W., Candi, E., Chung, S. and Steinert, P., (1997). “The Fate of Trichohyalin.” *Journal of Biological Chemistry*, **272**(44), pp.27893-27901.

Tayama, M., Soeda, S., Kishimoto, Y., Martin, B., Callahan, J., Hiraiwa, M. and O'Brien, J., (1993). “Effect of saposins on acid sphingomyelinase.” *Biochemical Journal*, **290**(2), pp.401-404.

ter Horst, B., Chouhan, G., Moiemen, N. and Grover, L., (2018). “Advances in keratinocyte delivery in burn wound care.” *Advanced Drug Delivery Reviews*, **123**, pp.18-32.

Terrinoni, A., Didona, B., Caporali, S., Chillemi, G., Lo Surdo, A., Paradisi, M., Annichiarico-Petruzzelli, M., Candi, E., Bernardini, S. and Melino, G., (2018). “Role of the keratin 1 and keratin 10 tails in the pathogenesis of ichthyosis hystrix of Curth Macklin.” *PLOS ONE*, **13**(4), p.e0195792.

Theocharis, S., Margeli, A. and Kouraklis, G., (2003). “Peroxisome Proliferator Activated Receptor-Gamma Ligands as Potent Antineoplastic Agents.” *Current Medicinal Chemistry-Anti-Cancer Agents*, **3**(3), pp.239-251.

Thomas, S. and Bonchev, D., (2010). “A survey of current software for network analysis in molecular biology.” *Human Genomics*, **4**(5), p.353.

Thuong, N., Hawn, T., Chau, T., Bang, N., Yen, N., Thwaites, G., Teo, Y., Seielstad, M., Hibberd, M., Lan, N., Caws, M., Farrar, J. and Dunstan, S., (2011). “Epiregulin (EREG) variation is associated with susceptibility to tuberculosis.” *Genes & Immunity*, **13**(3), pp.275-281.

Ting, S., Caddy, J., Wilanowski, T., Auden, A., Cunningham, J., Elias, P., Holleran, W. and Jane, S., (2005). “The Epidermis of Grhl3-Null Mice Displays Altered Lipid Processing and Cellular Hyperproliferation.” *Organogenesis*, **2**(2), pp.33-35.

Toivola D.M., P. Boor, C. Alam, P. Strnad., (2015). “Keratins in health and disease.**”** *Curr Opin Cell Biol*, **32**, pp. 73-81.

Tominaga, H., Ishiyama, M., Ohseto, F., Sasamoto, K., Hamamoto, T., Suzuki, K. and Watanabe, M., (1999). “A water-soluble tetrazolium salt useful for colorimetric cell viability assay.” *Analytical Communications*, **36**(2), pp.47-50.

Toouli, C., Huschtscha, L., Neumann, A., Noble, J., Colgin, L., Hukku, B. and Reddel, R., (2002). “Comparison of human mammary epithelial cells immortalized by simian virus 40 T-Antigen or by the telomerase catalytic subunit.” *Oncogene*, **21**(1), pp.128-139.

Trapnell, C., Hendrickson, D., Sauvageau, M., Goff, L., Rinn, J. and Pachter, L., (2012). "Differential analysis of gene regulation at transcript resolution with RNA-seq." *Nature Biotechnology*, **31**(1), pp.46-53.

Trombetta, A., Maggiora, M., Martinasso, G., Cotogni, P., Canuto, R. and Muzio, G., (2007). "Arachidonic and docosahexaenoic acids reduce the growth of A549 human lung-tumor cells increasing lipid peroxidation and PPARs." *Chemico-Biological Interactions*, **165**(3), pp.239-250.

Trzeciak, M., Olszewska, B., Sakowicz-Burkiewicz, M., Sokołowska-Wojdyło, M., Jankau, J., Nowicki, R. and Pawełczyk, T., (2020). "Expression Profiles of Genes Encoding Cornified Envelope Proteins in Atopic Dermatitis and Cutaneous T-Cell Lymphomas." *Nutrients*, **12**(3), p.862.

Tsuchida, S., Bonkobara, M., McMillan, J., Akiyama, M., Yudate, T., Aragane, Y., Tezuka, T., Shimizu, H., Cruz, P. and Ariizumi, K., (2004). "Characterization of Kdap, A Protein Secreted by Keratinocytes." *Journal of Investigative Dermatology*, **122**(5), pp.1225-1234.

Tunggal, J. A., Helfrich, I., Schmitz, A., Schwarz, H., Gunzel, D., Fromm, M., Kemler, R., Krieg, T., and Niessen, C. M. (2005). "E-cadherin is essential for in vivo epidermal barrier function by regulating tight junctions." EMBO J. **24**, 1146–1156

Turksen, K. and Troy, T., (2002). "Permeability barrier dysfunction in transgenic mice overexpressing claudin 6." *Development*, **129**(7), pp.1775-1784.

Tyagi, S., Sharma, S., Gupta, P., Saini, A. and Kaushal, C., (2011). "The peroxisome proliferator-activated receptor: A family of nuclear receptors role in various diseases." *Journal of Advanced Pharmaceutical Technology & Research*, 2(4), p.236.

Tyrrell, V., Ali, F., Boeglin, W., Andrews, R., Burston, J., Birchall, J., Ingram, J., Murphy, R., Piguet, V., Brash, A., O'Donnell, V. and Thomas, C., (2021). "Lipidomic and transcriptional analysis of the linoleoyl-omega-hydroxyceramide biosynthetic pathway in human psoriatic lesions." *Journal of Lipid Research*, **62**, p.100094.

Tzeng, J., Byun, J., Park, J., Yamamoto, T., Schesing, K., Tian, B., Sadoshima, J. and Oka, S., (2015). "An Ideal PPAR Response Element Bound to and Activated by PPARα." *PLOS ONE*, 10(8), p.e0134996.

Uchida, Y. and Holleran, W., (2008). "Omega-O-acylceramide, a lipid essential for mammalian survival." *Journal of Dermatological Science*, **51**(2), pp.77-87.

Vahlquist, A., Gånemo, A. and Virtanen, M., (2008). "Congenital Ichthyosis: An Overview of Current and Emerging Therapies." *Acta Dermato-Venereologica*, **88**(1), pp.4-14.

Vandamme, T., (2014). "Use of rodents as models of human diseases." *Journal of Pharmacy and Bioallied Sciences*, **6**(1), p.2.

van Beelen, V., Roeleveld, J., Mooibroek, H., Sijtsma, L., Bino, R., Bosch, D., Rietjens, I. and Alink, G., 2007. A comparative study on the effect of algal and fish oil on viability and cell proliferation of Caco-2 cells. Food and Chemical Toxicology, 45(5), pp.716-724.

van Meer, G., Voelker, D. and Feigenson, G., (2008). "Membrane lipids: where they are and how they behave." *Nature Reviews Molecular Cell Biology*, **9**(2), pp.112-124.

van Smeden, J., Janssens, M., Gooris, G. and Bouwstra, J., (2014). "The important role of stratum corneum lipids for the cutaneous barrier function." *Biochimica et Biophysica Acta (BBA) - Molecular and Cell Biology of Lipids*, **1841**(3), pp.295-313.

Varga, T., Czimmerer, Z. and Nagy, L., (2011). "PPARs are a unique set of fatty acid regulated transcription factors controlling both lipid metabolism and inflammation." *Biochimica et Biophysica Acta (BBA) - Molecular Basis of Disease*, **1812**(8), pp.1007-1022.

Vasireddy, V., Uchida, Y., Salem, N., Kim, S., Mandal, M., Reddy, G., Bodepudi, R., Alderson, N., Brown, J., Hama, H., Dlugosz, A., Elias, P., Holleran, W. and Ayyagari, R., (2007). "Loss of functional ELOVL4 depletes very long-chain fatty acids (≥C28) and the unique ω-O-acylceramides in skin leading to neonatal death." *Human Molecular Genetics*, **16**(5), pp.471-482.

Velagaleti, R., Massaro, J., Vasan, R., Robins, S., Kannel, W. and Levy, D., (2009). "Relations of Lipid Concentrations to Heart Failure Incidence." *Circulation*, **120**(23), pp.2345-2351.

Viswakarma, N., Jia, Y., Bai, L., Vluggens, A., Borensztajn, J., Xu, J. and Reddy, J., (2010). "Coactivators in PPAR-Regulated Gene Expression." *PPAR Research*, **2010**, pp.1-21.

Volker, D., Fitzgerald, P., Major, G. and Garg, M., (2000). "Efficacy of fish oil concentrate in the treatment of rheumatoid arthritis." *The Journal of Rheumatology*, **27**(10), pp.6-2343.

Vona, R., Iessi, E. and Matarrese, P., (2021). "Role of Cholesterol and Lipid Rafts in Cancer Signaling: A Promising Therapeutic Opportunity?". *Frontiers in Cell and Developmental Biology*, **9**.

Wahl SM. (1992). "Transforming growth factor beta (TGF-beta) in inflammation: a cause and a cure." *J Clin Immunol,* **12**(2):61–74.

Wang, Y., Lee, C., Tiep, S., Yu, R., Ham, J., Kang, H. and Evans, R., (2003). "Peroxisome-Proliferator-Activated Receptor δ Activates Fat Metabolism to Prevent Obesity." *Cell*, **113**(2), pp.159-170.

Wang, K. and Wong, Y., (2009). "G protein signaling controls the differentiation of multiple cell lineages." *BioFactors*, **35**(3), pp.232-238.

Wang, Z., Gerstein, M. and Snyder, M., (2009). "RNA-Seq: a revolutionary tool for transcriptomics." *Nature Reviews Genetics*, **10**(1), pp.57-63.

Wang, B., Shi, L., Sun, X., Wang, L., Wang, X. and Chen, C., (2016). "Production of CCL20 from lung cancer cells induces the cell migration and proliferation through PI3K pathway." *Journal of Cellular and Molecular Medicine*, **2**-(5), pp.9-920.

Wang, B., Kumar, V., Olson, A. and Ware, D., (2019). “Reviving the Transcriptome Studies: An Insight Into the Emergence of Single-Molecule Transcriptome Sequencing.” *Frontiers in Genetics*, **10**.

Watt, F., (1983). “Involucrin and Other Markers of Keratinocyte Terminal Differentiation.” *Journal of Investigative Dermatology*, **81**(1), pp. S100-S103.

Wawryk-Gawda, E., Chylińska-Wrzos, P., Lis-Sochocka, M., Chłapek, K., Bulak, K., Jędrych, M. and Jodłowska-Jędrych, B., (2013). “P53 protein in proliferation, repair and apoptosis of cells.” *Protoplasma*, **251**(3), pp.525-533.

Weber, C., Fischer, J., Redelfs, L., Rademacher, F., Harder, J., Weidinger, S., Wu, Z. and Meyer-Hoffert, U., (2017). “The serine protease inhibitor of Kazal-type 7 (SPINK7) is expressed in human skin.” *Archives of Dermatological Research*, **309**(9), pp.767-771.

Welte, M. and Gould, A., (2017). “Lipid droplet functions beyond energy storage.” *Biochimica et Biophysica Acta (BBA) - Molecular and Cell Biology of Lipids*, **1862**(10), pp.1260-1272.

Werchau, S., (2011). “Keratitis-Ichthyosis-Deafness Syndrome: Response to Alitretinoin and Review of Literature.” *Archives of Dermatology*, **147**(8), p.993.

Wertz, P. and Downing, D., (1983). “Ceramides of pig epidermis: structure determination.” *Journal of Lipid Research*, **24**(6), pp.759-765.

Wertz, P., (1992). “Epidermal lipids.” *Seminars in Dermatology*, **11**(2), pp.13-106.

Westergaard, M., Henningsen, J., Kratchmarova, I., Kristiansen, K., Svendsen, M., Johansen, C., Jensen, U., Schrøder, H., Berge, R., Iversen, L., Bolund, L. and Kragballe, K., (2001). “Modulation of Keratinocyte Gene Expression and Differentiation by PPAR-Selective Ligands and Tetradecylthioacetic Acid.” *Journal of Investigative Dermatology*, **116**(5), pp.702-712.

Westergaard, M., Henningsen, J., Rasmussen, S., Kristiansen, K., Johansen, C., Svendsen, M., Jensen, U., Schrøder, H., Staels, B., Iversen, L., Bolund, L. and Kragballe, K., (2003). “Expression and Localization of Peroxisome Proliferator-Activated Receptors and Nuclear Factor κB in Normal and Lesional Psoriatic Skin.” *Journal of Investigative Dermatology*, **121**(5), pp.1104-1117.

Whelan, J. and Fritsche, K., (2013). “Linoleic acid.” *Advances in Nutrition*, **4**(3), pp.2-311.

White, S., Mirejovsky, D. and King, G., (1988). “Structure of lamellar lipid domains and corneocyte envelopes of murine stratum corneum. An x-ray diffraction study.” *Biochemistry*, **27**(10), pp.3725-3732.

Williams, M., (1992). “Ichthyosis: Mechanisms of Disease.” *Pediatric Dermatology*, **9**(4), pp.365-368.

Willson, T., Brown, P., Sternbach, D. and Henke, B., (2000). “The PPARs: From Orphan Receptors to Drug Discovery.” *Journal of Medicinal Chemistry*, **43**(4), pp.527-550.

Wolf, R., Orion, E., Ruocco, E. and Ruocco, V., (2012). “Abnormal epidermal barrier in the pathogenesis of psoriasis.” *Clinics in Dermatology*, **30**(3), pp.323-328.

Wong, W., Tian, X., Xu, A., Yu, J., Lau, C., Hoo, R., Wang, Y., Lee, V., Lam, K., Vanhoutte, P. and Huang, Y., (2011). "Adiponectin Is Required for PPARγ-Mediated Improvement of Endothelial Function in Diabetic Mice." *Cell Metabolism*, **14**(1), pp.104-115.

Wong, R., Geyer, S., Weninger, W., Guimberteau, J. and Wong, J., (2015). "The dynamic anatomy and patterning of skin." *Experimental Dermatology*, **25**(2), pp.92-98.

Woodley, D., Wysong, A., DeClerck, B., Chen, M. and Li, W., (2015). "Keratinocyte Migration and a Hypothetical New Role for Extracellular Heat Shock Protein 90 Alpha in Orchestrating Skin Wound Healing." *Advances in Wound Care*, **4**(4), pp.203-212.

Wright Muelas, M., Ortega, F., Breitling, R., Bendtsen, C. and Westerhoff, H., (2018). "Rational cell culture optimization enhances experimental reproducibility in cancer cells." *Scientific Reports*, **8**(1).

Wu, Z., Hansmann, B., Meyer-Hoffert, U., Gläser, R. and Schröder, J., (2009). "Molecular Identification and Expression Analysis of Filaggrin-2, a Member of the S100 Fused-Type Protein Family." *PLoS ONE*, **4**(4), p.e5227.

Wu, Z., Latendorf, T., Meyer-Hoffert, U. and Schröder, J., (2011). "Identification of Trichohyalin-Like 1, an S100 Fused-Type Protein Selectively Expressed in Hair Follicles." *Journal of Investigative Dermatology*, **131**(8), pp.1761-1763.

Wyman, M. and Schneiter, R., (2008). "Lipid signalling in disease." *Nature Reviews. Molecular Cell Biology*, **9**(2), pp.76-162.

Xu, S., Mueser, T., Marnett, L. and Funk, M., (2012). "Crystal Structure of 12-Lipoxygenase Catalytic-Domain-Inhibitor Complex Identifies a Substrate-Binding Channel for Catalysis." *Structure*, **20**(9), pp.1490-1497.

Xu, Z., Li, Z., Du, L., Li, J. and Wang, L., (2013). "Using bovine pituitary extract to increase proliferation of keratocytes and maintain their phenotype in vitro." *International Journal of Ophthalmology*, **6**(6), pp.65-758.

Yaar, M. and Park, H., (2012). "Melanocytes: A Window into the Nervous System." *Journal of Investigative Dermatology*, **132**(3), pp.835-845.

Yamamoto-Tanaka, M., Makino, T., Motoyama, A., Miyai, M., Tsuboi, R. and Hibino, T., (2014). "Multiple pathways are involved in DNA degradation during keratinocyte terminal differentiation." *Cell Death & Disease*, **5**(4), pp. e1181-e1181.

Yamasaki, K., Di Nardo, A., Bardan, A., Murakami, M., Ohtake, T., Coda, A., Dorschner, R., Bonnart, C., Descargues, P., Hovnanian, A., Morhenn, V. and Gallo, R., (2007). "Increased serine protease activity and cathelicidin promotes skin inflammation in rosacea." *Nature Medicine*, **13**(8), pp.975-980.

Yan, Y., Furumura, M., Numata, S., Teye, K., Karashima, T., Ohyama, B., Tanida, N. and Hashimoto, T., (2015). "Various peroxisome proliferator-activated receptor (PPAR)-γagonists differently induce differentiation of cultured human keratinocytes." *Experimental Dermatology*, **24**(1), pp.62-65.

Yan, B., Liu, N., Li, J., Li, J., Zhu, W., Kuang, Y., Chen, X. and Peng, C., (2020). "The role of Langerhans cells in epidermal homeostasis and pathogenesis of psoriasis." *Journal of Cellular and Molecular Medicine*, **24**(20), pp.11646-11655.

Yanagi, T., Akiyama, M., Nishihara, H., Ishikawa, J., Sakai, K., Miyamura, Y., Naoe, A., Kitahara, T., Tanaka, S. and Shimizu, H., (2010). "Self-Improvement of Keratinocyte Differentiation Defects During Skin Maturation in ABCA12-Deficient Harlequin Ichthyosis Model Mice." *The American Journal of Pathology*, **177**(1), pp.106-118.

Yang, Q., Yamada, A., Kimura, S., Peters, J. and Gonzalez, F., (2006). "Alterations in Skin and Stratified Epithelia by Constitutively Activated PPARα." *Journal of Investigative Dermatology*, **126**(2), pp.374-385.

Yang, Z., Miyahara, H., Iwasaki, Y., Takeo, J. and Katayama, M., (2013). "Dietary supplementation with long-chain monounsaturated fatty acids attenuates obesity-related metabolic dysfunction and increases expression of PPAR gamma in adipose tissue in type 2 diabetic KK-Ay mice." *Nutrition & Metabolism*, **10**(1), p.16.

Yang, S., Sun, Y., Geng, Z., Ma, K., Sun, X. and Fu, X., (2016). "Abnormalities in the basement membrane structure promote basal keratinocytes in the epidermis of hypertrophic scars to adopt a proliferative phenotype." *International Journal of Molecular Medicine*, **37**(5), pp.1263-1273.

Yang, R., Liu, F., Wang, J., Chen, X., Xie, J. and Xiong, K., (2019). "Epidermal stem cells in wound healing and their clinical applications." *Stem Cell Research & Therapy*, **10**(1).

Yin, L., Wei, Y., Wang, Y., Xu, Y. and Yang, Y., (2013). "Long Term and Standard Incubations of WST-1 Reagent Reflect the Same Inhibitory Trend of Cell Viability in Rat Airway Smooth Muscle Cells." *International Journal of Medical Sciences*, **10**(1), pp.68-72.

Yoo, H., Jeon, B., Jeon, M., Lee, H. and Kim, T., (2008). "Reciprocal regulation of 12- and 15-lipoxygenases by UV-irradiation in human keratinocytes." *FEBS Letters*, **582**(21-22), pp.3249-3253.

Yu, K., Bayona, W., Kallen, C., Harding, H., Ravera, C., McMahon, G., Brown, M. and Lazar, M., (1995). "Differential Activation of Peroxisome Proliferator-activated Receptors by Eicosanoids." *Journal of Biological Chemistry*, **270**(41), pp.23975-23983.

Yu, Z., Schneider, C., Boeglin, W. and Brash, A., (2005). "Mutations associated with a congenital form of ichthyosis (NCIE) inactivate the epidermal lipoxygenases 12-LOX and eLOX3." *Biochimica et Biophysica Acta (BBA) - Molecular and Cell Biology of Lipids*, **1686**(3), pp.238-247.

Yu, Y., Prassas, I., Dimitromanolakis, A. and Diamandis, E., (2015). "Novel Biological Substrates of Human Kallikrein 7 Identified through Degradomics." *Journal of Biological Chemistry*, **290**(29), pp.17762-17775.

Yun, S., Han, S. and Park, J., (2018). "Peroxisome Proliferator-Activated Receptor γ and PGC-1α in Cancer: Dual Actions as Tumor Promoter and Suppressor." *PPAR Research*, **2018**, pp.1-12.

Zeitvogel, J., Jokmin, N., Rieker, S., Klug, I., Brandenberger, C. and Werfel, T., (2017). "GATA3 regulates FLG and FLG2 expression in human primary keratinocytes." *Scientific Reports*, **7**(1).

Zhang, Y., Xue, R., Zhang, Z., Yang, X. and Shi, H., (2012). "Palmitic and linoleic acids induce ER stress and apoptosis in hepatoma cells." *Lipids in Health and Disease*, **11**(1).

Zhang, S., Jiang, J., Chen, Z., Wang, Y., Tang, W., Chen, Y. and Liu, L., (2018). "Relationship of PPARG, PPARGC1A, and PPARGC1B polymorphisms with susceptibility to hepatocellular carcinoma in an eastern Chinese Han population." *OncoTargets and Therapy*, **2018**(11), pp.4651-4660.

Zhang, X., Yin, M. and Zhang, L., (2019). "Keratin 6, 16 and 17—Critical Barrier Alarmin Molecules in Skin Wounds and Psoriasis." *Cells*, **8**(8), p.807.

Zheng, Y., Yin, H., Boeglin, W., Elias, P., Crumrine, D., Beier, D. and Brash, A., (2011). "Lipoxygenases Mediate the Effect of Essential Fatty Acid in Skin Barrier Formation." *Journal of Biological Chemistry*, **286**(27), pp.24046-24056.

Ziboh, V., (1992). "Prostaglandins, leukotrienes, and hydroxy fatty acids in epidermis." *Seminars in Dermatology*, **11**(2), pp.20-114.

Ziboh, V., Miller, C. and Cho, Y., (2000). "Metabolism of polyunsaturated fatty acids by skin epidermal enzymes: generation of antiinflammatory and antiproliferative metabolites." *The American Journal of Clinical Nutrition*, **71**(1), pp.361s-366s.

Zoete, V., Grosdidier, A. and Michielin, O., (2007). "Peroxisome proliferator-activated receptor structures: Ligand specificity, molecular switch and interactions with regulators." *Biochimica et Biophysica Acta (BBA) - Molecular and Cell Biology of Lipids*, **1771**(8), pp.915-925.

Appendix 1: MRM parameters for analysis of C32 oxidized ceramides.

Ceramide ID	Q1 Mass (*m/z*) [M-H+60]$^-$	Q3 Mass (*m/z*)
C32 EOS	1098.9	279.2
C32 EOH	1114.9	279.2
C32 EOP	1116.9	279.2

Ceramide ID	Q1 Mass (*m/z*) [M-H+60]$^-$	Q3 Mass (*m/z*)
C32 9-HODE EOS	1114.9	295.2
C32 9-HODE EOH	1130.9	295.2
C32 9-HODE EOP	1132.9	295.2

Ceramide ID	Q1 Mass (*m/z*) [M-H+60]$^-$	Q3 Mass (*m/z*)
C32 9R,10R,13R-TriHOME EOS	1148.9	329.2
C32 9R,10R,13R-TriHOME EOH	1164.9	329.2
C32 9R,10R,13R-TriHOME EOP	1166.9	329.2

Appendix 2: MRM chromatograms of C32 EOS, EOH and EOP ceramides. (A-C) hTERT media, (D-F) hTERT cells collected at 30% confluence, (G-I) hTERT cells collected at 100% confluence.

A

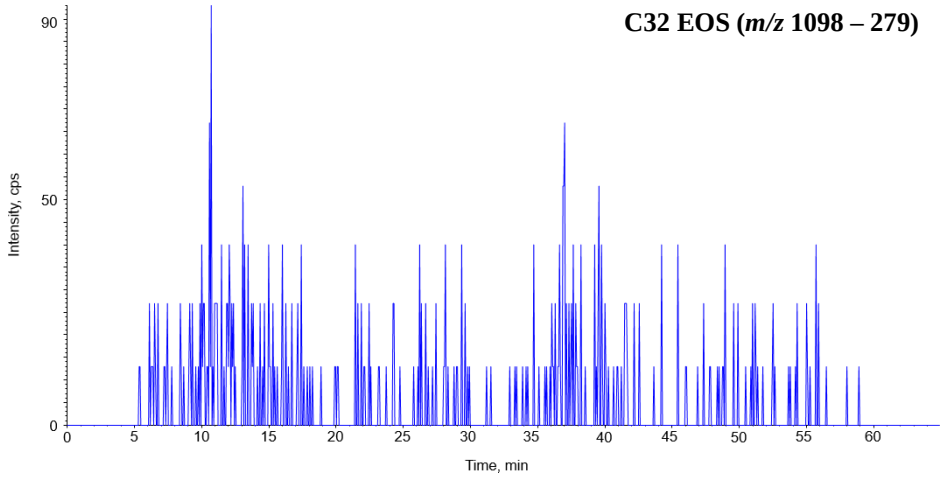

B

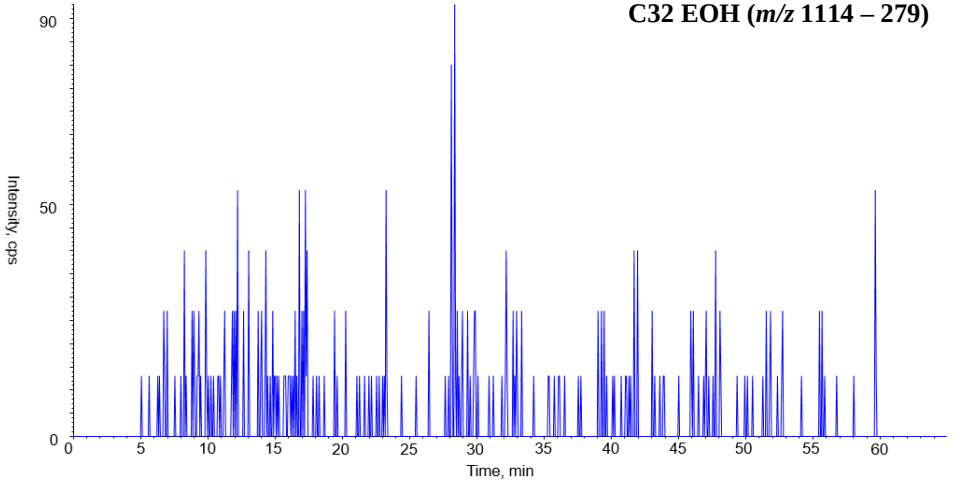

C

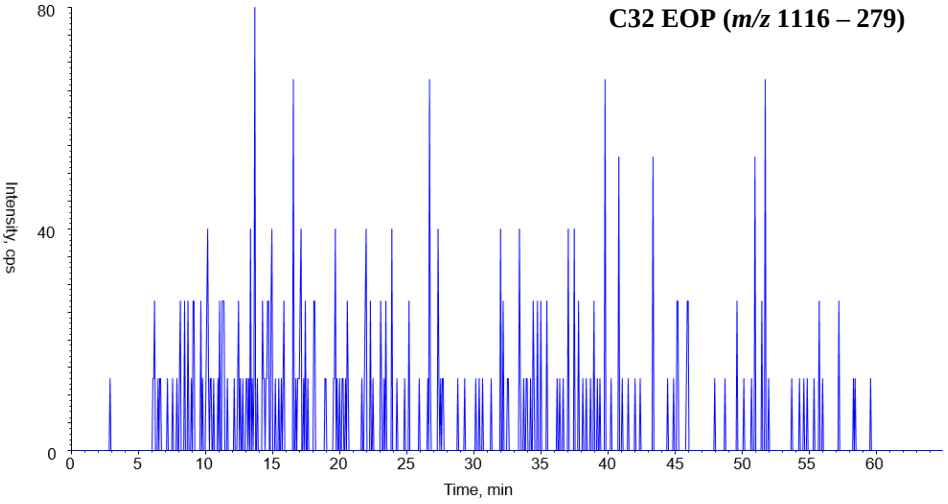

D

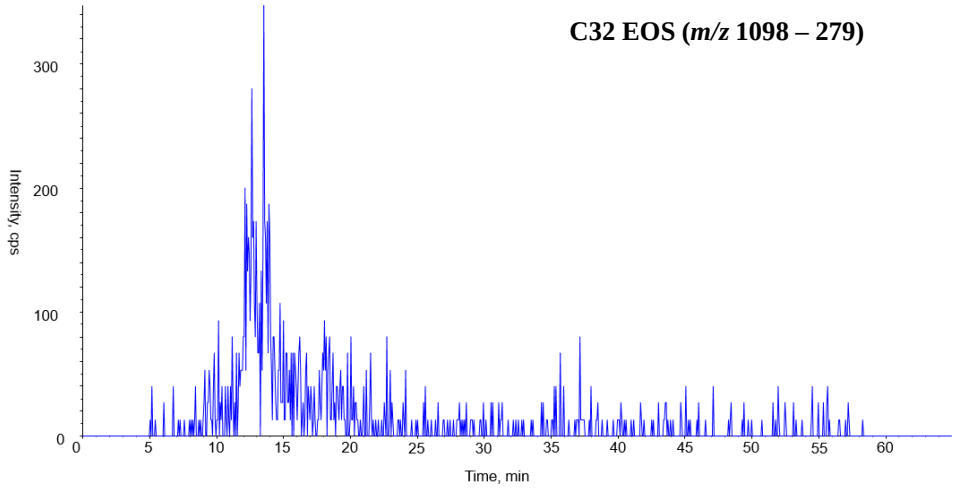
C32 EOS (*m/z* 1098 – 279)
Intensity, cps
300
200
100
0
0
5
10
15
20
25
30
35
40
45
50
55
60
Time, min

E

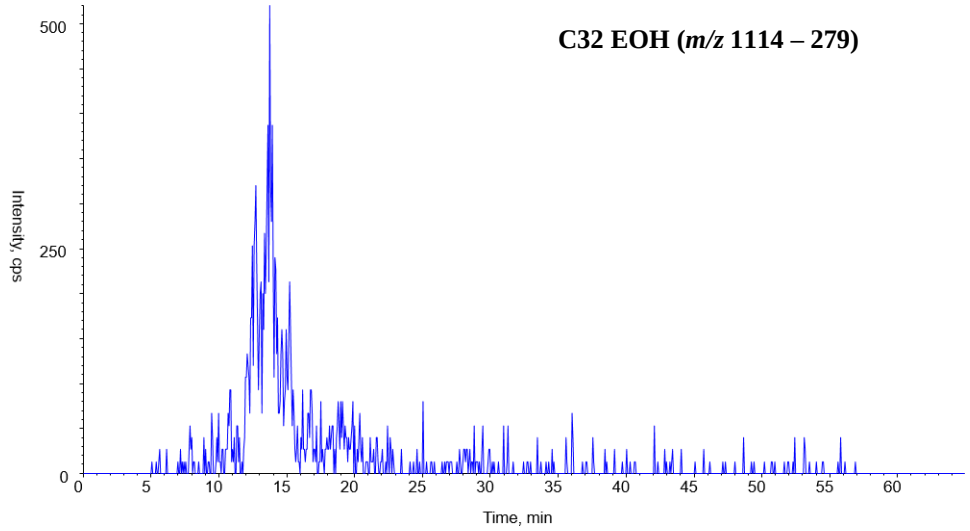
C32 EOH (*m/z* 1114 – 279)
Intensity, cps
500
250
0
0
5
10
15
20
25
30
35
40
45
50
55
60
Time, min

F

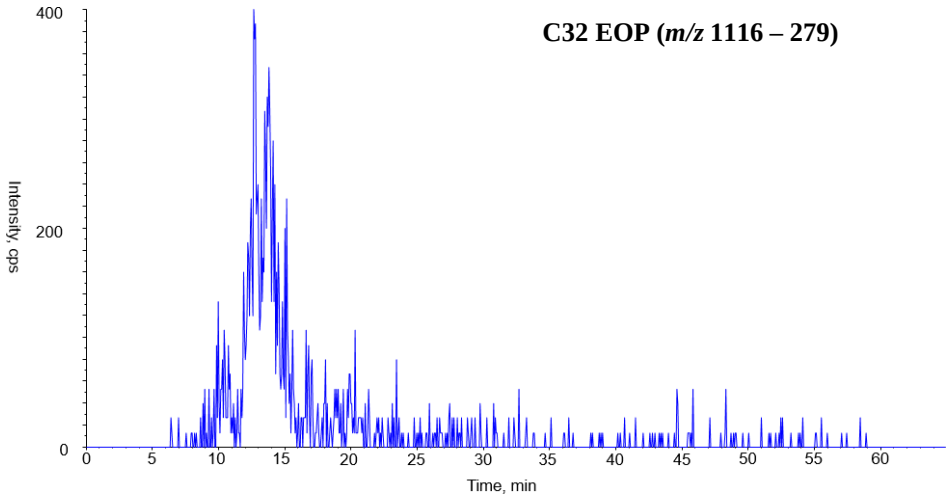
C32 EOP (*m/z* 1116 – 279)
Intensity, cps
400
200
0
0
5
10
15
20
25
30
35
40
45
50
55
60
Time, min

G

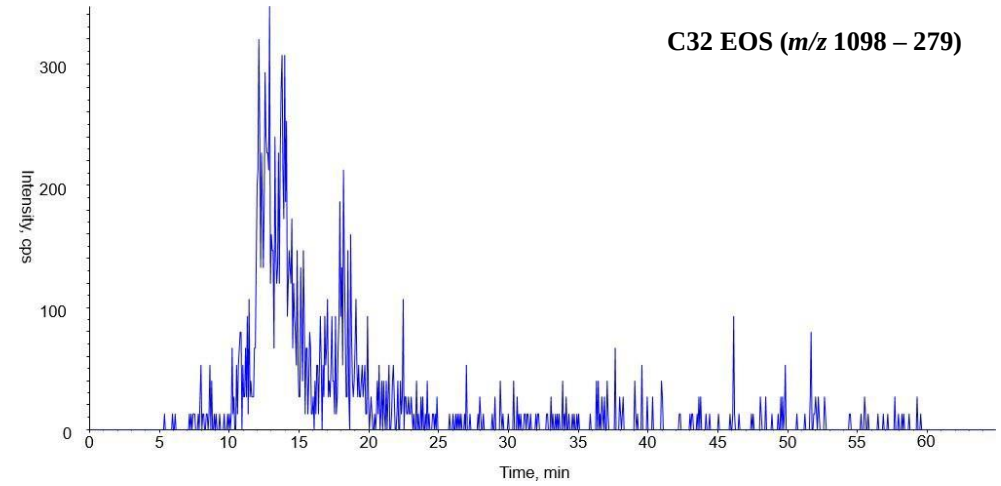
C32 EOS (*m/z* 1098 – 279)
Intensity, cps
Time, min

H

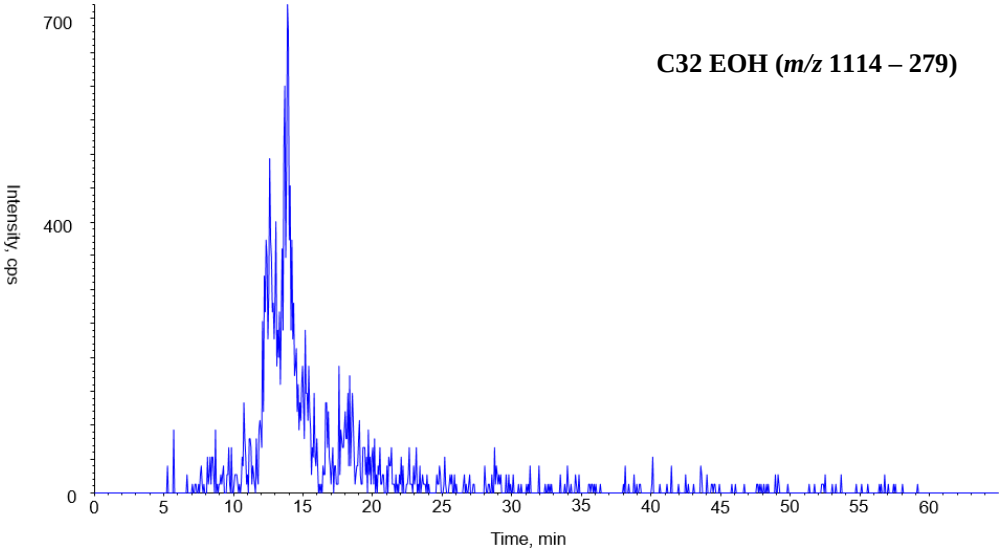
C32 EOH (*m/z* 1114 – 279)
Intensity, cps
Time, min

I

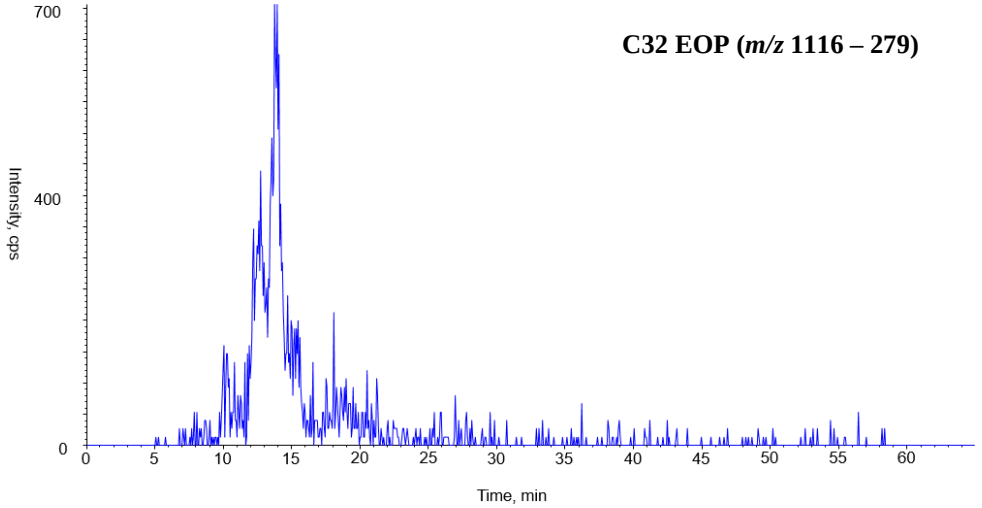
C32 EOP (*m/z* 1116 – 279)
Intensity, cps
Time, min

Appendix 3: List of upregulated (≥ 1.5-FC) and downregulated (≤ 1.5-FC) genes in the 12*R*-LOX knockout vs wildtype dataset.

Upregulated genes (≥ 1.5-FC)
Sult1c2, Sprr1b, Sprr2d, Tpm3-rs7, Sprr2a3, Teddm3, Klk14, Lce3f, Iqcj, Slc36a3, Tas1r2, Clec4b1, Spink14, Grm2, Trim69, Lce3d, Plac8l1, Cyp2c55, Pla2g2c, Serpina3a, Hsd17b1, Xcl1, Krt16, Lhcgr, Tmem235, Fsip2, Thegl, Hand1, Zdhhc11, Ccdc33, Lrit3, Chrnb4, Ccl20, Rp1l1, Sprr2e, Serpinb3c, Pglyrp3, Tmem145, Rptn, Serpinb12, Myo3a, Mrap2, Serpinb11, Lhfpl5, Sox3, Sprr2h, Pkd2l1, Prg2, Ccl8, Kcnj4, Krtap9-1, Skor1, Patl2, Il5ra, Otop3, Spata20, Lce3e, Krtap4-8, Krt10, Lipn, Mup20, Krt1, Slc45a1, Cnfn, Sprr2k, Serpinb2, Shisa8, Il1f6, Tmbim7, Nlrp1a, Tlr11, Spaca4, Fosl1, Ly6d, Krtdap, Krt6b, Krt24, Pou1f1, Them5, Epha10, Rnf224, Dnase1l3, Ankrd22, Fam71a, Krtap5-4, Alox12b, Sult2b1, Krt14, Gabra2, Pdyn, Csta1, Fnd3c2, Cysrt1, Serpinb3a, Ereg, Calm5, Gpr3, Mpped1, Mesp2, Tex35, Trpm2, Il1f9, Aadacl2 *Clps, Gkn2, Stfa1, Mup3, 1700007K09Rik, Izumo1r, Adam30, Defb48, Fam136b-ps, Dnase2b, Stfa3, Spata3, Sis, Gm10720, Gm10146, Olfr1373, Hist1h2ba, Dnajb8, Rxfp4, 2300005B03Rik, Trim75, BC100530, Gm10142, Fam183b, 4933425L06Rik, Cckar,* *Pabpn1l, Defb6, Aox4, Mar-10, 1700019B03Rik, Gja10, Gm10263, BC117090, Gm10577, 2610528A11Rik, Tdh, Mroh3*
Downregulated genes (≤ 1.5-FC)
Slco1a1, Klk1, Mefv, Hoxc12, Piwil4, Lman1l, Slc38a11, Ffar4, Pdk4, Ppargc1a, Pck1, Fam186b, Susd5, Dio2, Matn3, Ehhadh, Adra1a, Chst9, Ccl28, Gmpr, Adgrf3, Styxl1, Adam11, Pvalb, Olr1, Irf4, Epyc, Cited1, Prima1, Tfcp2l1, Arx, Opn4, Mylk4, Cpt1b, Nr4a3, Slc25a42, Musk, Kcnf1 *Gm6614, Rln1, Olfr458, Gm10775, Ucp1, 5330417C22Rik, Lman1l, RP24-134N2.1, Chil5, Lipi, 4933424G06Rik, BC049762, Apol10b, 4930426L09Rik, Gm11273*